

Topics in High-Energy Astrophysics

Jeremy Goodman
Princeton University Observatory

April 8, 2013

Contents

1	Special Relativity	7
1.1	Superluminal motion	7
1.2	Lorentz transformations and Lorentz invariance	8
1.2.1	Invariance of four-volumes	11
1.3	Four-vectors and four-momentum	11
1.3.1	Conservation of 4-momentum	12
1.4	Transformation of electromagnetic fields	13
1.5	Phase space	13
1.6	Specific intensity	15
1.7	Relativistic beaming	17
1.8	Conservation laws and energy-momentum tensor	18
1.9	Problems for Chapter 1	22
2	Synchrotron Radiation	25
2.1	Radiation from an accelerated charge	25
2.2	Basic principles of synchrotron radiation	27
2.2.1	Motion of charges in a magnetic field	27
2.2.2	Total emitted power	27
2.2.3	Characteristic emission frequency	28
2.3	Synchrotron spectrum	29
2.3.1	Cooling break	33
2.4	Synchrotron self-absorption	33
2.5	Equipartition energy and brightness temperature	36
2.6	Problems for Chapter 2	39
3	Gamma-Ray Bursts and Afterglows	41
3.1	Observed properties of GRBs	41
3.2	Basic theoretical considerations for GRBs	43
3.3	Afterglow observations	48
3.4	Basic theoretical considerations for afterglows	50
3.4.1	Relativistic shock dynamics	51
3.4.2	Afterglow emission	52
3.5	Problems for Chapter 3	56
4	Black-hole Basics	57
4.1	General-Relativistic kinematics	57
4.1.1	The Principle of Equivalence	57
4.1.2	Metric in general coordinates	58
4.1.3	Geodesics	59
4.1.4	Momentum	61

4.1.5	Constants of motion	62
4.2	Non-rotating black holes	62
4.2.1	Schwarzschild metric and coordinates	62
4.2.2	Null (photon) orbits	64
4.2.3	Timelike orbits	66
4.2.4	Tidal fields	67
4.3	Rotating black holes	68
4.3.1	Kerr metric	68
4.3.2	Horizon and ergosphere	68
4.3.3	Negative energies	69
4.3.4	Irreducible mass	71
4.3.5	Orbits	72
5	Accretion onto rotating black holes	73
5.1	Circular and marginally stable orbits	73
5.2	Growth of the hole	75
5.3	Steady, thin-disk accretion	76
5.3.1	Newtonian accretion disks	76
5.3.2	Relativistic conservation laws	78
5.4	Appendix: Invariant 4-volume and divergence formula	81
5.5	Problems for Chapter 5	83
6	Neutron Stars	85
6.1	Masses and radii	85
6.1.1	Radii	86
6.2	Type I X-ray bursts	87
6.2.1	Radiative transfer in the diffusion approximation	90
6.2.2	The graybody factor	91
7	The Blandford-Znajek mechanism	95
7.1	Faraday unipolar dynamo	95
7.2	Electrical conductivity of a black hole	96
7.3	Black hole as dynamo	97
7.4	Back-of-the-envelope AGN	99
8	Gravitational Waves	101
8.1	Overview	101
8.2	The Weak-Field Approximation	102
8.3	Analogy with Electromagnetism	102
8.4	The gravitational-wave equation	103
8.5	Solution for fields in the radiation zone	105
8.5.1	Transverse-traceless (“TT”) gauge	107
8.6	Gravitational waves from a binary star	108
8.7	Detection of gravitational waves	109
8.8	Energy of gravitational waves	110
9	Cosmic Rays	113
9.1	Energy spectrum	113
9.2	Detection of cosmic rays	115
9.3	Inferences from the composition of cosmic rays	116
9.3.1	Spallation model	116
9.3.2	Confinement time	117

CONTENTS

5

9.4 Acceleration mechanism	118
9.4.1 Energetics	121
10 Compton scattering	123
10.1 Compton cross section	123
10.2 Inverse Compton scattering	125
10.3 Kompaneets Equation	126

Chapter 1

Special Relativity

Newtonian approximations are adequate for much of astrophysics, but special relativity is essential to understand phenomena whose energy per unit mass is large. Presumably you have already studied special relativity in physics courses, but you may not have encountered certain applications that are particularly important to astrophysics, such as the Lorentz transformation of specific intensity or the jump conditions for relativistic shocks. Such applications form the main subject matter of the present chapter.

Appropriate supplementary reading for this lecture is chapter 4 of [53].

1.1 Superluminal motion

There is a difference between physics and astrophysics in the meaning of the word “observer.” In traditional physics textbooks concerned with special relativity, “observer” usually refers to an entire inertial reference frame, notionally consisting of an infinite array of clocks and meter sticks at rest with respect to one another and extending throughout spacetime. In astronomy, “observer” normally means an individual person and his or her telescope, receiving information about remote events by means of photons rather than recording them with local rods and clocks. The astronomical observer’s view of rapidly moving objects is therefore subject to distortions that are not often discussed in physics textbooks. Among the most basic of these is the illusion of motion faster than light. Superluminal motion (as this is called) is frequently seen in radio sources, gamma-ray bursts, and other situations where emitting material moves toward the observer at a speed close to (but of course less than) c and at a small angle to the line of sight. Some would say that superluminal motion is not really a relativistic effect at all, since no Lorentz transformations are involved.

Consider an emitting element with trajectory $\mathbf{r}(t_{\text{em}})$ in a reference frame where the observer is at rest at the origin, $\mathbf{r}_{\text{obs}} = 0$. Photons emitted at time t_{em} are received by the observer at time

$$t_{\text{rec}} = t_{\text{em}} + r(t_{\text{em}})/c, \quad r \equiv |\mathbf{r}|. \quad (1.1)$$

It is important to understand that both t_{em} and t_{rec} are defined in the same reference frame, namely that of the observer. They differ only because of light-travel time. Sometimes t_{em} is called “retarded time.”

Differentiating both sides of eq. (1.1)

$$\frac{dt_{\text{rec}}}{dt_{\text{em}}} = 1 + c^{-1} \mathbf{n} \cdot \frac{d\mathbf{r}}{dt_{\text{em}}},$$

where $\mathbf{n} \equiv \mathbf{r}/r$ is the unit vector along the line of sight from observer to emitter.¹ The physical

¹We shall try to use this convention consistently: $-\mathbf{n}$ is the direction of motion of a photon, so that the telescope receiving it points along \mathbf{n} .

velocity of the emitter is

$$\mathbf{v} = \frac{d\mathbf{r}}{dt_{\text{em}}}, \quad v < c.$$

The apparent velocity as the observer sees it is

$$\mathbf{v}_{\text{apparent}} = \frac{d\mathbf{r}}{dt_{\text{rec}}} = \frac{d\mathbf{r}}{dt_{\text{em}}} \frac{dt_{\text{em}}}{dt_{\text{rec}}} = \frac{\mathbf{v}}{1 + \mathbf{n} \cdot \mathbf{v}/c}. \quad (1.2)$$

Since the denominator can be as small as $1 - (v/c)$, it is possible to have $v_{\text{apparent}} > c$ if $v > c/2$.

In astronomy, radial velocities (= along the line of sight) are measured by doppler shifts. Doppler shifts are always finite so the astronomically inferred radial velocity is always $< c$, in contrast to $\mathbf{n} \cdot \mathbf{v}_{\text{apparent}}$ as defined by (1.2). Velocities transverse to the line of sight are measured as angular velocities (“proper motions”) multiplied by the distance from the observer to the source. Unlike the doppler velocity, the transverse velocity measured this way can appear to be superluminal:

$$\mathbf{v}_{\perp, \text{apparent}} = - \frac{\mathbf{n} \times (\mathbf{n} \times \mathbf{v})}{1 + \mathbf{n} \cdot \mathbf{v}/c}.$$

For a source at redshift z , the motion appears to be reduced by $(1+z)^{-1}$ —compared, that is to say, to what would have been seen by an astronomer comoving with the microwave background at redshift z .² This is because of cosmological time dilation. In other words, if $\dot{\theta}$ is the observed proper motion, then the apparent transverse velocity corrected for time dilation is $v_{\perp, \text{app}} = (1+z)d_A\dot{\theta}$. The distance d_A is the angular-diameter distance, defined as the ratio of the transverse proper size of an object to its angular size in the limit that the latter is small [46]. In a flat universe with matter density parameter $\Omega_m = 1 - \Omega_\Lambda$,

$$d_A = \frac{c}{(1+z)H_0} \int_0^z \frac{dz'}{\sqrt{1 + \Omega_m[(1+z')^3 - 1]}}, \quad (1.3a)$$

$$\approx 4300 \frac{z}{(1+z)(1+0.33z)} \text{Mpc}. \quad (1.3b)$$

Unfortunately the integral (1.3a) cannot be done exactly in elementary functions, but for the current best estimates of the cosmological parameters $H_0 = 70 \text{ km s}^{-1} \text{ Mpc}^{-1}$, $\Omega_m = 0.28$ [27], the approximation (1.3b) has a relative error $< 4\%$ for $z < 100$.

1.2 Lorentz transformations and Lorentz invariance

An event is a point in spacetime. Events are labeled by sets of four coordinates, which should be thought of as real-valued functions on spacetime. The functions are distinguished by letters, *e.g.* $txyz$, or by Greek indices ranging from 0 to 3:

$$x^\mu : x^0 \equiv t, x^1 \equiv x, x^2 \equiv y, x^3 \equiv z.$$

Lower-case roman indices $\dots ijk\dots$ will range from 1 to 3 (the spatial components). Upper-case roman letters $ABC\dots$ are particle labels rather than space-time indices. The locus of events occupied by a particle is a curve in spacetime called its worldline. Worldlines can be described by giving the coordinates of its events as functions of some parameter. For a massive particle, it is often convenient to use the proper time as the parameter, $x^\mu(\tau)$.

²In a cosmological context, the “redshift” of a source refers to that of its host galaxy, which is assumed to be approximately at rest with respect to the microwave background. It is rare for relativistically moving objects to display spectral lines from which their radial velocities can be directly determined.

In General Relativity, coordinates can be quite general functions, but in Special Relativity they are inertial unless stated otherwise. An inertial system is one in which the worldlines of all unaccelerated particles are described by linear relationships among the coordinates. Thus for example if $\Delta x^\mu \equiv x^\mu(Q) - x^\mu(P)$ are the coordinate differences between any two events P, Q on an unaccelerated worldline, then the ratios $\Delta x^i/\Delta x^0$ are independent of P, Q . Furthermore, the difference Δx^i in spatial coordinates between two particles that have a common velocity should be independent of x^0 . By this definition, spherical polar coordinates are not inertial.

The two postulates of Special Relativity (henceforth SR) are

- I. The laws of physics are the same in all inertial reference frames.
- II. The speed of light is a physical law, hence constant.

SR takes no account of gravitational effects.

It is often convenient to work in units such that the speed of light $c = 1$. The necessary factors of c can always be restored by dimensional analysis. As a consequence of postulate II, if the unaccelerated particle discussed above is a photon,

$$\sum_{i=1}^3 (\Delta x^i)^2 - (\Delta x^0)^2 = 0. \quad (1.4)$$

To simplify the writing of such formulae, lower indices are defined by changing the sign of the 0th component, *i.e.*

$$\Delta x_0 \equiv -\Delta x^0, \quad \Delta x_i \equiv \Delta x^i,$$

and repeated indices are implicitly to be summed from 0 to 3. Thus (1.4) is written

$$\Delta x_\mu \Delta x^\mu = 0.$$

One of the summed indices should always appear “upstairs” and the other “downstairs.” Still another way to write the above is $\eta_{\mu\nu} \Delta x^\mu \Delta x^\nu = 0$, where the symbol

$$\eta_{\mu\nu} = \eta^{\mu\nu} = \begin{cases} -1 & \mu = \nu = 0, \\ +1 & \mu = \nu = i, \\ 0 & \mu \neq \nu, \end{cases} \quad (1.5)$$

is called the Minkowski metric. It is a sin to equate an upstairs index to a downstairs index (as in $\eta_{\mu\nu} = \eta^{\mu\nu}$) because most such equations will not Lorentz transform properly. But $\eta_{\mu\nu}$ and $\eta^{\mu\nu}$ are invariant, *i.e.* the same in all inertial reference frames. In preparation for General Relativity, please regard $\eta_{\mu\nu}$ as the components of a (diagonal) matrix $\boldsymbol{\eta}$, and $\eta^{\mu\nu}$ as the components of the inverse matrix $\boldsymbol{\eta}^{-1}$ —even though these two matrices are numerically the same.

As a consequence of postulates I&II and some plausible symmetry assumptions, it can be shown that the interval

$$\Delta s^2 \equiv \Delta x_\mu \Delta x^\mu \quad (1.6)$$

is invariant not only for photons but for all unaccelerated particles, including massive ones. Of course the interval depends upon the events P, Q , but it doesn’t depend upon the reference frame. I won’t give the proof, since you have surely seen it before. When $\Delta s^2 = 0$, the separation between P and Q is null, and when $\Delta s^2 < 0$, it is timelike. If the separation between P and Q is timelike, it is possible for these events to lie on the worldline of a physical particle object with nonzero mass. In this case the time between the events as measured in the rest frame of the object is $\Delta\tau \equiv \sqrt{-\Delta s^2}$,

which is called proper time.³ Spacelike separations are those for which $\Delta s^2 > 0$. These cannot be traversed by physical particles.

Following [56], $x^{\bar{\mu}}$ and x^μ will denote coordinates in two inertial reference frames $\bar{\mathcal{O}}$ and \mathcal{O} , respectively. No particular relationship holds between μ and $\bar{\mu}$ except that both range from 0 to 3. Also, x^0 and $x^{\bar{0}}$ are different functions of spacetime. Since unaccelerated trajectories appear linear in both coordinate systems, they are related by a linear transformation,

$$\Delta x^{\bar{\mu}} = \Lambda^{\bar{\mu}}{}_{\mu} \Delta x^{\mu}. \quad (1.7)$$

The Lorentz transformation $\Lambda^{\bar{\mu}}{}_{\mu}$ depends upon the relative motion and orientation of the systems \mathcal{O} and $\bar{\mathcal{O}}$ but not upon the particular events P, Q . Invariance of Δs^2 implies that

$$\eta_{\bar{\mu}\bar{\nu}} \Lambda^{\bar{\mu}}{}_{\mu} \Lambda^{\bar{\nu}}{}_{\nu} = \eta_{\mu\nu}, \quad \text{or} \quad \mathbf{\Lambda}^T \boldsymbol{\eta} \mathbf{\Lambda} = \boldsymbol{\eta} \quad (1.8)$$

in matrix notation. Eq. (1.8) is the defining property of Lorentz transformations. Symmetric matrices $\mathbf{\Lambda}^T = \mathbf{\Lambda}$ describe boosts, wherein \mathcal{O} and $\bar{\mathcal{O}}$ are in relative motion but their spatial axes are aligned. A boost along the x^1 axis at relative velocity β is

$$\begin{pmatrix} \Delta x^{\bar{0}} \\ \Delta x^{\bar{1}} \\ \Delta x^{\bar{2}} \\ \Delta x^{\bar{3}} \end{pmatrix} = \begin{pmatrix} \gamma & -\gamma\beta & 0 & 0 \\ -\gamma\beta & \gamma & 0 & 0 \\ 0 & 0 & 1 & 0 \\ 0 & 0 & 0 & 1 \end{pmatrix} \begin{pmatrix} \Delta x^0 \\ \Delta x^1 \\ \Delta x^2 \\ \Delta x^3 \end{pmatrix}. \quad (1.9)$$

As usual, the Lorentz factor

$$\gamma \equiv \frac{1}{\sqrt{1 - \beta^2}}.$$

The inverse Lorentz boost is obtained by interchanging $\Delta x^\mu \leftrightarrow \Delta x^{\bar{\mu}}$ and changing the sign of the relative velocity: $\beta \rightarrow -\beta$. To remember which sign is needed, I find it helpful to note that according to (1.9), a particle at rest in \mathcal{O} has $\Delta x^i = 0$ so that $\Delta x^{\bar{1}} = -\gamma\beta\Delta x^0 = -\beta\Delta x^{\bar{0}}$; thus system \mathcal{O} moves at $-\beta$ with respect to $\bar{\mathcal{O}}$.

Spatial rotations are described by a subset of orthogonal transformations ($\mathbf{\Lambda}^{-1} = \mathbf{\Lambda}^T$) for which $\Lambda^{\bar{0}}_0 = 1$ and $\Lambda^{\bar{0}}_i = \Lambda^j_0 = 0$. For example, if \mathcal{O} has been rotated by angle θ with respect to $\bar{\mathcal{O}}$ around a common $x^1 x^{\bar{1}}$ axis,

$$\begin{pmatrix} \Delta x^{\bar{0}} \\ \Delta x^{\bar{1}} \\ \Delta x^{\bar{2}} \\ \Delta x^{\bar{3}} \end{pmatrix} = \begin{pmatrix} 1 & 0 & 0 & 0 \\ 0 & 1 & 0 & 0 \\ 0 & 0 & \cos \theta & -\sin \theta \\ 0 & 0 & \sin \theta & \cos \theta \end{pmatrix} \begin{pmatrix} \Delta x^0 \\ \Delta x^1 \\ \Delta x^2 \\ \Delta x^3 \end{pmatrix}. \quad (1.10)$$

An arbitrary Lorentz transformation can be decomposed into the product of a rotation and a boost.⁴ Lorentz transformations do not commute in general. Exceptions include boosts applied along the same direction and rotations around the same axis.

It is well known that times expand and lengths contract by factors of γ and γ^{-1} , respectively, upon transformation out of the rest frame. This reciprocal behavior can cause confusion in view of the symmetrical roles of x^0 and x^1 in the boost (1.9). But two very different kinds of measurement are involved.

³The meaning of ‘‘proper’’ in this term has little to do with correctness. It has the somewhat old-fashioned meaning ‘‘belonging/intrinsic to’’ or ‘‘own,’’ as in *property* and *proprietor*. Older British mathematics texts sometimes refer to ‘‘proper values’’ rather than ‘‘eigenvalues’’ of a matrix.

⁴The Polar Decomposition Theorem of linear algebra states that every non-singular, real-valued square matrix can be decomposed into the product of an orthogonal matrix and a positive-definite symmetric matrix: $\mathbf{M} = \mathbf{O}\mathbf{P}$, $\mathbf{O}\mathbf{O}^T = \mathbf{I}$, $\mathbf{S}^T = \mathbf{S}$, $\mathbf{S} > 0$. *Proof:* $\mathbf{M}^T \mathbf{M} > 0$, hence $\exists \mathbf{P} = (\mathbf{M}^T \mathbf{M})^{1/2} > 0$. Let $\mathbf{O} = \mathbf{M}\mathbf{P}^{-1}$.

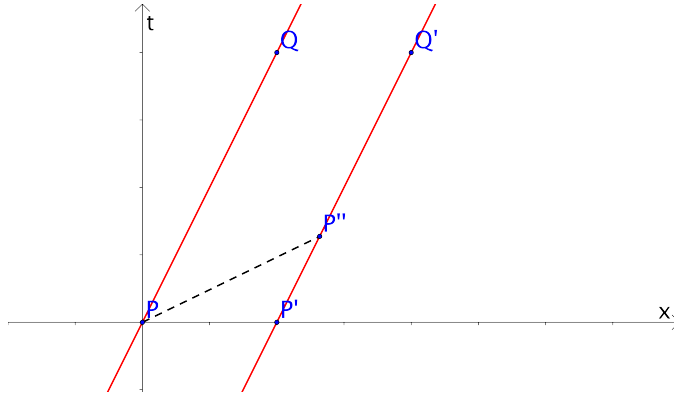


Figure 1.1: Two parallel worldlines PQ and $P'P''Q'$ as seen in the coordinates (x, t) of frame \mathcal{O} . The temporal separation between events P and Q on the first worldline is $t(Q)$, which is plainly greater than the proper time $\Delta\tau = \sqrt{t^2(Q) - x^2(Q)}$. This is time dilation. The spatial separation between the worldlines is measured on lines of simultaneity. In \mathcal{O} this means PP' or any parallel line. In the worldlines' restframe $\bar{\mathcal{O}}$, however, lines of simultaneity are parallel to PP'' , which is the reflection of PQ in the invariant null line $x = t$, $\bar{x} = \bar{t}$. Hence $\bar{t}(P) = \bar{t}(P'') > \bar{t}(P')$. The invariant interval $\Delta s^2(PP')$ is equal to $x^2(P')$ and also to $\bar{x}^2(P') - \bar{t}^2(P')$. It follows that $x^2(P') < \bar{x}^2(P') = \bar{x}^2(P'')$. In other words, the separation between parallel worldlines is largest in their rest frame. This is Lorentz contraction.

Time dilation compares the separation in proper time $\Delta\tau_{PQ}$ between events on the worldline of a particle, where τ is the time elapsed in the particle's rest frame, with the separation in coordinate t between the same events P & Q in a second frame: $\Delta t_{PQ} = \gamma\Delta\tau_{PQ}$, where γ is the Lorentz factor of the particle.

Lorentz contraction compares the spacelike separation between *two* given particles in a common rest frame with their separation in a frame where they move. (These particles could represent opposite ends of a meter stick, for example.) The separation in $\bar{\mathcal{O}}$ (the rest frame) is taken at $\Delta\bar{t} = 0$, while the separation in \mathcal{O} is taken at $\Delta t = 0$. Thus *different pairs of events* are used, since events simultaneous in one frame generally cannot be simultaneous in another. When the relative velocity between frames is parallel to the separation, the measurements are related by $\Delta x = \gamma^{-1}\Delta\bar{x}$.

In short, time dilation pertains to the temporal separation between two given *points* (events), while Lorentz contraction pertains to the spatial separation between parallel (world)*lines*.

1.2.1 Invariance of four-volumes

The area of the parallelogram $PP'Q'Q$ in Figure 1.1 is $[x(P') - x(P)] \times [t(Q) - t(P)] = x(P')t(Q)$ (base times height) in frame \mathcal{O} . In the rest frame $\bar{\mathcal{O}}$, the same four events define a transformed parallelogram with vertical sides and area $\bar{t}(Q)\bar{x}(P')$. It is easy to see from the discussion in the caption that these two areas are equal. The same result can be obtained more formally by noting that $\det(\Lambda) = \pm 1$ as a consequence of eq. (1.8)—in fact one usually insists on the positive sign here—and therefore the jacobian of the transformation $x^\mu \rightarrow \bar{x}^\mu$ is unity. Therefore $d^4x^\mu = d^4\bar{x}^\mu$.

1.3 Four-vectors and four-momentum

Any set of four quantities transforming according to the same rule (1.8) as Δx^μ is a 4-vector. Indices of general 4-vectors are raised and lowered in the same way, *viz* by changing the sign of the

0th component; or equivalently,

$$a_\mu = \eta_{\mu\nu} a^\nu \quad a^\mu = \eta^{\mu\nu} a_\nu.$$

If a^μ and b^μ are any two 4-vectors, then

$$a^\mu b_\mu = a^{\bar{\mu}} b_{\bar{\mu}} \Leftrightarrow a^\mu b_\mu \text{ is a Lorentz invariant.}$$

By definition, a Lorentz invariant has the same value in all inertial reference frames. It is usually more efficient and less confusing to calculate in terms of Lorentz invariants rather than Lorentz transformations whenever this is possible.

A 3-vector a^i is any triplet of quantities that preserves its length under rotations but not of course under boosts. It may or may not correspond to the last 3 components of a 4-vector. I often write 3-vectors in boldface, $a^i \Leftrightarrow \mathbf{a}$.

The 4-momentum of a particle consists of the particle's energy p^0 and the spatial components p^i of its momentum. If the particle has mass (not a photon) then there is a frame $\bar{\mathcal{O}}$ in which it is at rest, $p^{\bar{\mu}} = (m, 0, 0, 0)$, where m is the rest mass. In a general frame \mathcal{O} where its 3-velocity is

$$\frac{dx^i}{dt} = \beta^i \Leftrightarrow \frac{d\mathbf{x}}{dt} = \boldsymbol{\beta},$$

its 4-momentum is

$$p^\mu = (\gamma m, \gamma\beta^1 m, \gamma\beta^2 m, \gamma\beta^3 m) \equiv (\gamma m, \gamma\boldsymbol{\beta} m).$$

As with any 4-vector, the square $p_\mu p^\mu$ is Lorentz invariant. Evaluation in the rest frame shows that $p_\mu p^\mu = -m^2$.

Another important 4-vector is 4-velocity $u^\mu \equiv m^{-1} p^\mu$. In the rest frame, $u^{\bar{\mu}} = (1, 0, 0, 0)$, and in any frame, $u^\mu u_\mu = -1$. Massless particles such as photons do not have 4-velocities but they do have 4-momenta. It is often convenient to parametrize trajectories of massive particles by the proper time, τ . For an unaccelerated particle, τ is nothing but time measured in the particle's rest frame. But it can be generalized to accelerated worldlines⁵ by setting

$$d\tau \equiv (-dx^\mu dx_\mu)^{1/2} = \sqrt{-ds^2}, \quad (1.11)$$

where dx^μ is the infinitesimal coordinate separation between neighboring events along the worldlines. With this definition, the 4-velocity, 4-momentum, and 4-acceleration are

$$u^\mu = \frac{dx^\mu}{d\tau}, \quad p^\mu = m \frac{dx^\mu}{d\tau}, \quad a^\mu = \frac{du^\mu}{d\tau} = \frac{d^2 x^\mu}{d\tau^2}.$$

1.3.1 Conservation of 4-momentum

Total 4-momentum is conserved in a collision: that is,

$$\sum_{A=1}^N p_A^\mu = \sum_{B=1}^{N'} p_B'^\mu \equiv P^\mu \quad (1.12)$$

where the sums on the left and right run over the particles entering and leaving the collision, respectively. The identities of the particles may be changed by the collision; even their number may change. The invariant mass $M \equiv (-P^\mu P_\mu)^{1/2}$ is, *a fortiori*, also conserved. Note the distinction between *conserved*, meaning constant with time in a given reference frame, and *invariant*, meaning independent of reference frame. M^2 is both invariant and conserved, whereas P^μ is conserved but not invariant; also the rest masses of individual particles are always invariant but not always conserved.

⁵Perhaps one should speak of *worldcurves* for accelerated particles, but few do.

1.4 Transformation of electromagnetic fields

These are

$$\begin{aligned}\bar{E}_{\parallel} &= E_{\parallel}, & \bar{\mathbf{E}}_{\perp} &= \gamma(\mathbf{E}_{\perp} + \boldsymbol{\beta} \times \mathbf{B}) \\ \bar{B}_{\parallel} &= B_{\parallel}, & \bar{\mathbf{B}}_{\perp} &= \gamma(\mathbf{B}_{\perp} - \boldsymbol{\beta} \times \mathbf{E})\end{aligned}\quad (1.13)$$

the subscripts indicating components parallel and perpendicular to the motion $\boldsymbol{\beta}$ of frame $\bar{\mathcal{O}}$ with respect to \mathcal{O} . In tensor and matrix form,

$$F^{\bar{\mu}\bar{\nu}} = \Lambda^{\bar{\mu}}_{\mu} \Lambda^{\bar{\nu}}_{\nu} F^{\mu\nu} \quad \Leftrightarrow \quad \bar{\mathbf{F}} = \mathbf{\Lambda} \mathbf{F} \mathbf{\Lambda}^T, \quad (1.14)$$

where the field-strength tensor (or “Maxwell tensor”) is

$$F^{0i} = -F^{i0} = E^i, \quad F^{ij} = -F^{ji} = \epsilon^{ijk} B_k, \quad (1.15)$$

or

$$\mathbf{F} = \begin{pmatrix} 0 & E_x & E_y & E_z \\ -E_x & 0 & B_z & -B_y \\ -E_y & -B_z & 0 & B_x \\ -E_z & B_y & -B_x & 0 \end{pmatrix}. \quad (1.16)$$

It is clear from (1.14) that $F^{\mu\nu} F_{\mu\nu}$ and $\det(\mathbf{F})$ are invariant [for the latter, note eq. (1.8) implies $\det(\mathbf{\Lambda}) = \pm 1$]. Since these evaluate to $2(B^2 - E^2)$ and $(\mathbf{E} \cdot \mathbf{B})^2$,

$$\boxed{E^2 - B^2 \text{ and } \mathbf{E} \cdot \mathbf{B} \text{ are Lorentz invariants.}} \quad (1.17)$$

The equation of motion for a particle of mass m and charge q is

$$\frac{dp^{\mu}}{d\tau} = \frac{q}{m} F^{\mu\nu} p_{\nu}. \quad (1.18a)$$

The spatial components ($\mu \in 1, 2, 3$) of this equation are equivalent to (since $d\tau = \gamma^{-1} dt$)

$$\frac{d\mathbf{p}}{dt} = q \left(\mathbf{E} + \frac{\mathbf{v}}{c} \times \mathbf{B} \right) \quad (1.18b)$$

which is the good old Lorentz-force law. The temporal component ($\mu = 0$) is equivalent to

$$\frac{dE}{dt} = q \mathbf{E} \cdot \mathbf{v}. \quad (1.18c)$$

Eqs. (1.18b) & (1.18c) are Lorentz covariant, meaning that they take the same form in all inertial frames. This is not obvious because they are written in terms of 3-vectors and other quantities that transform messily. On the other hand, eq. (1.18a) is obviously covariant as a consequence of the linear Lorentz transformations associated with the 4-indices and the invariance of q , m , and $d\tau$.

1.5 Phase space

This section will prove that phase-space volumes are Lorentz invariant. The most important application of this fact in astrophysics is to photons, where it leads to the transformation law for specific intensity.

One might think that momentum space should be 4-dimensional in SR. But for particles of a given rest mass (including $m = 0$), the four components of momentum are constrained by

$$p^{\mu} p_{\mu} = -m^2 \quad \Leftrightarrow \quad p^0 = (p^i p_i + m^2)^{1/2}. \quad (1.19)$$

Thus $p^0 = -p_t = -p_0$ is a function of the 3-momentum \mathbf{p} rather than an independent dynamical coordinate. Hence single-particle momentum space is properly 3-dimensional. However, it is not a flat 3-space, but rather a hyperbolic 3-surface (“mass shell”) embedded in a 4-dimensional Lorentzian space, the surface being defined by the constraint (1.19). The metric in this 3-surface is non-Euclidean, with volume element (1.20).

Imagine a group of particles whose spatial positions lie in a small coordinate volume $d^3\mathbf{x} = dx dy dz$ (to avoid confusion between indices and exponents, t, x, y, z is sometimes used instead of x^0, x^1, x^2, x^3), and whose 3-momenta lie in a small phase-space volume $d^3\mathbf{p} = dp_x dp_y dp_z$, as seen in frame \mathcal{O} . In other words, the x coordinates of all these particles lie in the range $[x, x + dx]$, and the corresponding component of their momenta lie in $[p_x, p_x + dp_x]$; and similarly for y, z . The phase space volume they occupy is $d^3\mathbf{x}d^3\mathbf{p}$. In some other frame $\bar{\mathcal{O}}$, they occupy a different coordinate volume $d^3\bar{\mathbf{x}}$ and a different momentum-space volume $d^3\bar{\mathbf{p}}$. Yet it turns out that $d^3\bar{\mathbf{x}}d^3\bar{\mathbf{p}} = d^3\mathbf{x}d^3\mathbf{p}$.

There are many ways to prove phase-space invariance:

*McGlynn’s Proof:*⁶ The Uncertainty Principle is $\Delta p_x \Delta x = h$, and statistical mechanics counts states with $h^{-3}d^3\mathbf{x}d^3\mathbf{p}$. Clearly Planck’s constant h is a law of nature, and therefore (by the first postulate of Special Relativity) independent of inertial reference frame. The UP and the number of states must be invariant. Hence $d^3\mathbf{x}d^3\mathbf{p}$ must be invariant.

McGlynn’s “Proof” shows what is at stake physically, but it seems less than rigorous. Therefore we offer a more mathematical proof, which gives the useful byproducts (1.20) and (1.21).

Since $d^3\mathbf{x}$ and $d^3\mathbf{p}$ are separately invariant under rotations, it is enough to consider their transformations under a boost along the x^1 axis,

$$\begin{aligned} p^{\bar{1}} &= \gamma(p^1 - \beta p^0) \\ p^{\bar{2}} &= p^2 \\ p^{\bar{3}} &= p^3 \end{aligned}$$

which has the jacobian

$$\begin{vmatrix} \partial p^{\bar{1}}/\partial p^1 & \partial p^{\bar{1}}/\partial p^2 & \partial p^{\bar{1}}/\partial p^3 \\ \partial p^{\bar{2}}/\partial p^1 & \partial p^{\bar{2}}/\partial p^2 & \partial p^{\bar{2}}/\partial p^3 \\ \partial p^{\bar{3}}/\partial p^1 & \partial p^{\bar{3}}/\partial p^2 & \partial p^{\bar{3}}/\partial p^3 \end{vmatrix} = \begin{vmatrix} \gamma(1 - \beta \partial p^0/\partial p^1) & -\gamma\beta \partial p^0/\partial p^2 & -\gamma\beta \partial p^0/\partial p^3 \\ 0 & 1 & 0 \\ 0 & 0 & 1 \end{vmatrix}.$$

From (1.19), $\partial p^0/\partial p^i = p_i/p^0$, so the jacobian is $\gamma(p^0 - \beta p^1)/p^0 = p^{\bar{0}}/p^0$, and

$$d^3\bar{\mathbf{p}} = \frac{p^{\bar{0}}}{p^0} d^3\mathbf{p} \Leftrightarrow \boxed{\frac{d^3\mathbf{p}}{p^0} \text{ is invariant.}} \quad (1.20)$$

Next we transform $d^3\mathbf{x}$. Let A, B be two particles from the group that have parallel but distinct trajectories, whose \bar{x} coordinates as a function of time are

$$\begin{aligned} \bar{x}_A(t_A) &= \bar{v} \bar{t}_A + \bar{x}_A(0), \\ \bar{x}_B(t_B) &= \bar{v} \bar{t}_B + \bar{x}_B(0). \end{aligned}$$

Here $\bar{v} \equiv p^{\bar{1}}/p^{\bar{0}}$ is the \bar{x} component of their common velocity. The separation in $\bar{\mathcal{O}}$ is measured at $\bar{t}_A = \bar{t}_B$, hence $\Delta \bar{x} = \bar{x}_A(0) - \bar{x}_B(0)$. We may use the Lorentz transformations to eliminate \bar{t} & \bar{x} in favor of t & x :

$$\gamma(x_A - \beta t_A) = \bar{v} \gamma(t_A - \beta x_A) + \bar{x}_A(0),$$

$$\text{hence} \quad x_A(t_A) = \frac{\beta + \bar{v}}{1 + \beta \bar{v}} t_A + \frac{\bar{x}_A(0)}{\gamma(1 + \beta \bar{v})}.$$

⁶I first heard this argument in my youth from fellow graduate student Thomas McGlynn.

This presumes of course that \mathcal{O} and $\bar{\mathcal{O}}$ have a common origin of coordinates, *i.e.* a unique event E such that $x^\mu(E) = 0 = x^{\bar{\mu}}(E)$ —otherwise there should be additional constant terms here. Note the result for relativistic addition of velocities, $v = (\bar{v} + \beta)/(1 + \bar{v}\beta)$. Writing the corresponding equation for B , setting $t_A = t_B$, and subtracting, we find the separation in frame \mathcal{O} :

$$\Delta x = \frac{\Delta \bar{x}}{\gamma(1 + \beta\bar{v})}.$$

This is not the usual formula for Lorentz contraction unless $\bar{\mathcal{O}}$ is the rest frame so that $\bar{v} = 0$. Since $\bar{v} = p^1/p^0$, however, $\gamma(1 + \beta\bar{v}) = p^0/p^{\bar{0}}$, whence $\Delta \bar{x} = (p^0/p^{\bar{0}})\Delta x$, and therefore (since $\Delta \bar{y} = \Delta y$ & $\Delta \bar{z} = \Delta z$),

$$d^3 \bar{\mathbf{x}} = \frac{p^0}{p^{\bar{0}}} d^3 \mathbf{x} \quad \Leftrightarrow \quad \boxed{p^0 d^3 \mathbf{x} \text{ is invariant.}} \quad (1.21)$$

For particles with rest mass, results (1.20) and (1.21) are more easily derived by invoking a rest frame, but we have been at pains to prove them for photons. Combining the two results, we have the desired result

$$\boxed{d^3 \mathbf{p} d^3 \mathbf{x} \text{ is invariant.}} \quad (1.22)$$

1.6 Specific intensity

Specific intensity is defined so that [see 53, chap. 2]

$$I_\nu d\nu d \cos \theta d\phi dA_\perp dt \quad (1.23)$$

is the energy carried by photons of frequency in the range $(\nu, \nu + d\nu)$, travelling along directions within the solid angle $\sin \theta d\theta d\phi$, across an area dA_\perp normal to their direction, during time dt . The subscript on I_ν , the specific intensity, represents frequency, not a spacetime index—this notation is conventional. Specific intensity is the same as surface brightness provided that the latter is evaluated for a spectral filter of unit frequency width. I_ν is measured in units such as $\text{erg cm}^{-2} \text{s}^{-1} \text{sr}^{-1} \text{Hz}^{-1}$ [sr \equiv steradian] or Jy sr^{-1} [1 Jansky = $10^{-26} \text{W m}^{-2} \text{Hz}^{-1} = 10^{-23} \text{erg cm}^{-2} \text{s}^{-1} \text{Hz}^{-1}$].

If $-\mathbf{n}$ is a unit vector in the direction specified by the polar angles (θ, ϕ) (the sign follows the convention that the telescope points along \mathbf{n}) then the momentum of photons is

$$\mathbf{p} = -\frac{h\nu}{c} \mathbf{n}, \quad \text{whence} \quad d^3 \mathbf{p} = \left(\frac{h}{c}\right)^3 \nu^2 d\nu d \cos \theta d\phi.$$

The spatial volume occupied by these photons is a cylinder of height cdt and base dA_\perp , so $d^3 \mathbf{x} = cdt dA_\perp$, and therefore

$$2 \frac{\nu^2}{c^2} d\nu d \cos \theta d\phi dA_\perp dt = 2 \frac{d^3 \mathbf{p} d^3 \mathbf{x}}{h^3}. \quad (1.24)$$

This is the number of quantum-mechanical states in phase-space volume $d^3 \mathbf{p} d^3 \mathbf{x}$; the factor of 2 accounts for both polarizations. Comparison with (1.23) shows that $c^2 I_\nu / 2\nu^2$ is the energy per mode. (Traditionally, photon quantum states are called “modes”.) Each photon carries energy $h\nu$, so the occupation number, or number of photons per quantum state, is

$$n = \frac{c^2 I_\nu}{2h\nu^3}. \quad (1.25)$$

The result (1.22) means that the modes themselves are invariant. Since all observers will count the same number of photons, n is invariant, and it follows that

$$\boxed{I_\nu / \nu^3 \text{ is Lorentz invariant.}} \quad (1.26)$$

The specific intensity of a blackbody is such an important special case that it has its own symbol $B_\nu(T)$, where T is the temperature:

$$B_\nu(T) = \frac{2h\nu^3}{c^2} \frac{1}{\exp(h\nu/k_B T) - 1}. \quad (1.27)$$

From (1.25), the corresponding occupation number is

$$n_{BB} = \frac{1}{\exp(h\nu/k_B T) - 1}. \quad (1.28)$$

Conversely, if a radiation field has occupation number (1.28), then it is a blackbody and (1.27) is its specific intensity. The prefactor $2h\nu^3/c^2$ is the energy per photon ($h\nu$) times the number of modes per unit frequency per unit volume per unit solid angle ($2\nu^2/c^3$). The full range of solid angles is 4π , so

$$\frac{8\pi\nu^2}{c^3} = \# \text{ modes per unit frequency per unit volume.} \quad (1.29)$$

One important astrophysical application is to the Cosmic Microwave Background (CMB). If we ignore the very slight ($< 10^{-4}$) fluctuations responsible for structure formation, there is a frame (the CMB rest frame) in which I_ν^{CMB} would appear as a perfect blackbody at $T_{\text{CMB}} \approx 2.7\text{K}$. The Sun moves with respect to the CMB rest frame at $\sim 10^{-3}c$, so the CMB does not appear quite isotropic. Let \mathcal{O} and $\bar{\mathcal{O}}$ be the rest frames of the Sun and the CMB, respectively, and as usual, let $\boldsymbol{\beta}$ be the velocity of $\bar{\mathcal{O}}$ (the CMB) with respect to \mathcal{O} (the Sun). A radio telescope looking at CMB radiation in direction \mathbf{n} sees the same occupation number that it would in the CMB frame,

$$n_{BB} = [\exp(h\bar{\nu}/k_B T_{\text{CMB}}) - 1]^{-1}, \quad (1.30)$$

but $\bar{\nu}$ is related to the the frequency ν measured by a telescope looking in direction \mathbf{n} by

$$\bar{\nu} = \gamma(1 + \mathbf{n} \cdot \boldsymbol{\beta})\nu. \quad (1.31)$$

Let us pause to check the signs: if the telescope looks towards the direction of the Sun's motion through the CMB, $-\boldsymbol{\beta}$, then $\nu > \bar{\nu}$, *i.e.* the telescope sees a blueshift.

Let us define

$$\hat{T}_{\text{CMB}}(\mathbf{n}) \equiv \frac{T_{\text{CMB}}}{\gamma(1 + \mathbf{n} \cdot \boldsymbol{\beta})}. \quad (1.32)$$

Then eq. (1.30) can be rewritten as

$$n_{BB} = \left[\exp(h\nu/k_B \hat{T}_{\text{CMB}}) - 1 \right]^{-1}. \quad (1.33)$$

This means that the measured CMB spectrum (*i.e.*, its dependence on measured frequency ν) is exactly thermal but with a temperature (1.32) that depends upon direction. The CMB appears hottest in the direction towards which the Sun moves ($\mathbf{n} \propto -\boldsymbol{\beta}$). Since $\beta \ll 1$, the temperature variation has a simple $\cos\theta$ pattern across the sky (and an amplitude $\Delta T/T \sim 10^{-3}$), so it is called the ‘‘CMB dipole.’’ If the Earth were moving relativistically ($\gamma \gg 1$), the angular dependence would be a little more complicated, but the spectrum would still be exactly thermal in any given direction.

Another very important property of occupation number is that it is constant along light rays in vacuum, even in the presence of a gravitational field, and even in a transparent medium (one that neither absorbs nor emits):

$$\frac{dn}{dt} \equiv \frac{\partial n}{\partial t} + \frac{\partial n}{\partial \mathbf{x}} \cdot \frac{d\mathbf{x}}{dt} + \frac{\partial n}{\partial \mathbf{p}} \cdot \frac{d\mathbf{p}}{dt} = 0. \quad (1.34)$$

Here $n(t, \mathbf{x}, \mathbf{p})$ is a function of phase space position and time, and $[\mathbf{x}(t), \mathbf{p}(t)]$ is the trajectory of a light ray through phase space. This is a relativistic form of Liouville's theorem. It holds also for massive particles, provided that they suffer no collisions or decays, *etc.* We may often replace n with I_ν in (1.34)—but not, for example, when ν changes along the trajectory due to a gravitational redshift.

1.7 Relativistic beaming

Consider a uniformly bright emitting sphere of radius a , *i.e.* at the surface of the sphere, I_ν is independent of the direction in which the photons propagate as long as this makes an angle $\theta < 90^\circ$ with respect to the outward normal to the sphere. A black body has this property, since the Planck function (1.27) is independent of photon direction. The flux density through this surface is, in its rest frame,

$$F_\nu(a) = \int_0^1 d \cos \theta \int_0^{2\pi} d\phi I_\nu \cos \theta = \pi I_\nu. \quad (1.35)$$

The extra factor of $\cos \theta$ occurs because I_ν is defined in terms of area $d^2 A_\perp$ normal to the direction of the ray, which is inclined with respect to the fixed surface of the sphere by angle θ .

In vacuum and ignoring gravitational fields, it follows from (1.34) that specific intensity is constant along rays. Therefore at $r > a$, I_ν has the same value within the solid angle subtended by the emitting sphere, *viz.*

$$0 \leq \theta \leq \sin^{-1}(a/r) \equiv \theta_{\max}$$

and vanishes at larger angles. It follows that the flux at r is

$$F_\nu(r) = 2\pi I_\nu \int_{\cos \theta_{\max}}^1 \cos \theta d \cos \theta = \pi (1 - \cos^2 \theta_{\max}) I_\nu = \frac{\pi a^2}{r^2} I_\nu,$$

in agreement with the inverse-square law.

Now suppose there is a source of radiation with specific intensity $I_{\bar{\nu}}$ in its own rest frame, $\bar{\mathcal{O}}$, and that this frame moves at velocity $\boldsymbol{\beta}$ with respect to the telescope (frame \mathcal{O}). The frequencies transform according to eq. (1.31). Therefore, the telescope sees

$$I_\nu = \left(\frac{\nu}{\bar{\nu}}\right)^3 I_{\bar{\nu}} = [\gamma(1 + \mathbf{n} \cdot \boldsymbol{\beta})]^{-3} I_{\bar{\nu}}. \quad (1.36)$$

The term $\gamma(1 + \mathbf{n} \cdot \boldsymbol{\beta})$ is called Doppler factor in radio astronomy. To make this more concrete, suppose the rest-frame specific intensity is isotropic and follows power law in frequency, $I_{\bar{\nu}} = K \bar{\nu}^{-\alpha}$, and consider a source coming directly towards the observer ($\boldsymbol{\beta} = -|\boldsymbol{\beta}|\mathbf{n}$) at a highly relativistic speed

$$|\boldsymbol{\beta}| \approx 1 - \frac{1}{2\gamma^2} + O(\gamma^{-4}) \quad \gamma \gg 1,$$

so that $1 + \mathbf{n} \cdot \boldsymbol{\beta} \approx 1/(2\gamma^2)$, and therefore

$$I_\nu \approx (2\gamma)^{3+\alpha} K \nu^{-\alpha}$$

On the other hand, suppose the source moves at a small angle θ to the line of sight,

$$1 + \boldsymbol{\beta} \cdot \mathbf{n} = 1 - |\boldsymbol{\beta}| \cos \theta \approx \frac{1}{2} (\gamma^{-2} + \theta^2) + O(\gamma^{-2}\theta^2, \gamma^{-4}, \theta^4).$$

Then

$$I_\nu(\theta) \approx (1 + \gamma^2 \theta^2)^{-3-\alpha} I_\nu(0), \quad (1.37)$$

where $I_\nu(0)$ is the previous result for motion directly toward the observer. Hence the emission is concentrated at angles $\theta \lesssim \gamma^{-1}$ from the direction of motion. This effect is called “beaming.” Notice that the approximation (1.37) depends upon the assumption that the emission in the rest-frame is isotropic, because if the radiation makes angle $\theta \sim \gamma^{-1}$ with respect to β in the observer’s frame, then the corresponding angle in the source frame is $\bar{\theta} \sim \pi/2$.

Symptoms of beaming are evident in radio jets of AGN. A typical spectral index is $\alpha \sim 1.0$. Sometimes one sees two colinear jets, presumably ejected in opposite directions from the nucleus and extending up to ~ 1 Mpc from it. Usually one jet is much brighter (higher I_ν) than the other. Very often only one jet can be seen, yet the counterjet probably exists because one sees radio lobes on both sides of the nucleus, where the jets collide with an intergalactic medium and the bulk velocity becomes nonrelativistic.

1.8 Conservation laws and energy-momentum tensor

You are familiar with the differential form of charge conservation,

$$\frac{\partial \rho}{\partial t} + \nabla \cdot \mathbf{j} = 0, \quad (1.38)$$

in which ρ is the charge per unit volume and \mathbf{j} is the current. Integrated over an arbitrary volume V , eq. (1.38) says that

$$\frac{d}{dt} \int_V \rho d^3 \mathbf{x} = - \oint_{\partial V} \mathbf{j} \cdot d^2 \mathbf{A},$$

where ∂V is the boundary surface of V . Now $j^\mu \equiv (\rho, \mathbf{j})$ is a 4-vector. To see this, note first that $\rho d^3 \mathbf{x} = \bar{\rho} d^3 \bar{\mathbf{x}}$ since charge is Lorentz invariant. Then it follows from eq. (1.21) that $\bar{\rho}/\rho = \bar{p}^0/p^0$, so that $\rho = j^0$ indeed transforms as the 0th component of a 4-vector. Also, $\mathbf{j} = \rho \mathbf{v} = j^0 v^i$, where \mathbf{v} is the drift velocity of the positive charges relative to the negative ones; since v^i clearly transforms in the same way as p^i/p^0 , it follows that j^i transforms as the spatial components of a 4-vector.

It can be shown that $\partial_\mu \equiv \partial/\partial x^\mu$ transforms in the same way as p_μ , viz. $p_{\bar{\mu}} = p_\mu \Lambda^\mu_{\bar{\mu}}$, the inverse of $p^\mu = \Lambda^\mu_{\bar{\mu}} p^{\bar{\mu}}$. Therefore eq. (1.38) becomes

$$\partial_\mu j^\mu = 0 \quad \Leftrightarrow \quad j^\mu_{,\mu} = 0. \quad (1.39)$$

Note the use of commas to represent partial derivatives. Conservation laws for other Lorentz scalars (“scalar” \equiv “invariant”) take the same form. For example, if N^0 represents number of particles per unit volume and \mathbf{N} their flux (number/area/time), then

$$N^\mu_{,\mu} = 0 \quad (1.40)$$

states that these particles are locally conserved: “locally” because particles do not disappear from one spot and reappear at a distance, which would violate (1.40) even if total particle number were constant in some frame.

In continuous systems, such as fluids or electromagnetic fields, it is often necessary to consider energy or momentum per unit volume, energy or momentum flux, and so forth. Since energy and momentum are not scalars, their local conservation law takes a more complicated form than (1.39) and (1.40). The energy-momentum tensor $T^{\mu\nu}$ is defined as follows [see 56, chap. 4]:

$$\begin{aligned} T^{00} &= \text{energy density} \\ T^{0i} &= \text{energy flux in } i^{\text{th}} \text{ direction} \\ T^{i0} &= \text{density of } p^i \\ T^{ij} &= \text{flux of } p^i \text{ in } j^{\text{th}} \text{ direction} \end{aligned} \quad (1.41)$$

Here “X density” means “X per unit volume.” There is a standard argument from nonrelativistic mechanics to show that $T^{ij} = T^{ji}$: otherwise a small cube would experience a torque proportional to its volume times $T^{ij} - T^{ji}$, and the resulting angular acceleration would vary inversely with the square of its linear size. In relativity, the full tensor is symmetric in $c = 1$ units, *i.e.*

$$T^{\mu\nu} = T^{\nu\mu}. \quad (1.42)$$

In general units where $c \neq 1$, energy flux has units (mass)(time) $^{-3}$, whereas momentum density has units (mass)(length) $^{-2}$ (time) $^{-1}$, so that $T^{0j} = c^2 T^{j0}$.

The local conservation law for 4-momentum is

$$T^{\mu\nu}{}_{;\nu} = 0. \quad (1.43)$$

The transformation law is just what the number and placement of the indices indicate, namely

$$T^{\mu\nu} = \Lambda^\mu{}_{\bar{\mu}} \Lambda^\nu{}_{\bar{\nu}} T^{\bar{\mu}\bar{\nu}}. \quad (1.44)$$

The electromagnetic energy-momentum tensor, for example, is

$$T^{\mu\nu} = -\frac{1}{4\pi} \left(F^{\mu\alpha} F_{\alpha}{}^{\nu} + \frac{1}{4} \eta^{\mu\nu} F^{\alpha\beta} F_{\alpha\beta} \right). \quad (1.45)$$

The energy-momentum tensor of a perfect fluid will be seen more often in this course. “Perfect” means that viscosity and thermal conductivity are negligible. Assuming that the flow is slower than light, one can define the fluid 4-velocity $U^\mu(A)$ at every event A within the fluid. The local rest frame $\bar{O}(A)$ is defined by $U^{\bar{\mu}}(A) = (1, 0, 0, 0)$. Let $\rho(A)$ be the local energy density measured in this frame, and $P(A)$ be the pressure. Then

$$T^{\bar{0}\bar{0}} = \rho \quad \text{and} \quad T^{\bar{i}\bar{j}} = P\eta^{\bar{i}\bar{j}}.$$

Do not confuse ρ with charge density or P with momentum. Note that we don’t put overbars on ρ or P : in the context of relativistic fluids, it is implicit that thermodynamic quantities are defined in the local rest frame of each fluid element, hence are Lorentz scalars by fiat.

To comprehend $T^{\bar{i}\bar{j}}$, consider a small area element $d\bar{A}$ in the $\bar{y}\bar{z}$ plane of the local rest frame. The force exerted by the fluid at $\bar{x} < 0$ is $Pd\bar{A}$ in the $+\bar{x}$ direction; in other words, momentum $dp^{\bar{1}} = Pd\bar{A}d\bar{t}$ crosses the element from left to right in time $d\bar{t}$. Thus P represents a flux of \bar{x} -momentum in the $+\bar{x}$ -direction and therefore contributes to $T^{\bar{1}\bar{1}}$. The fluid at $\bar{x} > 0$ exerts an opposing force but the momentum flux is the same, since both $dp^{\bar{1}}$ and the direction of transport change sign. (So you might think $T^{\bar{i}\bar{j}} = 2P$, but that would count the momentum transfer twice.) Since there is no shear viscosity, there is no transfer of \bar{y} or \bar{z} momentum across the element, hence $T^{\bar{2}\bar{1}} = T^{\bar{3}\bar{1}} = 0$. Since the orientation of our element was arbitrary, we conclude that $T^{\bar{i}\bar{j}}$ has the form asserted above.

We can express the rest-frame energy-momentum tensor in a single formula:

$$T^{\bar{\mu}\bar{\nu}} = (\rho + P)U^{\bar{\mu}}U^{\bar{\nu}} + P\eta^{\bar{\mu}\bar{\nu}}.$$

Note how P cancels out of $T^{\bar{0}\bar{0}}$. In view of eq. (1.44) and the fact that $U^{\bar{\mu}}$ transforms as a four-vector, it follows that

$$T^{\mu\nu} = (\rho + P)U^\mu U^\nu + P\eta^{\mu\nu} \quad (1.46)$$

in a general frame. *Note that it is still the rest-frame ρ and P that appear.* In particular, the energy density of a moving but pressureless fluid is $T^{00} = \rho U^0 U^0 = \gamma^2 \rho$.

The relativistic equations of motion for the fluid result from applying eq. (1.43) to (1.46). There must also be an equation of state giving P as a function of ρ and perhaps also of a second thermodynamic variable (temperature or entropy), but the equation of state depends upon the nature of the fluid. The extreme cases—the most important for us—are

- (i) A “cold” fluid $P = 0$, meaning that the mean-square random velocities of the particles in the local fluid rest frame are negligible compared to c^2 (“dust”).
- (ii) A relativistic fluid $P = \rho/3$, meaning that the random velocities in the local rest frame are $\approx c$ and isotropically distributed (“radiation”).

The canonical example of (ii) is a photon gas ($\rho = aT^4$), but it also holds for a plasma if $k_B T \gg mc^2$ and m is the rest mass of the heaviest particles: m_p for a hydrogen plasma, m_e for an electron-positron plasma.

In the rest frame of a shock front with local normal \mathbf{n} ,

$$T^{\mu j} n_j \text{ is continuous across the shock,} \quad (1.47)$$

else eq. (1.43) would imply infinite $T^{\mu 0}$ at the shock. Note that the rest frame of the shock is not the same as the rest frame of the fluid.

We apply these results to a strong relativistic shock advancing into an ordinary (nonrelativistic) interstellar medium [ISM]. The shock moves along the x direction with velocity $-\beta$ as seen in the ISM rest frame, which has preshock $\rho \approx \bar{N}_H m_p c^2$, where $\bar{N}_H \equiv$ number of hydrogen atoms per unit volume, and negligible pressure $P \ll \rho$. In the rest frame of the shock, the ISM approaches with 4-velocity $U^\mu = (\gamma, \gamma\beta, 0, 0)$. With primes marking postshock quantities, the jump conditions are ⁷

$$\begin{aligned} (\rho + P)\gamma^2\beta &= (\rho' + P')\gamma'^2\beta' & [T^{01} = T'^{01}], \\ (\rho + P)\gamma^2\beta^2 + P &= (\rho' + P')\gamma'^2\beta'^2 + P' & [T^{11} = T'^{11}]. \end{aligned} \quad (1.48)$$

In gamma-ray-burst afterglows, pulsar winds, and probably radio jets, $\gamma \gg 1$ so that $\beta \approx 1$. Also $P \approx 0$ and $P' \approx \rho'/3$, *i.e.* the preshock flow is dust and the postshock flow is radiation. The equations above reduce to

$$\frac{4}{3}\rho'\gamma'^2\beta' \approx \rho\gamma^2 \approx \frac{4}{3}\rho'\gamma'^2\beta'^2 + \frac{1}{3}\rho'.$$

These are two relations for the unknowns ρ' , β' given prescribed values for ρ and γ . Eliminating ρ and γ and putting $\gamma'^2 = (1 - \beta'^2)^{-1}$ yields

$$(3\beta' - 1)(\beta' - 1) \approx 0.$$

Choosing the smaller root, we obtain

$$\begin{aligned} \beta' &\approx 1/3, \\ \rho' &\approx 2\gamma^2\rho. \end{aligned} \quad (1.49)$$

So the postshock bulk velocity is subrelativistic in the shock frame, almost all of the preshock energy having been converted to random motions. These results are based solely on conservation laws plus the assumption that the postshock pressure is isotropic. The mechanisms for randomizing the particle velocities in relativistic shocks are a subject for research.

There are only two shock jump conditions (1.48), but you probably recall that there are three (Rankine-Hugoniot) jump conditions for shocks in a nonrelativistic ideal gas. Shouldn't there be a third condition here too? The answer is yes, if there are conserved particles. In that case, the integral form of (1.40) says that

$$N^j n_j \text{ is continuous across the shock} \quad \Leftrightarrow \quad N\gamma\beta = N'\gamma'\beta', \quad (1.50)$$

where N (written without indices) is the number of conserved particles per unit volume in the rest frame of the fluid. The “four-current” associated with these conserved particles can be written

⁷Note that (ρ, P) and (ρ', P') are measured in different frames (the pre- and postshock fluid rest frames, respectively), whereas β and β' are both measured in the shock frame.

$N^\mu = NU^\mu$ if U^μ is the four-velocity of the local fluid rest frame, i.e. the frame in which the 3-velocities or 3-momenta of the local particles average to zero. The equation of state can then be written $P = P(\rho, N)$. Here N plays the role of density in the nonrelativistic case, and $\rho = (mc^2 + \bar{\varepsilon})N$, where m and $\bar{\varepsilon}$ are the rest mass and internal energy *per conserved particle*. We did not need the jump condition (1.50) earlier because P can be expressed in terms of ρ alone in the case of pure “dust” or “radiation” equations of state.

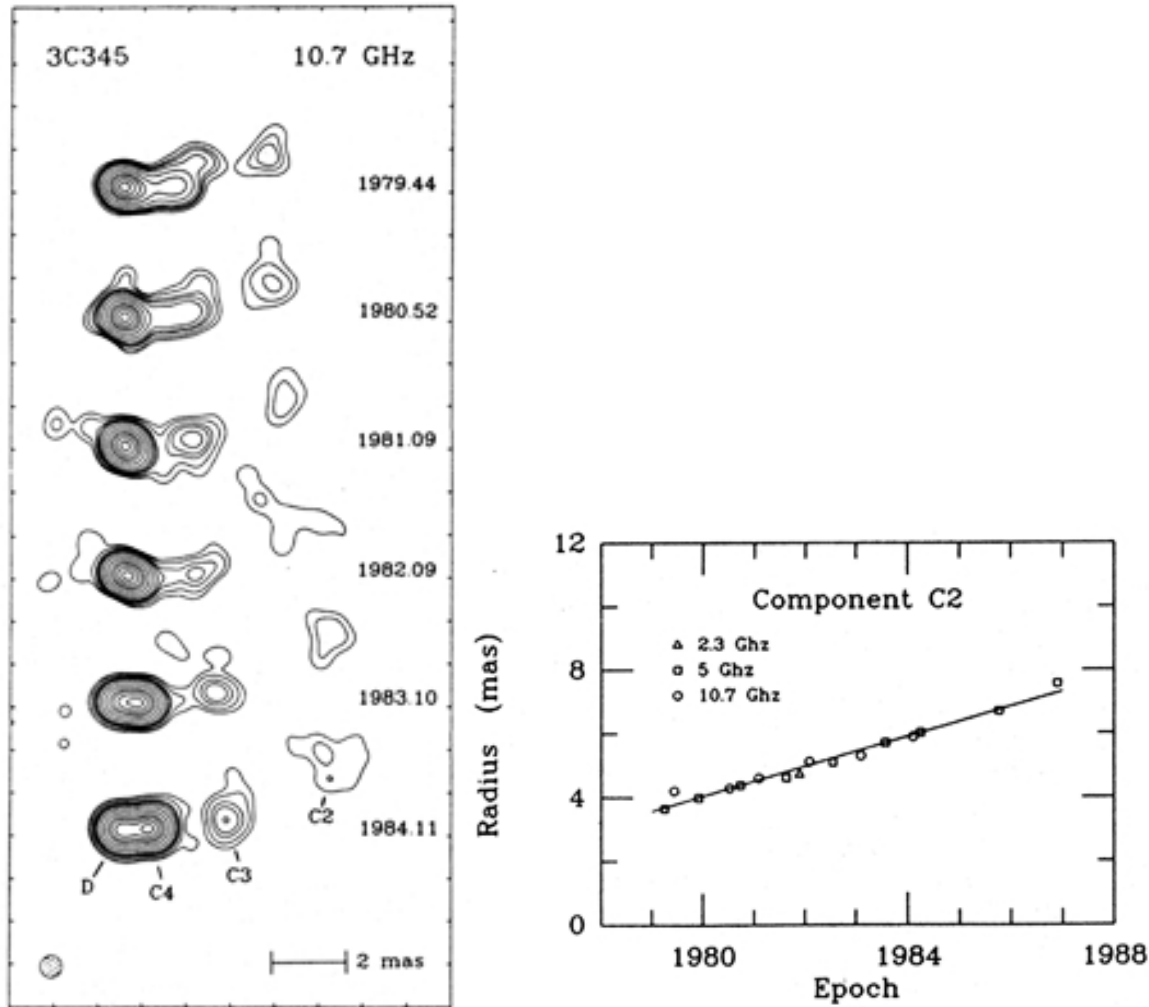


Figure 1.2: VLBI data for 3C 345 from [4]. Redshift of galaxy is $z = 0.595$. *Left panel:* Maps at successive epochs. *Right panel:* Proper motion of C2 fit to $0.47 \text{ milliarcsec yr}^{-1}$.

1.9 Problems for Chapter 1

- VLBI measurements of the radio source 3C 345 show large proper motions. (a) Estimate $v_{\perp, \text{apparent}}$ as described in the text, including the correction for relativistic time dilation; see Figure 1.2 and caption above for parameters.) (b) What is the minimum angle Lorentz factor γ of C2? (c) What are the minimum and maximum possible values for the angle θ between its motion and the line of sight? ($\theta = 0$ corresponds to motion directly toward us.)
- A high-energy cosmic ray proton can produce a pion by collision with a cosmic-microwave-background photon *via* the reaction $p + \gamma \rightarrow p + \pi^0$. Taking 1 GeV and 100 MeV for the rest masses of the proton and pion, respectively, and 10^{-3} eV for the energy of the photon, estimate the *minimum* proton energy at which this reaction occurs. *Hint:* Evaluate the invariant mass of a system consisting of a proton and pion at rest.
- (*) (a) Verify by matrix multiplication that (1.14) is equivalent to (1.13), using the matrices in (1.16) and (1.9) for \mathbf{F} and $\mathbf{\Lambda}$, respectively. (b) Express the components of the electromagnetic

energy-momentum tensor (1.45) in terms of \mathbf{E} and \mathbf{B}

4. Suppose that 4-vector \mathbf{v} is an eigenvector of a Lorentz matrix $\mathbf{\Lambda}$, i.e. $\mathbf{\Lambda}\mathbf{v} = \lambda\mathbf{v}$, where λ is the eigenvalue. **(a)** Show that if λ is real and $|\lambda| \neq 1$, then \mathbf{v} is a null vector: that is, $\mathbf{v}^T \boldsymbol{\eta} \mathbf{v} = 0 = v^\mu v_\mu$. **(b)** Show that every nontrivial boost has exactly two null eigenvectors.
5. (*) A spherical dust grain of radius $r = 1 \mu$ and density 2 g cm^{-2} follows a circular orbit around the Sun at semimajor axis $a = 1 \text{ AU}$. Assume that it perfectly absorbs all solar photons falling upon it and re-radiates them isotropically in its rest frame. What is the nonradial component of the force upon the grain due to this process, and at what rate does the orbit decay? *Hint:* Evaluate the specific intensity at the position of the grain in the solar rest frame, and transform this into the instantaneous rest frame of the grain. You may approximate the Sun as a perfect 5800 K black body.
6. A mass M is fired at Lorentz factor $\Gamma \gg 1$ from a “cannon” directly toward the observer. The muzzle flash reaches the observer at time t_1 in her frame, \mathcal{O} . The mass M later collides perfectly inelastically (i.e., collides and “sticks”) with a second mass m that is initially at rest in \mathcal{O} . Radiation from this collision reaches the observer at time t_2 . **(a)** What is the distance in frame \mathcal{O} travelled by M between the cannon and m ? **(b)** Express as a function of Γ the mass ratio m/M at which half of the initial kinetic energy is dissipated by the collision. (*This isn't a difficult problem, but first-rate high-energy astrophysicists were needed to point out its implications for gamma-ray bursts: (author?) [52].*)
7. An angularly resolved (e.g., with the VLA) radio jet is observed to have a typical synchrotron spectrum $I_\nu = K\nu^{-0.6}$. The counterjet is not observed, with a 1% upper limit on its brightness relative to the observed jet at the same observed frequency. Calculate the minimum Doppler factor of the observed jet on the assumption that the counterjet has an equal speed but oppositely directed velocity.

Problems marked () are extra credit*

Chapter 2

Synchrotron Radiation

Synchrotron radiation is emitted by relativistic charged particles (usually e^\pm) in a magnetic field. It is an efficient radiation mechanism when these ingredients are present, and it is observed in diverse astronomical sources: stellar coronae, the interstellar medium, radio galaxies and radio jets, and probably gamma-ray bursts. Synchrotron radiation is most often observed in the radio, but sometimes in optical, X-ray, and even gamma-ray ranges.

2.1 Radiation from an accelerated charge

This is perhaps worth reviewing briefly, as it demonstrates the power of relativistic notation, in which Maxwell's equations become

$$F^{\mu\nu}{}_{,\nu} = 4\pi J^\mu \quad F_{\mu\nu,\lambda} + F_{\lambda\mu,\nu} + F_{\nu\lambda,\mu} = 0. \quad (2.1)$$

The second equation is satisfied automatically by introducing a vector potential,

$$F_{\mu\nu} = A_{\nu,\mu} - A_{\mu,\nu} \quad (2.2)$$

and the first becomes

$$A^{\nu}{}_{,\nu}{}^{,\mu} - A^{\mu}{}_{,\nu}{}^{,\nu} = 4\pi J^\mu. \quad (2.3)$$

The physical fields $F_{\mu\nu}$ (equivalently \mathbf{E}, \mathbf{B}) are unaffected by the gauge transformation $A_\mu \rightarrow A_\mu - f_{,\mu}$. By choosing the function f appropriately, one can arrange that $A^\mu{}_{,\mu} = 0$ In this Lorentz gauge

$$\square A_\mu = -4\pi J_\mu \quad \text{where} \quad \square \equiv \partial^\nu \partial_\nu = -\frac{\partial^2}{\partial t^2} + \nabla^2. \quad (2.4)$$

The solution of this wave equation is

$$A_\mu(x) = 2 \int \delta[(x-x')^\nu(x-x')_\nu]_{\text{ret}} J_\mu(x') d^4x' = \int \frac{J_\mu(\mathbf{x}', t - |\mathbf{x} - \mathbf{x}'|)}{|\mathbf{x} - \mathbf{x}'|} d^3\mathbf{x}'. \quad (2.5)$$

Notice the elegance and manifest Lorentz-covariance of the first form of the solution. The argument of the delta function vanishes at $t' = t + |\mathbf{x} - \mathbf{x}'|$ and at $t' = t - |\mathbf{x} - \mathbf{x}'|$. The subscript “ret” means that we discard the first root in favor of the second (the retarded time) when using the delta function to perform the dt' integration, which yields the denominator $|\mathbf{x} - \mathbf{x}'|$ according to the standard prescription

$$\int \delta[f(z)] dz = \sum_{f(\zeta)=0} \frac{\delta(z-\zeta)}{|df/dz|}$$

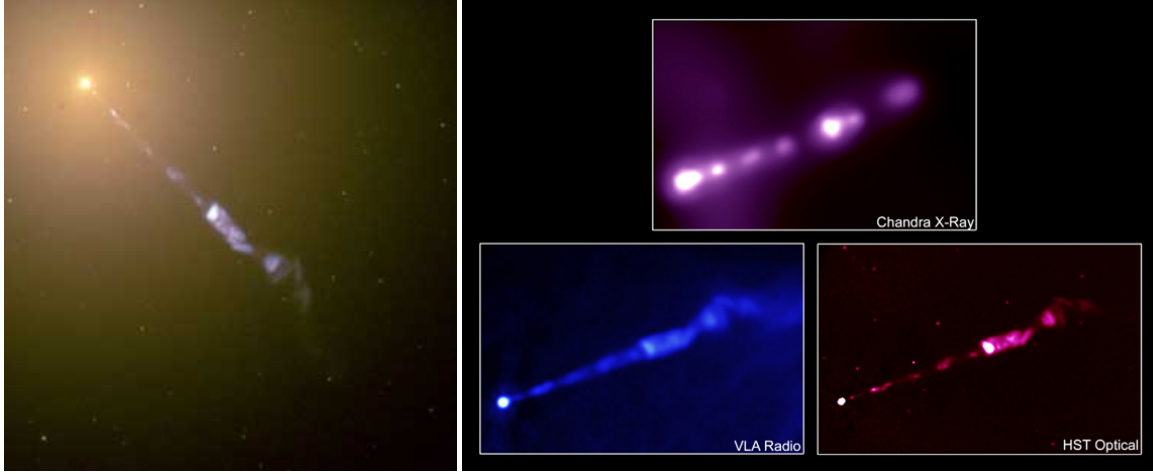


Figure 2.1: The jet of Messier 87, the central galaxy of the Virgo cluster. The emission is probably synchrotron radiation. *Left panel:* Optical view showing jet and host galaxy, *via* Hubble Space Telescope [34]. *Right panel:* Composite view of jet only, at optical, radio, and X-ray wavelengths [35].

The 4-current associated with a point charge q having worldline $X^\mu(\tau)$ and 4-velocity $U^\mu = dX^\mu/d\tau$ is

$$J^\mu(x') = q \int U^\mu(\tau) \delta^4[x' - X(\tau)] d\tau = q U^\mu(t') \frac{\delta^3[\mathbf{x}' - \mathbf{X}(t')]}{U^0(t')}. \quad (2.6)$$

Note that $\delta^4(x) = \delta(t)\delta^3(\mathbf{x})$ is the four-dimensional delta function, which is Lorentz-invariant. Putting the first form of eq. (2.6) into the first form of eq. (2.5) gives the relativistic form of Coulomb's law:

$$A_\mu(t, \mathbf{x}) = \left[q \frac{U_\mu}{U_\nu (X - x)^\nu} \right]_{\text{ret}} = \left[\frac{q}{R} \cdot \frac{U_\mu / U^0}{1 - \mathbf{n} \cdot \mathbf{v}} \right]_{\text{ret}}. \quad (2.7)$$

Here $v^i \equiv U^i/U^0 = dX^i/dt_{\text{ret}}$ is the 3-velocity, $R \equiv |\mathbf{x} - \mathbf{X}|$ is the distance, $t_{\text{ret}} = t - R$, and $\mathbf{n} \equiv (\mathbf{x} - \mathbf{X})/R$ is a unit vector from the charge to the field point.¹

Now $E_i = \partial_i A_0 - \partial_0 A_i$ and $B_i = \epsilon_{ijk} \partial_j A_k$. In the radiation zone (large R), R and \mathbf{n} can be treated as constants except in the argument of U^μ and \mathbf{v} :

$$\frac{d\mathbf{v}}{dt} = \frac{d\mathbf{v}}{dt_{\text{ret}}} \frac{dt_{\text{ret}}}{dt} = \frac{d\mathbf{v}/dt_{\text{ret}}}{1 - \mathbf{n} \cdot \mathbf{v}}.$$

Therefore, writing $\mathbf{a} \equiv d\mathbf{v}/dt_{\text{ret}}$ for the 3-acceleration, one finds after some algebra that

$$\begin{aligned} \mathbf{E} &= \left\{ \frac{q}{R} \frac{\mathbf{n} \times [(\mathbf{n} - \mathbf{v}) \times \mathbf{a}]}{(1 - \mathbf{n} \cdot \mathbf{v})^3} \right\}_{\text{ret}} + O\left(\frac{q}{R^2}\right), \\ \mathbf{B} &= \mathbf{n} \times \mathbf{E} + O\left(\frac{qv}{R^2}\right). \end{aligned} \quad (2.8)$$

For nonrelativistic motion, $\mathbf{v} \ll \mathbf{n}$ and $\mathbf{n} \cdot \mathbf{v} \ll 1$ so that the Poynting flux reduces to

$$\frac{c}{4\pi} \mathbf{E} \times \mathbf{B} \approx \frac{q^2}{4\pi c^3 R^2} |\mathbf{n} \times \mathbf{a}|^2 \mathbf{n},$$

¹Note this is the opposite of our usual sign convention for \mathbf{n} !

in which the factors of c have been restored. Integrating over all directions \mathbf{n} gives the Larmor formula for the total power radiated by the charge:

$$P_L = \frac{2q^2}{3c^3} |\mathbf{a}|^2, \quad (2.9)$$

2.2 Basic principles of synchrotron radiation

Typical Lorentz factors for radiating electrons are $\gamma \gtrsim 10^2$, so the first one or two terms of the expansion for the 3-velocity

$$v \approx 1 - \frac{1}{2\gamma^2} + O(\gamma^{-4})$$

are therefore usually adequate.

2.2.1 Motion of charges in a magnetic field

Let $\mathbf{B} = B\mathbf{e}_z$ be a constant field. Assuming that $\mathbf{E} = 0$,² the equations of motion (1.18a) for a point particle of charge q and mass m become

$$\frac{d}{d\tau} \begin{pmatrix} U^0 \\ U^1 \\ U^2 \\ U^3 \end{pmatrix} = \frac{qB}{mc} \begin{pmatrix} 0 & 0 & 0 & 0 \\ 0 & 0 & 1 & 0 \\ 0 & -1 & 0 & 0 \\ 0 & 0 & 0 & 0 \end{pmatrix} \begin{pmatrix} U^0 \\ U^1 \\ U^2 \\ U^3 \end{pmatrix}.$$

It follows that U^0 and U^3 are constants of the motion, while U^1 and U^2 trace out a circle. The complete solution (up to an arbitrary shift in the origin of τ) is

$$U^\mu = (\gamma, \gamma v_\perp \cos \omega_c \tau, -\gamma v_\perp \sin \omega_c \tau, \gamma v_\parallel), \quad (2.10)$$

in which $\gamma = (1 - v^2)^{-1/2} = \text{constant}$; α , called the pitch angle, is the angle between \mathbf{v} and \mathbf{B} and is constant; and the components of \mathbf{v} parallel and perpendicular to \mathbf{B} are $v_\parallel \equiv v \cos \alpha$, $v_\perp \equiv v \sin \alpha$. This is helical motion around a field line. The cyclotron frequency,

$$\omega_c \equiv \frac{qB}{mc} \approx (2\pi) \times 2.8 \left(\frac{B}{\text{Gauss}} \right) \text{ MHz}, \quad (2.11)$$

in which the numerical value is for a positron. One writes $\nu_c \equiv \omega_c/2\pi$ for the frequency in cycles rather than radians per unit time. Although the orbital frequency in the particle rest frame is always ω_c , the frequency in the “lab” frame where the four velocity is (2.10) is

$$\gamma^{-1} \omega_c \equiv \omega_B, \quad (2.12)$$

since $dt = \gamma d\tau$.

2.2.2 Total emitted power

Although nonrelativistic, the Larmor formula (2.9) is exact in the instantaneous rest frame of an accelerated charge. In the rest frame \bar{O} , $U^0 \equiv 1$, $a^0 = 0$, and so $\mathbf{a} \cdot \mathbf{a} = a_\mu a^\mu$. The latter is Lorentz invariant, so we can evaluate it in the lab frame using (2.10):

$$\begin{aligned} a^\mu &\equiv \frac{dU^\mu}{d\tau} = -\gamma v_\perp \omega_c (0, \sin \omega_c \tau, \cos \omega_c \tau, 0), \\ a^\mu a_\mu &= \gamma^2 v_\perp^2 \omega_c^2 = \omega_c^2 (\gamma^2 - 1) \sin^2 \alpha. \end{aligned} \quad (2.13)$$

²Recall that if $\mathbf{E} \cdot \mathbf{B} = 0$, then there is a frame in which $\mathbf{E} = 0$. When $\mathbf{E} \cdot \mathbf{B} \neq 0$, charges can be accelerated to very large energies along field lines; such voltages tend to be “shorted out” if there is free charge.

Hence the radiated power in \bar{O} is

$$\left(\frac{d\bar{E}}{d\tau}\right)_{\text{sync}} = \frac{2q^2}{3c}\omega_c^2(\gamma^2 - 1)\sin^2\alpha. \quad (2.14)$$

The dipole radiation carries no net momentum in \bar{O} . Therefore, if $\Delta\bar{E}$ is the change in energy in the rest frame during a small interval of proper time $\Delta\tau$, the corresponding change in the lab frame O is

$$\Delta E = \gamma(\Delta\bar{E} + \mathbf{v} \cdot \Delta\bar{\mathbf{p}}) = \gamma\Delta\bar{E} = \gamma\Delta\tau \frac{d\bar{E}}{d\tau} = \Delta t \frac{d\bar{E}}{d\tau}$$

Under these circumstances, the power is invariant:

$$\frac{dE}{dt} = \frac{d\bar{E}}{d\tau} \quad \text{if} \quad \frac{d\bar{\mathbf{p}}}{d\tau} = 0. \quad (2.15)$$

Therefore, (2.14) is also the total radiated power in the lab frame.

For an isotropic velocity distribution, $\langle \sin^2\alpha \rangle = 2/3$, so with $q \rightarrow e$, $m \rightarrow m_e$, and $q^2\omega_c^2 \rightarrow r_e^2 B^2 = 3\sigma_T B^2/8\pi$, the average synchrotron power per electron or positron is

$$\langle P_{\text{sync}} \rangle_\alpha = \frac{4}{3}(\gamma^2 - 1)c\sigma_T \frac{B^2}{8\pi}. \quad (2.16)$$

2.2.3 Characteristic emission frequency

Although the lab-frame orbital frequency $\omega_B = \omega_c/\gamma$, we will see that the lab-frame emission spectrum peaks at $\sim \gamma^2\omega_c$, *i.e.* a factor γ^3 larger than the orbital frequency.

Argument #1: The emitted radiation, although axisymmetric around \mathbf{a} in the instantaneous rest frame, is beamed into a cone of half-angle $\Delta\theta \sim \gamma^{-1}$ centered on the direction of motion as seen in the lab. This beam sweeps over the observer in a time $\Delta t_{\text{ret}} \sim \Delta\theta/\omega_B \sim \omega_c^{-1}$. However, because the time t at which the radiation is received and the time t_{ret} at which it is emitted are related by

$$\frac{dt}{dt_{\text{ret}}} = 1 - \mathbf{n} \cdot \mathbf{v}, \quad (2.17)$$

where \mathbf{n} is a unit vector from the source to the observer, and since beam is centered on $\mathbf{n} \parallel \mathbf{v}$, it follows that

$$\Delta t \approx (1 - v)\Delta t_{\text{ret}} \approx \frac{\Delta t_{\text{ret}}}{2\gamma^2} \approx \frac{1}{\gamma^2\omega_c}.$$

Finally, the Fourier transform of the radiated electric field has a characteristic width $\Delta\omega \sim (\Delta t)^{-1} \sim \gamma^2\omega_c$.

Argument #2: In its rest frame, the electron sees a constant magnetic field $\bar{\mathbf{B}} = \gamma\mathbf{B}$, and an electric field $\gamma\mathbf{v} \times \mathbf{B}$ that is approximately equal to $\bar{\mathbf{B}}$ in magnitude but perpendicular in direction, and rotating about \mathbf{e}_z at angular frequency $\bar{\Omega}$. Shaken by this electric field, the electron radiates photons of the same rest-frame frequency $\bar{\Omega}$. Now one might suppose that $\bar{\Omega} = \omega_c$, the rest-frame orbital frequency. But in fact $\bar{\Omega} \sim \gamma\omega_c$ because of the phenomenon of Thomas precession: that is, a perfect gyroscope used by an accelerated observer to define a fixed spatial direction will precess as seen by an inertial observer. In the restricted form needed here, this result can be derived by projecting $da^\mu/d\tau$ onto a unit spacelike vector m^μ in the direction of motion:

$$\bar{\Omega} \equiv -m_\mu \frac{da^\mu}{d\tau} \bigg/ \sqrt{a^\nu a_\nu}. \quad (2.18)$$

For nonrelativistic motion, the spatial parts of m^μ would be $\mathbf{m} = \mathbf{v}/v$, so that eq. (2.18) would reduce to

$$-\mathbf{m} \cdot \frac{d\mathbf{a}}{dt} |\mathbf{a}|^{-1} = -\frac{\mathbf{v}}{v} \cdot \frac{\omega_c \mathbf{a} \times \mathbf{e}_z}{|\mathbf{a}|} = \omega_c \frac{\mathbf{e}_z \cdot (\mathbf{a} \times \mathbf{v})}{|\mathbf{a}||\mathbf{v}|} = \omega_c.$$

In the relativistic case, we can evaluate the invariant expression (2.18) in the lab frame. The spatial components of m^μ should still be parallel to \mathbf{v} , but $m_\mu U^\mu = 0$ so that $m^{\bar{0}} \rightarrow 0$ in the rest frame. The unique 4-vector satisfying these conditions and the normalization $m_\mu m^\mu = 1$ has the lab-frame components $m^\mu = (\gamma v, \gamma \mathbf{v}/v)$. From eq. (2.13), $\sqrt{a^\nu a_\nu} = \gamma \omega_c v_\perp$ and

$$\frac{da^\mu}{d\tau} = (0, -\gamma \omega_c^2 \mathbf{v}_\perp) .$$

Hence $m_\mu da^\mu/d\tau = \gamma^2 \omega_c^2 v_\perp^2/v$, and finally

$$\bar{\Omega} = \gamma \omega_c v_\perp/v = \gamma \omega_c \sin \alpha \quad \text{Q.E.D.} \quad (2.19)$$

Since for $\gamma \gg 1$, this is much larger than the orbital frequency ω_c , the frequency of the emitted radiation in the instantaneous rest frame is reasonably well-defined at $\bar{\Omega}$. The frequency of these photons in the lab frame depends upon their direction of emission but is typically $\gamma \bar{\Omega} = \gamma^2 \omega_c \sin \alpha$, as claimed above. Notice that the photons are elliptically polarized.

Although the derivation of Thomas precession is correct, argument #2, if pursued further, does not lead to the exact lab-frame emission spectrum. So the physical reasoning cannot be entirely correct. Perhaps the trouble is that there is no such thing as a well-defined instantaneous frequency in an accelerated reference frame.

2.3 Synchrotron spectrum

The correct way to derive the spectrum is *via* retarded potentials in an inertial (lab) frame. The spatial part of the vector potential (2.7) emitted by a single charge is (in this section $\boldsymbol{\beta} \equiv \mathbf{v}/c$ because we want to keep track of the factors of c):

$$\mathbf{A}(t, \mathbf{x}) = \frac{q}{R} \left[\frac{\boldsymbol{\beta}}{1 - \mathbf{n} \cdot \boldsymbol{\beta}} \right]_{\text{ret}} . \quad (2.20)$$

Here (t, \mathbf{x}) are the coordinates of the astronomer. The origin of coordinates is somewhere in the radiating region, so that $R \approx |\mathbf{x}|$ and $\mathbf{n} \approx \mathbf{x}/R$ can be treated as constants except in the argument of $\boldsymbol{\beta}$, which is $t_{\text{ret}} = t - R$. Consequently, spatial derivatives can be replaced by temporal ones:

$$\nabla \mathbf{A} = -\mathbf{n} \frac{\partial}{\partial t} \mathbf{A} + O(R^{-2}). \quad (2.21)$$

Since the motion is periodic, \mathbf{A} can be expanded as a Fourier series:

$$\mathbf{A}_k(\mathbf{x}) \equiv \frac{\omega_B}{2\pi} \int_{-\pi/\omega_B}^{\pi/\omega_B} dt \mathbf{A}(t, \mathbf{x}) e^{ik\omega_B t}, \quad \mathbf{A}(t, \mathbf{x}) = \sum_{k=-\infty}^{\infty} \mathbf{A}_k(\mathbf{x}) e^{-ik\omega_B t} .$$

In view of (2.21), the corresponding expansion for the radiated magnetic field is

$$\mathbf{B}_k(\mathbf{x}) = \nabla \times \mathbf{A}_k(\mathbf{x}) = \frac{ik\omega_B}{c} \mathbf{n} \times \mathbf{A}_k(\mathbf{x}) . \quad (2.22)$$

Using (2.17) & (2.20),

$$\mathbf{B}_k(\mathbf{x}) = \frac{ik\omega_B^2 q}{2\pi c R} \int_{-\pi/\omega_B}^{\pi/\omega_B} dt_{\text{ret}} \mathbf{n} \times \boldsymbol{\beta}(t_{\text{ret}}) \exp[ik\omega_B t(t_{\text{ret}})] . \quad (2.23)$$

Since the full treatment from this point is rather involved, let's consider the special case that $\sin \alpha = 1$ (*i.e.* $\beta_{\parallel} = 0$), and furthermore, that the observer is in the plane of motion at a great distance along the x axis. Then $\mathbf{n} \rightarrow \mathbf{e}_x$. Putting $\phi \equiv \omega_B t_{\text{ret}}$, we have $1 - \mathbf{n} \cdot \boldsymbol{\beta} \rightarrow 1 - \beta \cos \phi$, and

$$t \rightarrow \omega_B^{-1} (\phi - \beta \sin \phi) + \frac{R}{c},$$

ignoring an unimportant constant of integration. Also, $\mathbf{n} \times \boldsymbol{\beta} \rightarrow \mathbf{e}_z \beta \sin \phi$, so that eq. (2.23) reduces to

$$\mathbf{B}_k(\mathbf{x}) = \mathbf{e}_z \frac{iq\omega_B\beta}{cR} e^{ik\omega_B R/c} k \int_{-\pi}^{\pi} \frac{d\phi}{2\pi} \sin \phi \exp [ik(\phi - \beta \sin \phi)] \quad (2.24)$$

$$\begin{aligned} &= \left(-\mathbf{e}_z \frac{q\omega_B\beta}{cR} e^{ik\omega_B R/c} \right) \frac{\partial}{\partial \beta} \int_{-\pi}^{\pi} \frac{d\phi}{2\pi} \exp [ik(\phi - \beta \sin \phi)] \\ &= \left(-\mathbf{e}_z \frac{q\omega_B\beta}{cR} e^{ik\omega_B R/c} \right) k J'_k(k\beta). \end{aligned} \quad (2.25)$$

We have used the integral representation of $J_k(z)$, the Bessel function of order k [1, §9], and $J'_k(z)$ is its derivative.

Up to this point we have not made any mathematical approximations, so the result applies to any value of β . Suppose $\beta \ll 1$. The function $J_k(z) \approx (z/2)^k/k!$ when $z \ll k$, so

$$|\mathbf{B}_{\pm 1}| \approx \frac{q\beta\omega_c}{2cR} \quad (\beta \ll 1),$$

and the higher harmonics are smaller by factors $\sim \beta^k$. This is cyclotron radiation: the radiated fields are almost monochromatic at $\omega = \omega_c$ independently of particle energy.

In the ultrarelativistic limit $\beta \rightarrow 1$, it turns out that the most important harmonics are $k \sim \gamma^3$. The behaviour of $k J'_k(k\beta)$ at large k is not immediately obvious, since k appears in three places. Using asymptotic expansions from [1]³ and $\beta \approx 1 - \gamma^{-2}/2$, it can be shown that

$$\mathbf{B}_k \approx \left(-i\mathbf{e}_z \frac{\sqrt{3}}{\pi} \frac{q\omega_c}{cR} e^{ik\omega_B R/c} \right) \eta K_{2/3}(\eta), \quad \eta \equiv \frac{k}{3\gamma^3}. \quad (2.26)$$

where $K_{2/3}(z)$ is a modified Bessel function of the second kind:

$$\eta K_{2/3}(\eta) \approx \begin{cases} \Gamma\left(\frac{2}{3}\right) (\eta/2)^{1/3} & \eta \ll 1 \\ e^{-\eta} (\eta\pi/2)^{1/2} & \eta \gg 1 \end{cases}$$

This function is of order unity when $\eta \sim O(1)$. Thus most important harmonics are $k \sim \gamma^3$, corresponding to frequencies $\omega \sim \gamma^2\omega_c \sim \gamma^3\omega_B$.

In principle, η is a discrete variable because it is defined in terms of k by (2.26). However, in a realistic case, the electrons will have a range of Lorentz factors and hence different spacings $\Delta\eta = (3\gamma^3)^{-1}$ between their harmonics. The effect is to smear the individual harmonics into a continuous spectrum.

The time-averaged energy flux received by this observer in the orbital plane of the radiating charge is

$$\frac{c}{4\pi} \sum_{k=-\infty}^{\infty} |\mathbf{B}_k|^2 \approx \gamma^3 \frac{9}{\pi^2} \left(\frac{q\omega_c}{cR} \right)^2 \int_0^{\infty} \eta^2 K_{2/3}^2(\eta) d\eta.$$

³*op cit*, §9.3.4 & §10.4.16

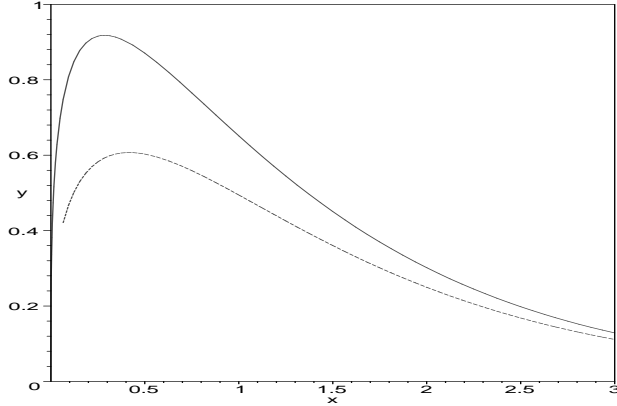


Figure 2.2: Synchrotron functions $F(x)$ (solid) and $G(x)$ (dashed).

The summation over k has been approximated by an integration, and a factor $3\gamma^3$ has been inserted for the Jacobian $dk/d\eta$. The final integral ≈ 0.4798 . The flux above has one factor of γ more than the total power per electron (2.16), because it applies to observers who lie within the solid angle swept out by the emitted beam. Observers more than $\Delta\theta \approx \gamma^{-1}$ above or below the xy plane receive negligible flux from this charge. So the power integrated over solid angle is $\propto \gamma^2$ in agreement with (2.16).

In the general case that the pitch angle $\alpha \neq \pi/2$ and the observer lies in some direction $\theta \neq \alpha$, the calculation proceeds along similar lines, but there are a few changes and complications:

- The minimum value of $dt/dt_{\text{ret}} \rightarrow \cos(\theta - \alpha)/2\gamma^2$.
- There are two linear polarizations of generally comparable strength: the perpendicular polarization (as in the special case above) where the radiated electric field lies along $\mathbf{n} \times \mathbf{B}_0$, and the parallel polarization, where it lies along $\mathbf{n} \times (\mathbf{n} \times \mathbf{B}_0)$.
- The definition of η changes to $\omega/(3\gamma^3\omega_B \sin \alpha)$.

The power per unit frequency in these two polarizations, after integration over solid angle, can be shown to be

$$P_{\perp}(\omega) = \frac{\sqrt{3}q^2\omega_c \sin \alpha}{2c} [F(x) + G(x)], \quad (2.27)$$

$$P_{\parallel}(\omega) = \frac{\sqrt{3}q^2\omega_c \sin \alpha}{2c} [F(x) - G(x)], \quad (2.28)$$

where

$$x \equiv \frac{2\omega}{3\gamma^2\omega_c \sin \alpha} \quad (= 2\eta), \quad (2.29)$$

$$F(x) \equiv x \int_x^{\infty} K_{5/3}(x') dx' \quad (2.30)$$

$$G(x) \equiv xK_{2/3}(x). \quad (2.31)$$

These formulae (and somewhat more detail on their derivation) can be found in [53]. But when integrating over frequency, we always associate a factor $(2\pi)^{-1}$ with $d\omega$, so that

$$\frac{d\omega}{2\pi} = d\nu \quad (\text{since } \nu \equiv \omega/2\pi),$$

and therefore our formulae (2.27)-(2.28) are larger than theirs by $\times 2\pi$. The function $F(x)$, which determines the total power summed over polarizations, has the asymptotic forms

$$F(x) \approx \begin{cases} 4.225 x^{1/3} & x \ll 1, \\ 1.253 x^{1/2} e^{-x} & x \gg 1, \end{cases} \quad (2.32)$$

and its maximum is $F(0.2858) \approx 0.9180$.

Relativistic particles are often accelerated to a power-law distribution of energies, so that the number of electrons plus positrons with energies in the range $(E, E + dE)$ per unit volume is

$$\mathcal{N}(\gamma)d\gamma = K \gamma^{-p} d\gamma \quad \gamma_{\min} \leq \gamma \leq \gamma_{\max}. \quad (2.33)$$

Typically, $p \approx 2$ for either of two reasons:

1. First-order Fermi acceleration⁴ at collisionless shock fronts is probably one of the main ways that relativistic particles are produced, and simple models of the process predict $p \approx 2$.
2. If by any means electrons are injected at a constant rate at some high energy E_1 and corresponding Lorentz factor $\gamma_1 = E_1/m_e c^2$, and if thereafter they lose energy mainly by synchrotron and/or inverse Compton emission without further acceleration, then a $p = 2$ distribution results.

$p = 2$ implies equal energy densities in equal intervals of $\log E$. The total synchrotron emissivity (power per unit volume per unit frequency) due to the distribution (2.33) is

$$\varepsilon(\nu) = \frac{\sqrt{3} K q^2 \omega_c}{c} \frac{\Gamma\left(\frac{p+5}{4}\right)^2 \Gamma\left(\frac{3p-1}{12}\right) \Gamma\left(\frac{3p+19}{12}\right)}{(p+1)\Gamma\left(\frac{p+5}{2}\right)} \left(\frac{\nu}{3\nu_c}\right)^{(1-p)/2}, \quad (2.34)$$

which we have chosen to write in terms of $\nu \equiv \omega/2\pi$ and $\nu_c \equiv \omega_c/2\pi$, and we have assumed an isotropic distribution of pitch angles. This spectrum applies when

$$\gamma_{\min}^2 \omega_c \lesssim 2\pi\nu \lesssim \gamma_{\max}^2 \omega_c. \quad (2.35)$$

The degree of linear polarization is measured by

$$\Pi \equiv \frac{P_{\perp} - P_{\parallel}}{P_{\perp} + P_{\parallel}} = \frac{G}{F}. \quad (2.36)$$

For a power-law electron distribution (2.33), it can be shown that $\Pi \rightarrow (p+1)/(p+\frac{7}{3})$ [53]. The observed polarization is usually smaller, because \mathbf{B} varies in direction along the line of sight through the source. Nevertheless, high linear polarization is a telltale sign of synchrotron emission.

⁴Briefly, energetic particles repeatedly cross the shock front, deflected and scattered by magnetic fields carried in the plasma; the average increase in energy per crossing is $\Delta E/E \sim |\beta_s|/(1-\beta_s^2)$, where $c\beta_s$ is the shock velocity relative to the pre-shock plasma [8].

2.3.1 Cooling break

Sometimes it is appropriate to describe the energy distribution of the electrons as they are injected—i.e., immediately after they are accelerated to their relativistic velocities—rather than as they are found later, possibly after having suffered energy losses. Thus let $\dot{\mathcal{N}}(\gamma)d\gamma$ be the number of electrons accelerated to Lorentz factors in the interval $(\gamma, \gamma+d\gamma)$ per unit volume per unit time. To the extent that subsequent energy losses can be neglected, the energy distribution $\mathcal{N}(\gamma)$ is simply the integral of the injection spectrum $\dot{\mathcal{N}}(\gamma)$ over time, so that if the latter is a power-law $\propto \gamma^{-p}$, then so is the former, and the emissivity $\varepsilon_\nu \propto \nu^{(1-p)/\nu}$ as we have seen.

At sufficiently large Lorentz factor, however, the energy losses due to synchrotron emission itself cannot be ignored. One can define a cooling time as a function of γ and B by $|d \ln \gamma / dt|^{-1} \equiv \gamma m_e c^2 / P_{\text{sync}}(\gamma)$, in which $P_{\text{sync}}(\gamma)$ is the radiated power per electron [eq. (2.16)]. Thus $|d \ln \gamma / dt|^{-1} \approx \gamma^{-1} (6\pi m_e c^2 / c\sigma_T B^2)$. Above some value γ_b , the cooling time is less than age of the source, i.e. the effective duration over which the injection process has been acting. We may regard the electron distribution as being in steady state for $\gamma \gg \gamma_b$, meaning that $\partial \mathcal{N} / \partial t = 0$, whereas \mathcal{N} is still growing with time at $\gamma \ll \gamma_b$. In particular, if the injection spectrum is itself steady, then

$$\mathcal{N}(\gamma) \left| \frac{d\gamma}{dt} \right| = \int_{\gamma}^{\infty} \dot{\mathcal{N}}(\bar{\gamma}) d\bar{\gamma} \quad \text{if } \gamma \gg \gamma_b, \quad (2.37)$$

because all the electrons injected above γ have had time to cool past γ to still lower Lorentz factors. Consequently, if $\dot{\mathcal{N}} \propto \gamma^{-p}$, then

$$\mathcal{N}(\gamma) \propto \begin{cases} \gamma^{-p} & \gamma \ll \gamma_b, \\ \gamma^{-p-1} & \gamma \gg \gamma_b, \end{cases}$$

and therefore

$$\varepsilon_\nu \propto \begin{cases} \nu^{(1-p)/2} & \nu \ll \nu_b, \\ \nu^{-p/2} & \nu \gg \nu_b, \end{cases} \quad (2.38)$$

where $\nu_b \approx \gamma_b^2 \nu_c$ is the synchrotron frequency corresponding to γ_b . The frequency ν_b is called the *cooling break*, because the spectrum (2.38) is a broken power law. When ν_b can be identified in the observed spectrum, it constrains a combination of the the magnetic field and source age.

2.4 Synchrotron self-absorption

One normally assumes that the emission is incoherent, meaning that the relative phase of the waves emitted by different electrons is randomly determined. In such a case, the power emitted by N electrons is just N times the power emitted by one, and their spectra simply add. In an artificial source such as a radio antenna, and in some natural sources (*e.g.* pulsars), electrons accelerate in phase, so that their emitted *amplitudes* add coherently and the total power is N^2 times that of a single charge.

Emission by a thermal distribution is incoherent almost by definition. Imagine a perfectly conducting box filled with relativistic but thermally-distributed electrons and positrons and magnetic field. Suppose that emission processes other than synchrotron can be neglected. We still expect that the radiation field should eventually reach thermal equilibrium with the charges. But equilibrium is impossible under emission alone; there must be an accompanying absorption related to the inverse of the emission process.

For a general (not necessarily thermal) incoherent distribution of electrons and photons, let $\Gamma(\mathbf{p}, \mathbf{k})$ represent the transition rate for the emission of a synchrotron photon of momentum $\hbar \mathbf{k}$ by

an isolated electron of initial momentum \mathbf{p} and final momentum $\mathbf{p}' = \mathbf{p} - \hbar\mathbf{k}$. In the presence of a pre-existing radiation field, the actual rate of this process is

$$\Gamma(\mathbf{p}, \mathbf{k}) n_e(\mathbf{p}) [1 + n_{\text{ph}}(\mathbf{k})] ,$$

where n_e and n_{ph} are mode occupation numbers, and the presence of the latter reflects boson statistics—or equivalently, stimulated emission. We assume that the electrons are completely non-degenerate (meaning that $n_e(\mathbf{p}) \ll 1$), else the above should be multiplied by $[1 - n_e(\mathbf{p}')]$ since the electrons obey Fermi statistics. The rate of the inverse process—absorption of a photon—is

$$\Gamma(\mathbf{p}, \mathbf{k}) n_e(\mathbf{p}') n_{\text{ph}}(\mathbf{k}) .$$

The transition rate Γ has the same value as before because of microscopic time-reversibility. There is no final-state factor because there is no photon in the final state. The net rate of change of $n_{\text{ph}}(\mathbf{k})$ is therefore

$$\begin{aligned} \frac{dn_{\text{ph}}}{dt}(\mathbf{k}) &= \sum_{\mathbf{p}} \Gamma(\mathbf{p}, \mathbf{k}) \{n_e(\mathbf{p}) [1 + n_{\text{ph}}(\mathbf{k})] - n_e(\mathbf{p} - \hbar\mathbf{k}) n_{\text{ph}}(\mathbf{k})\} \\ &= \underbrace{\sum_{\mathbf{p}} \Gamma(\mathbf{p}, \mathbf{k}) n_e(\mathbf{p})}_{\text{classical emission rate}} - \underbrace{\left\{ \sum_{\mathbf{p}} \Gamma(\mathbf{p}, \mathbf{k}) [n_e(\mathbf{p} - \hbar\mathbf{k}) - n_e(\mathbf{p})] \right\}}_{\text{classical absorption rate}} n_{\text{ph}}(\mathbf{k}) . \end{aligned}$$

Notice that the classical absorption rate, the sum of all terms $\propto n_{\text{ph}}(\mathbf{k})$, is the difference between true quantum-mechanical absorption and stimulated emission. The term in curly braces is the absorption coefficient per unit time. One normally deals with the absorption rate per unit length, α_ν . For an isotropic distribution, n_e can be considered a function of energy rather than momentum:

$$\alpha_\nu = c^{-1} \sum_{\mathbf{p}} \Gamma(\mathbf{p}, \mathbf{k}) [n_e(E - h\nu) - n_e(E)] , \quad E \equiv \sqrt{\mathbf{p}^2 + m_e^2}, \quad \nu \equiv c|\mathbf{k}|/2\pi . \quad (2.39)$$

The synchrotron power per electron is related to $\Gamma(\mathbf{p}, \mathbf{k})$ by the number of states available to the photon:

$$P(\nu, E) = h\nu \times \underbrace{\int d\Omega_{\mathbf{k}} V \frac{2\nu^2}{c^3}}_{d(\#\text{states})/d\nu} \Gamma(\mathbf{p}, \mathbf{k}) .$$

where V is the total volume of the system, which will cancel out later. So

$$\int d\Omega_{\mathbf{k}} \alpha_\nu = \frac{c^2}{2h\nu^3 V} \sum_{\mathbf{p}} P(\nu, E) [n_e(E - h\nu) - n_e(E)]$$

Because of isotropy, α_ν does not depend on the direction of \mathbf{k} , so the integration simply multiplies α_ν by 4π . Next, we approximate the sum over electron states by an integral:

$$\sum_{\mathbf{p}} \approx V \int \frac{d^3\mathbf{p}}{h^3} \rightarrow \frac{4\pi V}{(hc)^3} \int E^2 dE \quad (E \gg m_e c^2) ,$$

in which isotropy has been invoked once again, and $|\mathbf{p}| \approx E/c$. So

$$4\pi\alpha_\nu = \frac{c^2}{2h\nu^3} \int dE \frac{4\pi E^2}{(hc)^3} [n_e(E - h\nu) - n_e(E)] P(\nu, E);$$

V has cancelled out, as promised. Introducing the number density of electrons per unit energy,

$$\mathcal{N}(E) = \frac{4\pi E^2}{(hc)^3} n_e(E) ,$$

we have

$$\alpha_\nu = \frac{c^2}{8\pi h\nu^3} \int dE E^2 \left[\frac{\mathcal{N}(E - h\nu)}{(E - h\nu)^2} - \frac{\mathcal{N}(E)}{E^2} \right] P(\nu, E) .$$

Recall that we are generally dealing with ultrarelativistic electrons and radio photons, so that $h\nu \ll E$. It makes sense to expand the contents of [...] to first order in $h\nu$, yielding

$$\alpha_\nu = -\frac{c^2}{8\pi\nu^2} \int dE P(\nu, E) E^2 \frac{d}{dE} \left[\frac{\mathcal{N}(E)}{E^2} \right] . \quad (2.40)$$

Notice that Planck's constant has disappeared from this final form, which indicates that the result could have been obtained classically.

Let us evaluate (2.40) for a power-law distribution of electrons (2.33). First, taking a single pitch angle (absorption coefficients due to multiple pitch angles simply add),

$$\begin{aligned} P(\nu, E) &= P_0 F\left(\frac{2\nu}{\gamma^2\nu_\alpha}\right), \\ P_0 &\equiv \frac{\sqrt{3}q^2\omega_c \sin \alpha}{c}, \quad \nu_\alpha = \frac{3\omega_c \sin \alpha}{2\pi}. \end{aligned}$$

Here $P(\nu, E) = P_\perp(\omega) + P_\parallel(\omega)$ as given by (2.27) & (2.28) with $\omega = \nu/2\pi$ and $E = \gamma mc^2$. Then, making use of the integral

$$\int_0^\infty x^a F(x) dx = \frac{2^{a+1}}{a+2} \Gamma\left(\frac{a}{2} + \frac{7}{3}\right) \Gamma\left(\frac{a}{2} + \frac{2}{3}\right), \quad (2.41)$$

one can show that

$$\alpha_\nu = \frac{P_0}{4\pi m\nu_\alpha^2} K \Gamma\left(\frac{3p+2}{12}\right) \Gamma\left(\frac{3p+22}{12}\right) \left(\frac{\nu}{\nu_\alpha}\right)^{-(p+4)/2},$$

presuming once again that ν lies in the range (2.35). For an isotropic distribution of pitch angles, one can average this over $\sin \alpha$ to obtain (recall $r_e \equiv e^2/mc^2$ and $\nu_c = eB/2\pi mc$)

$$\begin{aligned} \alpha_\nu &= C(p) \frac{cr_e}{\nu_c} K \left(\frac{\nu}{\nu_c}\right)^{-(p+4)/2} \\ C(p) &= \frac{3^{(p+1)/2} \pi^{1/2}}{8} \frac{\Gamma[(p+4)/4] \Gamma[(3p+2)/12] \Gamma[(3p+22)/12]}{\Gamma[(p+6)/4]}. \end{aligned} \quad (2.42)$$

Note $C(2) \approx 1.645$ and $C(3) \approx 2.411$.

The important point about this formula, aside from its proportionality to the density of electrons (via K), is the rapid increase towards lower frequencies: $\alpha_\nu \propto \nu^{-3}$ if $p = 2$. At sufficiently low frequency, the emitting region becomes optically thick. Deep inside an optically thick region, the specific intensity at each frequency must saturate at a value S_ν , the source function, satisfying

$$\alpha_\nu S_\nu = \frac{\varepsilon(\nu)}{4\pi c} :$$

the righthand side is the increment to the intensity per unit length, the factor $(4\pi)^{-1}$ being necessary because the emissivity ε includes all solid angles, while the lefthand is corresponding decrement by absorption. Since the synchrotron emissivity (2.34) scales as $\nu^{(1-p)/2}$, it follows that

$$S_\nu^{(\text{sync})} \propto \nu^{5/2}, \quad (2.43)$$

with a coefficient easily derived from (2.34) and (2.42). This of course is steeper than a Rayleigh-Jeans law

$$S_\nu^{(\text{RJ})} = \frac{2k_B T_b}{c^2} \nu^2, \quad (2.44)$$

where T_b is the brightness temperature: this is equal to the actual temperature of the emitting particles if the source is thermal and optically thick, but otherwise T_b is *defined* by this relation. The emission at a given frequency ν is dominated by electrons (or positrons) whose synchrotron frequency $\nu_c \gamma^2 \sim \nu$; if one considers these electrons to have a “temperature” proportional to their energy, then that temperature is related to the frequency by

$$k_B T(\nu) = \left(\frac{\nu}{\nu_c} \right)^{1/2} m_e c^2.$$

The synchrotron source function can then be said to follow the Rayleigh-Jeans law (2.44), but with a frequency-dependent brightness temperature $T(\nu) \propto \nu^{1/2}$.

The specific intensity at the surface of an optically thick emission region will be $I_\nu \approx S_\nu^{(\text{sync})} \propto \nu^{5/2}$ at low frequencies, and at high frequencies, $I_\nu \approx L\bar{\varepsilon}(\nu)/4\pi \propto \nu^{(1-p)/2}$, where L is geometric depth of the source, and $\bar{\varepsilon}$ is the depth-averaged emissivity. The frequency at which these two powerlaws match is the self-absorption frequency.

2.5 Equipartition energy and brightness temperature

We now enter the realm of order-of-magnitude estimates. In the following, F_ν denotes flux density, the energy per unit frequency per unit area per unit time received by a radio telescope. It is usually measured in Janskys:

$$1 \text{ Jy} \equiv 10^{-23} \text{ erg cm}^{-2} \text{ s}^{-1} \text{ Hz}^{-1} = 10^{-26} \text{ W m}^{-2} \text{ s}^{-1} \text{ Hz}^{-1}. \quad (2.45)$$

The angular diameter of the source $\equiv \theta$, its distance $\equiv D$, and its linear diameter $\equiv d = D\theta$. We will also use $L_\nu \equiv 4\pi D^2 F_\nu$ for the luminosity per unit frequency. For simplicity, all factors of $(1+z)$ are ignored—but these factors can be important because radio sources are detected out to redshifts of a few.

If observed near its peak, νL_ν is an estimate of the total luminosity of the source. Taking the emission region to be roughly homogeneous, we have from eq. (2.16) that

$$\nu L_\nu \approx \frac{4}{3} \gamma^2 c \sigma_T \mathcal{U}_B N_e V,$$

where $V \sim d^3$ is the volume of the source, and $\mathcal{U}_B \equiv B^2/8\pi$ is the energy density of the magnetic field. Since the energy per unit volume in the electrons (plus positrons) is

$$\mathcal{U}_e = \gamma m c^2 N_e,$$

$$\text{it follows that } \nu L_\nu \approx \gamma \frac{4\sigma_T}{3mc} \mathcal{U}_B \mathcal{U}_e V.$$

But the radiation at frequency ν is produced by electrons with Lorentz factor

$$\gamma \approx \sqrt{\frac{\nu}{\nu_c}} \approx \left(\frac{m\nu^2}{r_e \mathcal{U}_B} \right)^{1/4},$$

where $r_e \equiv e^2/mc^2 = \sqrt{3\sigma_T/8\pi}$ is the classical radius of the electron. Putting this together,

$$\nu L_\nu \approx \frac{32\pi}{9} \left(\frac{\pi}{2}\right)^{1/4} \left(\frac{r_e^7 \nu^2}{m^3 c^4}\right)^{1/4} \mathcal{U}_B^{3/4} \mathcal{U}_e V. \quad (2.46)$$

Again, the lefthand side is evaluated at its maximum (with respect to ν). On the other hand, the total energy in particles and fields is at least (since the following ignores energy in nuclei, *etc.*)

$$E = (\mathcal{U}_e + \mathcal{U}_B)V \quad (2.47)$$

It is a simple matter to show that the minimum energy at fixed values of the observables ν , L_ν , and V (the latter two require an estimate of the distance of course) is achieved at

$$\mathcal{U}_B = \frac{3}{4}\mathcal{U}_e \quad (2.48)$$

$$E_{\min} \approx (2^{27} 3^{-12} \pi^5)^{-1/7} \left(f^{-4/7} + \frac{4}{3} f^{3/7}\right) \left(\frac{m^3 c^4}{r_e^7}\right)^{1/7} \nu^{2/7} L_\nu^{4/7} V^{3/7} \quad (2.49)$$

$$B_{\text{eq}} \approx 2.56 f^{-2/7} \left(\frac{m^3 c^4}{r_e^7}\right)^{1/14} \nu^{1/7} L_\nu^{2/7} V^{-2/7}, \quad (2.50)$$

where $f \equiv 3\mathcal{U}_e/4\mathcal{U}_B$, so that $f = 1$ for the minimum energy.

Maximum Brightness Temperature

Let us now switch gears and estimate the maximum expected brightness temperature. For a given source, T_b peaks at $\nu = \nu_a$ where the source is marginally self-absorbed. Thus

$$\varepsilon(\nu_a) d \approx \frac{8\pi\nu_a^2}{c^2} k_B T_b.$$

On the other hand,

$$\nu_a \varepsilon(\nu_a) \approx \frac{4}{3} \gamma^2 N_e c \sigma_T \mathcal{U}_B = \frac{4}{3} \gamma \frac{\sigma_T}{mc} \mathcal{U}_e \mathcal{U}_B \equiv \gamma \frac{\sigma_T}{mc} f \mathcal{U}_B^2,$$

Now

$$3kT_b \approx \gamma mc^2 \quad (2.51)$$

if γ is also the Lorentz factor of the electrons whose synchrotron frequency $\approx \nu_a$, with which the radiation field is in approximate equilibrium. Eliminating T_b from the three equations above, we find after some algebra that

$$\frac{3}{\pi^2} \nu_a^3 \approx f \frac{d}{c} \nu_c^4.$$

On the other hand,

$$\nu_a \approx \gamma^2 \nu_c \approx \left(\frac{3k_B T_b}{mc^2}\right)^2 \nu_c.$$

Eliminating ν_c between these last two yields

$$\left(\frac{3k_B T_b}{mc^2}\right)^8 \approx \frac{\pi^2}{3} f \frac{d}{c} \nu_a. \quad (2.52)$$

But the flux density and specific intensity are related by the angular size of the source:

$$F_\nu \approx \frac{\pi}{4} \theta^2 I_\nu = \frac{\pi}{2} \theta^2 \frac{\nu_a^2}{c^2} k_B T_b$$

Solving for ν_a from this last equation and substituting into eq. (2.52) yields (with $d = D\theta$)

$$\begin{aligned}\frac{k_B T_b}{mc^2} &\approx \frac{1}{3} \left(\frac{\pi^2}{6}\right)^{1/17} f^{2/17} \left(\frac{4\pi D^2 F_\nu}{mc^2}\right)^{1/17}, \\ T_{b,\text{eq}} &\approx 4 \times 10^{11} D_{\text{Gpc}}^{2/17} F_{\nu,\text{Jy}}^{1/17} f^{2/17} \text{ K}.\end{aligned}\tag{2.53}$$

This is [51]’s equipartition brightness temperature (except that we have not included the $1+z$ factors). It represents an approximate upper limit for a source that is not Doppler boosted (by bulk motion of the emitting blob). Of course it depends on the uncertain dimensionless parameter f , but only weakly, so that the source would have to be very far from equipartition in order to exceed this limit substantially. Another numerically similiar limit on T_b can be derived by requiring that inverse-Compton losses against the synchrotron radiation be less important for the relativistic electrons than synchrotron losses [28].

From the brightness temperature we can also derive the equipartition angular size:

$$\begin{aligned}\theta &\approx \left(\frac{6}{\pi}\right)^{1/2} \left(\frac{3}{2\pi^3}\right)^{1/34} f^{-1/17} \left(\frac{c}{\nu_a D}\right)^{1/17} \left(\frac{F_\nu}{m\nu_a^2}\right)^{8/17} \\ &\approx 1.5 f^{-1/17} D_{\text{Gpc}}^{-1/17} F_{\nu,\text{Jy}}^{8/17} \nu_{\text{GHz}}^{-1} \text{ milliarcsec}.\end{aligned}\tag{2.54}$$

Since f has been included, this is valid even if equipartition doesn’t hold (*i.e.* $f \neq 1$), but obviously the dependence on f is extremely weak.

2.6 Problems for Chapter 2

1. *Cyclotron radiation.* Calculate, for a nonrelativistic electron ($v \ll c$) in a uniform magnetic field, the power emitted in each linear and circular polarization. You may assume pitch angle $\alpha = \pi/2$.
2. Estimate the constraints on γ and B such that for an electron,
 - (a) the energy loss per period $2\pi/\omega_B$ is small compared to the energy itself;
 - (b) the angular momentum is large compared to Planck's constant.
3. An electron in a uniform field \mathbf{B} is released at $t = 0$ with Lorentz factor $\gamma(0)$ and pitch angle $\alpha(0)$.
 - (a) Calculate the evolution of $\gamma(t)$ and $\alpha(t)$, assuming that $\gamma \gg 1$ at all times of interest.
 - (b) Show that the time-integrated energy emitted per unit frequency

$$\frac{dE}{d\nu} \propto \nu^{-1/2}$$

at frequencies $\nu_c \ll \nu \ll \gamma^2(0)\nu_c$ ($\nu_c \equiv \omega_c/2\pi$), and estimate the coefficient of this power law. You may take $\alpha = \pi/2$.

4. VLBI observations of compact radio components of 3C273 (redshift $z = 0.158$) at 10.7 GHz find flux density $F_\nu \approx 10 \text{ Jy}$ and angular size $\theta_* \lesssim 4 \text{ m.a.s.}$ (m.a.s. \equiv milliarcsecond)[11]. Assume synchrotron emission.
 - (a) Estimate the equipartition angular size and compare with θ_* . Comment.
 - (b) Estimate the minimum energy of these components.

Chapter 3

Gamma-Ray Bursts and Afterglows

3.1 Observed properties of GRBs

Gamma-ray bursts [GRBs] were discovered serendipitously in the late 1960s by the VELA satellites, which were put in orbit to monitor atmospheric nuclear tests. The abstract of the first unclassified paper on GRBs still serves well to define them [29]:

Sixteen short bursts of photons in the energy range 0.2–1.5 MeV have been observed between 1969 July and 1972 July using widely separated spacecraft. Burst durations ranged from less than 0.1 s to ~ 30 s, and time-integrated flux densities from $\sim 10^{-5}$ erg cm $^{-2}$ to $\sim 2 \times 10^{-4}$ erg cm $^{-2}$ in the energy range given. Significant time structure within bursts was observed. Directional information eliminates the Earth and Sun as sources.

The nature of GRB sources was, and still is, mysterious. For decades, the general opinion held that GRBs had something to do with neutron stars in the Galaxy. But a minority argued for cosmological distances **refs**. Two principal observations supported the latter view:

1. The events are isotropically distributed.
2. The number of events $N(> S)$ brighter than threshold S does not scale as expected for a uniform population of sources in euclidean space.

Regarding the second point, suppose for the moment that all sources had the same intrinsic luminosity. By the inverse square law, the observed flux scales with distance as $F \propto D^{-2}$, so that the volume of space within which a GRB could be seen with $F > S$ scales as $S^{-3/2} \propto D_{\max}^3$. Therefore, if the sources were uniformly distributed, $N(> S) \propto S^{-3/2}$. It can be shown that the same scaling applies to sources having a distribution of luminosities provided only that the distribution is independent of distance. But in fact the observed GRB counts rise more slowly at the faint end, *i.e.* $d \log N / d \log S > -3/2$. This might indicate that the sources are not distributed inhomogeneously, for example if they belonged to the Galactic halo and were concentrated towards the center of the Galaxy, or not isotropically, for example if they belonged to the Galactic disk. In both examples one would expect some anisotropy in the distribution of bursts on the sky, since the Sun is some 8 kpc from the Galactic center. On the other hand, cosmologically distant sources would naturally satisfy both properties, since the inverse-square law is not satisfied on scales comparable to the horizon—and also since it is natural to suppose that the burst population may evolve with cosmic time.

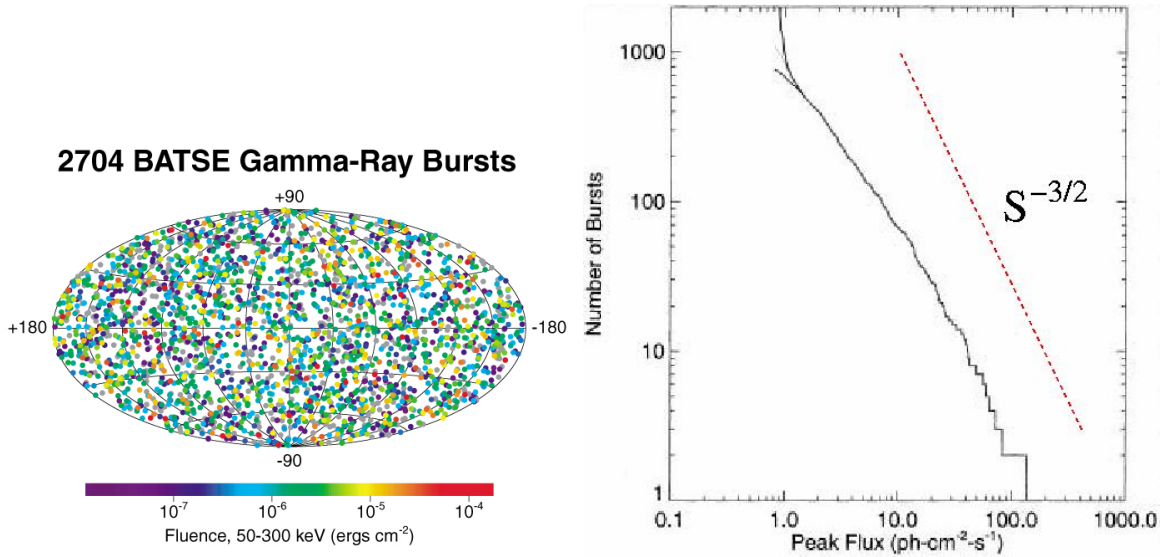


Figure 3.1: *Left panel:* Angular distribution of GRBs detected by BATSE, color-coded by fluence, in an equal-area projection[22]. *Right panel:* Cumulative number versus peak flux in 64-msec time bins, with alternative corrections for trigger efficiency at faint end[40].

However, the actual situation before 1991 was murkier than the discussion above suggests. For one thing, since scintillators have very little angular discrimination, directions could be obtained only for bursts detected by more than one spacecraft, using time of arrival; these tended to be the brightest ones, which presumably occur nearer to us and might be expected to be more isotropically distributed (if less distant than the thickness of the disk, for example). Furthermore, the roll-off in $N(> S)$ at the faint end was caused in part by variable detector thresholds; this was made worse in some discussions by defining S as the fluence—the time integral of burst flux—whereas the detectors usually triggered on peak flux itself. Resistance to the cosmological interpretation was due in part perhaps to the enormous energies it implied: $\gtrsim 10^{53}$ erg for an isotropically emitting source at $z \sim 1$. There were also more technical arguments against large distances. And then there were red herrings. Notably, there is a small class of *repeating* sources, now called Soft Gamma Repeaters (SGRs), with a clear concentration to the Galactic Center. A spectacularly bright event on March 5, 1979, was angularly coincident with a supernova remnant in the Large Magellanic Cloud, and its “light curve” showed an eight-second oscillation, perhaps indicative of a slowly rotating neutron star. On 27 Dec. 2004, the previously known Galactic source SGR 1806-20 erupted in an even more energetic hard gamma-ray flare— $> 10^{46}$ erg, equivalent to about a third of the rest mass of the moon [44]. After a short (~ 0.5 s) hard ($\gtrsim 0.5$ MeV) pulse, it too displayed an oscillating “tail” consistent with the known periodicity of SGR 1806-20. It is believed that SGRs are indeed neutron stars, but with extraordinary magnetic fields $\sim 10^{15}$ G rather than the $10^8 - 10^{13}$ G deduced for pulsars. The hard initial pulse seen in these two SGR events resembles that of the short & hard population of GRBs except in received flux, suggesting that the latter objects may be extragalactic cousins of the former. At present, it is difficult to reconcile this hypothesis with the apparent isotropy of the short GRBs, since even the 27 December flare would not have been detected beyond ~ 40 Mpc. Perhaps SGRs are capable of even brighter outbursts visible to greater distances—but that is also difficult to understand if they are indeed magnetars, whose total magnetic energy is only $\sim 10^{47} (B/10^{15} \text{ G})^2$ erg.

Some of the confusion was dispelled after a large homogeneous dataset was gathered by the Burst and Transient Source Experiment (BATSE) on board the Compton Gamma-Ray Observatory (CGRO), which launched in 1991 and de-orbited in 2000. BATSE consisted of a set of NaI scin-

tillators “pointing” in different directions from the corners of the spacecraft; directions (with $\sim 4^\circ$ precision) were found for all detected bursts by comparing the signal strengths among scintillators. As shown by Figure 3.1, BATSE data established both the isotropy and the non-euclidean $N(> S)$ distribution of GRBs. This convinced most astrophysicists that the sources are cosmological. But “proof” was found only with the detection of GRB afterglows, as will be discussed later.

As shown in Figure 3.2, GRB light curves show great variety. Some are quite smooth apart from counting statistics; others fluctuate wildly on the smallest measureable timescales. It is not clear whether this diversity is intrinsic or a function of aspect angle, since it is now believed on other grounds that GRBs are jets of some sort rather than isotropic emitters. Still, we may be dealing with multiple populations of sources. Evidence for at least two classes of GRB—“short” and “long”—is seen in the distribution of burst durations, as seen in Figure 3.3. The short bursts tend to have harder spectra, and none has yet been associated with an afterglow.

In a plot of fluence per logarithmic interval of photon energy (νF_ν), the spectrum of the typical BATSE burst appears to peak at ~ 100 keV, but the spectrum is often rather broad, and there is a wide variation in the peak energy, so that composite spectra are rather flat (Fig. 3.4). In some cases, hard tails are seen extending up to $\gtrsim 1$ GeV. Such tails may be more common than they appear to be in the database, because limited photon statistics would make them difficult to detect in most bursts.

3.2 Basic theoretical considerations for GRBs

For the purpose of rough estimates, we can use euclidean geometry even though the typical burst source probably lies at $z \gtrsim 1$. We write d_{28} for the distance in units of 10^{28} cm ≈ 3.2 Gpc $\sim cH_0^{-1}$.

One of the first important conclusions is that the source must have highly relativistic bulk velocities. Let Γ be the characteristic bulk Lorentz factor (γ is reserved for other purposes). The duration of burst events covers a broad range: $10^{-1} \lesssim \Delta t \lesssim 10^3$ (Fig. 3.3), but even long bursts often fluctuate violently on much shorter timescales $\delta t \lesssim 10^{-2}$ s (Fig. 3.2). If $\Gamma \sim 1$, we would expect that the size of the source (R) should be $\lesssim \delta t/c$, else different parts of the source would not be in causal contact over the time δt and would fluctuate independently; this would lead to an overall amplitude of variability $\sim (c\delta t/R)^{1/2} \ll 1$, in conflict with the observations. If the source moves relativistically towards the observer, however, then the observed timescales are smaller than the intrinsic ones by a factor $1 - \beta \sim \Gamma^{-2}$ (see §1.1), whence the limit becomes

$$R \lesssim \Gamma^2 c \delta t \sim 3000 \Gamma^2 \delta t_{-2} \text{ km}, \quad (3.1)$$

where $\delta t_{-2} \equiv \delta t / (10^{-2} \text{ s})$. If the source emits isotropically and produces a fluence $J \equiv 10^{-5} J_{-5} \text{ erg s}^{-1}$ at Earth, its luminosity is

$$L \sim \frac{4\pi d^2 J}{\Delta t} \approx 10^{51} d_{28}^2 J_{-5} \Delta t_1, \quad (3.2)$$

where $\Delta t_1 \equiv \Delta t / (10 \text{ s})$. Often, much of this luminosity emerges in photons with energies above the pair-creation threshold, $h\nu > m_e c^2 = 511$ keV. Let us estimate the optical depth of the source to pair creation *via* the reaction $\gamma\gamma \rightarrow e^+e^-$, assuming for the moment that the source is not relativistic ($\Gamma \sim 1$). The number of photons within the source at any one time is $N \sim L\delta t/m_e c^2$. The pair-creation threshold per photon is $\sim \sigma_T$, so the total optical depth is

$$\tau_p \sim \frac{N\sigma_T}{\pi R^2} \sim \frac{\sigma_T L}{m_e c^4 \delta t} \sim \frac{4\sigma_T d^2 J}{m_e c^4 \delta t \Delta t} \sim 4 \times 10^{13} d_{28}^2 J_{-5} (\delta t_{-2} \Delta t_1)^{-1}. \quad (3.3)$$

One would therefore expect that the source should be extremely optically thick to its own pairs, and hence the emitted spectrum should be thermal. But it is not. Indeed, essentially this argument was used in pre-BATSE days to “prove” that GRBs could be no more distant than ~ 1 kpc since $\tau_p \propto d^2$ [55].

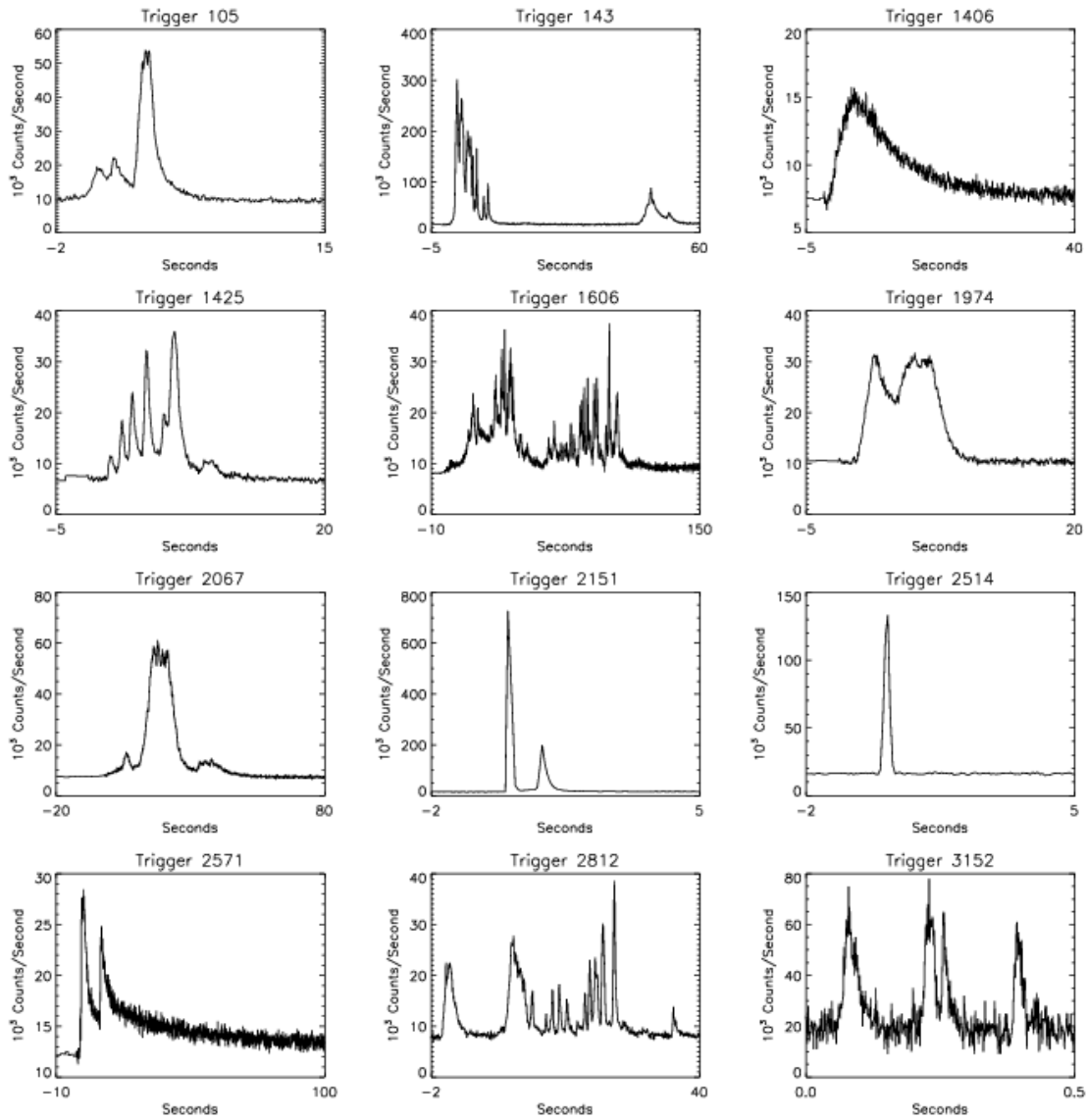


Figure 3.2: A sample of GRB lightcurves determined by BATSE [22].

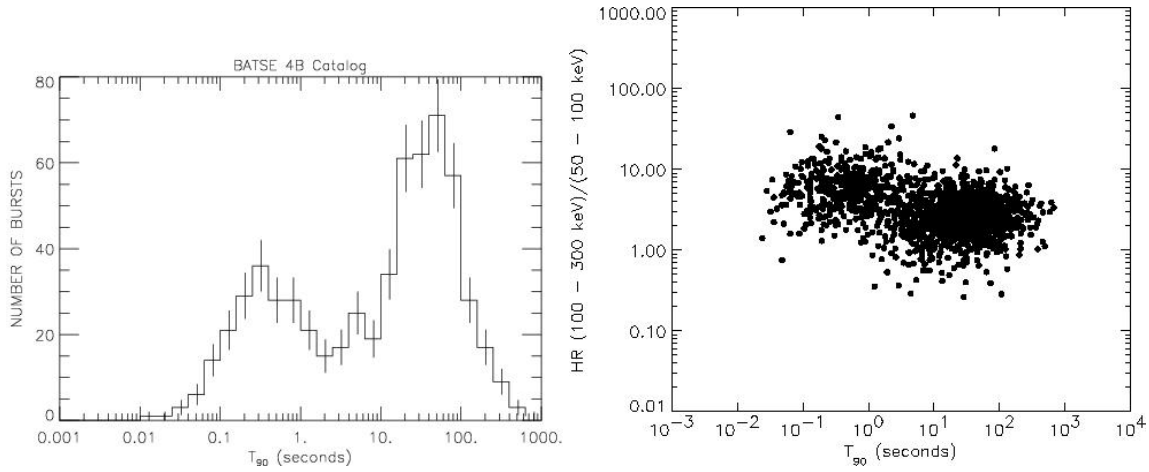


Figure 3.3: *Left:* Histogram of durations of BATSE bursts defined as the time within which 90% of the fluence was collected (T_{90}).[40]. *Right:* Distribution of GRBs in a plane of T_{90} and spectral hardness [16].

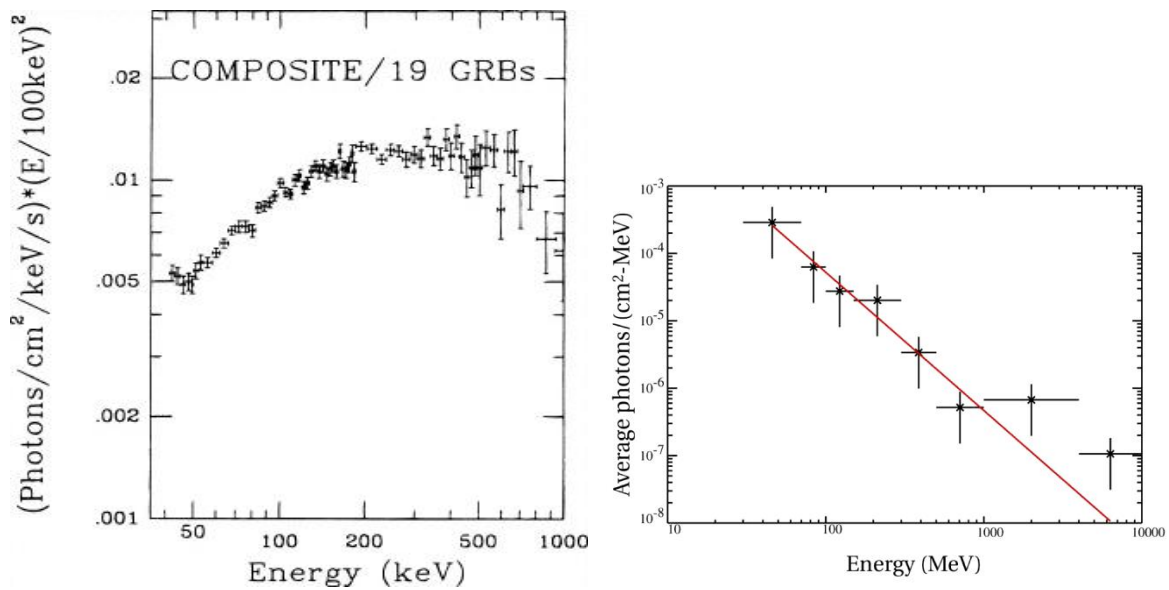


Figure 3.4: *Left:* Composite spectrum of 19 bright bursts[54]. *Right:* A burst with a very hard tail [22].

If the source moves relativistically toward the observer, τ_p is reduced for at least three reasons:

1. The source size can be larger by a factor $\sim \Gamma^2$ [(3.1)].
2. The luminosity in the rest frame of the source is smaller by $\sim \Gamma^{-2}$.¹
3. The photon energies in the rest frame are smaller by $\sim \Gamma^{-1}$, hence fewer are above threshold.

For a source whose high-energy spectrum is a power-law $F_\nu \propto \nu^{-\beta}$, these three effects in combination reduce the optical depth by $\sim \Gamma^{-4-\beta}$. Thus for $\beta \sim 1$ (as seen for example in the burst of Fig. 3.4), the rest-frame optical depth for the parameters of (3.3) would be $\lesssim 1$ if $\Gamma \gtrsim (4 \times 10^{13})^{1/(4+\beta)} \sim 170$.

A separate argument for relativistic motions is that the source is likely to be explosive. The radiative force on an electron at distance R from the source is

$$f_e \sim \frac{\sigma_T L}{4\pi R^2 c} \sim \frac{\sigma_T J d^2}{c \Delta t R^2}.$$

If the source were confined by gravity, then this would have to be balanced by the gravitational force on a proton (even a slight charge separation would be resisted by strong electric fields),

$$f_p \sim -\frac{GM m_p}{R^2},$$

where M is the mass of the source. The net force on the two particles is positive (outward) unless

$$M \gtrsim \frac{\sigma_T L}{4\pi G m_p c}. \quad (3.4)$$

This is called the Eddington limit. Note that it is independent of the distance R . If pairs are present, the limit must be increased by the total number of e^\pm per proton. Substituting for L from (3.2) implies $M \gtrsim 10^{13} d_{28}^2 J_{-5} \Delta t_1 M_\odot$. On the other hand, the source cannot vary faster than the light-travel time across its Schwarzschild radius ($R_S = 2GM/c^2$), whence

$$M \lesssim \Gamma^2 \frac{c^3 \delta t}{G} \sim 10^3 \delta t_{-2} M_\odot.$$

Thus gravity fails to confine the source by at least ten orders of magnitude. While the source might be held together nongravitationally, scenarios along these lines tend to be very exotic: for example, emission from a neutron star composed of strange matter (if such exists), so that the emitting material is bound to the star's surface by strong nuclear forces **refs**; and even in this probably fails, since the emission would probably be thermal.

Early models for GRBs at cosmological distances invoked a relativistic wind [41] or “fireball” [20] consisting purely of pairs and photons. In both cases, the source would in fact be extremely optically thick to pairs, but with an energy density so high that the mean energy per photon $\langle h\nu \rangle \sim m_e c^2$. Absent any admixture of baryons, $\langle h\nu \rangle$ would be approximately conserved: as the optically thick plasma adiabatically cools, the pairs annihilate, returning their energy to the photon gas, whose random motions are increasingly converted to radial streaming. However, even a small baryon loading—a fraction $\eta \sim 10^{-4}$ of the energy in baryonic rest mass—prolongs the optically thick phase in a smoothly expanding wind until most of the energy has been converted to kinetic energy of the baryons. Even when $\eta \ll 10^{-4}$, simple fireball models produce spectra that are too nearly thermal [20].

¹Luminosity is equivalent to emitted power, which is invariant when no net momentum is emitted in the rest frame [§2.2.2 & eq. (2.15)]. However, since the time over which the energy is received and the time over which it is emitted are related by $\Delta t_{\text{rec}} = (1-\beta)\Delta t_{\text{em}}$ —even though both times are measured in the astronomer's frame—the luminosity (3.2) overestimates the emitted power by the corresponding factor.

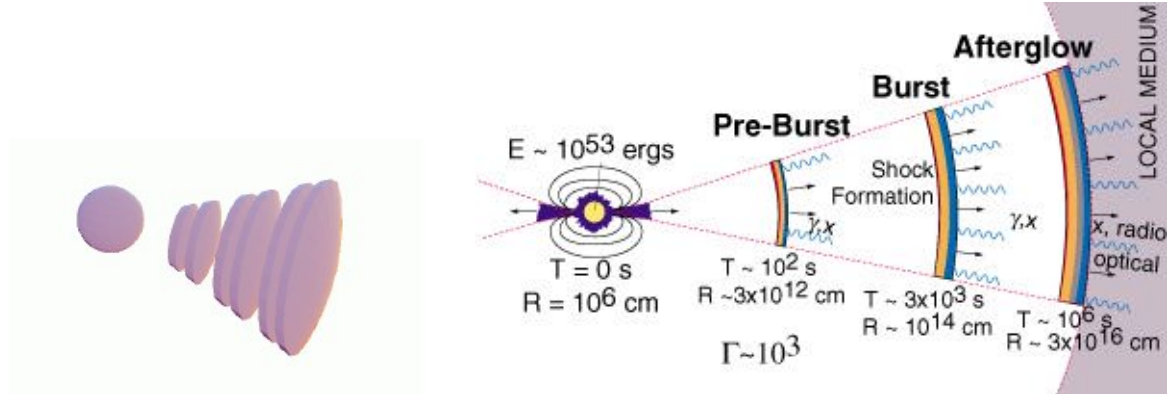


Figure 3.5: *Left*: Internal shock model: partially collimated pulses/shells with widely differing Lorentz factors [49]. *Right*: Cartoon of internal shock and afterglow phases, with nominal dimensions [22].

The currently most popular theory of GRB emission is the internal shock model. A stationary source of unspecified nature and size $\lesssim c\delta$ emits a relativistic wind or jet with variable Γ , $\langle\Gamma\rangle \gtrsim 10^2 - 10^3$. Faster shells overtake the slower, leading to optically thin shocks at distances $R \sim (\Gamma)^2 c\delta t \sim 10^{14}$ cm, which emit synchrotron and perhaps inverse-compton radiation. This model is able to explain the rapid variability and non-thermal spectra of GRBs. It has difficulty explaining why a large fraction of the outflow energy is converted to radiation. This difficulty is in two parts.

The first difficulty is purely kinematic. Consider two shells of Lorentz factors Γ_1, Γ_2 ($\Gamma_2 > \Gamma_1 \gg 1$) and rest masses M_1, M_2 . We assume that before collision, the shells are “cold” in their individual rest frames, so that M_1 and M_2 are essentially their baryonic masses. The invariant mass of the two is given by

$$M_{\text{COM}}^2 = -\eta_{\mu\nu}(p_1 + p_2)^\mu(p_1 + p_2)^\nu \approx (M_1 + M_2)^2 + \frac{(\Gamma_2 - \Gamma_1)^2}{\Gamma_1\Gamma_2} M_1 M_2. \quad (3.5)$$

and $\Delta M c^2 \equiv (M_{\text{COM}} - M_1 - M_2)c^2$ is the energy available to be dissipated in the center-of-mass frame. Clearly one wants $\Gamma_2 \gg \Gamma_1$ to make this as large as possible, yet one also wants a large value for

$$\Gamma_{\text{COM}} = \frac{M_1\Gamma_1 + M_2\Gamma_2}{M_{\text{COM}}},$$

since the radiated energy that the astronomer sees is $E_{\text{rad}} \lesssim \Gamma_{\text{COM}} M_{\text{COM}} c^2$. It is certainly possible to design a variable wind that satisfies these constraints.

The second difficulty is to radiate $\Delta M c^2$ efficiently [31, 23]. The primary radiative process is probably synchrotron emission. In order to radiate efficiently, the shocked plasma must have comparable energy densities in relativistic protons, electrons (or positrons), and magnetic field. In a simple first-principles collisionless shock model, the electrons would receive only a fraction $m_e/m_p = 1/1836$ of the energy. Flux freezing implies that a perpendicular field would increase over its pre-shock value by the shock compression ratio $\gamma\sqrt{8}$ in the relativistic limit [(1.50)], hence the magnetic energy density would increase by $\lesssim 8\gamma^2$, whereas the energy density in particles increases by $2\gamma^2$ [(1.49)] over its initial rest-mass energy density:

$$\left(\frac{u_B}{u_b}\right)_{\text{postshock}} \sim \left(\frac{u_B}{u_b}\right)_{\text{preshock}} \sim \left(\frac{B^2}{8\pi\rho c^2}\right)_{\text{ISM}} \ll 1$$

where the last inequality follows because in the interstellar medium, one observes that magnetic and *thermal* (not rest-mass) energy densities are comparable: $B^2/8\pi \sim (\rho/m_p)k_B T \ll \rho c^2$. “Anoma-

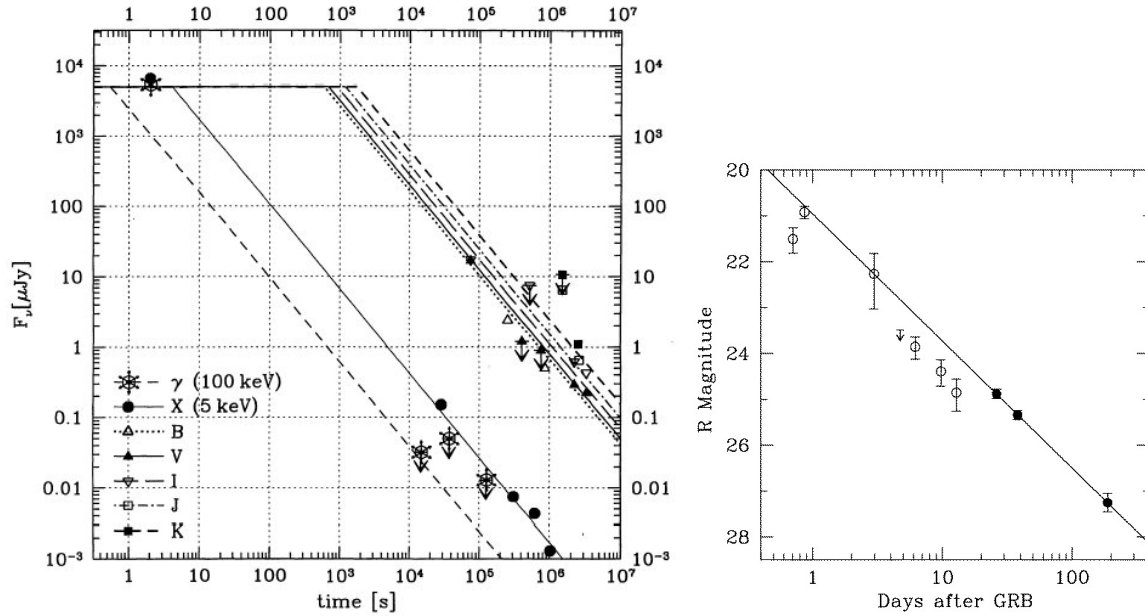


Figure 3.6: Light curves of GRB 970228. *Left*: Early observations in all available bands, from [67]. Symbols with downward arrows are upper limits. *BVR* and *IJK* are optical and near-IR wavelength bands, respectively. *Right*: *R* magnitudes only from ground (open symbols) and HST (solid symbols), from [17]. Solid line is a powerlaw fit to HST points, brightness $\propto (t - t_{\text{burst}})^{-1.1 \pm 0.1}$

lous” processes are required to transfer energy from the protons to the leptons and to the field, and these processes are not understood. This “equipartition” problem—which is really two problems, one for the leptons and another for the field—is not unique to the internal-shock model of GRBs, although it is especially severe in that context. It arises for many other collisionless astrophysical shocks, such as supernova remnants.

3.3 Afterglow observations

While the resolution of BATSE and—for especially bright bursts—the Interplanetary Network [IPN]² was sufficiently accurate to establish the isotropy of GRB sources, but not sufficiently accurate for follow-up at other wavelengths. A typical optical research telescope, for example, has a field of view measured in arc minutes rather than degrees. Nor was notification very timely, and as we now know, the afterglows fades with time as $t^{-1} - t^{-2}$ at X-ray through optical wavelengths.

The laurels for first detection of GRB afterglows belong to the Italian-Dutch X-ray satellite BeppoSAX. GRB science was a minor consideration in its design, but BeppoSAX carried two instruments of critical importance: the Gamma Ray Burst Monitor, and the two [X-ray] Wide-Field Cameras [WFC1,2]. The large field of view (20° each) of these cameras offered a reasonable probability of monitoring a GRB in X-rays (1.8 – 28 keV) simultaneously with the γ -rays event itself, while the angular resolution (5 arc minutes) was sufficient for optical followup. The satellite was in operation for many months, however, before procedures were established to localize and report

²Many interplanetary probes, such as the Pioneer, Venera, and Ulysses spacecraft, carried small scintillators capable of detecting very strong bursts. By comparing the times of arrival at different spacecraft, burst directions could be determined by triangulation.

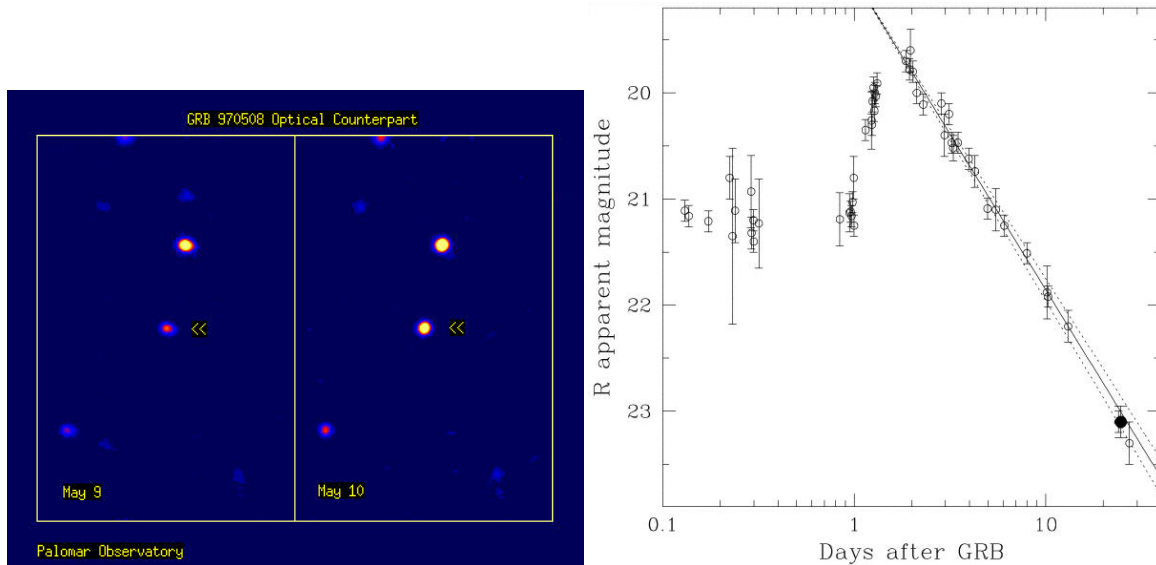


Figure 3.7: Optical afterglow of GRB 970508. *Left*: Initial brightening seen at Palomar 200-inch (S. G. Djorgovski, unpublished). *Right*: Optical light curve [47]. The optical source brightened initially but was consistent with flux $\propto t^{-1}$ after May 10.

the X-ray detections promptly. (Reducing their “reaction time” has been a continuing challenge for GRB astronomers.) The first success was the burst of 28 February 1997 (GRBs are often referred to by their date of detection, hence this one is named GRB 970228). A rapidly fading X-ray counterpart to the GRB was seen by the WFC1 and was still visible to other X-ray instruments (with narrower fields but better sensitivity) when they slewed to the source hours later [12]. The X-ray errorbox was small enough to allow detection of a fading optical transient 20 hours later [63], which was followed for days thereafter as it faded and reddened into the IR (Fig. 3.6).

The remarkable afterglow of GRB 970508 (Fig. 3.7) gave direct proof of its cosmological origin with the detection of absorption lines at $z = 0.835$ [38]. In fact, a number of afterglows now have measured redshifts, either through the detection of absorption lines in the optical transient itself, or by later observations of the host galaxy—that is, the galaxy (usually very faint and blue) in which the source is believed to reside on the basis of angular coincidence. A fascinating and useful compilation of data, images, and references on all GRB afterglows is <http://www.mpe.mpg.de/~jcg/grbgen.html>. As of April 2005, the redshifts of $\gtrsim 40$ afterglows have been measured, ranging from $z \sim 0.4$ to $z = 4.5$. The number of redshifts will likely increase rapidly with the advent of the SWIFT satellite (launched Nov. 2004) and its precise X-ray positions.

GRB 970508 received intense observational coverage and was observed at wavelengths ranging from γ -rays to the radio. Longer wavelengths brightened at later times, a trend that can be seen even within the radio spectrum (Fig. 3.8, left panel). The spiky behavior at early times may be caused by interstellar scintillation [21].³

Beyond confirming the cosmological distance scale, afterglows have revealed a number of important properties of GRBs:⁴

³ The refractive index of the interstellar medium [ISM] varies with electron density (n_e) and frequency ν as

$$\frac{c}{\lambda\nu} = [1 - (n_e e^2 / \pi m_e \nu^2)^2]^{1/2};$$

inhomogeneities of n_e lead to the radio equivalent of the twinkling of starlight in the Earth’s atmosphere. The interstellar effect is negligible at optical or higher frequencies because of the ν^{-2} dependence above.

⁴All of these inferences presume, of course, that the burst and the afterglow have a common ultimate source

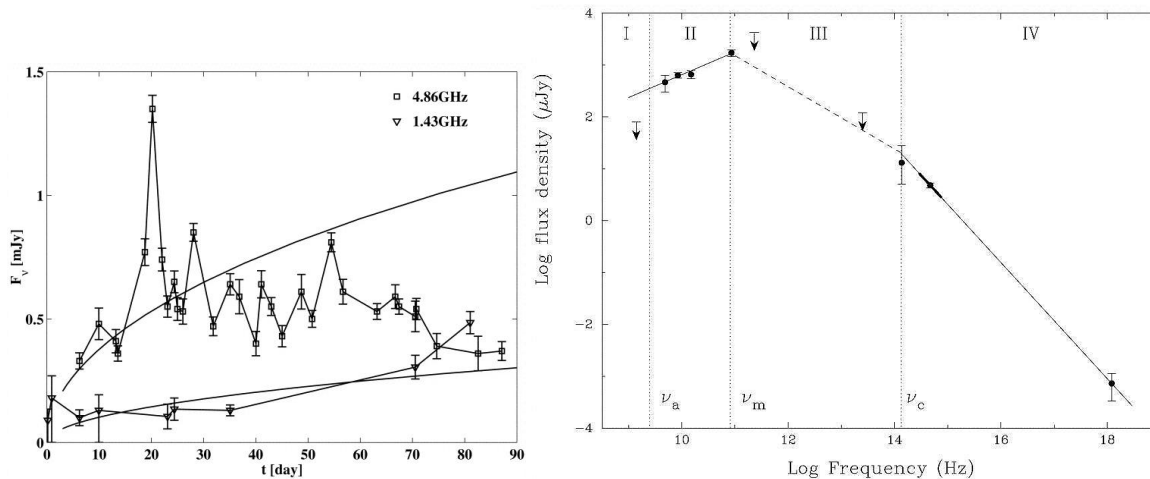


Figure 3.8: *Left:* Radio lightcurves of 970508 [65]. *Right:* The X-ray to radio spectrum of 970508 12 days after the burst [18].

1. The sources appear to reside in distant galaxies (“hosts”).
2. In view of the blue colors of the hosts, GRBs are probably associated with young stars or recent remnants thereof. Furthermore, in a handful of cases, spectra of peculiar Type Ic supernovae have been detected late in the afterglow [36].
3. The afterglow is produced by synchrotron emission from a relativistic shock driven into the interstellar medium near the central engine.
4. The outflow responsible for the burst and the afterglow is probably jet-like rather than spherical, and is directed towards the observer. (The latter is obviously a selection effect.)

The first two are fairly direct astronomical inferences from observation. The last two involve some theoretical modeling and additional physical assumptions, but there are a number of cross checks that strengthen our confidence in the conclusions. Some of these will be discussed in the sequel.

It is important to remember, however, that only a small minority of GRB burst are associated with detectable afterglows, so that the inferences above may not apply to the “silent” majority. In particular, no afterglows have yet been associated with short bursts (see §3.1 & 3.3).

3.4 Basic theoretical considerations for afterglows

Afterglows were in effect predicted. [52] showed that a “baryon-loaded” fireball would eventually shock against the interstellar medium [ISM] and convert its relativistic bulk velocity into random particle velocities in the shock rest frame. If a significant fraction of the energy could be converted to magnetic field (as appears to occur in many extragalactic radio sources, for example) then observable synchrotron emission would be produced. However, in the original 1992 paper, the distinction between the afterglow and the GRB itself was not very clear. A definite prediction that GRBs should be followed by radio emission due to an ISM shock was made by [42].

(“central engine”). This seems probable on direct observational grounds, as well as indirect theoretical ones.

3.4.1 Relativistic shock dynamics

Consider a relativistic spherical shock expanding into a uniform external medium of mass density $\bar{\rho} = \bar{N} m_p c^2$ and negligible pressure (*i.e.* dust). For simplicity, we assume that the total energy E of the explosion is conserved, *i.e.* we neglect the loss of energy to radiation, and we use ideal-fluid approximations. These appear to be reasonable approximations for afterglow shocks. When the shock radius r_s becomes much larger than the initial region of energy input, it can be expected to evolve self-similarly. Exact results have been obtained under these assumptions by [7], but this discussion will be limited to approximate scaling laws.

Using results from §1.8, the shock jump conditions imply

$$\begin{aligned} \gamma &= \Gamma, \quad \beta \approx 1, \quad T^{00} \approx \Gamma^2 \bar{\rho}, \quad N^0 \approx \Gamma \bar{N}, \\ \beta' &\approx 1/3 \quad \gamma' \approx 3/\sqrt{8}, \quad \bar{\rho}' \approx 2\Gamma^2 \bar{\rho}, \quad \bar{N}' \approx \sqrt{8}\Gamma \bar{N}, \end{aligned} \quad (3.6)$$

where $\Gamma \gg 1$ is the shock Lorentz factor and the primes denote postshock quantities. We are assuming that no baryon are created in the shock, so that the baryon current N^μ is conserved, *i.e.* $N^\mu_{,\mu} = 0$. It follows that the mean energy per baryon in the restframe of the postshock fluid is

$$\bar{\varepsilon}' = \frac{\bar{\rho}'}{\bar{N}'} = \frac{\Gamma m_p c^2}{\sqrt{2}}.$$

Henceforth, in the interests of speed, we will generally ignore dimensionless factors of order unity. Thus for example, $\bar{\varepsilon} \sim \Gamma m_p c^2$. Since the postshock bulk velocity (not the individual particle speeds!) is nonrelativistic in the shock frame, it follows that the mean energy per baryon in the rest frame of the pre-shock ISM (“lab frame”) is $\bar{\varepsilon}' \sim \Gamma^2 m_p c^2$. Thus the energy carried by the swept-up ISM is

$$\Delta E_{\text{ISM}} \sim \Gamma^2 \frac{4\pi}{3} r_s^3 \bar{N} m_p c^2.$$

Initially, $\Gamma \sim \Gamma_0 = \text{constant}$, but since energy conservation demands $\Delta E_{\text{ISM}} \leq E = \Gamma_0 M_0 c^2$, where M_0 is the initial mass of the ejecta, the shock must begin to decelerate at a radius

$$r_{s,0} \sim \left(\frac{3E}{4\pi \bar{N} m_p c^2 \Gamma_0^2} \right)^{1/3} \sim 10^{17} E_{53}^{1/3} \bar{N}_0^{-1/3} \Gamma_{0,2}^{-2/3} \text{ cm}, \quad (3.7)$$

where $E_{53} \equiv E/(10^{53} \text{ erg})$, $\bar{N}_0 \equiv \bar{N}/(1 \text{ proton cm}^{-3})$, and $\Gamma_{0,2} \equiv \Gamma_0/100$. The coordinate time in the lab frame at which the shock reaches this radius is $\approx r_{s,0}/c \sim 1$ month, but the time as observed by astronomers is compressed by a factor $(1 - \beta_{\text{shock}}) \approx 1/2\Gamma_0^2$, so that (we will use t for the astronomer’s time)

$$t_0 \approx 200 E_{53}^{1/3} \bar{N}_0^{-1/3} \Gamma_{0,2}^{-8/3} \text{ s}. \quad (3.8)$$

Thereafter,

$$\Gamma \approx \left(\frac{3E}{4\pi \bar{N} m_p c^2 r_s^3} \right)^{1/2} \approx 10 \cdot \left(\frac{E_{53}}{\bar{N}_0} \right)^{1/8} \left(\frac{t}{1 \text{ day}} \right)^{-3/8}. \quad (3.9)$$

and

$$t(r_s) \approx \int_0^{r_s} \frac{dr'_s}{2\Gamma^2(r'_s)c} \approx t_0 \left(\frac{r_s}{r_{s,0}} \right)^4.$$

Inverting this,

$$\begin{aligned} r_s &\approx r_{s,0} \left(\frac{t}{t_0} \right)^{1/4} \\ \Gamma &\approx \Gamma_0 \left(\frac{t}{t_0} \right)^{-3/8}, \end{aligned} \quad (3.10)$$

but note from (3.9) that Γ depends on E/\bar{N} rather than Γ_0 when $t > t_0$.

The shock becomes nonrelativistic at

$$t_1 \approx 1 E_{53}^{1/3} \bar{N}_0^{-1/3} \text{yr}. \quad (3.11)$$

Thus, the later radio observations shown in the first panel of Fig. (3.8) were probably in the nonrelativistic regime.

This discussion has assumed a spherical outflow and shock. More likely, the initial outflow is a jet of opening angle $\theta_j \ll 1$ and solid angle $\Omega_j \approx \pi\theta_j^2$. At the same energy per unit solid angle, the total energy is then smaller than we have assumed by a factor Ω_j . However, at early times when $\Gamma \gg \theta_j^{-1}$, the shock evolves as if it were spherical because there has not been enough time in the shock rest frame for signals to have been transmitted from one side of the jet to the other. Although we have neglected radiation, it will be shown below that the flux density observed from the shock is predicted to decline as a powerlaw with time during this early phase, as observed, if constant fractions of the postshock energy go into electrons and magnetic field. We may expect a change in the slope of this powerlaw when Γ drops to θ_j^{-1} , which happens at a time

$$t_j \sim 1. E_{\text{iso},53}^{1/3} \bar{N}_0^{-1/3} (10\theta_j)^{8/3} \text{days}, \quad (3.12)$$

after the GRB, the jet angle being measured in radians. Here and henceforth, E_{iso} is the ‘‘equivalent isotropic energy:’’ that is, the energy of a spherical shock with the same energy per steradian as the jet. The actual energy is

$$E = E_{\text{iso}} \times \frac{\Omega_j}{4\pi}. \quad (3.13)$$

3.4.2 Afterglow emission

All of this is purely hypothetical unless the shock is observable, which requires an emission mechanism. It is likely that this is synchrotron radiation. If it is anything like that of the Galaxy, the pre-shock ISM contains magnetic field as well as hydrogen. In the Galactic ISM, the energy density in the field is comparable to the thermal pressure of the plasma:

$$B \sim 3\mu\text{G} \frac{B^2}{8\pi} \sim 0.2 \text{eV cm}^{-3}; \quad p = \bar{N}k_B T \sim 0.3 \text{eV cm}^{-3}. \quad (3.14)$$

⁵ There is also a comparable energy density in cosmic rays. All of these are much less than the energy density in rest mass, $\bar{N} m_p c^2 \sim 1 \text{GeV cm}^{-3}$. A shock will compress the particles and fields, causing a great enhancement in the synchrotron emissivity since this scales as $\propto \langle \gamma_e \rangle \mathcal{U}_B \mathcal{U}_e$, where \mathcal{U}_B and \mathcal{U}_e are the energy densities in field and e^\pm , and $\langle \gamma_e \rangle$ is the mean Lorentz factor of the electrons measured in the local rest frame of the plasma.

To estimate the field that results from shock compression, it is useful to divide \mathbf{B} into components parallel and perpendicular to the shock plane: B_{\parallel} , B_{\perp} . (The present convention for ‘‘parallel’’ and ‘‘perpendicular’’ is opposite to that used for the Lorentz transformations of \mathbf{E} & \mathbf{B} in (1.13).) B_{\perp} is unaffected by the shock, but conservation of magnetic field lines implies⁶ that B_{\parallel} is increased by the same factor as the baryon number density,

$$\frac{\bar{B}'_{\parallel}}{\bar{B}_{\parallel}} = \frac{\bar{N}'}{\bar{N}} \approx \sqrt{8}\Gamma, \quad (3.15)$$

⁵ Actually, if \bar{N} represents the number of nucleons per unit volume, then the pressure is more like $1.7\bar{N}k_B T$ when the ISM is fully ionized, allowing for the electrons and for the fact that $\sim 30\%$ of the gas by weight is in helium and other elements heavier than hydrogen. It is found that p itself is more nearly constant than \bar{N} or T separately.

⁶ Actually a second assumption is involved here: that the field lines comove with the plasma (‘‘flux freezing’’). This is a very good approximation since the plasma is a good conductor.

where as usual overbars denote quantities measured in the local rest frame of the fluid, and primes distinguish postshock from preshock values. So if $B_{\parallel} \sim B_{\perp}$ ahead of the shock, then $B'_{\parallel} \gg B'_{\perp}$ behind it. Expressed as a fraction of the total energy density, that of the field is

$$f'_B \approx \frac{(B'_{\parallel})^2}{8\pi\rho'c^2} = \frac{8\Gamma^2 B_{\parallel}^2}{16\pi\Gamma^2 \bar{N} m_p c^2} \sim 10^{-9}.$$

Thus f'_B is independent of the shock Lorentz factor, but it is very small simply because $U_B \ll \bar{N} m_p c^2$ in the preshock ISM. Now in fact, if f'_B were really so small as this, then synchrotron radiation from the shock would be unobservable. Models fit to afterglow data suggest that typically $f'_B \sim 10^{-4} - 10^{-1}$ [45]. This requires amplification of the field far beyond what is achieved by compression alone. The amplification mechanism may be a microscopic plasma instability near the shock front [37], or perhaps macroscopic turbulence in the postshock flow. Hence

$$B' \sim (16\pi f'_B \Gamma^2 \bar{N} m_p c^2)^{1/2} \sim 0.3 \Gamma \bar{f}'^{1/2} \bar{N}_0^{1/2} \text{ G.} \quad (3.16)$$

Collisionless shocks tend to produce power-law spectra of relativistic ions and electrons. The ions scarcely radiate directly, so we concentrate on the electrons. Their spectrum is of the form (2.33) in the rest frame of the postshock fluid, presumably matching onto a roughly Maxwellian distribution at low energies. Studies of particle acceleration by relativistic shocks indicate that $p \approx 2.2 - 2.3$. We shall assume that $p > 2$. Then most of the energy is at the low end of the spectrum:

$$U_e = m_e c^2 \int_{\bar{\gamma}_{\min}}^{\bar{\gamma}_{\max}} \bar{\gamma} m_e c^2 K \bar{\gamma}^{-p} d\bar{\gamma} \approx (p-2)^{-1} K m_e c^2 \left(\bar{\gamma}_{\min}^{2-p} - \bar{\gamma}_{\max}^{2-p} \right) \approx (p-2)^{-1} K m_e c^2 \bar{\gamma}_{\min}^{2-p}$$

The characteristic emission frequency at $\bar{\gamma}_{\min}$ is

$$\bar{\nu}_{\min} = \bar{\gamma}_{\min}^2 \frac{e\bar{B}'}{2\pi m_e c}. \quad (3.17)$$

What is $\bar{\gamma}_{\min}$? If the shock simply randomizes the direction of motion of most particles, then $\bar{\gamma}_{\min} \sim \Gamma$. If energy equipartition between the ions and electrons is achieved, then

$$\bar{\gamma}_{\min} = f'_e \frac{m_p}{m_e} \Gamma, \quad (3.18)$$

with $f'_e \approx 1$. It is usually assumed (or found by model fitting, see [45]) that $f'_e \gtrsim 10^{-2}$ despite the fact that two-body collisions are far too slow to establish equipartition, so that some collective process or instability is required. The characteristic emission frequency in the observer's frame is $\nu_{\min} = \Gamma \bar{\nu}_{\min}$, or

$$\begin{aligned} \nu_{\min} &\sim 3 \times 10^{12} f_e'^2 f_B'^{1/2} \Gamma^4 \bar{N}_0^{1/2} \text{ Hz} \\ &\sim 3 \times 10^{11} (10^2 f_e')^2 (10^2 f_B')^{1/2} (E_{\text{iso},53}/\bar{N}_0)^{1/2} t_d^{-3/2} \text{ Hz,} \end{aligned} \quad (3.19)$$

where $t_d = t/(1 \text{ day})$. The observed spectrum should peak at ν_{\min} , and scale as $\nu^{1/3}$ below this frequency and as $\nu^{(1-p)/2}$ above it.

Sufficiently energetic electrons cool (*i.e.* radiate most of their energy) in a time than the age of the shock. The condition for this is $\bar{\gamma} \gtrsim \bar{\gamma}_{\text{cool}}$, where

$$\bar{\gamma}_{\text{cool}}^2 c \sigma_T \frac{B'^2}{8\pi} \Gamma t = \bar{\gamma}_{\text{cool}} m_e c^2.$$

Note that the age of the shock in its rest frame is $\sim r_s/\Gamma c \sim \Gamma t$, where t (as usual) is the observed time after the burst. The corresponding frequency in the observer's frame is

$$\nu_{\text{cool}} \approx \Gamma \bar{\gamma}_{\text{cool}}^2 \left(\frac{e\bar{B}'}{2\pi m_e c} \right) = \frac{32\pi m_e c e}{\sigma_{\text{T}}^2 \bar{B}'^3 \Gamma t^2}.$$

Combining this with (3.9) & (3.16) yields

$$\nu_{\text{cool}} \sim 2 \times 10^{15} E_{\text{iso},53}^{-1/2} \bar{N}_0^{-1} (10^2 f'_B)^{-3/2} t_{\text{day}}^{-1/2} \text{ Hz}. \quad (3.20)$$

The spectrum is predicted to steepen above ν_{cool} , *i.e.* ν^{-p} instead of $\nu^{(1-p)/2}$. If the spectral break at ν_{cool} can be identified in the data, it gives a useful constraint on the uncertain parameter f'_B .

Gaze now at the second panel of Fig. 3.8, showing the spectrum of GRB 970508 at $t = 12$ day. The authors [18] have identified three spectral breaks, defining four spectral regions—perhaps a bold interpretation of only ten data points, but then these points span nine orders of magnitude in frequency. The lowest-frequency break is identified with the self-absorption frequency, which we have not discussed. Evidently, ν_{min} and ν_{cool} (labeled ν_m, ν_c in the figure) are approximately where one might expect to find them, following (3.19) & (3.20), but probably with $f'_e \sim 10^{-1}$ instead of $\sim 10^{-2}$. [45] find the following best-fit parameters for this burst: $f'_e \approx 0.11$, $f'_B \approx 0.045$, $\bar{N} \approx 0.75 \text{ cm}^{-3}$, $p = 2.18$, $\theta_j \approx 0.32 \text{ rad}$, and $E_{\text{iso}} \approx 2 \times 10^{53} \text{ erg}$.

It remains to determine the normalization of the spectrum. Following the discussion of §2.5, the total synchrotron power radiated in a logarithmic interval of frequency centered around ν_{min} is

$$\left(\frac{d\bar{P}}{d \ln \bar{\nu}} \right)_{\nu_{\text{min}}} \approx \frac{\sigma_{\text{T}}}{m_e c} \gamma'_{\text{min}} \bar{U}'_e \bar{U}'_B \bar{V}'.$$

where \bar{V}' is the volume of the emission region. This has been expressed in the postshock rest frame, but the *emitted* power is Lorentz invariant [see §2.15], and so is the power per $\ln \nu$ since $\ln \nu$ and $\ln \bar{\nu}$ differ by an additive constant. The *received* power is larger than the emitted power by a factor $(1 - \beta)^{-1}$, however, because the emitted energy is received over a time $dt_{\text{rec}} = (1 - \beta)dt_{\text{emit}}$. Thus

$$\left(\frac{dP}{d \ln \nu} \right)_{\nu_{\text{min,rec}}} \approx \Gamma^2 \left(\frac{d\bar{P}}{d \ln \bar{\nu}} \right)_{\nu_{\text{min}}} \approx \Gamma^2 \frac{\sigma_{\text{T}}}{m_e c} \gamma'_{\text{min}} \bar{U}'_e \bar{U}'_B \bar{V}'. \quad (3.21)$$

(Note: the factor $dt_{\text{emit}}/dt_{\text{rec}} \approx \Gamma^2$ not $2\Gamma^2$ because the postshock flow has Lorentz factor $\Gamma/\sqrt{2}$.) Now

$$\bar{V}' \bar{N}' \approx \frac{4\pi r_s^3}{3} \bar{N} \Rightarrow \bar{V}' = \frac{4\pi r_s^3}{3\sqrt{8}\Gamma} \approx \frac{E}{\Gamma^3 \bar{N} m_p c^2},$$

using (3.6) & (3.9). Using this relation and (3.18), (3.17), & the first line of (3.16) to eliminate \bar{V}' , $\bar{\gamma}$, and $\bar{\nu}$ from (3.21) yields

$$\left(\frac{dP}{d \ln \nu} \right)_{\nu_{\text{min,rec}}} \approx \sqrt{2} \bar{f}'_B (\bar{f}'_e)^2 \frac{c\sigma_{\text{T}} m_p^2}{m_e^2} \bar{N} E \Gamma^4. \quad (3.22)$$

Notice that the frequency (3.19) is also $\propto \Gamma^4$. Dividing (3.22) by $4\pi d^2 \nu_{\text{min}}$ gives an estimate for the flux density at the peak of the spectrum:

$$F_{\nu_{\text{min}}} \sim 0.03 (10^2 f'_B)^{1/2} \bar{N}_0^{-1/2} E_{\text{iso},53} d_{28}^{-2} \text{ Jy}. \quad (3.23)$$

Thus, a simple and convenient prediction of the synchrotron blastwave model of afterglows is that *the flux density at the peak of the spectrum is independent of time*—presuming, of course, that the external density (\bar{N}) and equipartition factor f'_B are constant. Another caveat is that the equivalent

isotropic shock energy E_{iso} will decrease both because of actual radiative losses, and perhaps more importantly, because the energy per solid angle declines after the time (3.12) as the jet opens up (this is ~ 20 day if $\theta_j \approx 0.3$ rad as found for GRB 970508).

In view of the number of simplifying assumptions that have been made, it is very reassuring that the predictions $F_{\nu_{\text{min}}} \approx \text{constant}$ and $\nu_{\text{min}} \propto t^{-3/2}$ are indeed satisfied, at least at early times (before the break attributed to the jet). Another prediction that one can make is that the exponent p of the electron spectrum controls both the slope of the spectrum at a fixed time ($F_\nu \propto \nu^{(1-p)/2}$ for $\nu_{\text{min}} < \nu < \nu_{\text{cool}}$) the decline of F_ν with time at a fixed frequency:

$$F_\nu \approx F_{\nu_{\text{min}}} \left(\frac{\nu}{\nu_{\text{min}}} \right)^{(1-p)/2} \propto \nu_{\text{min}}^{(p-1)/2} \propto t^{-3(p-1)/4}, \quad (3.24)$$

as long as $t < t_j$ and $\nu_{\text{cool}} > \nu > \nu_{\text{min}}$. Thus if the observations are fit to a double powerlaw of the form $F_\nu \propto t^{-\alpha} \nu^{-\beta}$, then one expects $\alpha = 3\beta/2$. Indeed, for $p \approx 2.3$ as predicted by models of particle acceleration at shocks, (3.24) predicts $F_\nu \propto \nu^{-0.7} t^{-1}$, approximately as observed.

This discussion has largely avoided the complications arising after t_j when the jet-like nature of the outflow becomes important. But qualitatively, perhaps the best evidence for jets is from those afterglows that have been observed at late times in the radio. In this phase, at $t \sim 1$ yr, even a spherical blastwave should be marginally nonrelativistic, so that beaming effects are not dominant and the entire outflow should contribute to the light curve. The fact that the radio flux at late times is substantially less than the predictions of a spherical model, as shown in Fig. 3.8, indicates that the initial outflow was not spherically symmetric ($\Omega_j \ll 4\pi$ and that the total energy is $\ll 10^{53}$ erg. In fact, the inferred total energy $E = (\theta_j^2/4)E_{\text{iso}}$ seems to show less variation than E_{iso} and θ_j separately: $E \approx 10^{50.7 \pm 1.0}$ [45].

3.5 Problems for Chapter 3

1. (a) Suppose that the preshock medium is not uniform but has a power-law dependence on distance from the source,

$$\bar{N}(r) = K r^{-w}, \quad K, w \text{ constant}; \quad w < 3.$$

Evaluate for the afterglow phase the powerlaw indices x_1, \dots, x_8 in the following relations: $\Gamma \propto t^{x_1}$, $t_j \propto \theta_j^{x_2}$, $\nu_{\min} \propto t^{x_3}$, $F_{\nu_{\min}} \propto t^{-x_4}$, and

$$F_\nu \propto \begin{cases} \nu^{x_5} t^{x_6} & \nu < \nu_{\min} \\ \nu^{x_7} t^{x_8} & \nu > \nu_{\min} \end{cases}$$

You may assume $t < t_j$ except when calculating x_2 .

(b) Evaluate the constants K and w assuming that the progenitor of the GRB was a massive star that emitted a steady spherically symmetric wind with constant mass-loss rate $\dot{M} = 10^{-4} M_\odot \text{ yr}^{-1}$ and constant outflow speed $v = 10^3 \text{ km s}^{-1}$. At what radius does the number density of the wind fall to 1 cm^{-3} ?

Chapter 4

Black-hole Basics

4.1 General-Relativistic kinematics

This chapter and the next discuss parts of General Relativity that are most relevant to present-day astrophysics. They are no substitute for a full course in GR¹ but are meant to be self-contained. The equations of motion of a test particle in a prescribed metric are derived from the principle of least action (which is enough to understand orbits around black holes) eschewing covariant derivatives. In the next chapter, the orbital results will be used to explain some basic properties of accretion onto black holes, such as the maximum efficiency of conversion of mass to energy in a thin disk, spin-up of black holes, and irreducible mass. The field equations are not discussed, except in Chapter 8 where we treat gravitational waves; that chapter gives a self-contained derivation of the linearized form of the field equations directly from Lorentz and gauge invariance.

4.1.1 The Principle of Equivalence

Newton wrote that bodies free of external forces move uniformly in straight lines. Einstein's revision says that bodies free of external *nongravitational* forces move on spacetime geodesics, a term originally from cartography meaning the straightest/shortest paths possible on a curved surface. GR views gravitational forces as fictitious, just as newtonian mechanics views centrifugal and Coriolis forces as artifacts of an accelerated frame of reference. Nevertheless tidal fields, which are felt as relative accelerations between freely-falling particles (geodesics), *are* physically real. Tidal fields are a manifestation of curvature. The source of curvature is mass.

The elimination of gravitational forces is possible because of the Principle of Equivalence (PE), which began with Galileo's observation that all bodies accelerate equally in a gravitational field regardless of mass or composition. Newton tested this experimentally at a level $\approx 10^{-3}$ using pendulums. Another formulation of the PE is that external gravitational effects can be removed by adopting a freely-falling frame of reference, at least to the extent that the gravitational field is uniform and constant; this formulation appears explicitly in the *Principia*. The PE is essential to a geometric description of gravity. It would not make sense to say that free-particle motion follows the shape of spacetime if different materials or fundamental particles accelerated differently in gravitational fields.

Still another formulation of the PE is that *no local measurement can distinguish between a gravitational field and an acceleration*. This is really a statement about limits and is best clarified by examples, since otherwise it would seem to deny the reality of tidal fields. The critical word is "local": a longer time interval and/or a greater spatial separation is needed to measure a tide than an acceleration, so tides are less local.

¹An excellent introductory text is that of Schutz [56].

An important and experimentally tested application of the PE is gravitational redshift. Consider an observer in a rocket ship undergoing constant acceleration g in flat space (*i.e.*, no gravity). Inertial observer O comoves with the rocket at $t = 0$ and sees the rocket to have velocity gt at time t ($gt \ll c$). At $t = 0$, a photon of frequency ν is released from the back of the rocket cabin, and it is absorbed at the front of the cabin after time $t \approx h/c$, where h is the height of the cabin (not Planck's constant). The frequency is constant according to O , but because the rocket velocity has increased by $v \approx gt \approx gh/c$, the receiver accelerating with the cabin measures a frequency shift

$$\frac{\Delta\nu}{\nu} \approx -\frac{v}{c} \approx -\frac{gh}{c^2}.$$

The PE implies that two stationary observers separated vertically by h in the gravitational field g of the earth should see the same shift. This has actually been measured [50]; note that $\Delta\nu/\nu \approx 10^{-15}$ over $h = 10$ m. The generalization is

$$\frac{\nu_2 - \nu_1}{\nu} \approx -\frac{\Phi_2 - \Phi_1}{c^2} \quad (4.1)$$

for observers stationary in a newtonian gravitational potential Φ . This formula is approximate but accurate as long as $\Delta\nu/\nu \ll 1$.

One is forced to conclude that *time flows more slowly in deeper gravitational potentials*. To see why, imagine that the two observers keep time with atomic clocks, which essentially count cycles of a 9.2 GHz cesium hyperfine transition, and send one another microwaves at the frequencies that their clocks produce. Observer 2 will see the light sent by observer 1 to be redshifted. Yet both observers agree that the separation between them is constant, because for example the roundtrip travel time of light signals does not change. The redshift therefore cannot be ascribed to a steady increase in this travel time, *i.e.* it is not a first-order Doppler shift. So observer 2 will conclude that observer 1's clock runs slow by the amount (4.1).

4.1.2 Metric in general coordinates

As in special relativity [SR], events are labeled by four coordinates, but these coordinates may not be inertial—in fact cannot be inertial where there is curvature. In GR, the choice of coordinates is arbitrary,² although some choices are usually more convenient than others. But there is no universally most convenient system or class of systems—it depends upon the problem at hand, especially any symmetries that the spacetime may have. Therefore, the central concepts and equations of GR are designed to hold true in arbitrary coordinates.

Local properties of curved spacetime are described by the metric $g_{\mu\nu}$ (and its derivatives), which determines the interval associated with infinitesimal coordinate separations dx^μ :

$$ds^2 = g_{\mu\nu} dx^\mu dx^\nu. \quad (4.2)$$

Antisymmetric parts $g_{\mu\nu} - g_{\nu\mu}$ would have no effect on ds^2 , so $g_{\mu\nu} = g_{\nu\mu}$. In D dimensions, the metric has D^2 components but only $D(D+1)/2$ independent ones. The metric components are functions of the coordinates, which are arbitrary. Consider two coordinate systems $\{x^\mu\}$ and $\{x^{\bar{\mu}}\}$ valid in overlapping regions of spacetime. The metrics in the two systems are related by the invariance of the interval, so that

$$g_{\mu\nu} dx^\mu dx^\nu = ds^2 = g_{\bar{\mu}\bar{\nu}} dx^{\bar{\mu}} dx^{\bar{\nu}},$$

from which it follows that the metric transforms according to

$$g_{\mu\nu} = g_{\bar{\mu}\bar{\nu}} \frac{\partial x^{\bar{\mu}}}{\partial x^\mu} \frac{\partial x^{\bar{\nu}}}{\partial x^\nu}. \quad (4.3)$$

²except that the coordinates should be independent: If P and Q are distinct events, then $x^\mu(P) - x^\mu(Q)$ should be nonzero for at least one of the four values $\{0, 1, 2, 3\}$ of the index μ . There are also some technical restrictions on the smoothness of the coordinates when viewed as differentiable functions on spacetime.

Note carefully how the upstairs and downstairs indices balance. Here $\partial x^{\bar{1}}/\partial x^2$ means the partial derivative of the function $x^{\bar{1}}$ with respect to x^2 at constant x^0, x^1, x^3 . We could write this as $x^{\bar{1}}_{,2}$ but the comma notation for partial derivatives is rarely applied to the coordinate functions themselves. All functions appearing in eq. (4.3) [and similar transformation laws for other tensors] are evaluated at the same event.

Although a proof will not be given, the following very important fact is a consequence of the PE:

Near any nonsingular event E , coordinates $x^{\hat{\mu}}$ can be found such that

$$g_{\hat{\mu}\hat{\nu}}(E) = \eta_{\hat{\mu}\hat{\nu}} \quad \text{and} \quad g_{\hat{\mu}\hat{\nu},\hat{\lambda}}(E) = 0. \quad (4.4)$$

Such coordinates constitute a freely-falling reference frame [henceforth FFRF] at E . FFRF coordinates will be marked by hats on the indices. Although the freely-falling coordinates extend to at least a small neighborhood of E , the relations (4.4) are not guaranteed except at E ; in general, each event has its own FFRF. If the properties (4.4) can be extended to a finite region using a single coordinate system, then the spacetime in that neighborhood is flat. Whether or not the region is flat, geodesics passing through E satisfy

$$\frac{d^2 x^{\hat{\mu}}}{d\tau^2}(E) = 0, \quad (4.5)$$

just as one would expect for an unaccelerated trajectory written in inertial coordinates in Special Relativity [SR]. We will prove this shortly. Thus an FFRF is as close as one can come to an inertial reference frame in a general curved spacetime. Before trying to interpret a local quantity in GR, it is often a good idea to transform it into an FFRF so that one can appeal to physical laws as they are formulated in SR. Even at a given event E , FFRFs are not unique, since any Lorentz transformation

$$x^{\hat{\mu}'} \equiv \Lambda^{\hat{\mu}'}_{\hat{\mu}} x^{\hat{\mu}}$$

yields another FFRF at E as long as the coefficients $\Lambda^{\hat{\mu}'}_{\hat{\mu}}$ are constant. We are also free to add constant offsets $a^{\mu'}$ to the righthand side above, making it a local Poincaré rather than Lorentz transformation.

It can be shown that a necessary and sufficient condition for flatness is the vanishing—in *any* coordinates—of a certain set of $D^2(D^2 - 1)/12$ algebraic combinations of the metric and its first ($g_{\mu\nu,\kappa}$) and second ($g_{\mu\nu,\kappa\lambda}$) partial derivatives throughout the region in question. Gauss proved this for $D = 2$, where just one combination is involved, the intrinsic curvature. (Gauss also invented the idea of metric). In spacetime ($D = 4$) there are 20 relevant combinations, which are the independent components of the Riemann curvature tensor $R_{\mu\nu\kappa\lambda}$. In an FFRF, $R_{\hat{0}\hat{i}\hat{0}\hat{j}} = R_{\hat{0}\hat{j}\hat{0}\hat{i}}$ is the $i\hat{j}$ th component of the tidal field experienced by particles that are nearly at rest in that FFRF.

Problem 4.1. *Two neighboring and nearly comoving observers fall freely and nonrelativistically in a newtonian gravitational field. Express their relative 3-acceleration in terms of their spatial separation and derivatives of the newtonian potential.*

4.1.3 Geodesics

A path is a connected one-dimensional sequence of events. A curve is a path plus a choice of parametrization $x^\mu(\sigma)$, where σ is the parameter. If $\sigma = \sigma(\theta)$ then $x^\mu(\theta) \equiv x^\mu[\sigma(\theta)]$ is a new curve on the same path. The tangent to $x^\mu(\sigma)$ is $dx^\mu/d\sigma$, so

$$\frac{dx^\mu}{d\theta} = \frac{dx^\mu}{d\sigma} \frac{d\sigma}{d\theta}.$$

The direction of the tangent depends only on the path, but its length depends on the curve. In spacetime, paths are classified as timelike, spacelike, or null according as

$$g_{\mu\nu} \frac{dx^\mu}{d\sigma} \frac{dx^\nu}{d\sigma} \quad (4.6)$$

is < 0 , > 0 , or $= 0$, respectively. The classification is independent of parameter as long as $d\sigma/d\theta \neq 0$. A timelike path can always be parametrized by proper time

$$g_{\mu\nu} \frac{dx^\mu}{d\tau} \frac{dx^\nu}{d\tau} = -1.$$

We reserve the symbol τ for proper time. Then the tangent

$$u^\mu \equiv \frac{dx^\mu}{d\tau}, \quad u^\mu u_\mu = -1 \quad (4.7)$$

is the 4-velocity. 4-acceleration is more complicated than $d^2x^\mu/d\tau^2$ except in a FFRF.

The length of a timelike path between events A and B is

$$L = \int_a^b d\sigma \sqrt{-g_{\mu\nu} \frac{dx^\mu}{d\sigma} \frac{dx^\nu}{d\sigma}} \quad : \quad x^\mu(a) = x^\mu(A), \quad x^\mu(b) = x^\mu(B). \quad (4.8)$$

Note length is independent of parametrization.

Every child knows that a straight line gives the shortest distance between two points—in euclidean geometry. In general, a path is extremal if $\delta L = 0$, meaning that the length is unchanged to first order in δx^μ by the variation

$$x^\mu(\sigma) \mapsto x^\mu(\sigma) + \delta x^\mu(\sigma) \quad \delta x^\mu(a) = \delta x^\mu(b) = 0.$$

I write “extremal” rather than “shortest” because, as a consequence of the minus sign in the metric, the favored paths are actually *longest*.

Problem 4.2. Show that if events A and B are connected by a timelike path, then there exists a path of zero length between them.

Instead of $\delta L = 0$, consider the variational problem $\delta S = 0$, where

$$S \equiv \frac{1}{2} \int_a^b d\sigma \, g_{\mu\nu} \frac{dx^\mu}{d\sigma} \frac{dx^\nu}{d\sigma} \quad : \quad x^\mu(a) = x^\mu(A), \quad x^\mu(b) = x^\mu(B). \quad (4.9)$$

Lacking the square root, S does depend upon parametrization, unlike L . It looks a lot like the action of classical mechanics, with σ playing the role of time. The extremal curve for (4.9) solves the Euler-Lagrange equations

$$\frac{d}{d\sigma} \left(\frac{\partial \mathcal{L}}{\partial \dot{x}^\alpha} \right) - \frac{\partial \mathcal{L}}{\partial x^\alpha} = 0,$$

where $\dot{x}^\mu \equiv dx^\mu/d\sigma$ and the “lagrangian” is³

$$\mathcal{L}(x^\alpha, \dot{x}^\alpha) = \frac{1}{2} g_{\mu\nu}(x^\alpha) \dot{x}^\mu \dot{x}^\nu, \quad (4.10)$$

³The notation $g_{\mu\nu}(x^\alpha)$ means that the metric depends on the whole set (x^0, x^1, x^2, x^3) ; the α is not a free index when inside the arguments of functions.

so that
$$\frac{1}{2} \frac{d}{d\sigma} \left(g_{\alpha\nu} \frac{dx^\nu}{d\sigma} + g_{\mu\alpha} \frac{dx^\mu}{d\sigma} \right) - \frac{1}{2} g_{\mu\nu, \alpha} \frac{dx^\mu}{d\sigma} \frac{dx^\nu}{d\sigma} = 0.$$

Dummy indices such as μ and ν above can be renamed at will, and the metric is symmetric, so the two terms in parentheses can be combined:

$$\frac{d}{d\sigma} \left(g_{\alpha\nu} \frac{dx^\nu}{d\sigma} \right) - \frac{1}{2} g_{\mu\nu, \alpha} \frac{dx^\mu}{d\sigma} \frac{dx^\nu}{d\sigma} = 0. \quad (4.11)$$

The extremal curve for the action (4.9) has a path of extremal length (4.8), and therefore (4.11) is actually the general equation for geodesics. To see this, note first of all that since \mathcal{L} does not depend explicitly on σ , the ‘‘hamiltonian’’

$$\mathcal{H} = \dot{x}^\alpha \frac{\partial \mathcal{L}}{\partial \dot{x}^\alpha} - \mathcal{L} = \frac{1}{2} g_{\mu\nu}(x^\alpha) \dot{x}^\mu \dot{x}^\nu$$

is conserved, *i.e.* $d\mathcal{H}/d\sigma = 0$ along extremal curves, as can be checked using eq. (4.11). So one may as well restrict the search for solutions of $\delta S = 0$ to curves of constant \mathcal{H} , hence constant squared tangent (4.6). For any such curve, whether or not extremal, $L = (b - a)\sqrt{-2\mathcal{H}}$ and $S = (b - a)\mathcal{H}$, whence $S = -L^2/2(b - a)$. It follows that

$$\delta S = - \frac{L\delta L}{b - a}.$$

So a curve that is extremal for S has a path that is extremal for L . This argument fails for null paths, where $L = 0$. It can be shown by other means that (4.11) is in fact the correct equation even for null geodesics.

For timelike geodesics, σ differs from τ only by a constant factor and constant offset. A relationship of the form $Y = mX + b$ between variables X, Y is called ‘‘affine’’ (‘‘linear’’ only if $b = 0$) therefore σ is an affine parameter. Clearly σ can be replaced by τ in eq. (4.11) if the geodesic is timelike. In view of eq. (4.4), the geodesic equation indeed reduces to eq. (4.5) in a FFRF.

4.1.4 Momentum

According to classical mechanics, the momentum canonically conjugate to coordinate x^α is

$$\tilde{p}_\alpha \equiv \frac{\partial \mathcal{L}}{\partial \dot{x}^\alpha}.$$

For \mathcal{L} given by eq. (4.10),

$$\tilde{p}_\alpha = g_{\alpha\nu} \frac{dx^\nu}{d\sigma}.$$

In a FFRF this reduces to $\tilde{p}_{\hat{\alpha}} = \eta_{\hat{\alpha}\hat{\mu}} dx^{\hat{\mu}}/d\sigma$, which differs by a constant factor from the physical 4-momentum $p_{\hat{\alpha}} = m\eta_{\hat{\alpha}\hat{\mu}} dx^{\hat{\mu}}/d\tau$ for a particle of mass m . It is therefore usual to define the 4-momentum in general coordinates by

$$p_\alpha \equiv m g_{\alpha\nu} \frac{dx^\nu}{d\tau}, \quad (4.12)$$

provided $m > 0$. For massless particles, the affine parameter is usually scaled so that

$$p_\alpha \equiv g_{\alpha\nu} \frac{dx^\nu}{d\sigma} \quad (4.13)$$

becomes the physical momentum $p_{\hat{\alpha}}$ in a FFRF.

4.1.5 Constants of motion

In a symmetrical spacetime, such as a stationary black hole, it can be arranged that the metric is independent of at least one of the coordinates (by suitable choice of coordinates). If the metric is independent of x^3 , for example, then it follows from eq. (4.11) that p_3 is constant on a geodesic. This fact is a great help in finding solutions to the geodesic equation. Even without special symmetry, $g_{\mu\nu}\dot{x}^\mu\dot{x}^\nu$ is constant and provides a first integral of the four geodesic equations (4.11).

Problem 4.3. *The metric of flat spacetime in cylindrical polar coordinates $x^\mu \in (t, R, \phi, z)$ is defined by*

$$ds^2 = -dt^2 + dR^2 + R^2d\phi^2 + dz^2.$$

Find and interpret p_0 , p_2 , and p_3 .

4.2 Non-rotating black holes

The Schwarzschild metric describes a spherically symmetric, static, vacuum spacetime: in particular, the spacetime of a nonrotating black hole. The metric has just one free parameter—the mass M . It was the first nontrivial exact solution of Einstein’s equations discovered (in 1916). It is perhaps the most important, in part because of Birkhoff’s Theorem, which states that “any spherically symmetric vacuum solution is static,” and therefore described by the Schwarzschild metric for some M . Birkhoff’s Theorem is the analog in GR of Newton’s statement that the external gravitational field of a sphere depends only on its mass, not on its radius. For example, if small corrections due to the planets, the solar wind, and the sun’s rotation are neglected, then the Sun’s gravitational field obeys the Schwarzschild solution. The Sun lacks an event horizon because the Schwarzschild solution applies only to the vacuum region outside the Sun, and the Sun is much larger than its own Schwarzschild radius.

Another important application of Birkhoff’s Theorem is to cosmology. Of course GR is required to describe the metric on scales comparable to the horizon, but one often uses newtonian gravitational physics on scales $\lesssim 300 h^{-1}$ Mpc ($z \lesssim 0.1$). The justification for this is that if one imagines evacuating a comoving sphere from such a universe, then Birkhoff’s Theorem says that the interior is the Schwarzschild solution for $M = 0$ (because there is no interior mass), which is flat space.⁴ This is true despite the expansion of the rest of the universe, as long as it is spherically symmetric. Therefore in the actual universe where the sphere is not empty, the gravitational field inside the sphere is caused entirely by the matter it contains; if this field is weak and the sphere expands slowly compared to c , then the newtonian approximation is accurate.

4.2.1 Schwarzschild metric and coordinates

In Schwarzschild’s original choice of coordinates $x^\mu \in (t, r, \theta, \phi)$,

$$ds^2 = -\left(1 - \frac{2M}{r}\right) dt^2 + \left(1 - \frac{2M}{r}\right)^{-1} dr^2 + r^2(d\theta^2 + \sin^2\theta d\phi^2), \quad (4.14)$$

or in other words

$$g_{00} = -(g_{11})^{-1} = -\left(1 - \frac{2M}{r}\right), \quad g_{22} = r^2, \quad g_{33} = r^2 \sin^2\theta, \quad g_{0i} = 0.$$

As is customary in GR, we have adopted units $G = c = 1$ so that mass, length, and time are equivalent: one solar mass M_\odot corresponds approximately to 1.5 km and 5×10^{-6} s. In ordinary

⁴Birkhoff’s Theorem doesn’t strictly apply if the vacuum includes a cosmological constant, but it doesn’t make much difference on scales $\ll c/\sqrt{\Lambda}$.

units,

$$g_{00} \rightarrow -\left(c^2 - \frac{2GM}{r}\right).$$

Many other coordinate systems could be used, but Schwarzschild coordinates are both mathematically convenient and relatively easy to interpret.

The interpretation begins with the notion of a stationary observer [SO]. Mathematically, a SO sits at constant r, θ, t , and her 4-velocity

$$u^\mu = \frac{dx^\mu}{d\tau} = \frac{1}{\sqrt{-g_{00}}} (1, 0, 0, 0), \quad \text{so } g_{\mu\nu}u^\mu u^\nu = -1. \quad (4.15)$$

Physically, a SO recognizes herself as such by measuring a constant blueshift in the spectrum of each distant star (to the extent that intrinsic accelerations of the stars are negligible). If the black hole is at rest with respect to the stars, then they all show the same blueshift. To see this, note quite generally that an observer of 4-velocity u^μ measures the energy of a photon of 4-momentum p_μ as $(-p_\mu u^\mu) = -u^0 p_0$.

Problem 4.4. Verify the formula $-p_\mu u^\mu$ for the measured energy by evaluating it in a FFRF that is instantaneously at rest with respect to the observer, and then proving that the expression is invariant under transformation of coordinates.

But the photon travels to the observer on a null geodesic with conserved p_0 since the metric doesn't depend on x^0 ; and far from the black hole where space is flat, the photon was emitted with energy $h\nu_\infty$, hence $-p_0 = h\nu_\infty$ all along the geodesic. Thus the measured frequency is

$$\nu_r = u^0 \nu_\infty = \frac{\nu_\infty}{\sqrt{-g_{00}}} = \nu_\infty \left(1 - \frac{2M}{r}\right)^{-1/2}. \quad (4.16)$$

If one expands the square root to first order in $2GM/c^2 r$, this agrees with the gravitational-redshift formula derived in the last lecture,

$$\frac{\nu_r - \nu_\infty}{\nu_\infty} \approx -\frac{\Phi_r - \Phi_\infty}{c^2}.$$

Actually the correspondence can be made exact by rewriting the weak-field formula as

$$\frac{\nu_1}{\nu_2} = \frac{1 + \Phi_2/c^2}{1 + \Phi_1/c^2},$$

and interpreting

$$\frac{\Phi}{c^2} \rightarrow \sqrt{-g_{00}} - 1. \quad (4.17)$$

The SO needs a rocket to maintain her position and avoid falling into the black hole. The 4-acceleration she requires is simply the lefthand side of the geodesic equation evaluated on her worldline:

$$a_\alpha = \frac{d}{d\tau} \left(g_{\alpha\nu} \frac{dx^\nu}{d\tau} \right) - \frac{1}{2} g_{\mu\nu,\alpha} \frac{dx^\mu}{d\tau} \frac{dx^\nu}{d\tau} \rightarrow -\frac{1}{2} g_{00,\alpha} u^0 u^0 = \left(0, \frac{M/r^2}{-g_{00}}, 0, 0 \right).$$

The proper acceleration, which is what the SO measures with an accelerometer, can be determined by transforming this into a FFRF where she is instantaneously at rest. It is equivalent, and more convenient, to project a_α onto a radial unit vector:

$$l^\mu = \frac{1}{\sqrt{g_{11}}} (0, 1, 0, 0); \quad g_{\mu\nu} l^\mu l^\nu = 1, \quad g_{\mu\nu} l^\mu u^\nu = 0. \quad (4.18)$$

Thus the radial proper acceleration of the SO is

$$l^\alpha a_\alpha = \frac{M}{r^2} \left(1 - \frac{2M}{r}\right)^{-1/2}. \quad (4.19)$$

At large r this agrees with the newtonian formula, but the proper acceleration of stationary observers is infinite at the Schwarzschild radius

$$R_S \equiv \frac{2GM}{c^2} \approx 3.0 \left(\frac{M}{M_\odot}\right) \text{ km}. \quad (4.20)$$

In fact, one way to remember the result (4.19) is to compute the proper acceleration as $\Phi_{,i}$ with Φ given by eq. (4.17). (*Warning: although this works for slowly-moving objects in Schwarzschild coordinates, it is not a general result.*) The acceleration is outwards rather than inwards because GR considers freely-falling observers unaccelerated and SOs accelerated, while newtonian mechanics takes the opposite view.

The SO determines her angular coordinates θ, ϕ as those of the star she sees overhead, *i.e.*, in the direction of her acceleration. Consider two SOs at the same r separated by $(d\theta, d\phi)$ [they know they are at the same r because they see the same blueshift for distant stars]. Their proper separation

$$ds = \sqrt{g_{\mu\nu} dx^\mu dx^\nu} = r \sqrt{d\theta^2 + \sin^2 \theta d\phi^2},$$

just as in polar coordinates in flat space. It follows that the proper circumference of a circle of constant r is $2\pi r$, and the proper area of a sphere is $4\pi r^2$. This gives the physical interpretation of the r coordinate. On the other hand, r is not simply related to radial distance; the proper separation associated with a coordinate separation $dx^\mu = (0, dr, 0, 0)$ is not dr but $dr\sqrt{g_{11}}$.

Finally, the t coordinate is the proper time of SOs in the limit $r \rightarrow \infty$. This could be established by broadcasting a carrier signal of known ν_∞ to all SOs. Each SO at finite r knows that her own proper-time clock elapses more slowly than t :

$$d\tau = dt\sqrt{-g_{00}} \quad (4.21)$$

and corrects accordingly. (Here, as for radial acceleration, the newtonian or weak-field result becomes exact in Schwarzschild coordinates if $\Phi/c^2 \rightarrow -1 + \sqrt{-g_{00}}$.) Synchronization of t -time can be achieved using the round-trip delay of lightsignals exchanged between each SO and the standard clock.

4.2.2 Null (photon) orbits

By definition of a null curve, the squared tangent $g_{\mu\nu} \dot{x}^\mu \dot{x}^\nu = 0$, so from eq. (4.14),

$$0 = -\left(1 - \frac{2M}{r}\right) \left(\frac{dt}{d\sigma}\right)^2 + \left(1 - \frac{2M}{r}\right)^{-1} \left(\frac{dr}{d\sigma}\right)^2 + r^2 \left(\frac{d\theta}{d\sigma}\right)^2 + r^2 \sin^2 \theta \left(\frac{d\phi}{d\sigma}\right)^2. \quad (4.22)$$

For $\alpha = 2$, the geodesic equation (4.11) reads

$$\frac{d}{d\sigma} \left(r^2 \frac{d\theta}{d\sigma} \right) = r^2 \sin \theta \cos \theta \left(\frac{d\phi}{d\sigma} \right)^2. \quad (4.23)$$

Because of spherical symmetry, we can always rotate axes so that $\theta = \pi/2$ and $\dot{\theta} = 0$ at $\sigma = 0$. It then follows from eq. (4.23) that $d^2\theta(0)/d\sigma^2 = 0$, and by iterative differentiation of eq. (4.23), $d^n\theta(0)/d\sigma^n = 0$ for every $n > 0$. So the orbit remains in the plane $\theta = \pi/2$. Furthermore on

geodesics, the energy $E = -p_0$ and ϕ component of angular momentum $L_\phi = p_\phi$ are conserved because $g_{\mu\nu,0} = g_{\mu\nu,3} = 0$:

$$E = \left(1 - \frac{2M}{r}\right) \frac{dt}{d\sigma}, \quad L_\phi = r^2 \sin^2 \theta \frac{d\phi}{d\sigma}. \quad (4.24)$$

Eq. (4.22) now becomes, for geodesics,

$$0 = \left(1 - \frac{2M}{r}\right)^{-1} \left[-E^2 + \left(\frac{dr}{d\sigma}\right)^2 \right] + \frac{L^2}{r^2},$$

or equivalently,

$$\left(\frac{dr}{d\sigma}\right)^2 = E^2 - 2V(r, L), \quad (4.25)$$

$$\text{where} \quad V(r, L) \equiv \frac{L^2}{2r^2} \left(1 - \frac{2M}{r}\right). \quad (4.26)$$

With the total angular momentum L in place of L_ϕ , eqs. (4.25)-(4.26) hold for arbitrary orientations of the orbital plane.

The function $V(r, L)$ is an effective potential for radial motion. At $r < 2M$, $V < 0$ so that the righthand side of eq. (4.25) is positive, and it follows that $dr/d\sigma$ cannot change sign at $r < 2M$; this follows also from eq. (4.22), so it is true for all null paths, not just geodesics. Therefore if a photon is inside the Schwarzschild radius and travelling inward, it will have to continue to $r = 0$. The same can be demonstrated for massive particles. The surface $r = 2M$ is an event horizon: a point of no return.

Differentiating eq. (4.25) and dividing by $2dr/d\sigma$ yields

$$\frac{d^2r}{d\sigma^2} = -\frac{\partial V}{\partial r} = \frac{L^2}{r^3} \left(1 - \frac{3M}{r}\right). \quad (4.27)$$

Circular photon orbits exist. On such an orbit, $r = r_{\text{circ}} = \text{constant}$, so $dr/d\sigma = 0 = d^2r/d\sigma^2$. From eq. (4.27),

$$r_{\text{circ}} = 3M,$$

and substituting this into eq. (4.25),

$$(L/E)_{\text{circ}}^2 = 27M^2.$$

It's easy to see that the circular orbit is unstable, since r_{circ} is a local maximum of V .

More significantly, consider a photon approaching the black hole from $r \gg 2M$; then for $\theta \equiv \pi/2$,

$$\frac{L}{E} \rightarrow r^2 \frac{d\phi}{dt} = cb \quad \text{as } r \rightarrow \infty,$$

where b is the impact parameter: that is, the distance of closest approach that one would calculate by extrapolating the trajectory in flat space. Let the actual minimum radius be r_{min} , which is clearly an increasing function of b . If $r_{\text{min}} > 0$ then $dr/d\sigma = 0$ and $d^2r/d\sigma^2 \geq 0$ at $r = r_{\text{min}}$. But eq. (4.27) shows that the latter implies $r_{\text{min}} \geq 3M$, else the photon continues inward to $r = 0$. Evaluating eq. (4.25) at r_{min} , we find $(L/E)^2 \geq (L/E)_{\text{circ}}^2$. So the minimum impact parameter for which the photon can escape back to infinity is

$$b_{\text{min}} = \left(\frac{L}{E}\right)_{\text{circ}} = \frac{3\sqrt{3}}{2} R_S. \quad (4.28)$$

If one saw a black hole from a great distance against a uniformly bright background, its apparent radius would be $b_{\min} \approx 2.6 R_S$.

Finally, we show that although a null trajectory crossing the event horizon can never return, it takes an infinite time to get there. Eq. (4.25) can be solved as a quadrature:

$$d\sigma = - \frac{dr}{\sqrt{E^2 - 2V(r, L)}} . \quad (4.29)$$

Since $V = 0$ at $r = 2M$, it's clear that the Schwarzschild radius is reached after a finite increment in affine parameter σ , provided of course that $L/E < (L/E)_{\text{circ}}$. If one eliminates $d\sigma$ in favor of dt using eq. (4.24),

$$dt = - \frac{E r dr}{(r - 2M)\sqrt{E^2 - 2V(r, L)}} . \quad (4.30)$$

Upon integration from any $r > 2M$ down to $r = 2M$, the change in t diverges:

$$\begin{aligned} t - t_0 &\approx 2M \ln \left(\frac{\text{const.}}{r - 2M} \right) \quad \text{as } r \rightarrow 2M , \\ \text{or} \quad r - 2M &\approx (\text{const.}) \times \exp[-t/2M] \quad \text{as } t \rightarrow \infty . \end{aligned} \quad (4.31)$$

Problem 4.5. By eliminating $d\sigma$ from eq. (4.29) in favor of $d\phi$, or otherwise, show that a photon with $b \gg b_{\min}$ is deflected through angle $\approx 2R_S/b$ by mass M .

4.2.3 Timelike orbits

The first steps are the same as for null orbits, except that τ replaces σ on the righthand side of eq. (4.22), and -1 replaces 0 on the left. The conserved quantities E , and L_ϕ take the same form as in eq. (4.24) with $\sigma \rightarrow \tau$, so that $E \rightarrow -p_0/m$ and $L_\phi \rightarrow p_3/m$: *i.e.*, energy and angular momentum per unit mass. By an argument similar to the one for null geodesics, timelike geodesics also lie in a plane, so $L_\phi \rightarrow L$ in the radial equation (4.25). Instead of (4.26), the effective potential is

$$V(r, L) \equiv \frac{1}{2} \left(\frac{L^2}{r^2} + 1 \right) \left(1 - \frac{2M}{r} \right) , \quad (4.32)$$

where the “+1” reflects the replacement of 0 with -1 in eq. (4.22). As before, $\partial V/\partial r = 0$ on circular orbits, but now this condition yields

$$r_{\text{circ}} = \frac{L^2 \pm L\sqrt{L^2 - 12M^2}}{2M} . \quad (4.33)$$

Instead of a unique radius, there are in fact two possible circular orbits for every angular momentum $L > M\sqrt{12}$. Only the larger root for r_{circ} is stable, since $V \rightarrow -\infty$ as $r \rightarrow 0$, so that the smaller root corresponds to a local maximum of V . At $L = M\sqrt{12} \equiv L_{\min}$, the two roots merge, and

$$r_{\text{circ}}(L_{\min}) = 6M = 3R_S . \quad (4.34)$$

This defines the marginally stable orbit. Since $V(6M, \sqrt{12M^2}) = 4/9$, the energy per unit mass of the marginally stable orbit is [putting $dr/d\tau = 0$ in eq. (4.25)],

$$E_{\text{ms}} = \sqrt{\frac{8}{9}} \approx 1 - 0.057 . \quad (4.35)$$

Eq. (4.25) will be important to us when we discuss accretion disks. Notice that a geodesic escaping to $r = \infty$ must have $E \geq 1$.

Problem 4.6. Calculate the minimum impact parameter b_{\min} at which a timelike geodesic escapes capture, as a function of its 3-velocity at large distances, v_{∞} .

Now consider radial geodesics, $L = 0$. Furthermore, suppose that the particle is released from rest at some initial radius $r_0 > 2M$. Then $E^2 = 1 - 2Mr_0^{-1}$, and the analog of eq. (4.29) is

$$d\tau = - \frac{dr}{\sqrt{2M(r^{-1} - r_0^{-1})}} .$$

To simplify the discussion, take $r_0 \rightarrow \infty$, *i.e.* the particle falls from rest at some very large distance. A finite proper time elapses between any $r > 2M$ and the event horizon:

$$\tau(2M) - \tau(r) = \frac{4M}{3} \left(\frac{r}{2M} \right)^{3/2} .$$

However, as with the photon, an external SO says that the particle takes infinite time to reach the event horizon. Local SOs very near the horizon see the particle fall past them at almost the speed of light, but distant ones see it frozen at $r = 2M$. Actually they can't really "see" it for very long: if the infalling observer emits radial photons of constant frequency in his rest frame, then SOs at infinity see this signal redshifting exponentially with an e -folding time

$$\frac{R_S}{c} \approx 10^{-4} \left(\frac{M}{M_{\odot}} \right) \text{ s} .$$

Problem 4.7. Derive this last result. Hint: start from $p_{\mu}^{(\text{phot.})} u_{(\text{infall})}^{\mu} = -h\nu_0$.

4.2.4 Tidal fields

Suppose two particles are released from rest on the same radial line but separated by $\Delta r \ll r - 2M$. At the initial instant, both particles satisfy [cf. eqs. (4.25)&(4.32)]

$$\frac{dr}{d\tau}(0) = 0, \quad \frac{d^2r}{d\tau^2}(0) = -\frac{M}{r^2} ,$$

and therefore

$$\frac{d^2\Delta r}{d\tau^2}(0) = \frac{2M}{r^3} \Delta r .$$

Now the proper separation between the particles is actually $\Delta l = \Delta r \sqrt{g_{11}}$, but since $dg_{11}(0)/d\tau = 0$,

$$\frac{1}{\Delta l} \frac{d^2\Delta l}{d\tau^2} = \frac{1}{\Delta r} \frac{d^2\Delta r}{d\tau^2} = \frac{2M}{r^3} .$$

This is the $\hat{1}\hat{1}$ component of the tidal tensor: the ratio of proper relative radial acceleration to proper radial distance, measured in the instantaneous rest frame. By similar arguments using particles released from the same r but slightly different θ or ϕ , one finds that the $\hat{2}\hat{2}$ and $\hat{3}\hat{3}$ components of the tidal tensor are both $= -M/r^3$, and that the offdiagonal components vanish. All of this has exactly the same mathematical form as the newtonian tide, although r and τ are not exactly newtonian radius or time. Notice that the sum of the diagonal components of the tide vanishes; this is always true of the tidal field in vacuum (also true in newtonian theory). Finally, although we will not prove it, these tidal components are actually independent of velocity for radially falling observers. Thus an observer crossing the event horizon feels a finite radial tide $(2M)^{-2}$.

Problem 4.8. *An observer enclosed in a small windowless box is dropped from rest at an unknown (to him) radius from a black hole. Is there any way for him to know by local measurements, including tides, when he crosses the event horizon or what is the mass of the hole?*

4.3 Rotating black holes

Rotating blackholes have two parameters: mass (M) and angular momentum (J). For $G = c = 1$, the units of J are (mass)², and it is conventional to define $a \equiv J/M$. Rotating black holes are stationary but not static: that is, coordinates exist in which $g_{\mu\nu,0} \equiv 0$ but not also $g_{0i} = 0$. The “no-hair” theorem says that an isolated stationary black hole is completely determined by its total mass, angular momentum, and electrical charge. Astrophysically, any significant electrical charge would quickly be neutralized by selective accretion of ions or electrons, and episodes of significant nonstationarity are probably very brief, being damped by gravitational radiation on timescales $\approx GM/c^3$. Thus, the exact solution given below for an uncharged rotating black hole—the Kerr metric—describes all black holes likely to be encountered in astrophysics. Even better, despite superficial algebraic complexity, the Kerr metric conceals remarkable simplifications that one had no right to hope for, given the loss of spherical symmetry. Nature has been kind.

4.3.1 Kerr metric

$$ds^2 = -\frac{\Delta - a^2 \sin^2 \theta}{\rho^2} dt^2 - 2a \frac{2Mr \sin^2 \theta}{\rho^2} dt d\phi + \frac{(r^2 + a^2)^2 - a^2 \Delta \sin^2 \theta}{\rho^2} \sin^2 \theta d\phi^2 + \frac{\rho^2}{\Delta} dr^2 + \rho^2 d\theta^2, \quad (4.36)$$

$$\Delta \equiv r^2 - 2Mr + a^2, \quad (4.37)$$

$$\rho^2 \equiv r^2 + a^2 \cos^2 \theta. \quad (4.38)$$

In these Boyer-Lindquist coordinates, t is still the proper time of stationary observers [SOs] at infinity, and ϕ is clearly an angle in the direction of azimuthal symmetry. It is harder to interpret r and θ . They are topologically similar to the corresponding Schwarzschild coordinates, and in fact, eq. (4.36) reduces to Schwarzschild for $a = 0$.

4.3.2 Horizon and ergosphere

The event horizon occurs where $\Delta(r) = 0$ since for null curves, some rearrangement of terms involving $\dot{t} \equiv dt/d\sigma$ and $\dot{\phi}$ yields

$$-\frac{\rho^4}{\Delta} \dot{r}^2 = \rho^4 \dot{\theta}^2 + [a \dot{t} - (r^2 + a^2) \dot{\phi}]^2 \sin^2 \theta - \Delta [\dot{t} - a \sin^2 \theta \dot{\phi}]^2. \quad (4.39)$$

When $\Delta < 0$, the righthand side is positive, so that $\dot{r} \neq 0$. Therefore once an ingoing ($\dot{r} < 0$) photon enters the region $\Delta < 0$, it cannot reverse course to escape.⁵ For timelike curves, $+\rho^2$ is added to the righthand side of (4.39), so the same conclusion holds. Explicitly, the radius of the event horizon is

$$r_H = M + \sqrt{M^2 - a^2} \quad (\text{horizon}). \quad (4.40)$$

⁵There is a loophole: Δ changes sign again at $r_- \equiv M - \sqrt{M^2 - a^2}$, so it is conceivable that particles could reverse course inside r_- . But it can be shown that the inbound particle does not reach $r = r_H$ until $t = \infty$.

The event horizon disappears when $a \geq M$. This would allow outsiders to see the physical singularity at $r^2 = 0$. According to the Cosmic Censorship Hypothesis, such “naked” singularities are disallowed, hence one presumes $a < M$ for all physically realizable solutions.

Just *outside* the event horizon lies the ergoregion defined by $0 < \Delta \leq a^2 \sin^2 \theta$, or another words

$$r_H < r < M + \sqrt{M^2 - a^2 \cos^2 \theta} \quad (\text{ergoregion}). \quad (4.41)$$

The outer boundary of the ergoregion is the ergosphere, which meets the horizon at the poles $\theta = 0, \pi$. Particles and photons within the ergoregion cannot maintain constant ϕ , even with the aid of rockets, because if $d\phi = 0$ in eq. (4.36), then

$$-\frac{\Delta - a^2 \sin^2 \theta}{\rho^2} dt^2 = ds^2 - \frac{\rho^2}{\Delta} dr^2 - \rho^2 d\theta^2$$

But the lefthand side is positive (since $\Delta < a^2 \sin^2 \theta$), whereas the righthand side is negative (since $\Delta > 0$ and $ds^2 \leq 0$)—a contradiction.

Consider a null path on the horizon—or rather, just outside where $\Delta = 0^+$. The lefthand side of eq. (4.39) is either negative or zero, while the righthand side is either positive or zero (since the term $\propto -\Delta$ is negligible compared to the other terms). Therefore every term must vanish. It follows that $\dot{r} = \dot{\theta} = 0$ (so that the path stays on the horizon) and that (note $r_H^2 + a^2 = 2Mr_H$)

$$\left(\frac{d\phi}{dt}\right)_H = \frac{a}{2Mr_H} \equiv \omega_H, \quad (4.42)$$

which is called the angular velocity of the horizon.

4.3.3 Negative energies

As in the Schwarzschild case, the metric does not depend on t or ϕ , so p_0 and p_3 are conserved along geodesics:

$$E = -g_{0\mu} \dot{x}^\mu = \dot{t} \frac{\Delta - a^2 \sin^2 \theta}{\rho^2} + \dot{\phi} \frac{2aMr \sin^2 \theta}{\rho^2}, \quad (4.43)$$

$$L_\phi = g_{3\mu} \dot{x}^\mu = -\dot{t} \frac{2aMr \sin^2 \theta}{\rho^2} + \dot{\phi} \frac{(r^2 + a^2)^2 - a^2 \Delta \sin^2 \theta}{\rho^2} \sin^2 \theta. \quad (4.44)$$

For null curves, $E = -p_0$ and $L_\phi = p_3$, while for timelike ones, $E = -p_0/m$ and $L_\phi = p_3/m$ (energy and angular momentum per unit mass). The coefficients of \dot{t} and $\dot{\phi}$ in eqs. (4.43)-(4.44) define a 2×2 matrix whose determinant reduces to

$$D = \Delta \sin^2 \theta. \quad (4.45)$$

The equations can be inverted (except where $D = 0$):

$$\dot{t} = E \frac{(r^2 + a^2)^2 - a^2 \Delta \sin^2 \theta}{\rho^2 \Delta} - L_\phi \frac{2aMr}{\rho^2 \Delta}, \quad (4.46)$$

$$\dot{\phi} = E \frac{2aMr}{\rho^2 \Delta} + L_\phi \frac{\Delta - a^2 \sin^2 \theta}{\rho^2 \Delta \sin^2 \theta}. \quad (4.47)$$

E and L_ϕ are defined by eqs. (4.44)-(4.43) for all particles, but of course they are not guaranteed to be constant unless the particle follows a geodesic.

In Schwarzschild geometry we discussed stationary observers [SOs], defined as timelike worldlines with $dr = d\theta = d\phi = 0$. We've just seen that we can't have $d\phi = 0$ inside the ergoregion of Kerr spacetime, however. So we invoke timelike zero-angular-momentum observers [ZAMOs] with $L_\phi = 0$ instead of $\dot{\phi} = 0$, and $dr = 0 = d\theta$. From (4.44),

$$\left(\frac{d\phi}{dt}\right)_{ZAMO} = \frac{2aMr}{(r^2 + a^2)^2 - a^2\Delta \sin^2\theta} \equiv \omega, \quad (4.48)$$

which tends to ω_H as $r \rightarrow r_H$. The ZAMO 4-velocity, which is distinguished from general 4-velocities by a capital letter, is

$$U^\mu = E_Z^{-1}(1, 0, 0, \omega), \quad E_Z = \sqrt{\frac{\rho^2 \Delta}{(r^2 + a^2)^2 - a^2\Delta \sin^2\theta}}. \quad (4.49)$$

A quick route to the normalization factor begins with the observation that

$$p_\mu \dot{x}^\mu = -m. \quad (4.50)$$

For the ZAMOs, the only nonzero p_μ is $p_0 = -mE_Z$ so $\dot{t} = E_Z^{-1}$. Writing f for the coefficient of E_Z in eq. (4.46), the latter equation reduces to $\dot{t} = fE_Z$, whence $\dot{t} = E_Z^{-1} = f^{-1/2}$, thus establishing eq. (4.49).

In GR, energy can be a subtle concept. In SR, all physical observers agree on the sign of a given particle's energy, since it is preserved by Lorentz transformations and all physical observers move forward in time, $U^0 > 0$. This continues to be true in GR as long as one compares measurements made at the same event. But observers at different locations may not agree on the sign, even though in a stationary geometry such as Schwarzschild or Kerr, the conservation of $E \equiv -p_0$ gives a global definition of energy. E corresponds to the energy that a ZAMO or SO at $r = \infty$ would measure *locally* if the particle reached her. The energy measured by ZAMOs at finite r is not E , however, but rather $-p_\mu U^\mu$. The latter must be positive,⁶ so

$$E_Z^{-1}(E - \omega L_\phi) > 0 \quad \Leftrightarrow \quad E > \omega L_\phi. \quad (4.51)$$

where E and L_ϕ refer to the particle, and $E_Z > 0$ to the ZAMO. On the other hand, using eqs. (4.48) and (4.49), we can rewrite eq. (4.46) as

$$\dot{t} = E_Z^{-2}(E - \omega L_\phi),$$

and therefore the condition (4.51) is equivalent to the very reasonable requirement that the particle be future-directed, $\dot{t} > 0$. On the other hand, we can rewrite eq. (4.50) as

$$\dot{t}E = \dot{\phi}L_\phi + \rho^2 \left(\Delta^{-1} \dot{r}^2 + \dot{\theta}^2 \right) + \tilde{m}, \quad (4.52)$$

$$\text{where} \quad \tilde{m} \equiv \begin{cases} 1 & \text{if timelike} \\ 0 & \text{if null.} \end{cases}$$

In the ergoregion, $L_\phi \dot{\phi}$ can be negative, hence *orbits exist for which $E < 0$ even though $\dot{t} > 0$* . (E.g., choose initial conditions $\dot{r} = \dot{\theta} = 0$.) This is especially easy for photons but also happens for massive particles if they move fast enough so that the $+\tilde{m}$ is negligible. The negative- E orbits always have the opposite sign of angular momentum from that of the black-hole: $E - \omega L_\phi > 0$ hence $\omega L_\phi < 0$, and ω has the sign of a .

⁶because the Principle of Equivalence says that local physics is consistent with SR, and we do not have negative-energy particles in SR

Negative- E particles cannot reach $r = \infty$, but they can be produced in the ergoregion. For example, a π^0 (neutral pion) within the ergoregion could decay into “forward” ($L_\phi > 0$) and “backward” ($L_\phi < 0$) photon. The latter can have negative energy and eventually fall into the horizon, while the latter escapes to $r = \infty$ with greater energy than the π^0 !

There is some precedent for such negative energies within classical newtonian mechanics. A *change* in momentum $\Delta\mathbf{p}$ is galilean invariant: $\Delta\bar{\mathbf{p}} = \Delta\mathbf{p}$. But the associated energy changes are $\Delta E = \mathbf{p} \cdot \Delta\mathbf{p}/m$ and

$$\Delta\bar{E} = \bar{\mathbf{p}} \cdot \Delta\mathbf{p}/m = \Delta E + \mathbf{v} \cdot \Delta\mathbf{p},$$

if \mathbf{v} is the relative velocity of frame \bar{O} with respect to O . Thus it is possible to have $\Delta E > 0$ and $\Delta\bar{E} < 0$ if $\mathbf{v} \cdot \Delta\mathbf{p} < 0$. Similar remarks apply to rotating reference frames with momentum replaced by angular momentum and velocity by angular velocity. This gives rise to the important concept of negative-energy waves, since the creation of a wave in a medium generally changes the energy and momentum of the medium. A slow wave propagating against a current may have positive energy locally, but negative energy if it is seen to be borne downstream by an external observer. If we replace the wave by a particle and the current by the angular velocity ω in the ergoregion, then the analogy is rather close. [For an excellent and elementary discussion of negative-energy waves, see [48].]

4.3.4 Irreducible mass

For reasons too involved to discuss here, black holes are actually thermodynamic objects. The entropy of a black hole is proportional to the area of its event horizon:

$$S = \frac{k_B}{L_{\text{Pl}}^2} \times \frac{A}{4} \quad \text{where } L_{\text{Pl}} \equiv \sqrt{\frac{\hbar G}{c^3}} = \text{Planck length.}$$

For a nonrotating hole, the area simply $A = 4\pi R_S^2$. For a rotating hole, however, it is

$$A = \int_{r=r_H} \int \sqrt{g_{22}} d\theta \sqrt{g_{33}} d\phi = 4\pi(r_H^2 + a^2) = 4\pi(2M)^2 \left(\frac{1 + \sqrt{1 - (a/M)^2}}{2} \right). \quad (4.53)$$

This has the same area as a nonrotating black hole of mass

$$M_{\text{irred}} = \left(\frac{\sqrt{1 - a/M} + \sqrt{1 + a/M}}{2} \right) M, \quad (4.54)$$

which is less than M if $a \neq 0$. M_{irred} is called the irreducible mass, because $M - M_{\text{irred}}$ is the maximum energy that can be extracted from the rotating hole without reducing its entropy (and thereby violating the Second Law of black hole thermodynamics!). Up to 29% of the mass of a critically rotating ($a = M$) black hole can be extracted, in principle.

As a check on this result, it is straightforward to calculate from eqs. (4.40), (4.42), and (4.53) that

$$\left(\frac{\partial J}{\partial M} \right)_A = \frac{2Mr_H}{a} = \frac{1}{\omega_H},$$

which is just what one would expect for nondissipative extraction of energy from a flywheel: the change in energy (here, M) per unit change in angular momentum ($J = aM$) at constant entropy (A) is the angular velocity (ω_H).

In the subsequent lectures, we will discuss astrophysical scenarios for spinning up and spinning down the black hole.

4.3.5 Orbits

Miraculously, there is a simple “third integral” conserved by geodesics in Kerr geometry [10]:

$$K = (\rho^2 \dot{\theta})^2 + L_\phi^2 \csc^2 \theta + a^2(\tilde{m}^2 - E^2) \cos^2 \theta. \quad (4.55)$$

In the spherical limit $a \rightarrow 0$, K reduces to L^2 , the square of the total angular momentum. The existence of four first integrals of the geodesic equations (E , L_ϕ , K , and $\tilde{m}^2 = -g_{\mu\nu} \dot{x}^\mu \dot{x}^\nu$) allows the equations of motion to be reduced to four first-order equations:

$$\rho^2 \frac{dr}{d\sigma} = \pm \sqrt{[(r^2 + a^2)E - aL_\phi]^2 - \Delta[\tilde{m}^2 r^2 + aE(aE - 2L_\phi) + K]}, \quad (4.56)$$

$$\rho^2 \frac{d\theta}{d\sigma} = \pm \sqrt{K - L_\phi^2 \csc^2 \theta + a^2(E^2 - \tilde{m}^2) \cos^2 \theta}, \quad (4.57)$$

plus eqs. (4.46)-(4.47) for \dot{t} and $\dot{\phi}$. Dividing eq. (4.56) by eq. (4.57) yields an equation for $dr/d\theta$ in terms of r and θ . These results make it considerably easier to integrate orbits in the Kerr metric. Furthermore, the electromagnetic, Dirac, and linearized gravitational-wave equations all can be separated in Kerr geometry, despite the loss of spherical symmetry [59]. It seems likely that this reflects some hidden (super?)symmetry that has not yet been fully elucidated.

Chapter 5

Accretion onto rotating black holes

It is strongly believed that quasars derive their luminosities from dissipation of the orbital energy of gas surrounding a black holes with masses $\sim 10^8 - 10^9 M_\odot$ residing at the centers of galaxies. Since the gas reaching the hole comes from a much larger radius, it is very unlikely that its initial angular momentum is small enough to allow it to fall directly into the event horizon. (If the gas did so, there would probably be very little dissipation and very little radiation produced.) Therefore, the gas probably forms a rotating accretion disk around the hole. Its orbits are nearly circular, but because of strong differential rotation (variation of angular velocity with radius), hydrodynamic or magnetohydrodynamic turbulence results, leading to dissipation, radiation, and gradual inward radial drift of the gas. Accretion adds both mass and angular momentum to the hole, and under simple assumptions, this leads eventually to an extreme Kerr solution with $a \approx 0.998M$.

To understand these results, one must study the behavior of circular orbits in Kerr geometry.

5.1 Circular and marginally stable orbits

For timelike equatorial orbits (*i.e.* $\theta = \pi/2$, $d\theta = 0$), (4.36), (4.46), & (4.47) can be combined into

$$r^3 \dot{r}^2 = (r^3 + a^2 r + 2a^2 M)E^2 - 4aMEL + (2M - r)L^2 - r(r^2 + a^2 - 2Mr), \quad (5.1)$$

where $\dot{r} \equiv dr/d\tau$ as usual. For circular orbits (geodesics), the conditions $\dot{r} = 0$ and $\ddot{r} = 0$ yield two relations among (E, L, r) :

$$0 = (r^3 + a^2 r + 2a^2 M)E^2 - 4aMEL + (2M - r)L^2 - r(r^2 + a^2 - 2Mr), \quad (5.2)$$

$$L^2 = (3r^2 + a^2)(E^2 - 1) + 4Mr. \quad (5.3)$$

So the orbits form a one-parameter family. Using (5.3) to eliminate L from (5.2) gives

$$\begin{aligned} 0 &= r^3(r^3 + 9M^2 r - 6Mr^2 - 4Ma^2)E^4 \\ &\quad - 2r^2[r^4 - 7r^3 M + 16M^2 r^2 - 3M(4M^2 + a^2)r + 5a^2 M^2]E^2 \\ &\quad + (r^3 - 4Mr^2 + 4M^2 r - Ma^2)^2. \end{aligned} \quad (5.4)$$

There are two roots for E^2 at each r , both real and positive, corresponding to prograde and retrograde orbits. Having found a root, we can go back to eq. (5.3) to find the angular momentum. This procedure defines E and L as functions of r .

The following useful fact holds for *all circular orbits*:

$$\frac{dE}{dr} = \Omega \frac{dL}{dr}, \quad \text{where } \Omega \equiv \frac{d\phi}{dt} \quad (5.5)$$

is the angular velocity of the orbit. To prove this, write the geodesic equation in terms of the 4-velocity u^μ and its lower-index counterpart $u_\mu \equiv g_{\mu\nu}u^\nu = p_\mu/m$. The radial component of the geodesic equation becomes

$$\frac{du_1}{d\tau} = \frac{1}{2}g_{\mu\nu,1}u^\mu u^\nu.$$

Since $u_1 = 0$ for circular orbits, it follows that the righthand side above vanishes. Furthermore, since $g_{\mu\nu}u^\mu u^\nu = -1$,

$$0 = (g_{\mu\nu}u^\mu u^\nu)_{,1} = \underbrace{g_{\mu\nu,1}u^\mu u^\nu}_0 + g_{\mu\nu}u^\mu{}_{,1}u^\nu + g_{\mu\nu}u^\mu u^\nu{}_{,1} = 2u_\nu u^\nu{}_{,1}. \quad (5.6)$$

We have combined the final two terms by relabeling dummy indices, and we have used the definition of u_ν . On the other hand, since $g_{\mu\nu}u^\mu u^\nu = u_\nu u^\nu$,

$$0 = (u_\nu u^\nu)_{,1} = u_{\nu,1}u^\nu + u_\nu u^\nu{}_{,1}.$$

Therefore $u_\nu u^\nu{}_{,1} = -u_{\nu,1}u^\nu$ so that in view of (5.6),

$$u^\nu u_{\nu,1} = 0.$$

Since $u^\nu = (\dot{t}, 0, 0, \dot{\phi})$, (5.5) follows directly.

We are most interested in marginally stable orbits. As in the Schwarzschild case, these can be found from $dL/dr = 0$, since they have minimal angular momentum. In view of the theorem (5.5),

$$\frac{dE}{dr} = \frac{dL}{dr} = 0 \quad \text{at } r = r_{\text{ms}}, \quad (5.7)$$

Therefore, differentiating eq. (5.3) with respect to r ,

$$E_{\text{ms}}^2 = 1 - \frac{2M}{3r_{\text{ms}}}. \quad (5.8)$$

Similarly differentiating eq. (5.2) and eliminating E_{ms}^2 ,

$$L_{\text{ms}}^2 = \frac{2M}{3r_{\text{ms}}}(3r_{\text{ms}}^2 - a^2). \quad (5.9)$$

Finally, substituting these results for E and L in (5.3) gives an equation for r_{ms} itself:

$$r_{\text{ms}}^4 - 12Mr_{\text{ms}}^3 + 6(6M^2 - a^2)r_{\text{ms}}^2 - 28Ma^2r_{\text{ms}} + 9a^4 = 0. \quad (5.10)$$

To avoid having to solve a quartic, it is convenient to regard this last equation as a quadratic equation for a^2 given r_{ms} . The physically acceptable root is

$$a^2 = \frac{r_{\text{ms}}}{9} \left(3r_{\text{ms}} + 14M - 8\sqrt{3Mr_{\text{ms}} - 2M^2} \right). \quad (5.11)$$

This is plotted in Figure 5.1. There are two solutions for r_{ms} at each $a \neq 0$: the smaller and more tightly bound orbit is prograde ($aL_\phi > 0$), while the other is retrograde. The two converge at $a = 0$ (Schwarzschild). At $a = 1$ the prograde orbit lies at the event horizon, $r = M = r_H$ (recall that for $a > 1$ there is no event horizon). The binding energy per unit mass of prograde orbits varies between the limits

$$\epsilon = \begin{cases} 1 - \sqrt{8/9} \approx 0.057 & a = 0, \\ 1 - \sqrt{1/3} \approx 0.423 & a = 1. \end{cases} \quad (5.12)$$

Compare this with the efficiency of uranium fission ($\approx 10^{-3}$) and hydrogen fusion (≈ 0.007).

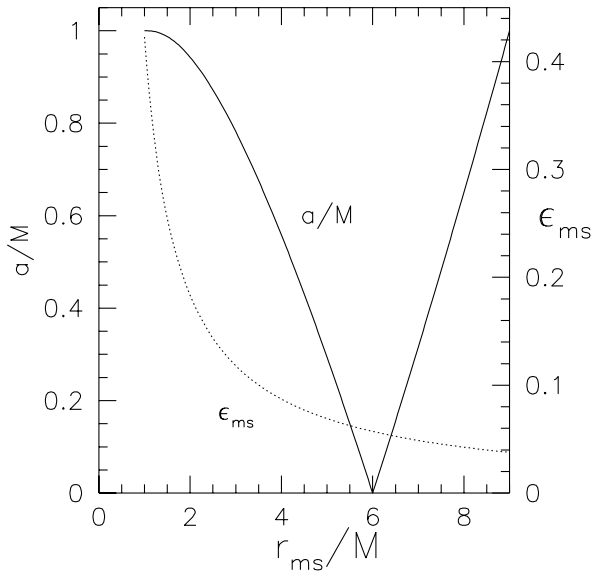


Figure 5.1: Black-hole spin, a/M (left axis), and the corresponding orbital binding energy per unit mass, $\epsilon \equiv 1 - E$ (right axis), versus the radius of the marginally stable orbit, r_{ms} .

5.2 Growth of the hole

The matter in a thin accretion disk gradually spirals inward through a succession of nearly circular orbits. In order to do so, the gas must shed angular momentum. It is generally believed that this occurs through some sort of friction between neighboring annuli, probably mediated by magnetic fields. Total angular momentum is conserved; some is radiated as photons, and perhaps rather more could be lost in a gaseous wind, but most of it is transferred outward through the disk itself by friction. Once the material reaches r_{ms} , any further loss of angular momentum is catastrophic since there is no circular orbit of lower L available. It is usually assumed that the gas then plunges quickly into the event horizon, conserving the energy and angular momentum that it had at r_{ms} .

Consider the effects of the accreted matter on mass and angular momentum of the black hole—and especially on the interesting ratio

$$a_* \equiv \frac{a}{M}. \quad (5.13)$$

Characterize an infalling parcel by its *rest mass* δm_0 : that is, the energy that it would have when at rest at $r = \infty$. The energy and angular momentum added to the hole when this parcel falls in are

$$\delta M = E_{\text{ms}} \delta m_0, \quad \delta J = L_{\text{ms}} \delta m_0.$$

Hence as the black hole grows,

$$\frac{dJ}{dM} = \frac{L_{\text{ms}}}{E_{\text{ms}}}.$$

Since $J = a_* M^2$, it follows that

$$M^2 \frac{da_*}{dM} = \frac{L_{\text{ms}}}{E_{\text{ms}}} - 2Ma_*.$$

Therefore, a_* will increase as the black hole accretes provided that the righthand side above is positive, or equivalently if $L_{\text{ms}} > 0$,

$$0 < \frac{L_{\text{ms}}^2}{E_{\text{ms}}^2} - (2Ma_*)^2 = 6M \cdot \frac{\Delta_{\text{ms}} + 2M(1 - a_*^2)}{3r_{\text{ms}} - 2M},$$

where we have substituted for L_{ms}^2 and E_{ms}^2 from eqs. (5.8)-(5.9). The righthand side of this last equation is clearly positive as long as $a_* < 1$, but note that it vanishes as $a_* \rightarrow 1$ because then $r_{\text{ms}} \rightarrow M$ and $\Delta_{\text{ms}} \rightarrow 0$. The conclusion is that *accretion from a thin disk causes the black hole to approach the critical value $a_* = 1$ ($a = M$).*

There are some caveats to this argument. First, it needn't be true if the direction of the angular momentum of the gas supplied to the hole varies as it grows, as may well happen. Second, the material plunging in from r_{ms} might be magnetically connected, if only briefly, to the inner parts of the disk, in which case it would probably enter the hole with $L/E < L_{\text{ms}}/E_{\text{ms}}$. [This idea, attributed by [60] to Zeldovich & Schwartzman, has been revised recently by Gammie, Krolik, and others]. Even if neither of these first two cases obtained, [60] showed that the increase would stop at $a_* \approx 0.998$ due to the fact that photons emitted from the disk on retrograde paths are more likely to be captured by the hole than prograde ones, hence de-spinning the hole. A glance at Fig. (5.1) makes this plausible, because the retrograde circular orbits terminate at larger r_{ms} , and hence larger L_{ms} , than prograde ones.

5.3 Steady, thin-disk accretion

In this section, we will show that the effective temperature of a steady disk can be expressed in terms of radius and accretion rate, plus a and M , without having to specify the viscosity mechanism responsible for transferring angular momentum outward through the disk. We consider disks that are axisymmetric (independent of ϕ) as well as time-independent, lie in the plane $\theta = \pi/2$, and are very thin ($\Delta\theta \ll 1$). The central mass M is at $r = 0$.

Much of this lecture is drawn from two classic papers: [43] and [60].

5.3.1 Newtonian accretion disks

We begin by reviewing the nonrelativistic case. Locally, such a disk is characterized by

$$\begin{aligned} \Sigma &\equiv \text{mass per unit area} = \text{surface density}, \\ v_r &\equiv \text{radial drift (accretion) velocity}, \\ F &\equiv T_{\text{eff}} = \text{energy/area/time emitted from one side of disk}. \end{aligned}$$

(The fluxes from the upper and lower sides of the disk are each equal to F). Also, the angular velocity and angular-momentum per unit mass are

$$\Omega = \sqrt{\frac{GM}{r^3}} \quad \text{and} \quad L = \Omega r^2 = \sqrt{GM}r,$$

respectively. In writing the above, one neglects the influence of pressure gradients on the rotation curve and assumes that the gravitational attraction of the central mass is balanced only by centrifugal acceleration. It can be shown that corrections are smaller by $\sim \Delta\theta^2$ since pressure also determines the thickness of the disk. The orbital energy per unit mass is

$$E \approx \frac{1}{2}(\Omega r)^2 - \frac{GM}{r} = -\frac{GM}{2r}.$$

The contribution of v_r to E_K is negligible since one assumes $v_r \ll \Omega r$. Also, since we are discussing nonrelativistic theory, the contribution $+c^2$ from the rest mass has been omitted from E . The accretion rate or mass flux $\dot{M}(r)$ is the mass per unit time crossing radius r in the inward direction:

$$\dot{M} = -2\pi r \Sigma v_r.$$

In a steady disk, \dot{M} is independent of r as well as t , else mass would accumulate or drain away from parts of the disk. At the inner edge, the accreting matter joins the central mass M . The angular-momentum flux is

$$f_J = -\dot{M}L + 2\pi rW.$$

The first term represents bodily transport by the mass itself (minus sign because $f_J > 0$ when transport is outwards). The second represents transport by stresses such as magnetic fields, turbulence (Reynolds stress), *etc.*—often called “viscous transport,” although true microscopic viscosity is almost always negligible in astrophysics. The rate of accumulation of angular momentum between r and $r + dr$ is

$$f_J(r) - f_J(r + dr) = -\frac{\partial f_J}{\partial r} dr.$$

Since this vanishes in a steady disk, f_J is also independent of radius; this would not be possible without the W term unless $\dot{M} = 0$, because $dL/dr \neq 0$. It follows that

$$2\pi rW = \dot{M}L + f_{J,\text{in}}, \quad (5.14)$$

where $f_{J,\text{in}}$ is the angular momentum flux at the inner edge of the disk.

The newtonian energy flux is

$$f_E = -\dot{M}E + 2\pi r\Omega W.$$

The second term arises because $2\pi rW$ is the torque exerted by the part of the disk interior to r on the part exterior, and this torque does mechanical work at the rate $2\pi r\Omega W$. Now f_E is not constant:

$$\begin{aligned} \frac{\partial f_E}{\partial r} &= -\dot{M} \frac{dE}{dr} + \frac{\partial}{\partial r} [\Omega(2\pi rW)] \\ &= -\dot{M}\Omega \frac{dL}{dr} + \frac{\partial}{\partial r} [\Omega(2\pi rW)] \\ &= \Omega \frac{\partial}{\partial r} (-\dot{M}L + 2\pi rW) + 2\pi rW \frac{d\Omega}{dr} \\ &= 2\pi rW \frac{d\Omega}{dr}. \end{aligned}$$

The second line above follows from the first because of the theorem (5.5) [which holds nonrelativistically also, as can easily be checked]. The fourth line follows from the third because $\partial f_J/\partial r = 0$. The divergence of the energy flux does not accumulate in the disk but is radiated from its surface. Thus

$$\begin{aligned} 2 \times 2\pi rF &= -\frac{\partial f_E}{\partial r} = 2\pi rW \frac{d\Omega}{dr} \\ \Rightarrow 4\pi r\sigma T_{\text{eff}}^4 &= -\left(\dot{M}L + f_{J,\text{in}}\right) \frac{d\Omega}{dr}. \end{aligned} \quad (5.15)$$

This is the promised relation between accretion rate and disk emission, from which the stress term has been eliminated. The constant $f_{J,\text{in}}$ is determined by an appropriate boundary condition at the inner edge of the disk.

5.3.2 Relativistic conservation laws

The equations for steady relativistic disks are similar to the newtonian ones, but there are a few predictable differences. First, since energy and mass are unified, and since energy is lost by radiation from the disk surface, the statement $\partial\dot{M}/\partial r = 0$ must be reinterpreted to mean something other than conservation of total mass within the disk. Second, while the newtonian theory neglects the angular momentum carried off by the radiated photons, the relativistic theory does not, leading to nonzero divergence of f_J . Finally, distinctions will have to be made between the measurements of various quantities in the “lab” frame and in local frames comoving with the gas.

Recall from the lectures on SR that if $N^\mu \equiv \bar{N}U^{\hat{\nu}}$ is the 4-current of a flow of particles having 4-velocity $U^{\hat{\nu}}$ (a function of spacetime) and number density \bar{N} in their rest frame, and if these particles are neither created nor destroyed, then

$$N^{\hat{\nu}}_{;\hat{\nu}} = 0. \quad (5.16)$$

The generalization of this to a general coordinate system is

$$g^{-1/2} \left(g^{1/2} N^\nu \right)_{;\nu} = 0, \quad (5.17)$$

where

$$g \equiv |\det\{g_{\mu\nu}\}|. \quad (5.18)$$

Many authors omit the absolute value signs from the definition of g and write $\sqrt{-g}$ in eq. (5.17). This result is proved in the §5.4, where it is also shown that the infinitesimal volume element

$$g^{-1/2} d^4x = \bar{g}^{-1/2} d^4\bar{x}. \quad (5.19)$$

is independent of the coordinates. Therefore if \mathcal{V} is an arbitrary 4-volume and f is any function that vanishes outside \mathcal{V} , eq. (5.17) implies

$$0 = \int_{\mathcal{V}} f \left(g^{1/2} N^\nu \right)_{;\nu} d^4x = - \int_{\mathcal{V}} N^\nu f_{;\nu} g^{1/2} d^4x \quad (5.20)$$

using integration by parts in each coordinate $dx^0 \dots dx^3$. In particular, if f is the characteristic function of \mathcal{V} , meaning

$$f(x) = \begin{cases} 1 & \text{if } x \in \mathcal{V}, \\ 0 & \text{otherwise,} \end{cases}$$

then the righthand side of eq. (5.20) becomes an integral over the boundary $\partial\mathcal{V}$, so that eq. (5.20) implies the integral form of the conservation law (5.17).

The generalization of $T^{\hat{\mu}\hat{\nu}}_{;\hat{\nu}} = 0$ is usually more complicated, but if the metric is independent of x^0 and x^3 , then it can be shown that

$$\left(g^{1/2} T_0^\nu \right)_{;\nu} = 0 \quad \text{and} \quad \left(g^{1/2} T_3^\nu \right)_{;\nu} = 0. \quad (5.21)$$

To make this plausible, consider the case of “dust” free of nongravitational forces: $T^\mu_\nu \rightarrow p_\mu N^\nu$, where p_μ is the 4-momentum of an individual particle and N^ν is their 4-current; then

$$\left(g^{1/2} T_\mu^\nu \right)_{;\nu} = p_\mu \left(g^{1/2} N^\nu \right)_{;\nu} + g^{1/2} N^\nu \frac{\partial p_\mu}{\partial x^\nu}.$$

The first term on the right vanishes if the particles are conserved, while the second term is proportional to the change in p_μ along the particle worldlines; but since the particles move along geodesics,

$p_0 = -E$ and $p_3 = L_\phi$ are constant on each worldline. The generalization of this to arbitrary energy-momentum tensors basically follows from Newton's Third Law: particles can exchange energy and angular momentum by exerting forces on one another, but E and L_ϕ are still locally conserved.

For the Kerr metric in Boyer-Lindquist coordinates,

$$g^{1/2} = \rho^2 \sin \theta \rightarrow r^2 \text{ at } \theta \approx \frac{\pi}{2}. \quad (5.22)$$

The relativistic version of $\dot{M} = \text{constant}$ follows by multiplying eq. (5.17) by $g^{1/2}$ and integrating over θ from the top ($\theta_t = \pi/2 - \Delta\theta/2$) to the bottom ($\theta_b = \pi/2 + \Delta\theta/2$) of the disk

$$0 = \int_{\theta_b}^{\theta_t} d\theta \partial_r (r^2 N^1) + [r^2 N^2]_{\theta_t}^{\theta_b}.$$

Replace $N^\mu \rightarrow \bar{N}U^\mu$, where \bar{N} is the number per unit volume in the fluid rest frame, which vanishes at the top and bottom of the disk. Then the second term above vanishes. In the first term, exchange the order of ∂_r and $\int d\theta$:

$$0 = \partial_r \left[r^2 \int_{\theta_b}^{\theta_t} d\theta \bar{N}U^1 \right].$$

Now define rest mass per unit area in the rest frame:

$$\Sigma(r) \equiv mr \int_{\theta_b}^{\theta_t} d\theta \bar{N}(r, \theta). \quad (5.23)$$

where m is the rest mass of a single particle. Assuming that U^1 does not vary much across the disk, we then have

$$\partial_r \dot{M} = 0, \quad \dot{M} \equiv -2\pi r \Sigma U^1. \quad (5.24)$$

Although \dot{M} has the dimensions of mass/time, it is really just a rescaling of (number of particles)/time.

To get the energy and angular-momentum conservation laws, we start by defining a bare-bones energy-momentum tensor in the local rest frame of the gas. Using orthonormal axes aligned with the radial, azimuthal, and vertical directions, this is

$$T^{\hat{\mu}\hat{\nu}} = \begin{pmatrix} m\bar{N} & 0 & F & 0 \\ 0 & 0 & 0 & S \\ F & 0 & 0 & 0 \\ 0 & S & 0 & 0 \end{pmatrix} \quad (5.25)$$

$$= m\bar{N}U^{\hat{\mu}}U^{\hat{\nu}} + F(r, \theta) (U^{\hat{\mu}}b^{\hat{\nu}} + U^{\hat{\nu}}b^{\hat{\mu}}) + S(r, \theta) (a^{\hat{\mu}}c^{\hat{\nu}} + a^{\hat{\nu}}c^{\hat{\mu}}). \quad (5.26)$$

F is the vertical (*i.e.*, θ direction) energy flux, and S is the offdiagonal stress responsible for angular momentum transport, *i.e.* azimuthal force per unit area perpendicular to r . In the second line, $a^{\hat{\mu}}$, $b^{\hat{\mu}}$, and $c^{\hat{\mu}}$ are unit vectors in the radial, vertical, and azimuthal directions, orthogonal to one another and to the 4-velocity $U^{\hat{\mu}}$, *e.g.*

$$\eta_{\hat{\mu}\hat{\nu}}a^{\hat{\mu}}a^{\hat{\nu}} = 1, \quad \eta_{\hat{\mu}\hat{\nu}}a^{\hat{\mu}}b^{\hat{\nu}} = \eta_{\hat{\mu}\hat{\nu}}a^{\hat{\mu}}c^{\hat{\nu}} = \eta_{\hat{\mu}\hat{\nu}}a^{\hat{\mu}}U^{\hat{\nu}} = 0,$$

and so forth. In the “lab” frame, at rest with respect to the Boyer-Lindquist coordinates, the components of this tetrad are

$$\begin{aligned}
U^\mu &= (U^0, U^1, 0, U^3) & U^1 &\ll U^3 \& U^0 \\
a^\mu &= (a^0, a^1, 0, a^3) & a^0 \&a^3 &\ll a^1 \\
b^\mu &= (0, 0, r^{-1}, 0) \\
c^\mu &= (c^0, c^1, 0, c^3) & c^1 &\ll c^0 \& c^3.
\end{aligned} \tag{5.27}$$

The indicated relative sizes of these components follow from the fact that the relative velocity of the rest and lab frames is mostly along the ϕ direction, since the radial velocity of the gas is very small. Note furthermore that

$$U_\mu \equiv g_{\mu\nu} U^\nu = (-E, g_{rr} U^r, 0, L). \tag{5.28}$$

Now integrate the angular-momentum conservation law across the disk:

$$0 = \partial_r \left[r^2 \int_{\theta_b}^{\theta_t} d\theta T_3^1 \right] + r^2 [T_3^2]_{\theta_t}^{\theta_b} \tag{5.29}$$

Comparing eqs. (5.26), (5.27), and (5.28), $T_3^2 = FL/r$. Furthermore the energy fluxes at top and bottom are equal in magnitude but opposite in direction, so $F(r, \theta_t) = -F(r, \theta_b) \equiv F$. So the second term in eq. (5.29) yields $2rFL$. After performing the integration in the first term, we get a contribution $(-LM/2\pi)$ from the $m\bar{N}U_0U^3$ piece of (5.26), and the rest is

$$r^2 \int d\theta S(r, \theta) c_3 a^1 \equiv rW(r). \tag{5.30}$$

(There is also a negligibly small contribution proportional to $a_3 c^1$.) Putting it all together, we have the angular-momentum conservation law in the form

$$\partial_r [-L\dot{M} + 2\pi rW] + 4\pi rFL = 0. \tag{5.31}$$

The same procedure turns the energy-conservation law $(g^{1/2}T_0^\mu)_{,\mu} = 0$ into

$$\partial_r [E\dot{M} + 2\pi rW_E] - 4\pi rFE = 0,$$

where

$$rW_E(r) \equiv r^2 \int d\theta S(r, \theta) c_0 a^1.$$

However, W_E is related to W by the fact that

$$0 = c_\mu U^\mu \approx c_0 U^0 + c_3 U^3,$$

the term $c_1 U^1$ being smaller by $O[(U^1/U^0)^2] \ll 1$. But

$$\frac{U^3}{U^0} = \frac{d\phi}{dt} \equiv \Omega,$$

whence $c_0 = -\Omega c_3$. It follows that $W_E = \Omega W$, and therefore

$$\partial_r [E\dot{M} - 2\pi r\Omega W] - 4\pi rFE = 0. \tag{5.32}$$

Equations (5.24), (5.31), and (5.32) are the fundamental equations of a steady thin disk. The stress term W can be eliminated by adding Ω times eq. (5.31) to eq. (5.32) and invoking eq. (5.5), which leads to

$$W = -2F(E - \Omega L)/\partial_r \Omega. \quad (5.33)$$

Substituting this into eq. (5.31) gives a first-order differential equation for F :

$$\frac{d}{dr} \left[\frac{r(E - \Omega L)}{\partial_r \Omega} F \right] - rLF = -\frac{\dot{M}}{4\pi} \frac{dL}{dr}.$$

This equation has the integrating factor $\mu = (E - \Omega L)$, so

$$F(r) = \sigma T_{\text{eff}}^4 = \frac{rd\Omega/dr}{(E - \Omega L)^2} \left[(\text{constant}) - \frac{\dot{M}}{4\pi} \int^r (E - \Omega L) \frac{dL}{dr} dr \right] \quad (5.34)$$

Once again, the constant is fixed by boundary conditions at the inner edge of the disk.

5.4 Appendix: Invariant 4-volume and divergence formula

To prove eq. (5.18), let $\{x^{\hat{\mu}}\}$ be freely-falling coordinates, so that

$$g_{\mu\nu} = \frac{\partial x^{\hat{\mu}}}{\partial x^\mu} \eta_{\hat{\mu}\hat{\nu}} \frac{\partial x^{\hat{\nu}}}{\partial x^\nu}.$$

This can be regarded as a matrix equation, $\mathbf{g} = \mathbf{M}^T \boldsymbol{\eta} \mathbf{M}$, so by taking determinants of both sides,

$$g = \left| \left\{ \frac{\partial x^{\hat{\mu}}}{\partial x^\mu} \right\} \right|^2.$$

But the righthand side is the square of the jacobian of the transformation $\{x^{\hat{\mu}}\} \rightarrow \{x^\mu\}$, so $g^{1/2} d^4 x^\mu = d^4 x^{\hat{\mu}}$, which suffices to establish (5.19).

Next we will need the following theorem about matrices: If $d\mathbf{M}$ is a first-order derivative of a nonsingular $N \times N$ matrix \mathbf{M} , then the corresponding derivative of its determinant is

$$d(\det \mathbf{M}) = (\det \mathbf{M}) \text{Trace} (\mathbf{M}^{-1} d\mathbf{M}). \quad (5.35)$$

To prove this, consider that the contribution from the change in the i^{th} row of \mathbf{M} is, by Cramer's rule,

$$\sum_{j=1}^N (-1)^{i+j} C_{ij} dM_{ij} = (\det \mathbf{M}) \sum_{j=1}^N [\mathbf{M}^{-1}]_{ji} dM_{ij},$$

where C_{ij} is the ij^{th} minor of \mathbf{M} . Summing this expression over all rows i yields (5.35). Now

$$\begin{aligned} \frac{\partial}{\partial x^{\hat{\mu}}} (N^{\hat{\mu}}) &= \frac{\partial x^\mu}{\partial x^{\hat{\mu}}} \frac{\partial}{\partial x^\mu} \left(\frac{\partial x^{\hat{\mu}}}{\partial x^\nu} N^\nu \right) \\ &= \frac{\partial x^\mu}{\partial x^{\hat{\mu}}} \frac{\partial x^{\hat{\mu}}}{\partial x^\nu} N^\nu_{,\mu} + \frac{\partial x^\mu}{\partial x^{\hat{\mu}}} \frac{\partial^2 x^{\hat{\mu}}}{\partial x^\nu \partial x^\mu} N^\nu \\ &= \delta_\nu^\mu N^\nu_{,\mu} + \text{Trace} (\mathbf{M}^{-1} d_N \mathbf{M}), \\ &= N^\mu_{,\mu} + (\det \mathbf{M})^{-1} d_N (\det \mathbf{M}), \end{aligned}$$

$$\text{if } [\mathbf{M}]_{\nu}^{\hat{\mu}} \equiv \frac{\partial x^{\hat{\mu}}}{\partial x^\nu} \quad \text{and} \quad d_N \equiv N^\nu \frac{\partial}{\partial x^\nu}.$$

Finally, recognizing once again that $\det \mathbf{M} = g^{1/2}$, we have

$$N^{\hat{\mu}}{}_{,\hat{\mu}} = g^{-1/2} \left(g^{1/2} N^{\nu} \right)_{,\nu} \quad \text{QED.} \quad (5.36)$$

5.5 Problems for Chapter 5

1. (a) A nonrotating neutron star of mass M and radius¹ $R > 3M$ has an angular diameter $\delta \ll 1$ as seen by a distant stationary observer at $r \gg R$. Show that if the observer computes the apparent diameter as $D_{\text{app}} = r\delta$, then

$$D_{\text{app}} = 2R \left(1 - \frac{2M}{R} \right)^{-1/2}.$$

Evaluate this for the realistic (?) values $M = 1.4 M_{\odot}$ and $R = 10 \text{ km}$.

(b) Suppose that the entire surface radiates as a black body at temperature T_{surf} . What temperature T_{∞} does a stationary observer at $r \gg R$ see? [*Hint: Recall that the mode occupation number n is constant along photon trajectories in vacuum, even in GR.*] What is the relationship between the luminosity (radiated power) $L_{\text{surf}} = 4\pi R^2 \sigma T_{\text{surf}}^4$ computed by an observer standing on the surface and the luminosity L_{∞} measured by stationary observers at $r \gg R$? If you used part (a) to calculate this, can you justify the result for $L_{\infty}/L_{\text{surf}}$ in another way?

2. Show that the geodesic equations can be written in hamiltonian form

$$\frac{dx^{\mu}}{d\sigma} = \frac{\partial H}{\partial p_{\mu}}, \quad \frac{dp_{\mu}}{d\sigma} = -\frac{\partial H}{\partial x^{\mu}}, \quad (5.37)$$

where

$$H \equiv p_{\mu} \frac{dx^{\mu}}{d\sigma} - L = \frac{1}{2} g^{\alpha\beta} p_{\alpha} p_{\beta}.$$

Here and always, if \mathbf{g} is the 4×4 symmetric matrix whose components are $g_{\alpha\beta}$, then $g^{\alpha\beta}$ are the components of \mathbf{g}^{-1} , so that

$$g_{\mu\beta} g^{\beta\nu} = \delta_{\mu}^{\nu} \equiv \begin{cases} 1 & \text{if } \mu = \nu, \\ 0 & \text{if } \mu \neq \nu. \end{cases}$$

In the case of a massive particle, we take $d\sigma = m d\tau$ to make the dimensions of momentum work out right. You will need to make use of the identity

$$g^{\alpha\beta}{}_{,\mu} = -g_{\kappa\lambda,\nu} g^{\alpha\kappa} g^{\beta\lambda};$$

derive this by applying the product rule to

$$d(\mathbf{g} \cdot \mathbf{g}^{-1}) = d\mathbf{I} = 0,$$

where \mathbf{I} is the identity matrix and d is any derivative operator.

(b) (*Required of graduate students only.*) Write a computer program to integrate orbits (both timelike and null) in the Kerr metric using the hamiltonian equations (5.37) and any suitable numerical algorithm, *e.g.* Runga-Kutta4. (The only nondiagonal part of \mathbf{g} is the $t\phi$ block. You can read off g^{tt} , $g^{t\phi}$, $g^{\phi\phi}$ from (4.46) & (4.47), remembering that $(E, L_{\phi}) \equiv (-p_t, +p_{\phi})$.) Check the accuracy of your results by the constancy of H and of the third integral K given by (4.55). Plot some representative trajectories in the (r, θ) plane (with nonzero θ of course). Verify as many of the analytic results given in lecture as you have time and patience for, *e.g.* the radii of prograde and retrograde orbits, the angular velocity ω_H of the horizon.

¹in the sense of the Schwarzschild coordinate, *i.e.* the proper circumference is $2\pi R$

Chapter 6

Neutron Stars

The possibility of self-gravitating, macroscopic objects consisting solely of neutrons was recognized independently by Lev Landau and Fritz Zwicky shortly after the discovery of the neutron (by Chadwick) in the 1930s.

6.1 Masses and radii

While we are mainly concerned with the surfaces and atmospheres of neutron stars, and with their radiative processes, a few remarks on their internal structure are in order because an important motivation for studying these objects is to constrain the equation of state of matter under extreme conditions. For this purpose, a precise observational determination of the relationship between mass and radius is much desired, but so far elusive.

Nevertheless, it is possible to understand why neutron stars have roughly the masses and radii they do at the back-of-the-envelope level. Like white dwarfs, neutron stars are supported by degeneracy pressure rather than thermal pressure. But whereas the electrons in a white dwarf behave as a (degenerate) ideal gas to a good first approximation, the neutron fluid in a neutron star is definitely not ideal: inter-nucleonic forces play important roles. Still, the ideal-gas approximation is the place to start. Thus, let a star of total mass¹ M consist of M/m identical fermions each of mass m . The radius of the star is R , so that the total number of states in phase space at radii $r \leq R$ and momenta $p \leq p_F$ is, including a factor for spin, is

$$(2s + 1) \left(\frac{4\pi}{3} R^3 \right) \left(\frac{4\pi}{3} p_F^3 \right) h^{-3} \approx \frac{M}{m}. \quad (6.1)$$

This determines the Fermi momentum p_F in terms of (N, R) ; it is only an approximation, because in general the number density N will vary with radius, decreasing from $r = 0$ to $r = R$, and so will the local $p_F \sim \hbar N^{-1/3}$. We take $2s + 1 = 2$ henceforth, as appropriate for electrons, neutrons, and quarks.

On the other hand, the total energy of the “star” is

$$E \approx \frac{M}{m} \varepsilon_F - \frac{GM^2}{R}, \quad (6.2)$$

in which ε_F is the kinetic energy per particle corresponding to momentum p_F , and the second term above is the gravitational energy in the approximation of a Newtonian sphere of uniform mass density. Obviously there should be numerical factors in front of both the kinetic and potential

¹Where relativistic corrections to mass-energy are important, M is to be taken as the total rest mass, i.e. $\mathcal{N}m$, where m is the rest mass each fermion would have if it were not in a gravitational field, and \mathcal{N} is their number.

terms above, but these factors are similar for uniform density and therefore do not much alter the equilibrium radius, which is determined by the condition $(\partial E/\partial R)_M = 0$. Now

$$\left(\frac{\partial \varepsilon_F}{\partial R}\right)_M = \frac{d\varepsilon_F}{dp_F} \left(\frac{\partial p_F}{\partial R}\right)_M = -v_F \frac{p_F}{R},$$

where $v_F = \varepsilon'_F(p_F)$ is the 3-velocity at the Fermi surface, as can be verified from $\varepsilon(p) = \sqrt{p^2 c^2 + m^2 c^4} - mc^2$. Therefore

$$\left(\frac{\partial E}{\partial R}\right)_M \approx -\frac{M}{m} \frac{v_F p_F}{R} + \frac{GM^2}{R^2}, \quad (6.3)$$

If the fermions are nonrelativistic, then $v_F \approx p_F/m$, and in combination with (6.1), this leads to $R \propto M^{-1/3}$. But in sufficiently massive and compact stars $v_F \rightarrow c$, in which case (6.1) yields $p_F R \approx GMm/c$. Using this to eliminate $(p_F R)^3$ from (6.1) yields a unique mass:

$$M \approx \frac{3}{2} \pi^{1/2} \left(\frac{\hbar c}{G}\right)^{3/2} m^{-2} \approx 5 \left(\frac{m_p}{m}\right)^2 M_\odot, \quad (6.4)$$

which should be interpreted as a maximum mass that can be supported by degeneracy pressure in the ideal-gas approximation.

For a white dwarf, scrutiny of the steps above shows that m should be interpreted as the rest mass associated with each electron, which is not m_e but $(A/Z)m_p \approx 2m_p$ for compositions consisting of light elements heavier than hydrogen. This yields $M_{\max, \text{WD}} \approx 1.25 M_\odot$, which is not a bad approximation to the more correct value $1.4 M_\odot$, considering the simplicity of our approximations.

For a neutron star, two important corrections are required. First, the general-relativistic form of the differential equation for hydrostatic equilibrium must be used. This is called the Tolman-Openheimer-Volkoff Equation. For an ideal gas of neutrons, this leads to a maximum mass that is actually $< M_\odot$ because relativistic gravity is stronger than newtonian. The second correction is to the equation of state. As the neutrons are squeezed together, the forces between them make the ideal-gas approximation untenable. At densities above nuclear density, $\rho > \rho_{\text{nuc}} = 2.8 \times 10^{14} \text{ g cm}^{-3}$, these forces are repulsive. This is plausible because as the nucleons begin to overlap, the p_F of their constituent quarks starts to increase, leading to a decrease in the effective value of the fermion mass m in (6.4) (the u and d quarks probably have masses $\lesssim 10 \text{ MeV}/c^2$). Qualitatively, this is the same reason that atoms or molecules repel one another as their electron clouds are forced to overlap. This “stiffening” of the equation of state (EOS) partly compensates for the reduction of M_{\max} by the TOV equation. But the quantitative details of the EOS of nuclear matter are still uncertain, and consequently the maximum mass of neutron stars is still unknown. Several accurately measured masses have been obtained for pulsars in binary systems by means of accurate pulse timing and detection of various relativistic effects on the orbit. Most of these are in the range 1.3-1.6 M_\odot , but recently a well-determined mass of $1.97 \pm 0.04 M_\odot$ has been announced [14].

6.1.1 Radii

Neutron-star radii are more difficult to measure than masses. In principle, the moment of inertia $I \sim MR^2$ might be constrained in binary pulsars via gravitational versions of spin-orbit coupling, but this has not yet been achieved: the coupling is weak because R is extremely small compared to the orbital separation. From time to time, there are claims of detections of gravitationally redshifted spectral lines from neutron-star surfaces, but none of these claims has been generally accepted. Probably the best current constraints come from analysis of Type I X-ray bursts of accreting neutron stars, as described below.

Some simple upper and lower bounds on R can easily be derived. The star should be larger than its own Schwarzschild radius, hence $R > 6(M/2 M_\odot) \text{ km}$. Relativistic considerations dictate that

R must actually be larger than this bound by at least a factor of 9/8 in order that the speed of sound implied by the EOS be $< c$. Some pulsars are rapidly rotating; the current record-holder is PSR J1748-2446ad, with a rotation rate $\Omega/2\pi = 716$ Hz [26]. Since the equatorial rotation velocity must be less than that of a circular orbit, $R < (GM/\Omega^2)^{2/3} \approx 24(M/2M_\odot)^{1/3}$ km; a more careful consideration of relativistic effects leads to $R_0 < 16(M/2M_\odot)^{1/3}$ km, where R_0 is the radius that the star would have if it were nonrotating [32]. The geometric mean of these upper and lower bounds is $\bar{R} \approx 10$ km. Calculations based on plausible equations of state predict $R \approx 8 - 15$ km for a canonical $M = 1.4 M_\odot$ [32].

6.2 Type I X-ray bursts

These are thermonuclear flashes on the surfaces of neutron stars accreting from a binary companion. For reviews, see [58, 19], which have theoretical and observational emphases, respectively.

Matter falling onto the surface of a neutron star releases a gravitational energy

$$\dot{E} = \frac{z}{1+z} \dot{M} c^2 \approx 0.23 \dot{M} c^2, \quad (6.5)$$

where z is the gravitational redshift defined by eq. (6.7) below, $z \approx 0.31$ for $M = 1.4 M_\odot$ and $R = 10$ km. This is much larger than the energy released by (hydrogen) fusion, $0.007 \dot{M} c^2$. If the accreting material burned continuously, then the heat of fusion would be difficult to detect. However, at accretion rates below 1% of the Eddington accretion rate

$$\begin{aligned} \dot{M}_{\text{Edd}} &= \frac{1+z}{zc^2} L_{\text{Edd},\infty} = \frac{8\pi GMm_p}{(1+X)\sigma_{\text{T}} cz} \\ &\approx 1.0 \times 10^{-8} \left(\frac{M}{M_\odot} \right) \left(\frac{10 \text{ km}}{R} \right) \frac{2}{1+X} M_\odot \text{ yr}^{-1}, \end{aligned} \quad (6.6)$$

where X is the hydrogen mass fraction of the accreted material ($X_\odot \approx 0.7$), this material accumulates until it reaches a mass column $\Sigma_{\text{ign}} \sim 2 \times 10^8 \text{ g cm}^{-2}$ and a pressure $P_{\text{ign}} \sim 3 \times 10^{22} \text{ dyn cm}^{-2}$, whereupon it ignites, reaching peak temperatures in the burning layer $\sim (P_{\text{ign}}/a)^{1/4} \sim 10^9 \text{ K}$, at which point radiation pressure causes the layer to expand. These bursts last 10s of seconds and recur at intervals of a few hours to a few days, depending on \dot{M}). At accretion rates $10^{-2} \dot{M}_{\text{Edd}} < \dot{M} < 10^{-1} \dot{M}_{\text{Edd}}$, the hydrogen burns steadily to helium but the helium accumulates until it ignites. At still higher rates but $\lesssim 0.3 \dot{M}_{\text{Edd}}$, the hydrogen cannot burn quickly enough to keep up with the accretion, so that it bursts together with the helium. At still higher rates, everything burns steadily. Or such at least is the theoretical expectation; the actual behavior appears to deviate somewhat from this expectation as judged by comparisons between the time-integrated emission between bursts, which measures \dot{M} via eq. (6.5). The neutron stars involved in Type I bursts appear to be relatively weakly magnetized compared to normal (i.e., non-millisecond) pulsars, but it is possible that because of magnetic channeling or other reasons, the accreting material is not uniformly distributed over the surface, in which case what matters for these various burning regimes is not the total accretion rate but rather the local rate per unit area.

Interest in these events is motivated in part by the possibility of determining the neutron star mass, radius, and distance from the X-ray light curve and spectral energy distribution [62]. An example of such an event is shown in Figure 6.1. The light curve shown in the top panel has a flat portion: this is interpreted as emission at the effective Eddington limit. Note that the peak X-ray luminosity is $\gtrsim 6 \times 10^{38} \text{ erg s}^{-1}$, which is $5 L_{\text{Edd}}$ for $1 M_\odot$ of hydrogen. This probably does not indicate a $5 M_\odot$ neutron star but rather an atmosphere consisting of helium and heavier elements, for which the mass per electron is twice what it would be for pure hydrogen, with a corresponding

increase in L_{Edd}/M .² The second panel shows the radiation temperature inferred from the X-ray spectral energy distribution (SED), i.e. the color temperature. At the circled point, corresponding to the peak flux, $k_{\text{B}}T_{\text{c}} \approx 2.5$ keV, whence $T_{\text{c}} \approx 2.9 \times 10^7$ K. Naïvely interpreted, this implies a photospheric radius $R_{\text{ph}} \approx (L_{\text{max}}/4\pi\sigma_{\text{T}}T_{\text{c}}^4)^{1/2} \approx 11$ km.

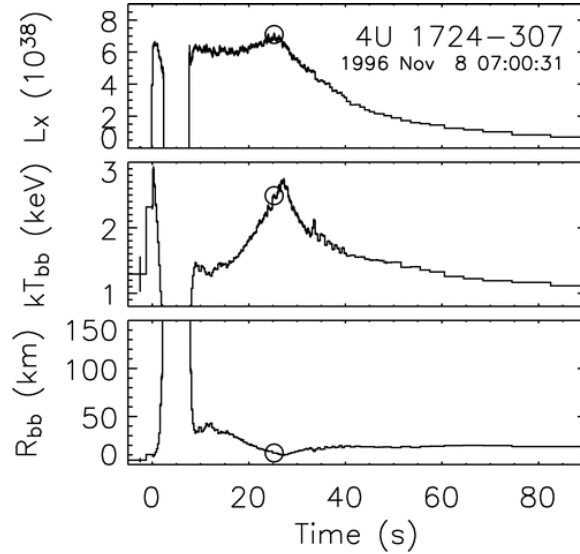


Figure 6.1: An extreme photospheric-expansion burst in the globular cluster Terzan 2 observed by RXTE [19]

In rough outline, postponing possible complications, the logic by which mass (M), radius (R), and distance (D) may all be determined can be summarized as follows. The peak bolometric flux received at Earth determines L_{pk}/D^2 and therefore M/D^2 if $L_{\text{pk}} = L_{\text{Edd}}$. The SED gives T_{c} , and therefore $(R/D)^2 \approx F_{\text{pk}}/T_{\text{c}}^4$. Eliminating D between these expressions gives M/R^2 . Now there are corrections to L and T as observed “at infinity” compared to their local values at the photosphere, which scale as powers of the gravitational redshift

$$1 + z \equiv (-g_{00})^{-1/2} = \left(1 - \frac{2GM}{c^2 R_{\text{ph}}}\right)^{-1/2}. \quad (6.7)$$

These corrections would be degenerate with the quantities already determined if R_{ph} were constant, but in fact it appears to vary during the outburst, as judged by variations in F/T_{c}^4 . The interpretation is that the luminosity gets so close to the Eddington limit that scale height of the atmosphere becomes comparable to or larger than R itself: this is indicated by the bottom panel of Fig. 6.1. The gap in the light curve shown in the top panel around 5-10 seconds is caused by the shift of the color temperature $T_{\text{c}} \propto R_{\text{ph}}^{-1/2}$ to values lower than those to which the detector is sensitive; the bolometric luminosity is presumed to be almost constant within $\sim \pm 0.01 L_{\text{Edd}}$, at least during the period when R_{ph} is substantially larger than R .

The reason that the luminosity must be so close to L_{Edd} during a photospheric radius expansion (“PRE” in the literature) is as follows. We have seen that the temperature at which a neutron star radiates L_{Edd} from its surface is $\sim 2 \times 10^7$ K. If radiation pressure forces were unimportant, the scale

²Even so, the implied mass is somewhat overlarge in this case. It is suspected that the inner part of the accretion disk acts as a mirror, concentrating flux towards the observer and giving the illusion of a larger isotropic luminosity. The average peak flux from bright bursts with well-determined distances is $3\text{--}4 \times 10^{38}$ erg s⁻¹, in line with expectations for a hydrogen-poor atmosphere above a $\sim 1.4 M_{\odot}$ star [19].

height for the gas pressure and density at this temperature would be $H_0 \sim k_B T / (m_p g) \sim 10$ cm (!), where

$$g(r) = (1+z) \frac{GM}{r^2} \quad (6.8)$$

is the proper gravitational acceleration experienced by a stationary observer Schwarzschild radial coordinate r : note the redshift factor (Chap. 4). Thus, if the atmosphere is in hydrostatic equilibrium with an actual scale height $\sim R_{\text{ph}} - R \gg H_0$, the radiative forces *cannot* be negligible but must cancel the gravitational ones to an accuracy $\sim H_0 / (R_{\text{ph}} - R)$. Why must the atmosphere be hydrostatic rather than a wind? In fact, there may be some outflow near or beyond R_{ph} , but the bulk of the atmosphere cannot be ejected because, as we have also seen, the energy available from fusion is much less than its binding energy.

Now the *local* Eddington luminosity at finite radius r is different from the luminosity defined by a stationary observer at infinity, even if this is based on the correct mass M and chemical composition (X, Z) (i.e, the correct opacity), because of the gravitational redshift. On the one hand, $L_{\text{Edd}}(r)$ is increased relative to the nonrelativistic result by the factor $(1+z)$ in the proper acceleration (6.8). On the other hand, for any luminosity $L(r)$ measured by a stationary observer at radius r , the corresponding luminosity measured at infinity is $L(\infty) = L(r)/(1+z)^2$: each photon is redshifted by a factor $(1+z)^{-1}$ as it climbs out of the potential well, and the rate of emission of these photons suffers time dilation by the same factor. The upshot is that

$$L_{\text{Edd}}(\infty) = \frac{L_{\text{Edd}}(r)}{1+z(r)}. \quad (6.9)$$

Thus, insofar as $L_{\text{Edd}}(R_{\text{ph}})$ is constant while R_{ph} expands and recontracts, the astronomer's received flux $\propto L_{\text{Edd}}(\infty)/D^2$ should vary as described by eqs. (6.9) & (6.7). with a fractional amplitude $\lesssim 30\%$. If this variation is measured, and to the extent that it can be attributed to this effect,³ one has a measure of M/R .

Recently, [39] have attempted to measure the mass and radius of the Type I burster EXO 1745-248 in the globular cluster Terzan 5. The advantage of using a burster in a globular cluster is that the distance to the cluster can be estimated independently, removing the need to rely on the relativistic effects to provide the third relation among the three *a priori* unknowns $\{M, R, D\}$. They find that the apparent emitting area $A = 4\pi D^2 F / [\sigma_{\text{T}}(T_c/f_c)^4]$ is constant during the fading part of the burst, as expected if the photosphere lies at the neutron-star surface during this phase. In this formula for A , the quantity f_c —the *color correction factor*—relates the color temperature measured from the SED to the effective temperature (which expresses the emitted bolometric flux). After making the appropriate relativistic corrections to A , these authors find two solutions that fit the data well: $\{M, R\} \approx \{1.7 M_{\odot}, 9 \text{ km}\}$ and $\{1.4 M_{\odot}, 11 \text{ km}\}$, both with 1σ errors of order 10%. These values are eminently reasonable and consistent with popular equations of state, but one ought to be concerned about the possibility of systematic errors [25, 24].

Under the conditions relevant to the expanded photosphere of a Type I burst, the absorption opacity (κ_a) is much smaller than the electron-scattering opacity (κ_s). This inevitably leads to a discrepancy between the color temperature and the effective temperature. The former determines the *shape* of the spectral energy distribution to the extent that it can be described as a blackbody, while the latter determines the normalization of the spectrum. In other words, if $f_c \equiv T_c/T_{\text{eff}}$, then

$$I_{\nu}(\theta, \phi) = f_c^{-4} B_{\nu}(T_c)$$

$$F = \sigma_{\text{SB}} T_{\text{eff}}^4 \equiv \int I_{\nu}(\theta, \phi) \cos \theta d^2 \Omega = f_c^{-4} \sigma_{\text{SB}} T_c^4. \quad (6.10)$$

³There should also be a small variation due to the dependence of the Klein-Nishina cross section on T_c , but this is only a few percent at keV energies, and in any case is predictable. Much more important uncertainties are due to possible variations in opacity, instrumental errors, reflection of flux by the accretion disk, etc.

In the second line, F is the frequency-integrated flux emerging from the surface of the atmosphere, and the polar angle θ is defined with respect to the outward-pointing normal. Note that the effective temperature T_{eff} is a measure of the (fourth root of) the flux F ; the effective temperature can therefore be defined even for spectral energy distributions that bear little resemblance to a black body. A source that emits with a spectrum having the shape of a black body but a different normalization is sometimes called a *gray body*, and the normalization $f_g < 1$ is called the *graybody factor*. With the color correction factor f_c defined as above, $f_g = f_c^{-4}$.

In particular, the color correction factor has to be predicted from a theory of the radiative transfer in the atmosphere, using assumptions about the atmospheric composition. We give a simplified discussion of this issue below. But first, we digress to introduce the equation of radiative transfer itself

6.2.1 Radiative transfer in the diffusion approximation

The purpose of this section is to motivate the approximate equations (6.16). If these are already familiar, then skip ahead.

In a form sufficiently general for present purposes, the equation of radiative transfer is

$$\frac{dI_\nu}{ds}(\Omega, s) = -\rho(\kappa_a + \kappa_s)I_\nu + \rho\kappa_a B_\nu(T_m) + \rho\kappa_s \int I_\nu(\Omega', s) \frac{d\sigma}{d\Omega}(\Omega' \rightarrow \Omega) d^2\Omega' \quad (6.11)$$

Here s is arc length along a ray, Ω is a shorthand for the direction (θ, ϕ) of the ray, T_m is the internal temperature of the matter that emits and absorbs the radiation, and $d\sigma/d\Omega$ is the differential cross section for scattering from direction Ω' to Ω , normalized according to

$$\int \frac{d\sigma}{d\Omega}(\Omega' \rightarrow \Omega) d^2\Omega = 1, \quad (6.12)$$

so that the integral term returns just as much energy to the radiation field as the term $-\kappa_s I_\nu$ removes from it. More generally, when the matter has no well-defined internal temperature—as in the case of nonthermal synchrotron radiation, for example—the combination $\kappa_a B_\nu(T_m)$ would be replaced by a source function $S_\nu(\Omega)$. Also, one generally has to allow for a change in frequency under scattering (due, for example, to electron recoil). But the simplified form (6.11) is adequate for X-ray burst atmospheres in the first approximation.

The distinction between absorption and scattering is sometimes hard to draw precisely, but one should think of scattering as changing some properties of a photon without entirely destroying it—mainly its direction—whereas absorption replaces the original photon with photons drawn at random from a distribution determined by T_m or other internal parameters of the radiating matter. Absorption may change the number of photons, whereas scattering does not. In particular, Compton scattering conserves photon number, bremsstrahlung emission and free-free absorption do not.

It is not hard to see that if the matter is at a uniform temperature, then eq. (6.11) has the particular solution $I_\nu = B_\nu(T_m)$, in which case the lefthand side vanishes and the radiation field is isotropic. This solution holds deep in the atmosphere. Close to the photosphere, however, it cannot hold because there the specific intensity $I_\nu(\Omega)$ becomes anisotropic. If there is no radiation impinging upon the photosphere from outside, then $I_\nu(\theta, \phi; s_{\text{ph}}) = 0$ for $\cos\theta < 0$ if θ is measured with respect to the outward pointing normal.

Even eq. (6.11) is too complicated to solve directly without a lot of numerical work. So we adopt the diffusion approximation: The radiation field is presumed only mildly anisotropic, so that its angular dependence can be expanded in Legendre polynomials:

$$I_\nu(\Omega, s) = \sum_{n=0}^{\infty} I_\nu^{(n)}(z) P_n(\cos\theta).$$

For simplicity, the spatial dependence depends on a single spatial coordinate, z , which measures height in the atmosphere and increases along the outward normal; this is related to arc length along a ray by $dz = \cos \theta ds$. The specific intensity is independent of the azimuthal angle ϕ . In the diffusion approximation, one further discards all terms in the above series except the first two, i.e. $n = 0$ and $n = 1$: these are the minimum set needed to describe a net outward flux. The surviving terms are given special names and symbols:

$$U_\nu(z) \equiv c^{-1} \int I_\nu(\Omega, s) d^2\Omega \quad \rightarrow \quad \frac{4\pi}{c} I_\nu^{(0)}(z), \quad (6.13a)$$

$$F_\nu(z) = \int I_\nu(\Omega, z) \cos \theta d^2\Omega \quad \rightarrow \quad 2\pi I_\nu^{(1)}(z), \quad (6.13b)$$

$$P_\nu(z) = c^{-1} \int I_\nu(\Omega, z) \cos^2 \theta d^2\Omega \quad \rightarrow \quad \frac{1}{3} U_\nu(z). \quad (6.13c)$$

Here $U_\nu(z)$ is the energy density per unit frequency at height z ; $F_\nu(z)$ is the corresponding flux density, which vanishes for an isotropic field; and $P_\nu(z)$ is the radiation pressure, which is defined in general by the first equality in eq. (6.13c) but reduces to $U_\nu/3$ when $I_\nu^{(n)} \rightarrow 0$ for $n \geq 2$.

With the further assumption that $d\sigma/d\Omega$ is front-back symmetric, i.e. that the rates for scattering from (θ', ϕ') to (θ, ϕ) and to $(\pi - \theta, \phi + 2\pi)$ are the same—this is true of nonrelativistic Thompson scattering—one obtains coupled equations for the energy density and flux:

$$\frac{dF_\nu}{dz} = -\rho\kappa_a [cU_\nu - 4\pi B_\nu(T_m)] \quad (6.14a)$$

$$\frac{c}{3} \frac{dU_\nu}{dz} = -\rho(\kappa_a + \kappa_s) F_\nu. \quad (6.14b)$$

Eq. (6.14a) results from integrating (6.11) over $d^2\Omega$ after replacing $ds \rightarrow dz/\cos \theta$ on the left side.⁴ The scattering terms annihilate because of the normalization (6.12). Eq. (6.14b) results from a similar integration over $d^2\Omega$ after first multiplying both sides of eq. (6.11) by $\cos \theta$; the final term in (6.11) gives no contribution when weighted by $\cos \theta$ because of the assumed front-back symmetry.

It is often convenient to change the independent variable from z to *optical depth*

$$\tau \equiv \int_z^\infty (\kappa_a + \kappa_s) \rho dz. \quad (6.15)$$

Equations (6.14) then become

$$\frac{dF_\nu}{d\tau} = \alpha [cU_\nu - 4\pi B_\nu(T_m)] \quad (6.16a)$$

$$\frac{c}{3} \frac{dU_\nu}{d\tau} = F_\nu, \quad (6.16b)$$

where $\alpha \equiv \kappa_a/(\kappa_a + \kappa_s)$ is the fraction of the total opacity represented by absorption.

6.2.2 The graybody factor

Equations (6.16) constitute two ordinary differential equations in z (for each frequency ν) and therefore require two initial or boundary conditions. One condition is

$$cU_\nu - 4\pi B_\nu(T_m) \rightarrow 0 \quad \text{as } \tau \rightarrow \infty, \quad (6.17)$$

⁴Do not confuse z as vertical coordinate with z as redshift.

i.e., the radiation and matter temperatures are at equilibrium deep in the atmosphere.

The other boundary is $\tau = 0$, which is notionally a surface from which photons escape freely. In reality the gas density never quite falls to zero, and so $\tau = 0$ corresponds to $z = +\infty$. However, if the atmosphere were truly plane-parallel, it would asymptotically occupy half the sky as seen from increasingly large heights and correspondingly low optical depths. At such large heights, $F_\nu \rightarrow f_E c U_\nu$, where f_E is a positive constant less than unity (because all photons move outward, but not directly upward). This leads to the boundary condition $f_E = 1/2$.

$$F_\nu \rightarrow f_E c U_\nu \quad \text{at } \tau \rightarrow 0. \quad (6.18)$$

In the *Eddington approximation*, one supposes that at $\tau \ll 1$, the specific intensity is constant along ingoing rays—i.e., $I_\nu(\theta, \tau) \approx I_\nu(0, 0)$ at angles $\theta < \pi/2$ measured from the outward normal—and vanishes on ingoing rays ($\theta > \pi/2$). With these assumptions, $f_E = 1/2$.

If (for simplicity) the matter temperature T_m and the fractional absorption α are constants, then eqs. (6.16) are linear inhomogeneous equations with constant coefficients. A particular solution is $(U_\nu, F_\nu) = (4\pi/c)B_\nu, 0$, and the homogeneous solutions are $\propto \exp(\pm\tau\sqrt{3\alpha})$. The solution for the flux that satisfies the boundary conditions (6.17) & (6.18) is

$$F_\nu(\tau) = 4\pi \left(\frac{1}{f_E} + \sqrt{\frac{3}{\alpha}} \right)^{-1} B_\nu(T_m) e^{-\tau\sqrt{3\alpha}}. \quad (6.19)$$

In the limit $\alpha = 1$, corresponding to negligible scattering, the atmosphere should radiate as a black body, so that $F_\nu(0) \rightarrow \pi B_\nu$. This will be the case if $f_E = (4 - \sqrt{3})^{-1} \approx 0.441$, close enough to the Eddington approximation $f_E = 1/2$.

In the opposite limit of weak absorption,

$$F_\nu(0) \approx 4\sqrt{\frac{\alpha}{3}} \pi B_\nu(T_m) \quad \alpha \ll \frac{3}{16}, \quad (6.20)$$

so that the graybody factor $f_g \ll 1$.

The square-root dependence deserves a heuristic explanation. If $\kappa_a \ll \kappa_s$, the number of scatterings that a photon typically undergoes while random-walking between $\tau \gg 1$ and $\tau \sim 0$ is $N_{\text{scatt}} \sim \tau^2$. The probability of absorption per scattering is $\sim \alpha \ll 1$. Therefore, equilibrium between the radiation and matter temperatures will be maintained at optical depths such that $\alpha N_{\text{scatt}} > 1$, i.e. for $\tau \gtrsim \alpha^{-1/2} \equiv \tau_{\text{eq}}$. At smaller optical depths, the photons diffuse by scattering with little change in their numbers or energies (since we neglect electron recoil). Hence the color temperature remains approximately constant at $\tau \leq \tau_{\text{eq}}$. However, a gradient in the energy density is required at $\tau \leq \tau_{\text{eq}}$ to drive the diffusive flux [eq. (6.16b)], so that

$$F_\nu(0) \sim c \frac{U_\nu(\tau_{\text{eq}})}{3\tau_{\text{eq}}} \sim \frac{4\pi}{3c} \alpha^{1/2} B_\nu(T_m).$$

since $U_\nu = (4\pi/c)B_\nu$ in thermal equilibrium.

The main source of absorption opacity is free-free, for which the following Kramers formula is a reasonable first approximation (B. Paczynski, private communication):

$$\begin{aligned} \kappa_a &\approx 13(1+X)(Z+0.001) \left(\frac{\rho}{1 \text{ g cm}^{-3}} \right) \left(\frac{T}{10^7 \text{ K}} \right)^{-7/2} \text{ cm}^2 \text{ g}^{-1} \\ &\approx 0.2 \frac{P_{\text{gas}}}{P_{\text{rad}}} \frac{(Z+0.001)(1+X)(5X-Z+3)}{4} \left(\frac{T}{10^7 \text{ K}} \right)^{-1/2} \text{ cm}^2 \text{ g}^{-1}, \end{aligned} \quad (6.21)$$

where X and Z are the mass fractions in hydrogen and “metals” (\equiv elements heavier than He). Note that in the second line, most of the temperature dependence has been absorbed into the ratio

of gas pressure to radiation pressure $\propto \rho/T^3$. For a neutron star radiating at its Eddington limit, the radiation temperature is $\sim 2 \times 10^7$ K⁵. The pressure ratio

$$\frac{P_{\text{gas}}}{P_{\text{rad}} + P_{\text{gas}}} \approx 1 - \frac{L}{L_{\text{Edd}}} \quad (6.22)$$

as a direct consequence of the hydrostatic and (frequency-integrated) radiative-transfer equation. In the case at hand, this ratio is $\ll 1$. Therefore, it is indeed expected that $\kappa_a \ll \kappa_s$ in Type-I X-ray bursts. The graybody factor $f_g \approx 4\sqrt{\kappa_a/3\kappa_s}$ is small and scales with the composition of the atmosphere as $(Z/Z_\odot)^{1/2}$.

⁵Actually, this is T_{eff} , since the Eddington limit applies to the flux. T_c and T_m are somewhat larger, making κ_a even smaller.

Chapter 7

The Blandford-Znajek mechanism

We have seen that

1. accretion from a thin disk can spin a black hole up nearly to its critical angular momentum $J_{\text{crit}} = GM^2/c$, or equivalently, $a \equiv J/M = 1$;
2. at $a/M = 1$, the accretion efficiency of a thin disk is $\epsilon = 1 - 3^{-1/3} \approx 0.42$: that is, of every parcel of rest mass accreted, a fraction $3^{1/2}$ is added to the mass of the hole, while the rest can be radiated¹;
3. thermodynamics permits a fraction $\leq 1 - 2^{-1/2} \approx 29\%$ of M to be extracted from the black hole by spinning it down.

It follows that by first growing a black hole up from a very small initial mass and then spinning it down again, a net efficiency of $1 - 3^{-1/2} \cdot 2^{-1/2} \approx 59\%$ might in principle be achieved, leaving more “headroom” to meet the constraints imposed by comparison of the quasar population with inert black holes in galactic nuclei [68, and references therein]. Also, one wants to explain how radio galaxies emit large amounts of radio, gamma-ray, and mechanical energy in relativistic jets with relatively little associated thermal emission; this points to the need for a “cleaner” power source than standard disk accretion.

To achieve these goals astrophysically, one requires a means of achieving step 3 above. An important theoretical model of how this might occur is the Blandford Znajek mechanism [henceforth BZM], which in effect wires the spinning black hole as a Faraday unipolar dynamo. This model is by no means universally accepted. There is no observational proof of it, and furthermore, it still requires a disk, whose properties upon close theoretical inspection are perhaps implausible. Nevertheless, it brings together GR and electrodynamics in an astrophysically interesting context. The ultimate theory of radio galaxies and their jets (and possibly other sources such as GRBs) may well incorporate elements of the BZM.

7.1 Faraday unipolar dynamo

Imagine a conducting disk made to rotate around its symmetry axis in an imposed magnetic field. For simplicity (this is not essential) let the field be uniform and parallel to the axis. The rotation velocity is $\mathbf{v} = \boldsymbol{\omega} \times \mathbf{r}$ at position \mathbf{r} within the disk, where $\boldsymbol{\omega}$ is the angular velocity. In locally corotating frame, the motion contributes a radial electric field $(\mathbf{v} \times \mathbf{B})/c$. The total electromotive

¹ Taking into account preferential capture of retrograde photons by the hole, however, $(a/M)_{\text{max}} \approx 0.998$ and $\epsilon_{\text{max}} \approx 0.30$ [60].

force due to this is

$$\mathcal{E} = \int_0^R \frac{\omega B r}{c} dr = \frac{\omega B R^2}{2c} = \frac{\omega \Phi}{2\pi c}, \quad (7.1)$$

where $\Phi \equiv \int \mathbf{B} \cdot d\mathbf{A} = \pi R^2 B$ is the total magnetic flux through the disk.

If the disk is electrically isolated (no wires or brushes attached) and the rotation is steady, the net electric field parallel to the surface of the conductor must vanish. Charges redistribute themselves within the disk so as to create a radial electrostatic field that just cancels the $\mathbf{v} \times \mathbf{B}/c$ contribution. Hence there is a nonzero normal component $E_{\perp} = 4\pi\sigma$, where σ is the surface charge density, and therefore a nonzero $\mathbf{E} \cdot \mathbf{B}$. But $\mathbf{E} \cdot \mathbf{B}$ is Lorentz invariant, so it follows that there will be a nonzero E_{\perp} in the lab (nonrotating) frame also. Also, since \mathbf{E} and \mathbf{B} are perpendicular to the disk in the rotating frame, the electric field in the lab frame has the radial component $\mathbf{E}_{\parallel} = \mathbf{v} \times \mathbf{B}/c$, and so the voltage from the center to the edge of the disk is

$$V_0 - V_R = \frac{\omega \Phi}{2\pi c}, \quad (7.2)$$

just equal to \mathcal{E} .

What Faraday did next, of course, was to make electrical contact with the outer edge of the disk using a wire brush, and thereby complete a circuit through an electrical load to the center of the disk. As long as mechanical energy is supplied to keep the disk turning, a current $I = \mathcal{E}/(Z_L + Z_D)$ flows through the circuit, and a total electrical power

$$P = I\mathcal{E} = \frac{\mathcal{E}^2}{Z_L + Z_D}$$

is generated, where Z_D and Z_L are the impedences (resistances) of the disk and the load, respectively. The power supplied to the load is

$$P_L = I^2 Z_L = Z_L \frac{\mathcal{E}^2}{(Z_L + Z_D)^2},$$

so the efficiency of the dynamo $P_L/P = Z_L/(Z_L + Z_D)$, which is maximized for $Z_L \gg Z_D$. However, P_L itself is maximized when $Z_L = Z_D$ —for a fixed \mathcal{E} , that is, fixed Φ and ω .

7.2 Electrical conductivity of a black hole

From the point of view of external observers, the event horizon behaves as an imperfectly conducting surface. The proof proceeds in a few steps.

1. *Infalling geodesic observers move radially at the speed of light as seen by local observers who are stationary with respect to the horizon.* Consider the Schwarzschild case. In a previous lecture, the radial equation of motion was shown to be

$$\left(\frac{dr}{d\tau}\right)^2 = E^2 - \left(1 - \frac{2M}{r}\right) \left(1 + \frac{L^2}{r^2}\right), \quad \text{and} \quad E = \left(1 - \frac{2M}{r}\right) \frac{dt}{d\tau}$$

Thus $dr/d\tau \rightarrow -E$ as $r \rightarrow 2M$ regardless of the angular momentum. It follows that

$$\frac{dr}{dt} \rightarrow -\left(1 - \frac{2M}{r}\right) \quad \text{as } r \rightarrow 2M.$$

regardless of both E and L . Now a local stationary observer has proper time $d\tau_{\text{so}} = dt \sqrt{-g_{00}}$, and the radial proper length corresponding to dr is $dr \sqrt{g_{11}}$, so according to the stationary observer, the radial 3-velocity is

$$\frac{dr \sqrt{g_{11}}}{dt \sqrt{-g_{00}}} \rightarrow -1. \quad \text{Q.E.D.}$$

In the case of a rotating black hole, “stationary with respect to the horizon” means keeping constant r and θ but rotating at the angular velocity of the horizon itself,

$$\left(\frac{d\phi}{dt}\right)_H = \omega_H = \frac{a}{2Mr_H}. \quad (7.3)$$

Otherwise, the proof goes through similarly, but with more algebra.

2. *Charges and currents outside the horizon produce electric and magnetic fields at the horizon that are finite as seen by freely infalling observers.* For our purposes this is a postulate. It is plausible because we have already seen that there is nothing special about the horizon from the point of view of the infalling observer (finite tidal fields, *etc.*). Also, for example, it is easy to show that an infalling observer sees finite energies for all infalling photons, so the electric and magnetic fields associated with those photons are finite.

Using FFRF instantaneously comoving with the infalling and stationary observers (“orthonormal frames,” for short), the transformation between the electric and magnetic fields seen by these two sets of observers is

$$\begin{aligned} \mathbf{E}_{\parallel} &= \gamma(\bar{\mathbf{E}}_{\parallel} + \mathbf{v} \times \bar{\mathbf{B}}_{\parallel}) & E_{\perp} &= \bar{E}_{\perp}, \\ \mathbf{B}_{\parallel} &= \gamma(\bar{\mathbf{B}}_{\parallel} - \mathbf{v} \times \bar{\mathbf{E}}_{\parallel}) & B_{\perp} &= \bar{B}_{\perp}, \end{aligned}$$

as in SR. Here the subscript \parallel means parallel to the *horizon*, hence *perpendicular* to the 3-velocity $\mathbf{v} \rightarrow -\hat{\mathbf{r}}$ of the infalling observer, whose electromagnetic fields are denoted by the overbars. The Lorentz factor $\gamma \rightarrow \infty$ as $r \rightarrow r_H$. So unless $\bar{\mathbf{E}}_{\parallel} = 0 = \bar{\mathbf{B}}_{\parallel}$, the stationary observer’s fields are almost parallel to the horizon, and

$$\mathbf{E} \rightarrow \hat{\mathbf{r}} \times \mathbf{B} \quad \text{as } r \rightarrow r_H \quad (\text{if } \bar{\mathbf{E}}_{\parallel} \neq 0). \quad (7.4)$$

As a check that all this makes sense, consider the electromagnetic 3-velocity defined by the ratio of the Poynting flux to the energy density:

$$\mathbf{v}_{em} \equiv \frac{c(\mathbf{E} \times \mathbf{B})/4\pi}{(\mathbf{E}^2 + \mathbf{B}^2)/8\pi}.$$

Eq. (7.4) implies that $\mathbf{v}_{em} \rightarrow -c\hat{\mathbf{r}}$ at the horizon, as one might expect.

Next, imagine immersing a nonrotating hole in a purely electrostatic field. Presumably \mathbf{B} vanishes everywhere, hence $\mathbf{B}_{\parallel} = 0$ at the horizon, and it follows that $\mathbf{E}_{\parallel} = 0$. Hence the electric field is normal to the horizon, just as one would expect if the horizon were a conductor.

To quantify the conductivity of the horizon, consider that it should perfectly absorb any incident Poynting flux $c(\mathbf{E}_{\parallel} \times \mathbf{B}_{\parallel})/4\pi$. On the other hand, if there were a surface current \mathcal{J} [dimensions: current/(transverse length)] flowing on the horizon, the power dissipated by Joule heating would be $\mathcal{J} \cdot \mathbf{E}_{\parallel}$ per unit area. Equating these two powers and recognizing that $|\mathbf{E}_{\parallel}| = |\mathbf{B}_{\parallel}|$ yields $\mathcal{J} = (c/4\pi)\mathbf{E}_{\parallel}$. This looks like Ohm’s law for a two-dimensional conductor with surface conductivity

$$\Sigma_H = \frac{c}{4\pi}. \quad (7.5)$$

Σ_H^{-1} has units of resistance and equates to 377 Ohms in the SI system.

7.3 Black hole as dynamo

[5] proposed to replace the disk in Faraday’s dynamo by a black hole with the angular velocity (7.3). [Their paper is important but difficult. For a more readable account of the main ideas, see [6]. For a thorough pedagogical discussion of black-hole physics, see [61].]

[64] analyzed the simplest analog of the electrically isolated dynamo: a Kerr black hole embedded in a stationary, asymptotically uniform magnetic field B_0 parallel to the spin axis [cf. 61]. He found an exact solution, with total flux through the upper half of the horizon

$$\Phi_H = 4\pi B_0 M (r_H - M),$$

so that $\Phi_H \rightarrow \pi R_S^2 B_0$ in the nonrotating limit $a \rightarrow 0$, $r_H \rightarrow 2M = R_S$. As with Faraday's disk, the horizon develops a surface charge to cancel the parallel component of the induced $(\mathbf{v} \times \mathbf{B})_H$ electric field in its corotating frame:

$$\sigma_H = -B_0 a \sqrt{M^2 - a^2} \frac{4Mr_H P_2(\cos \theta) + (a \sin^2 \theta)^2}{4\pi(r_H^2 + a^2 \cos^2 \theta)^2}.$$

Here $P_2(\cos \theta) \equiv (3 \cos^2 \theta - 1)/2$ is the usual Legendre polynomial. So for $a \ll M$, the electric field is quadrupolar, just as one expects for a rotating spherical conductor in a uniform field. σ_H changes sign at mid-latitude, and the net electric charge on the horizon is zero.

Wald's solution has nonzero $\mathbf{E} \cdot \mathbf{B}$: for example, the electric field at the "north pole" is parallel to the axis and of magnitude

$$4\pi\sigma_H(0) = -B_0 a \sqrt{M^2 - a^2} \frac{4M}{r_H^3}.$$

The voltage difference between the horizon and $r = \infty$ is of order $r_H B_0 (a/M)$, or numerically,

$$\Delta V \sim 10^{20} \left(\frac{a}{M}\right) \left(\frac{M}{10^9 M_\odot}\right) \left(\frac{B_0}{10^4 \text{ Gauss}}\right) \text{ Volt}, \quad (7.6)$$

for parameters thought relevant to quasars and radio galaxies. With such a huge voltage drop along field lines, one expects that any stray electron in the vicinity of such a hole would be accelerated to huge energies and, upon colliding with stray photons or charges of opposite sign, produce a cascade of e^+e^- pairs. Very quickly therefore, the vacuum surrounding the black hole would be filled with a highly conducting plasma. The plasma-loaded field lines can serve as "wires" to complete a circuit between the pole and equator of the horizon. The EMF around this circuit is [cf. eq. (7.1)]

$$\mathcal{E} = \frac{\omega_H \Phi_H}{2\pi},$$

which is numerically comparable to (7.6). Because of the plasma mentioned above, the black-hole "magnetosphere" is almost completely short-circuited ($\mathbf{E} \cdot \mathbf{B} \approx 0$), so this voltage drop occurs mostly in two places:

- (i) across the horizon itself, where the impedance $Z_L \sim 4\pi/c$;
- (ii) and possibly at some distance from the hole where the circuit is closed.

The latter is called the "astrophysical load." The thought is that the load is due either to bulk acceleration of matter, or else the magnetosphere becomes charged-starved so that individual charges accelerate to very high Lorentz factors. In hope is that this occurs mainly near the axis and powers a well-collimated relativistic jet. However, the problem is at least as difficult as (and in many ways perhaps similar to) the acceleration of pulsar winds. At the present stage, it is perhaps best described as a scenario rather than theory. Relativistic MHD simulations may provide insight. In any case, the same considerations concerning the power dissipated in the load and in the dynamo itself apply to this case, so that the maximum power one may hope to extract is of order [61]

$$P_L \lesssim \frac{1}{128} \left(\frac{a}{M}\right)^2 B_0^2 r_H^2 \approx 10^{45} \left(\frac{a}{M} \cdot \frac{M}{10^9 M_\odot} \cdot \frac{B}{10^4 \text{ G}}\right)^2 \text{ erg s}^{-1}, \quad (7.7)$$

comparable to what is required to explain powerful radio galaxies.

7.4 Back-of-the-envelope AGN

There must be matter surrounding the black hole—presumably an accretion disk—to sustain the magnetic field. Otherwise, since the hole behaves like an imperfect conductor, the flux would diffuse away from the horizon on a timescale of order $[M_9 \equiv M/(10^9 M_\odot)]$

$$\frac{GM}{c^3} \approx 5 \times 10^3 M_9^{-1} \text{ sec.}$$

But if the disk is a good conductor, the field lines cannot easily cross it, and the flux will be trapped on the horizon. In fact the disk will probably be turbulent and accreting, in which case it can probably serve as a *magnetic* dynamo to generate the large-scale magnetic flux necessary to tap the spin energy of the black hole. The disk will have its own luminosity, which is likely to be comparable to the maximum power (7.7) extracted from the hole.

To develop some sense for the orders of magnitude involved, recall that the maximum luminosity of an accreting mass is believed to be the Eddington limit,

$$L_E \equiv \frac{4\pi GMm_p c}{\sigma_T} \approx 1.3 \times 10^{47} M_9 \text{ erg s}^{-1}. \quad (7.8)$$

At this point, the outward radiation force on an electron, $L\sigma_T/4\pi r^2 c$ just balances the inward gravitational force on its associated proton, GMm_p/r^2 , at all radii $r \gg R_S$ (electrostatic fields will prevent any significant separation of the charges). At any higher luminosity, ordinary matter is more likely to be driven off by radiation pressure than to accrete. The energy density of the radiation field at the Eddington limit is

$$\rho_E c^2 \sim \frac{L_E}{4\pi R_S^2 c} \approx 4 \times 10^6 M_9^{-1} \text{ erg cm}^{-3}.$$

If the inner parts of the accretion disk are radiation-pressure-dominated, as seems likely, then the energy density within the disk will be comparable to ρ_E (but larger by a factor of the disk optical depth, which might be substantial). A characteristic magnetic field strength can be defined by equating this to $B^2/8\pi$:

$$B_E \approx 1.0 \times 10^4 M_9^{-1/2} \text{ Gauss}; \quad (7.9)$$

it is unlikely that a stronger field could be generated or stably confined by the disk. Similarly, one can derive a characteristic temperature for the emission from the disk by setting $aT_E^4 = \rho_E c^2$:

$$T_E \approx 1.5 \times 10^5 M_9^{-1/4} \text{ K} \approx 13 k_B^{-1} M_9^{-1/4} \text{ eV}, \quad (7.10)$$

comparable to the ionization potential of hydrogen for AGN disks.

These estimates suggest that the energy extracted from the spin of the hole, and hence perhaps the energy in the jet, is likely to be comparable to the luminosity of the disk.

Chapter 8

Gravitational Waves

Despite our earlier disclaimers, we have decided to include a short discussion of gravitational waves, even though their discussion requires use of the field equations, for which we give a brief self-contained derivation in the weak-field limit. The topic is timely and interesting because of the prospects for direct detection by upcoming gravitational-wave detectors, especially LISA, and because these detections will probe sources of great astrophysical interest that will be difficult to study electromagnetically, such as merging supermassive black holes at redshifts $z \gtrsim 1$.

For a more complete discussion, see [56], whose notation we follow by and large.

8.1 Overview

Gravitational waves (henceforth GW) are perturbations in the metric and its derivatives that propagate at the speed of light. The source of GW is (oscillatory parts of) the energy-momentum tensor, $T^{\mu\nu}$, or sometimes (since GR is nonlinear) the gravitational field itself—as in the case of merging black holes, for instance.

Perhaps 99% of practical astrophysical applications *to date* have used nothing more than the Quadrupole Formula, which gives the energy loss rate (“luminosity”) in gravitational waves of sources whose internal bulk speeds are $\ll c$:

$$L_{GW} = \frac{G}{5c^5} \langle \ddot{I}_{ij} \ddot{I}^{ij} \rangle, \quad (8.1)$$

in which I^{ij} is the traceless part of the quadrupole moment of the mass distribution,

$$I^{ij}(t) \equiv c^{-2} \int \left(x^i x^j - \frac{1}{3} \eta^{ij} x^k x_k \right) T^{00}(t, \mathbf{x}) d\mathbf{x}, \quad (8.2)$$

and $\ddot{I}^{ij} \equiv d^2 I^{ij} / dt^2$. We have divided by c^2 in (8.2) to convert the energy density T^{00} to a mass density. The Quadrupole Formula is the analog for GW of the Larmor formula (2.9) for the electromagnetic luminosity of an oscillating electrical dipole. Like the Larmor formula, (8.1) is valid when the period of oscillation is large compared to the light-crossing time R/c across the source, or in other words, when the emitted wavelength $\lambda \gg R$, which is normally true if the internal velocities are $\ll c$.

In the usual GR units $G = c = 1$, \ddot{I}^{ij} is dimensionless (*check this*), and therefore so is L_{GW} . It follows that there must be a unit of luminosity that can be constructed from G and c alone:

$$L_0 = \frac{c^5}{G} \approx 3.6 \times 10^{59} \text{ erg s}^{-1}. \quad (8.3)$$

Roughly speaking, this is the luminosity that an object of size comparable to its Schwarzschild radius would produce if it radiated all of its rest mass in its light-crossing time. Since the characteristic frequency of a nonrelativistic source with internal velocities $\sim v$ and size $\sim R$ is $\omega \sim v/R$, it follows that $\ddot{I} \sim Mv^3R^{-1}$ and $L_{GW} \sim (v/c)^6(R_S/R)^2L_0 \ll L_0$. Thus, typical sources radiate inefficiently because they are slow ($v \ll c$) and because they are not compact ($R \gg GM/c^2$).

8.2 The Weak-Field Approximation

In order to calculate the production of GW, it is practically unavoidable to linearize the Field Equations around some exact solution, normally Minkowski space. Thus we assume that the metric perturbation $h_{\mu\nu} \equiv g_{\mu\nu} - \eta_{\mu\nu}$ is small and work to first order. Obviously this depends as much upon our choice of coordinates as upon the intrinsic geometry, since it would not be true even in flat space if we chose, *e.g.*, polar coordinates. Even in strongly curved space, the Principle of Equivalence ensures that coordinates can be found such that $h_{\mu\nu}$ is small in the neighborhood of any given event. One can't necessarily find a single set of coordinates that makes $h_{\mu\nu}$ small everywhere, but this is true often enough for the Weak-Field Approximation to be very useful.

8.3 Analogy with Electromagnetism

Recall that Maxwell's equations

$$\begin{aligned} \nabla \times \mathbf{B} - \frac{1}{c} \frac{\partial \mathbf{E}}{\partial t} &= \frac{4\pi}{c} \mathbf{J}, & \nabla \times \mathbf{E} + \frac{1}{c} \frac{\partial \mathbf{B}}{\partial t} &= 0, \\ \nabla \cdot \mathbf{E} &= 4\pi\rho, & \nabla \cdot \mathbf{B} &= 0, \end{aligned} \quad (8.4)$$

lead to wave equations

$$\begin{aligned} \left(\nabla^2 - \frac{1}{c^2} \frac{\partial^2}{\partial t^2} \right) \mathbf{E} &= 4\pi \left(\frac{1}{c} \frac{\partial \mathbf{J}}{\partial t} + \nabla \rho \right) \\ \left(\nabla^2 - \frac{1}{c^2} \frac{\partial^2}{\partial t^2} \right) \mathbf{B} &= -\frac{4\pi}{c} \nabla \times \mathbf{J}. \end{aligned}$$

But while all solutions of (8.4) satisfy these wave equations, not all solutions of the latter satisfy (8.4): for example,

$$\mathbf{B} \propto \mathbf{e}_x \cos(\omega t - kx),$$

which has $\nabla \cdot \mathbf{B} \neq 0$. To avoid this, and for other reasons, one introduces scalar and vector potentials \mathbf{A} & Φ such that

$$\begin{aligned} \mathbf{B} &= \nabla \times \mathbf{A}, & \text{which guarantees} & & \nabla \cdot \mathbf{B} &= 0; \\ \mathbf{E} &= -\nabla \Phi - \frac{1}{c} \frac{\partial \mathbf{A}}{\partial t}, & \text{which guarantees} & & \nabla \times \mathbf{E} + \frac{1}{c} \frac{\partial \mathbf{B}}{\partial t} &= 0. \end{aligned}$$

Substitution into the first of eqs. (8.4) then yields

$$\nabla(\nabla \cdot \mathbf{A}) - \nabla^2 \mathbf{A} + \frac{1}{c^2} \frac{\partial^2}{\partial t^2} \mathbf{A} + \frac{1}{c} \frac{\partial}{\partial t} \nabla \Phi = \frac{4\pi}{c} \mathbf{J}. \quad (8.5)$$

For any arbitrary function $f(t, \mathbf{x})$, the gauge transformation

$$\mathbf{A} \rightarrow \mathbf{A} + \nabla f \quad \Phi \rightarrow \Phi - \frac{1}{c} \frac{\partial f}{\partial t} \quad (8.6)$$

has no effect on \mathbf{E} and \mathbf{B} . One can show that f may be chosen so that, after the transformation,

$$\nabla \cdot \mathbf{A} + \frac{1}{c} \frac{\partial \Phi}{\partial t} = 0. \quad (8.7)$$

This is called Lorentz Gauge. Then the wave equation (8.5) simplifies to

$$\square \mathbf{A} \equiv \left(\nabla^2 - \frac{1}{c^2} \frac{\partial^2}{\partial t^2} \right) \mathbf{A} = -\frac{4\pi}{c} \mathbf{J}. \quad (8.8)$$

Note that we have defined the D'Alembertian operator $\square \equiv \eta^{\mu\nu} \partial_\mu \partial_\nu$ in passing. Furthermore, $\nabla \cdot \mathbf{E} = 4\pi\rho$ leads in Lorentz Gauge to

$$\square \Phi = -4\pi\rho. \quad (8.9)$$

Equations (8.8) & (8.9) can be combined into one equation for the four-potential $A^\mu \equiv (\Phi, \mathbf{A})$ in terms of the 4-current $J^\mu \equiv (\rho, \mathbf{J}/c)$:

$$\square A^\mu = -4\pi J^\mu. \quad (8.10)$$

Gauge transformations (8.6) and the Lorentz gauge (8.7) are expressed as

$$A_\mu \rightarrow A_\mu + \partial_\mu f \quad \text{and} \quad \partial_\mu A^\mu = 0, \quad (8.11)$$

respectively, in this notation. Finally, the solution of (8.8) for outgoing waves is expressed in terms of the retarded Lienard-Weichert potential:

$$A^\mu(t, \mathbf{x}) = \int \frac{J^\mu(t_{\text{ret}}, \mathbf{x}')}{|\mathbf{x} - \mathbf{x}'|} d\mathbf{x}', \quad t_{\text{ret}} \equiv t - \frac{|\mathbf{x} - \mathbf{x}'|}{c}. \quad (8.12)$$

8.4 The gravitational-wave equation

Just as A^μ can undergo a gauge transformation without affecting the physical electromagnetic fields \mathbf{E}, \mathbf{B} , the metric perturbation can undergo an infinitesimal change of coordinates without affecting the intrinsic geometry and tidal fields. Such a coordinate change is

$$\bar{x}^\mu = x^\mu + \epsilon^\mu, \quad (8.13)$$

where ϵ^μ is of the same order of smallness as $h_{\mu\nu}$. Note that contrary to our (and Schutz's) usual convention, the bar has been put on the coordinate itself rather than its index, *i.e.* \bar{x}^μ instead of $x^{\bar{\mu}}$, in order to make equations like (8.13) easier to write, where μ has the same value in both coordinate systems. Expanding to first order in ϵ_μ and $h_{\mu\nu}$ the metric transformation law

$$\eta_{\mu\nu} + h_{\mu\nu} = \frac{\partial \bar{x}^\alpha}{\partial x^\mu} \frac{\partial \bar{x}^\beta}{\partial x^\nu} (\eta_{\alpha\beta} + \bar{h}_{\alpha\beta})$$

yields the required "gauge transformation,"

$$\bar{h}_{\mu\nu} = h_{\mu\nu} + \epsilon_{\mu,\nu} + \epsilon_{\nu,\mu}. \quad (8.14)$$

It doesn't matter whether $\epsilon_{\mu,\nu}$ means $\partial \epsilon_\mu / \partial x^\nu$ or $\partial \epsilon_\mu / \partial \bar{x}^\nu$ since these differ at second order. (By the way, indices on first-order quantities are raised and lowered using the zeroth-order metric, *e.g.* $\epsilon_\mu = \eta_{\mu\nu} \epsilon^\nu$ and $h^\mu{}_\nu = \eta^{\mu\alpha} h_{\alpha\nu}$.)

We will now sketch the derivation of the linear wave equation in a way that closely parallels the derivation of the exact nonlinear field equations (see, *e.g.*, [66]). (If you are willing to take the result, (8.19) on faith, skip ahead to that equation; but know that that form of the wave equation applies in harmonic gauge (8.17) only.) The ingredients are

1. All terms should involve two derivatives of $h_{\mu\nu}$ except the source term, which is $T_{\mu\nu}$.
2. The equation should be Lorentz covariant, meaning that all terms should be tensors with the same free indices upstairs and downstairs.
3. It should be invariant under “gauge transformations” (8.14).
4. It should imply $T^{\mu\nu}{}_{,\nu} = 0$ (just as Maxwell’s Equations imply charge conservation).
5. It should be consistent with Poisson’s equation $\nabla^2\Phi = 4\pi\rho$ in the Newtonian limit.

These are the same assumptions as those of exact GR, except that the second and third would then be combined into the requirement that all terms transform as tensors under arbitrary coordinate changes, and the fourth would become $T^{\mu\nu}{}_{,\nu} = 0$. In our case, the difference between the covariant derivative, indicated by the semicolon, and the ordinary partial derivative is second-order of smallness.

The most general form satisfying the first two assumptions is

$$A\Box h_{\mu\nu} + C(h^{\alpha}{}_{\mu,\alpha\nu} + h^{\alpha}{}_{\nu,\alpha\mu}) + Dh_{,\mu\nu} + \eta_{\mu\nu} (B\Box h + Eh^{\alpha\beta}{}_{,\alpha\beta}) = T_{\mu\nu} \quad (8.15)$$

Here $h \equiv h^{\lambda}{}_{\lambda}$ is shorthand for the trace of the metric perturbation, and A, B, C, D, E are constants. Assumption 3 implies that the lefthand side would vanish if $h_{\kappa\lambda}$ were replaced by $\epsilon_{\kappa,\lambda} + \epsilon_{\lambda,\kappa}$. With a little algebra (*check this*), this leads to

$$A + C = 0, \quad C + D = 0, \quad B + E = 0.$$

Assumption 4 leads to

$$A + C = 0, \quad B + D = 0, \quad C + E = 0.$$

So $A = D = E = -B = -C$, and (8.15) reduces to

$$\Box h_{\mu\nu} - (h^{\alpha}{}_{\mu,\alpha\nu} + h^{\alpha}{}_{\nu,\alpha\mu}) + h_{,\mu\nu} + \eta_{\mu\nu} (-\Box h + h^{\alpha\beta}{}_{,\alpha\beta}) = A^{-1}T_{\mu\nu}. \quad (8.16)$$

The Newtonian limit means weak fields (already assumed) and slow motions, so that $\partial_0 \ll \partial_i$, and $T_{ij} \ll T_{0i} \ll T_{00} \rightarrow \rho$. By the Principle of Equivalence—specifically, the thought experiments about gravitational redshifts in static Newtonian potentials, Φ —it also means $h_{00} \approx -2\Phi$. So we require

$$-2\nabla^2\Phi - (-\Box h + h^{\alpha\beta}{}_{,\alpha\beta}) = A^{-1}\rho \equiv -8\pi\rho.$$

By taking the trace of (8.16), one shows that the parenthesized term on the left equals $\frac{1}{2}A^{-1}T^{\lambda}{}_{,\lambda} \approx -A^{-1}\rho$. So we conclude that $\boxed{A^{-1} = -16\pi}$.

Like (8.5), (8.16) is rather messy, so we are motivated to find a gauge in which it simplifies. [In both equations, while the lefthand side as a whole is gauge invariant, individual terms can be made to vanish by appropriate choice of gauge.] The four free functions $\{e^{\mu}\}$ in (8.14) can be chosen to impose four constraints on $h_{\mu\nu}$: in particular, the “harmonic gauge conditions”

$$(h^{\mu\nu} - \frac{1}{2}\eta^{\mu\nu}h)_{,\nu} = 0. \quad (8.17)$$

In this gauge, the linearized Einstein Field Equations become

$$\Box (h^{\mu\nu} - \frac{1}{2}\eta^{\mu\nu}h) = -16\pi T^{\mu\nu}.$$

To save writing, we will use the abbreviation

$$H^{\mu\nu} \equiv h^{\mu\nu} - \frac{1}{2}\eta^{\mu\nu}h, \quad (8.18)$$

(Schutz calls this $\bar{h}^{\mu\nu}$), so that the wave equation becomes, in harmonic gauge,

$$\Box H^{\mu\nu} = -16\pi T^{\mu\nu}. \quad (8.19)$$

8.5 Solution for fields in the radiation zone

Equation (8.19) has the same form as the electromagnetic wave equation (8.10), except for an extra index, and therefore can be solved in the same way:

$$H^{\mu\nu}(t, \mathbf{x}) = 4 \int \frac{T^{\mu\nu}(t_{\text{ret}}, \mathbf{x}')}{|\mathbf{x} - \mathbf{x}'|} d\mathbf{x}'. \quad (8.20)$$

The next step, as in E&M, is to Fourier transform in time:

$$\begin{aligned} \tilde{H}^{\mu\nu}(\omega, \mathbf{x}) &= \int H^{\mu\nu}(t, \mathbf{x}) e^{i\omega t} dt, \\ H^{\mu\nu}(t, \mathbf{x}) &= \int \tilde{H}^{\mu\nu}(\omega, \mathbf{x}) e^{-i\omega t} \frac{d\omega}{2\pi}. \end{aligned}$$

With a similar definition for $\tilde{T}^{\mu\nu}(\omega, \mathbf{x}')$, (8.20) becomes

$$\tilde{H}^{\mu\nu}(\omega, \mathbf{x}) = 4 \int e^{i\omega|\mathbf{x}-\mathbf{x}'|} \frac{\tilde{T}^{\mu\nu}(\omega, \mathbf{x}')}{|\mathbf{x} - \mathbf{x}'|} d\mathbf{x}'. \quad (8.21)$$

Thus, in the transform, the time of propagation $t_{\text{ret}} - t$ is expressed by the phase of the exponential factor above. Next, we suppose that the source is confined to a region $|\mathbf{x}'| \lesssim R$, and that we are interested in the fields in the far field where $r \equiv |\mathbf{x}| \gg R$. Then we may expand

$$|\mathbf{x} - \mathbf{x}'| \approx r - \frac{\mathbf{x}}{r} \cdot \mathbf{x}' + O(|\mathbf{x}'|^2/r).$$

Let $\mathbf{n} \equiv \mathbf{x}/r$ be the unit vector from the center of the source to the distant field point; note that the sign convention differs from previous chapters. Then

$$\tilde{H}^{\mu\nu}(\omega, \mathbf{x}) = 4 \frac{e^{i\omega r}}{r} \int e^{-i\omega \mathbf{n} \cdot \mathbf{x}'} \tilde{T}^{\mu\nu}(\omega, \mathbf{x}') d\mathbf{x}'. \quad (8.22)$$

We have set $|\mathbf{x} - \mathbf{x}'| \rightarrow r$ in the denominator because this is insensitive to \mathbf{x}' , but we have been more careful in the exponential because if the source is large compared to a wavelength, *i.e.* $\omega R > 1$, then the phase may go through several cycles as \mathbf{x}' varies along the line of sight. In fact, (8.22) may be written succinctly in terms of the four-dimensional Fourier transform of $T^{\mu\nu}$,

$$\hat{T}^{\mu\nu}(\omega, \mathbf{k}) \equiv \iint T^{\mu\nu}(t, \mathbf{x}) e^{i\omega t - i\mathbf{k} \cdot \mathbf{x}} dt d\mathbf{x},$$

as

$$\tilde{H}^{\mu\nu}(\omega, \mathbf{x}) = 4 \frac{e^{i\omega r}}{r} \hat{T}^{\mu\nu}(\omega, \omega \mathbf{n}). \quad (8.23)$$

This solution is asymptotically exact in the limit $r \gg R$ (within the weak-field approximation, of course).

If internal motions of the source are slow, then since typical frequencies [*i.e.*, those at which $\tilde{T}^{\mu\nu}$ is appreciably large] are $\omega \sim v/R$, it follows that $|\omega \mathbf{n} \cdot \mathbf{x}'| \lesssim v \ll 1$. Thus to leading order in v (actually v/c), we can replace the exponential inside the integrand of (8.22) by unity. We will focus on the spatial components \tilde{H}^{ij} , since \tilde{H}^{i0} & \tilde{H}^{00} can be expressed in terms of them (see below):

$$\tilde{H}^{ij}(\omega, \mathbf{x}) \approx 4 \frac{e^{i\omega r}}{r} \int \tilde{T}^{ij}(\omega, \mathbf{x}') d\mathbf{x}', \quad (8.24)$$

with corrections that are smaller by powers of v/c .

For the next step, we will need the identity

$$\int T^{ij}(t, \mathbf{x}) d\mathbf{x} = \frac{1}{2} \frac{d^2}{dt^2} \int x^i x^j T^{00}(t, \mathbf{x}) d\mathbf{x}. \quad (8.25)$$

To prove this, start with

$$\frac{\partial^2}{\partial x^k \partial x^\ell} (x^i x^\ell) = \delta_k^i \delta_\ell^j + \delta_k^j \delta_\ell^i.$$

Therefore

$$\frac{1}{2} \frac{\partial^2}{\partial x^k \partial x^\ell} (x^i x^\ell) T^{k\ell} = \frac{1}{2} (T^{ij} + T^{ji}) = T^{ij}.$$

Substituting this into (8.25) and integrating twice by parts, we have

$$\int T^{ij}(t, \mathbf{x}) d\mathbf{x} = \frac{1}{2} \int x^i x^j T^{k\ell}{}_{,\ell,k} d\mathbf{x}. \quad (8.26)$$

Using $T^{\mu\nu}{}_{,\nu} = 0$ ¹ we have

$$(T^{k\ell}{}_{,\ell})_{,k} = (-T^{k0}{}_{,0})_{,k} = -(T^{k0}{}_{,k})_{,0} = +T^{00}{}_{,0,0}.$$

Using this substitution in (8.26) leads to (8.25). In the Fourier transform, $\partial_t \rightarrow -i\omega$, so (8.25) implies that (8.24) can be written

$$\tilde{H}^{ij}(\omega, \mathbf{x}) \approx -2 \frac{e^{i\omega r}}{r} \omega^2 \int x^i x^j \tilde{T}^{00}(\omega, \mathbf{x}') d\mathbf{x}'. \quad (8.27)$$

Whether we use the general form (8.23) or the slow-motion approximation (8.24), the spatial dependence of $\nabla \tilde{H}^{\mu\nu}(\omega, \mathbf{x})$ in the radiation zone $\omega r \gg 1$ is dominated by the phase factor $\exp(i\omega r)$, whose gradient is $i\omega \mathbf{n} \exp(i\omega r)$, so that

$$\nabla \tilde{H}^{\mu\nu}(\omega, \mathbf{x}) = i\omega \mathbf{n} \tilde{H}^{\mu\nu}(\omega, \mathbf{x}) + O(r^{-2}). \quad (8.28)$$

From now on, unless otherwise specified, let us ignore the $O(r^{-2})$ parts since they are asymptotically negligible compared to the $O(r^{-1})$ radiated fields. The harmonic gauge condition (8.17) then becomes, using (8.28) for the spatial derivatives,

$$-i\omega \tilde{H}^{\mu 0} + i\omega n_j \tilde{H}^{\mu j} = 0.$$

This implies that

$$\begin{aligned} \tilde{H}^{i0}(\omega, \mathbf{x}) &= n_j H^{ij} \\ \text{and } \tilde{H}^{00}(\omega, \mathbf{x}) &= n_i n_j H^{ij}, \end{aligned} \quad (8.29)$$

which confirms that all components of $\tilde{H}^{\mu\nu}$ can be expressed in terms of the nine space-space components \tilde{H}^{ij} .

¹which is true to first order since $T^{\mu\nu}$ is already small, although derivatives of the metric would enter the mix at higher orders

8.5.1 Transverse-traceless (“TT”) gauge

Note that it is the full quadrupole moment that appears in (8.27),

$$I^{ij} \equiv \int x^i x^j \tilde{T}^{00}(\omega, \mathbf{x}') d\mathbf{x}',$$

rather than its traceless counterpart $\mathcal{I}^{ij} = I^{ij} - \frac{1}{3}\eta^{ij}I^k_k$. So it would appear that (8.27) allows radiation from a spherical source, for which $I^{ij} = \frac{1}{3}\eta^{ij}I^k_k$, contrary to Birkhoff’s Theorem. This is not just a feature of the slow-motion approximation, since (8.23) says that $\tilde{H}^{ij} \propto \hat{T}^{ij}(\omega, \omega\mathbf{n})$, and the latter does not generally vanish for a pulsating spherical source.

Once again, there is an analogy in in E&M. In Lorentz gauge, $\tilde{\mathbf{A}}(\omega, \mathbf{x}) \propto \hat{\mathbf{J}}(\omega, \omega\mathbf{n}) \neq 0$ for a pulsating spherical charge distribution. In the latter case, rotational symmetry clearly implies that $\hat{\mathbf{J}}(\omega, \mathbf{k}) \parallel \mathbf{k}$, so that $\tilde{\mathbf{A}}(\omega, \mathbf{x}) \parallel \mathbf{n}$: that is, the vector potential is parallel to its local direction of propagation, in other words, it is *longitudinal* rather than *transverse*. We know that the physical radiation fields $\tilde{\mathbf{E}}$ & $\tilde{\mathbf{B}}$ must be transverse, however. In fact, since $\nabla \tilde{A}^\mu = i\omega\mathbf{n}\tilde{A}^\mu + O(r^{-2})$ [by the same logic that lead to (8.28)], $\tilde{\mathbf{B}} = \nabla \times \tilde{\mathbf{A}} = O(r^{-2})$ when $\tilde{\mathbf{A}}$ is longitudinal. So, there is no radiated magnetic field from a spherical source (actually no external magnetic field at all).

The longitudinal part of the vector potential is a gauge “phantom”: it can be eliminated from the radiation zone, at least locally, by a further restriction of the gauge. The Lorentz gauge condition (8.11) is obviously preserved by any further transformation in which $\square f = 0$. In particular, a plane-wave $f(t, \mathbf{x}) = F \exp(ik_\mu x^\mu)$, where F is constant, satisfies $\square f = 0$ provided that $k_\mu k^\mu = 0$. In the radiation zone, \tilde{A}^μ is *locally* well approximated by a plane wave, $\tilde{A}^\mu \approx a^\mu \exp(ik_\nu x^\nu)$, where $k^\mu = (\omega, \omega\mathbf{n})$, with a^μ a constant 4-vector. In these terms, the remaining gauge freedom is $a^\mu \rightarrow a^\mu + ik^\mu F$. We may choose the constant F so that $a^0 \rightarrow 0$ after the transformation (assuming $\omega \neq 0$). The general Lorentz gauge condition, which has not been spoiled, means that $k_\mu a^\mu = O(r^{-2})$, so that $a^0 = 0$ requires $\mathbf{k} \cdot \mathbf{a} = O(r^{-2})$. In short, this supplementary gauge choice makes $\Phi = 0$ and $\nabla \cdot \mathbf{A} = 0$, at least to leading order in r^{-1} . In this gauge, which is often called “radiation gauge,” the radiated part of \tilde{A}^μ is has just two, rather than four, degrees of freedom, which are the two transverse spatial components, *i.e.* those orthogonal to \mathbf{n} . These can be thought of as the two polarizations.

Note, however, that radiation gauge is available only locally, in the radiation zone. It is not actually restricted to plane waves, but it can’t be used where there is a nonzero charge density, at least not without violating Lorentz gauge, since (8.9) demands $\rho = 0$ in regions where $A^0 = 0$.

Correspondingly, the harmonic gauge condition (8.17) is preserved by transformations such that $\square \epsilon_\mu = 0$.

Exercise: Verify this.

In particular, we may use any plane wave $\epsilon_\mu(t, \mathbf{x}) = \epsilon_\mu(0) \exp(ik_\nu x^\nu)$ with $k_\nu k^\nu = 0$. In the radiation zone where $\tilde{H}^{\mu\nu}(\omega, \mathbf{x})$ and $\tilde{h}^{\mu\nu}(\omega, \mathbf{x})$ are locally planar, the infinitesimal coordinate transformation (8.14) translates to

$$\tilde{h}_{\mu\nu} \rightarrow \tilde{h}_{\mu\nu} + ik_\mu \tilde{\epsilon}_\nu(0) + ik_\nu \tilde{\epsilon}_\mu(0)$$

with $k^\mu \equiv (\omega, \omega\mathbf{n})$. By adjusting the four constants $\epsilon_\mu(0)$, we can impose four conditions on $\tilde{H}^{\mu\nu}$. It is convenient to use three of these to make $\tilde{H}^{0j} = 0$. It then follows from (8.29), which is true in any Lorentz gauge, that $n_j \tilde{H}^{ij} = 0 = \tilde{H}^{00}$. We still have one degree of freedom left among the four $\tilde{\epsilon}_\mu(0)$, which we use to make the trace $\tilde{h} = 0$. To summarize, we have achieved a “transverse traceless gauge” such that

$$0 = \tilde{h} = \tilde{h}^{00} = \tilde{h}^{0i} = \tilde{h}^{ij} n_j. \quad (8.30)$$

Since these conditions hold for every frequency component $\tilde{h}^{\mu\nu}(\omega, \mathbf{x})$, they hold also for the inverse temporal Fourier transforms $h^{\mu\nu}(t, \mathbf{x})$.² Without loss of generality, we may rotate our coordinates

²Actually our supplementary gauge choices depended upon $\omega \neq 0$, so $h^{\mu\nu}(t, \mathbf{x})$ is allowed to have a nonzero time

so that $\mathbf{n} = (0, 0, 1)$, *i.e.* the wave is locally propagating parallel to the z axis. Then the conditions (8.30) imply that

$$\tilde{h}_{\mu\nu}^{\text{TT}} = \tilde{H}_{\mu\nu}^{\text{TT}} = \begin{pmatrix} 0 & 0 & 0 & 0 \\ 0 & \frac{1}{2}(\tilde{h}_{xx} - \tilde{h}_{yy}) & \tilde{h}_{xy} & 0 \\ 0 & \tilde{h}_{xy} & \frac{1}{2}(\tilde{h}_{yy} - \tilde{h}_{xx}) & 0 \\ 0 & 0 & 0 & 0 \end{pmatrix} \quad \text{if } \mathbf{n} = (0, 0, 1) \text{ \& } \omega \neq 0. \quad (8.31)$$

Note: on the righthand side, the components shown are the radiation fields derived from the (asymptotically) “exact” solution (8.23) for the radiation field in a globally valid Lorentz gauge, whereas $h_{\mu\nu}^{\text{TT}}$ are the components in the more specialized *local* TT gauge.

As in the electromagnetic case, there are just two independent polarizations, represented here by $\tilde{h}_{xy} = \tilde{h}_{yx}$ and $\tilde{h}_{xx} = -\tilde{h}_{yy}$. Also in parallel with E&M, the TT gauge is available only in source-free regions, as one can easily see from the original wave equation (8.19).

The *form* of (8.31) is valid for a sufficiently distant observer (on the z axis) receiving radiation from any finite source, even a strong one, since the field is weak in the far field; but the actual values of the nonzero components are those given by (8.19) only if the source is weak. If the source is not only weak but also slow, we have from (8.27) that

$$\begin{aligned} \tilde{h}_{\text{TT}}^{xx}(\omega, \mathbf{x}) &= -\tilde{h}_{\text{TT}}^{yy} = -\frac{e^{i\omega r}}{r} \omega^2 (\tilde{I}^{xx} - \tilde{I}^{yy}), \\ \tilde{h}_{\text{TT}}^{xy} &= \tilde{h}_{\text{TT}}^{yx} = -2\frac{e^{i\omega r}}{r} \omega^2 \tilde{I}^{xy}. \end{aligned} \quad (8.32)$$

Recalling that the phase shift $\exp(i\omega r)$ simply reflects the time delay of propagation from 0 to r , or by explicitly performing the inverse Fourier transform, we have also that

$$\begin{aligned} h_{\text{TT}}^{xx}(t, \mathbf{x}) &= -h_{\text{TT}}^{yy} = \frac{1}{r} [\ddot{I}^{xx}(t-r) - \ddot{I}^{yy}(t-r)] = \frac{1}{r} [\ddot{I}^{xx} - \ddot{I}^{yy}]_{t_{\text{ret}}}, \\ h_{\text{TT}}^{xy} &= h_{\text{TT}}^{yx} = \frac{2}{r} \ddot{I}^{xy}(t-r) = \frac{2}{r} \ddot{I}^{xy}(t_{\text{ret}}). \end{aligned} \quad (8.33)$$

8.6 Gravitational waves from a binary star

This is perhaps the most reliable astrophysical source in practice: we know that close binaries exist, even a few very close ones involving white dwarfs and neutron stars, though no double-black-hole or even bh-ns pairs have been identified to date.

Let the component masses be M_1 & M_2 , the binary semimajor axis a , and the orbital frequency Ω . For simplicity, assume a circular orbit. (Dissipative processes, including energy loss by GW emission, usually tend to circularize orbits.) If the orbit lies in the xy plane with center of mass at the origin, then the instantaneous positions $\mathbf{x}_{(1)}$, $\mathbf{x}_{(2)}$ evolve as

$$\mathbf{x}_{(1)}(t) = -\frac{M_2}{M_1} \mathbf{x}_{(2)}(t) = \frac{M_2}{M_1 + M_2} a (\cos \Omega t, \sin \Omega t, 0),$$

so that the quadrupole moment

$$I^{ij}(t) = M_1 x_{(1)}^i x_{(1)}^j + M_2 x_{(2)}^i x_{(2)}^j = \mu a^2 \begin{pmatrix} \cos^2 \Omega t & \sin \Omega t \cos \Omega t & 0 \\ \sin \Omega t \cos \Omega t & \sin^2 \Omega t & 0 \\ 0 & 0 & 0 \end{pmatrix},$$

average that doesn't satisfy the analog of (8.30). In fact $\langle h_{00} \rangle_t$ has the $O(r^{-1})$ piece $2M/r$, where M is the total mass of the source.

where $\mu = M_1 M_2 / (M_1 + M_2)$ is the reduced mass. Therefore

$$\ddot{I}^{ij}(t) = -2\Omega^2 \mu a^2 \begin{pmatrix} \cos 2\Omega t & \sin 2\Omega t & 0 \\ \sin 2\Omega t & -\cos 2\Omega t & 0 \\ 0 & 0 & 0 \end{pmatrix},$$

which is already traceless. So

$$h_{\text{TT}}^{xx}(t, \mathbf{x}) = h_{\text{TT}}^{xy} \left(t + \frac{\pi}{4\Omega}, \mathbf{x} \right) = 2 \frac{\mu \Omega^2 a^2}{r} \cos 2\Omega(t - r). \quad (8.34)$$

Note that the frequency of the wave is *twice* the frequency of the orbit; this is because the quadrupole moment is invariant under $\mathbf{x}' \rightarrow -\mathbf{x}'$, which advances the system by half its orbital period. Since the metric is dimensionless, the expressions (8.34) have to be multiplied by G/c^4 in conventional units. However, let us continue with relativistic unit for now. With $M \equiv M_1 + M_2$, Kepler's Law is $\Omega^2 = M/a$, so the semiamplitude of both polarizations is

$$h_{ij,\text{max}}^{\text{TT}} = 2 \frac{\mu}{r} \frac{M}{a}.$$

Consider, for example, a $10^3 M_\odot$ black hole orbiting around a much heavier one in a galactic nucleus at redshift $z = 1$: a plausible source for LISA, according to some theorists. Then $r \approx cH_0^{-1} \approx 1.3 \times 10^{28}$ cm, and the length equivalent of $\mu \approx 3 \times 10^8$, so that $h_{ij,\text{max}}^{\text{TT}} \approx 2 \times 10^{-20} (M/a)$. At the marginally stable orbit, M/a ranges from $1/6$ if the larger black hole is nonrotating, to 1 if it is maximally rotating. So we are talking about (dimensionless) wave amplitudes of order 10^{-20} . In order to have a sense of whether this is interesting and detectable, we have to examine the physical effects of the wave.

8.7 Detection of gravitational waves

The simplest and perhaps most effective wave detectors involve precise measurement of the time-dependent separation between test masses in free fall. This is the basic idea for LISA.

The geodesic equation can be put in the form

$$\frac{d^2 x^\mu}{d\tau^2} = -g^{\mu\nu} \left(g_{\alpha\nu,\beta} - \frac{1}{2} g_{\alpha\beta,\nu} \right) \frac{dx^\alpha}{d\tau} \frac{dx^\beta}{d\tau}, \quad (8.35)$$

which reduces in the weak-field limit to

$$\frac{d^2 x^\mu}{d\tau^2} = - \left(h_{\alpha\beta}^{\mu} - \frac{1}{2} h_{\alpha\beta,\mu} \right) \frac{dx^\alpha}{d\tau} \frac{dx^\beta}{d\tau}, \quad (8.36)$$

So in TT gauge, where $h_{0\mu} = 0$, trajectories $x^i(\tau) = \text{constant}$ are actually geodesics. This doesn't mean that the wave has no effect; the spatial separation between these geodesics is modulated by h_{ij} even though their spatial coordinates are constant. Specifically, for a detection system far from the source along the z direction, the physical separation of between test masses at $\mathbf{r}_{(a)}$ and $\mathbf{r}_{(b)} = \mathbf{r}_{(a)} + \Delta\mathbf{r}$ is

$$\begin{aligned} l(t) &= [\Delta\mathbf{r} \cdot \Delta\mathbf{r} + h_{xx}(\Delta x)^2 + 2h_{xy}\Delta x\Delta y + h_{yy}(\Delta y)^2]^{1/2} \\ &= l_0 + \frac{1}{2l_0} \{ h_{xx}^{\text{TT}}(t) [(\Delta x)^2 - (\Delta y)^2] + 2h_{xy}^{\text{TT}}(t)\Delta x\Delta y \}, \end{aligned} \quad (8.37)$$

where $l_0 = |\Delta\mathbf{r}|$ is the unperturbed separation, assuming for simplicity that $\Delta z = 0$ so that h_{ij}^{TT} has exactly the same instantaneous value at both masses. Thus for a given h —meaning now the

wave amplitude rather than the trace—the oscillation in the separation is linearly proportional to the separation itself: $\delta l = l - l_0 \sim h \times l_0$. With laser metrology for example, the directly measured quantity is δl (in wavelengths of light) rather than $\delta l/l_0$, so other things being equal, larger l_0 makes for a more sensitive detector.

The LISA detector, which is currently projected to launch in 2012 or 2013, will have three spacecraft forming an equilateral triangle with sides of 5×10^6 km and will use lasers of wavelength $\lambda = 1 \mu\text{m}$. Thus the oscillations in separation to be measured are on the order of $\sim 10^{-8}$ cm = $10^{-4}\lambda$. Ideally, if we consider only photon shot noise, the laser measurement error is $\sigma = \lambda N_\gamma^{-1/2}$ when N_γ photons are detected. If laser power P is transmitted through an aperture of area A_1 to a receiving aperture A_2 at distance R , the rate at which photons are received is

$$\dot{N}_\gamma = \frac{P}{h\nu} \times \frac{A_1 A_2}{(\lambda R)^2}, \quad (8.38)$$

in which $h\nu = hc/\lambda$ is of course the energy per photon. In practice the rate of photons detected will be smaller by an efficiency factor $\eta \sim 0.30$ because of imperfect reflectivity of the optical surfaces, quantum efficiency of the detectors, *etc.*, but we ignore this for purposes of rough estimates. LISA will use $R = 5 \times 10^{11}$ cm, $P \approx 1$ W, and $A_1 = A_2 \approx 700 \text{ cm}^2$ (apertures diameters = 30 cm), so $\dot{N}_\gamma \approx 10^9 \text{ s}^{-1}$. Thus, the predicted error is $\sigma \sim 3 \times 10^{-5} \lambda (t_{\text{int}}/1 \text{ s})^{-1/2}$, where t_{int} is the integration time. This seems more than good enough, especially considering that the integration time can probably be much longer than a second: for $M = 10^6 M_6 M_\odot$, the wave period is $\pi M (a/M)^{3/2} \rightarrow 16 M_6 (a/M)^{3/2}$ s, and one can probably integrate coherently over many wave periods.

8.8 Energy of gravitational waves

Like most linear waves, weak-field GW carry an energy density and flux that is quadratic in wave amplitude. The energy and flux cannot be first-order quantities because all quantities linear in the wave vanish upon averaging over oscillations. We will derive the expression for the flux in harmonic and TT gauge by considering the backreaction on the source, *i.e.*, on the matter.

Start from the geodesic equation (4.11), which reduces to

$$\frac{d}{d\tau} (\eta_{\mu\nu} \dot{x}^\nu + h_{\mu\nu} \dot{x}^\nu) = \frac{1}{2} h_{\alpha\beta, \mu} \dot{x}^\alpha \dot{x}^\beta,$$

for weak fields. Dots indicate $d/d\tau$ of course. Expand the derivative on the lefthand side to obtain

$$\eta_{\mu\nu} \ddot{x}^\nu + h_{\mu\nu, \lambda} \dot{x}^\lambda \dot{x}^\nu$$

after discarding $h_{\mu\nu} \ddot{x}^\nu$ because it is second order. Then after some obvious rearrangement and raising of indices (using $\eta^{\mu\nu}$, remember), we have

$$\ddot{x}^\mu = \left(\frac{1}{2} h_{\alpha\beta, \mu}{}^\mu - h^\mu{}_{\alpha, \beta} \right) \dot{x}^\alpha \dot{x}^\beta. \quad (8.39)$$

Now imagine a whole cloud of particles following geodesics and having similar 4-velocities—in other words, a dust-like fluid. We can then consider the four-velocities U^μ to be a smooth vector field to which the particles' world lines are tangent, so that

$$\begin{aligned} \frac{dx^\mu}{d\tau} &= U^\mu(x^0, x^1, x^2, x^3) \\ \frac{d^2 x^\mu}{d\tau^2} &= \frac{dU^\mu}{d\tau} = U^\nu U^\mu{}_{, \nu} \end{aligned}$$

Making this replacement in (8.39) and multiplying both sides by the rest-frame number density of particles, \bar{N} , we have

$$\bar{N}U^\nu U^\mu{}_{,\nu} = \left(\frac{1}{2} h_{\alpha\beta,}{}^\mu - h^\mu{}_{\alpha,\beta} \right) U^\alpha U^\beta.$$

Now $N^\nu = \bar{N}U^\nu$ is the 4-current associated with particle number, which is conserved,

$$(\bar{N}U^\nu)_{,\nu} = 0.$$

Multiplying this last equation by mU^μ , where m is the rest mass per particle, and adding it to the previous one gives

$$T^{\mu\nu}{}_{,\nu} = \left(\frac{1}{2} h_{\alpha\beta,}{}^\mu - h^\mu{}_{\alpha,\beta} \right) T^{\alpha\beta} \quad (8.40)$$

since $m\bar{N}U^\mu U^\nu$ is the energy-momentum tensor of dust. Although we have derived it for dust only, we will assume that (8.40) holds for any mass distribution in the weak-field approximation. It is second order, because $h^{\mu\nu}$ and $T^{\mu\nu}$ are individually of first order. The lefthand side would vanish to first order, so we should regard the lefthand $T^{\mu\nu}$ as accurate through second order. Sometimes we will write this as $T_{(2)}^{\mu\nu}$ to distinguish it from versions of the energy-momentum tensor that may be accurate to first order only. On the righthand side of (8.40), it doesn't matter to second order whether we use $T_{(2)}^{\mu\nu}$ or its less accurate counterparts $T_{(1)}^{\mu\nu}$, because of the explicit factors of $h_{\mu\nu}$. Physically, the righthand side can be regarded roughly as the work done on the first-order mass distribution by the first-order gravitational field, *i.e.* the backreaction, and it ought to describe the exchange of energy (and momentum) between matter and outgoing waves. However, it also includes terms that merely redistribute energy within the source without carrying it off as radiation, as we shall see shortly.

Let us integrate (8.40) over all space:

$$\int d\mathbf{x} T^{\mu\nu}{}_{,\nu} = \int d\mathbf{x} T^{\mu 0}{}_{,0} + \int d\mathbf{x} T^{\mu i}{}_{,i} = \frac{d}{dt} \int d\mathbf{x} T^{\mu 0} \quad (8.41)$$

because the integral of $T^{\mu i}{}_{,i}$ vanishes by Gauss's theorem (or integration by parts) if the matter is confined to a finite spatial region, as we assume it is. The integral of part of the righthand side of (8.40) is

$$\begin{aligned} - \int d\mathbf{x} h^\mu{}_{\alpha,\beta} T^{\alpha\beta} &= - \int d\mathbf{x} h^\mu{}_{\alpha,0} T^{\alpha 0} - \int d\mathbf{x} h^\mu{}_{\alpha,i} T^{\alpha i} \\ &= - \int d\mathbf{x} h^\mu{}_{\alpha,0} T^{\alpha 0} + \int d\mathbf{x} h^\mu{}_{\alpha} T^{\alpha i}{}_{,i} \\ &= - \int d\mathbf{x} h^\mu{}_{\alpha,0} T^{\alpha 0} - \int d\mathbf{x} h^\mu{}_{\alpha} T^{\alpha 0}{}_{,0} \\ &= - \frac{d}{dt} \int d\mathbf{x} h^\mu{}_{\alpha} T^{\alpha 0} \end{aligned}$$

[We used the fact that $T^{\alpha\nu}{}_{,\nu}$ vanishes to first order between the second and third lines above.] Because this is a total time derivative, it is useful to group it with (8.41), so that the complete integrated form of (8.40) becomes

$$\frac{d}{dt} \int d\mathbf{x} (T^{\mu 0} + h^\mu{}_{\alpha} T^{\alpha 0}) = \frac{1}{2} \int d\mathbf{x} h_{\alpha\beta,}{}^\mu T^{\alpha\beta}.$$

Now let us set $\mu = 0$ (because we are interested in energy) and integrate over a finite time interval $t_1 \leq t \leq t_2$:

$$\int d\mathbf{x} (T^{\mu 0} + h^\mu{}_{\alpha} T^{\alpha 0}) \Big|_{t=t_1}^{t=t_2} = \frac{1}{2} \int_{t_1}^{t_2} dt - \int d\mathbf{x} \dot{h}_{\alpha\beta,}{}^\mu T^{\alpha\beta}. \quad (8.42)$$

The dot on h now means $\partial/\partial t$. Now if the source were to be stationary before t_1 and to stop oscillating well before t_2 , then there would be no waves near the source at t_1 (because they had not been created yet), nor at t_2 (because they would have propagated away). Although there may be nonzero metric perturbations in the source, they are near-field rather than radiation terms. If the source were to return to *exactly* its original configuration, the left side would vanish; it is the difference of some function of state. Thus the lefthand side can be regarded as the change in the energy of the source, to second order, ΔE_{source} . The righthand side clearly is not a function of state, since it would be nonzero even if the source were to return to its original configuration. Thus it is fair to regard it as (or at least to contain) the energy carried off by waves.

Let us now specialize to harmonic gauge. We can then use (8.14) to eliminate $T_{(1)}^{\alpha\beta}$ from (8.42) in favor of $H^{\alpha\beta}$ and beat the result into a symmetrical shape by integration by parts:

$$\begin{aligned}
\Delta E_{\text{source}} &= \frac{1}{32\pi} \int_{t_1}^{t_2} dt \int d\mathbf{x} \dot{h}_{\alpha\beta} \square H^{\alpha\beta} \\
&= \frac{1}{32\pi} \int_{t_1}^{t_2} dt \int d\mathbf{x} \left(\dot{h}_{\alpha\beta} \square h^{\alpha\beta} - \frac{1}{2} \dot{h} \square h \right) \\
&= \frac{1}{32\pi} \int_{t_1}^{t_2} dt \int d\mathbf{x} \left[-\dot{h}_{\alpha\beta} \ddot{h}^{\alpha\beta} + \dot{h}_{\alpha\beta} \nabla^2 h^{\alpha\beta} + \frac{1}{2} (\dot{h} \ddot{h} - h \nabla^2 h) \right] \\
&= \frac{1}{32\pi} \int_{t_1}^{t_2} dt \int d\mathbf{x} \left[-\ddot{h}_{\alpha\beta} \dot{h}^{\alpha\beta} - \nabla \dot{h}_{\alpha\beta} \cdot \nabla h^{\alpha\beta} + \frac{1}{2} (\ddot{h} \dot{h} + \nabla \dot{h} \cdot \nabla h) \right] \\
&= \frac{1}{32\pi} \int_{t_1}^{t_2} dt \int d\mathbf{x} \frac{\partial}{\partial t} \left[-\dot{h}_{\alpha\beta} \dot{h}^{\alpha\beta} - \nabla h_{\alpha\beta} \cdot \nabla h^{\alpha\beta} + \frac{1}{2} (\dot{h}^2 + |\nabla h|^2) \right] \\
&= - \int d\mathbf{x} \frac{1}{64\pi} \left[\dot{h}_{\alpha\beta} \dot{h}^{\alpha\beta} \nabla h_{\alpha\beta} \cdot \nabla h^{\alpha\beta} - \frac{1}{2} (\dot{h}^2 + |\nabla h|^2) \right] \Big|_{t_1}^{t_2}
\end{aligned}$$

Oops—the right side is a function of state after all! But in order to make it so, we had to transform it into something no longer local to the source; it can now be nonzero at large distances where $T^{\mu\nu} = 0$. So in these regions, the quantity

$$F_{\text{GW}} = \frac{1}{64\pi} \left\langle \dot{h}_{\alpha\beta} \dot{h}^{\alpha\beta} + \nabla h_{\alpha\beta} \cdot \nabla h^{\alpha\beta} - \frac{1}{2} (\dot{h}^2 + |\nabla h|^2) \right\rangle. \quad (8.43)$$

can be identified as the energy density of the waves. The angle brackets indicate that the expression should be averaged over oscillations. Since the waves propagate radially outward, the flux is simply $c\mathbf{n}F$. With these interpretations, (8.42) states that $\Delta E_{\text{source}} = -\Delta E_{\text{GW}}$.

We can make two further simplifications to F . First, since it is a local expression, we may evaluate it in TT gauge, where $h = 0$. Second, we may use the property (8.28) to replace spatial derivatives with temporal ones: *i.e.*, a radially propagating wave depends upon (t, \mathbf{x}) mainly in the combination $t - r$, so $\nabla = -\mathbf{n}\partial_t + O(r^{-1})$. Thus we have

$$F_{\text{GW}} = \frac{1}{32\pi} \left\langle \dot{h}_{ij}^{\text{TT}} \dot{h}_{\text{TT}}^{ij} \right\rangle. \quad (8.44)$$

Chapter 9

Cosmic Rays

Almost all of what astrophysics knows about the universe outside the solar system has been learned through the collection of photons. Cosmic rays, however, are material samples from distant parts of the Galaxy, and probably beyond. This would be enough to justify scientific interest in cosmic rays, even if there were not still many unsolved questions about their sources, their acceleration to high energies, and their propagation through the interstellar medium.

The term “cosmic ray” is often applied to high-energy photons and leptons (e^\pm , $\nu\bar{\nu}$), but here it will refer to hadronic particles unless stated otherwise.

9.1 Energy spectrum

As shown in Figure 9.1, the energies of cosmic rays observed at Earth span an enormous range. The spectrum is roughly a power law,

$$N(> E) \approx 5000(E_{\text{GeV}} + 1)^{-1.6} \text{ m}^{-2} \text{ sr}^{-1} \text{ s}^{-1}. \quad (9.1)$$

It is conventional to state the flux per steradian per unit area normal to the velocity, as here.

At the low-energy end, the observed spectrum is significantly distorted by solar modulation: these cosmic rays have difficulty penetrating the solar system against the flow of the solar wind. The solar wind is quite variable, but typically at the Earth (1 AU), $V_{\text{SW}} = 350 \text{ km s}^{-1}$, $B_{\text{SW}} = 50 \mu\text{G}$, $N_{\text{SW}} = 10 \text{ cm}^{-3}$. The gyroradius of a CR of momentum p ($= \sqrt{(E/c)^2 - (mc)^2}$) and charge Ze is

$$r_g = \frac{R}{B}, \quad R \equiv \frac{pc}{Ze}. \quad (9.2)$$

The quantity R is called the rigidity and is often measured in gigavolts (GV); note that for a relativistic CR, the energy in GeV is Z times R in GV. Thus for $R = 1 \text{ GV}$, $r_g \approx 7 \times 10^{10} \text{ cm} \approx 4 \times 10^{-3} \text{ AU}$. Hence these cosmic rays are rather closely coupled to the wind. They must diffuse “upstream” against the wind, so that their number density satisfies an equation of the form

$$\frac{\partial N}{\partial t} + \nabla \cdot (N\mathbf{V}_W - D\nabla N) = 0, \quad (9.3)$$

where D is a diffusion coefficient. By analogy with the kinetic theory of gases, $D \approx \lambda v/3$, where $v \approx c$ is the speed of the CR. The mean free path λ is associated with “scatterings” of the CR against the field \mathbf{B} . This can hardly be less than r_g , but it is possible that $\lambda \gg r_g$ if the field lines are open and very smooth, since particles could then stream along them.¹ In a steady state, (9.3)

¹Even in a smooth field, adiabatic invariance of $r_g p_\perp$ (where p_\perp is the momentum perpendicular to the field) can limit the distance along the line to which the CR penetrates (“magnetic mirroring”).

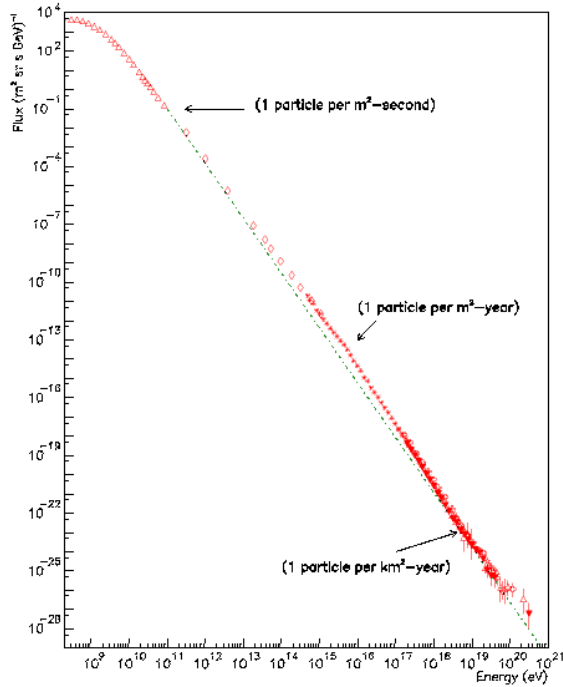


Figure 9.1: Cosmic ray energy spectrum, from <http://www.cosmic-ray.org/reading/>.

implies, assuming approximate spherical symmetry,

$$\frac{1}{N} \frac{\partial N}{\partial r} \approx \frac{V_W}{D}$$

Therefore the CR flux at Earth will be strongly modified for energies low enough so that $D/V_W \lesssim 1$ AU. If we take $D = vr_g/3$, then this occurs at $E \sim 100$ MeV for protons according to the numbers above.

Although the approximate agreement of this simple estimate with the low-energy cutoff seen in Figure 9.1 is reassuring, there are a number of complications that have not been taken into account. For one thing, λ could be larger than r_g as already noted. For another, equation (9.3) does not take into account energy changes of the CR due to their interaction with the wind: these occur primarily because the wind is an expanding flow, so that the CR “cool” adiabatically. On the other hand, one has direct observational evidence for the influence of the solar wind on the CR spectrum: the low-energy cutoff varies with time in correlation with the solar cycle; and it varies with distance from the Sun (as measured by interplanetary spacecraft). By fitting a diffusive model like (9.1) (including energy losses) to such data, it is possible to correct the CR spectrum for solar modulation and estimate its form beyond the heliopause (where the solar wind meets the ISM). The corrected spectrum still flattens at $E \lesssim$ GeV. This not unreasonable, since it represents the transition between relativistic and nonrelativistic motion.

Although it is barely visible in Fig. 9.1, there is a slight but highly statistically significant steepening of the powerlaw slope at $E \sim 10^{15.5}$ eV, from $-2.7 \rightarrow -3.1$. This is called the “knee”. The spectrum appears to flatten again above 10^{18} eV (10^{18} eV \equiv 1 EeV: “exa-” electron-volt), a feature referred to as the “ankle.” In a typical interstellar field of 3μ G, a rigidity $R = 10^{15.5}$ eV corresponds to a gyroradius of ≈ 1 pc, and $R = 10^{18}$ eV corresponds to $r_g \sim 360$ pc.

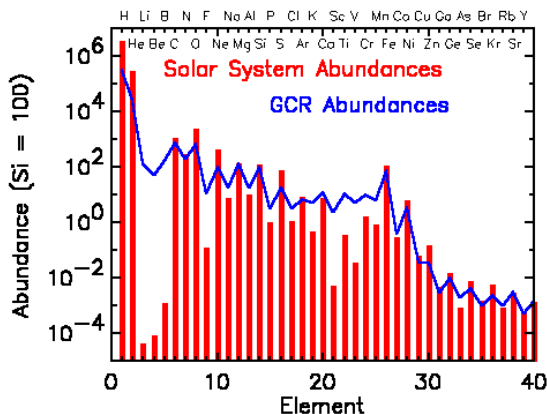


Figure 9.2: Cosmic ray composition, from imagine.gsfc.nasa.gov/Images/science.

9.2 Detection of cosmic rays

Primary cosmic rays generally do not reach the ground, but their secondaries do. The term “primary” is used to denote the original interplanetary particle, whose interactions with the Earth’s atmosphere creates a cascade of “secondary” CR as collision products.

The atmosphere is a very effective shield against primaries. At sea level, the column density at zenith is about 1 kg cm^{-2} . Total nuclear cross sections are typically $\sigma \sim 1 \text{ (fermi)}^2 = 10^{-26} \text{ cm}^2$ per nucleon. So a primary CR entering at zenith angle θ has probability $\sim \exp(-6 \sec \theta)$ of reaching sea level without collision. (A more accurate value is $\exp(-8 \sec \theta)$ for protons.) Thus, to obtain relatively pristine samples of primary cosmic rays, high-altitude balloons or spacecraft are necessary. (The exponential scale height of the atmosphere is $\sim 10 \text{ km}$.)

The composition of relatively low-energy cosmic rays ($E \lesssim 10 \text{ GeV}$) can be determined at high altitudes by the tracks they leave in nuclear emulsions, plastics, and other suitable materials. The material should be thick enough so that the CR slows completely to rest within it due to ionization losses.

Higher-energy cosmic rays are usually measured indirectly, through their secondaries. The first nuclear collision of the primary usually occurs high in the atmosphere (after $\sim 10^2 \text{ g cm}^{-2}$) and creates a pion— π^+ , π^- , or π^0 with roughly equal probability. The charged pions decay into muons and the π^0 into gamma rays. These particles in turn collide and create more particles, so that a cascade or air shower is initiated. At its peak, the air shower contains $\sim 1. \cdot (E_{\text{primary}}/\text{GeV})$ particles, which can be measured with detectors of the kind used in experimental particle physics, *e.g.* scintillation counters and proportional counters. At very high energies $> 10^{14} \text{ eV}$, air showers ionize the air itself extensively, and the recombining electrons and ions release optical photons that can be sensed at a distance by telescope mirrors and phototubes. (That is, the air itself serves as the scintillator.) The latter method has been used by the Fly’s Eye experiment (1981-1993) to measure CR up to $3 \times 10^{20} \text{ eV}$, roughly the energy of a baseball thrown by a major-league pitcher. (For web links to this and many other high-energy CR observatories, see www.mpi-hd.mpg.de/hfm/CosmicRay/CosmicRaySites.html.)

The energy of the shower is a good measure of the energy of the primary CR. Since only a fraction of the secondary particles are collected (to collect them all would require carpeting many square kilometers with detectors), statistical corrections are used to infer the shower energy. Since it is impossible to calibrate these methods directly by producing one’s own primaries, Monte Carlo methods must be relied on. Intercalibration of different experiments is therefore somewhat uncertain, probably at levels $\gtrsim 10\%$, especially if they use different methods to reconstruct the shower.

Nevertheless, it seems to be broadly accepted that energies in excess of 10^{20} eV have been observed.

9.3 Inferences from the composition of cosmic rays

As remarked above, detailed information about the composition of cosmic rays can be obtained at relatively low energies, as shown in figure 9.2. About 50 – 90% (authorities differ!) of the CR are protons (H nuclei), and the relative abundances of the heavier elements are broadly similar to those in the solar system and in the local ISM. From this it can be inferred that the mechanisms that accelerate cosmic rays act upon fairly conventional interstellar material.

However, the light elements Li, Be, B are overrepresented in the CR, as are the elements just below iron. These are understood to be consequences of spallation: the fragmentation of heavier CR nuclei in collisions with interstellar gas atoms. At the energies of interest, the cross sections can be measured experimentally or calculated reasonably reliably.

9.3.1 Spallation model

Following [33, chap. 20], let us develop a simplified “slab” model. One imagines that all cosmic rays traverse the same column density

$$\xi_{\oplus} = \int_{\text{source}}^{\text{Earth}} \rho ds.$$

where ρ is the mass density of the interstellar gas along the CR path,

$$\rho = (n_{\text{H}} + 4n_{\text{He}} + \dots) m_p = X^{-1} n_{\text{H}} m_p,$$

where n_{H} and $X \approx 0.7$ are the number density and the relative abundance by mass of interstellar hydrogen. Contrary to our usage in previous chapters, lower-case “n” is used here for number densities in the non-relativistic (with units of cm^{-3}), and upper-case “N” is used for fluxes of cosmic rays (units of $\text{cm}^{-2} \text{s}^{-1} \text{sr}^{-1} \text{GeV}^{-1}$). The flux of the i^{th} CR species (*i.e.*, nuclei of a particular isotope) is presumed to evolve along the path as

$$\frac{\partial N_i}{\partial \xi} = \frac{X}{m_p} \left(\sum_{j>i} N_j \sigma_{ji} - \sigma_i N_i \right) - \frac{X}{\rho c} \left(\frac{1}{\tau_{i,\text{esc}}} + \frac{1}{\tau_{i,\text{dec}}} \right) N_i, \quad (9.4)$$

in which ξ is now a variable along the path, σ_{ji} is the partial cross section for production of nucleus i as a result of collision of nucleus j with an interstellar proton, and σ_i is total cross section for destruction of nucleus i . To avoid having to solve a diffusion equation, escape of cosmic rays from the Galaxy is represented as a constant rate τ_{esc}^{-1} at all positions. Finally, $\tau_{i,\text{dec}}^{-1}$ is the radioactive decay rate of species i allowing for time dilation (hence it is a function of energy); of course $\tau_{i,\text{dec}} = \infty$ for stable isotopes. For simplicity, collisions with interstellar nuclei heavier than hydrogen have been ignored, and it is assumed that all CR have speed $\approx c$. Equation (9.4) takes no account of changes in particle energy due to the collisions and to ionization losses, *etc.*

To the extent that the escape time is the same for all species, which is probably a reasonable approximation at a common rigidity, we may eliminate the escape term by rewriting (9.4) in terms of new variables

$$\hat{N}_i(\xi) \equiv N_i(\xi) \exp \left(- \frac{X}{c\tau_{\text{esc}}} \int^{\xi} \frac{d\xi'}{\rho} \right),$$

satisfying

$$\frac{\partial \hat{N}_i}{\partial \xi} = \frac{X}{m_p} \left(\sum_{j>i} \hat{N}_j \sigma_{ji} - \sigma_i \hat{N}_i \right) - \frac{X}{\rho c \tau_{i,\text{dec}}} \hat{N}_i. \quad (9.5)$$

The exponential term cancels when one considers relative abundances, $\hat{N}_i/\hat{N}_j = N_i/N_j$.

Consider first the production of stable isotopes of Li, Be, B by spallation of CNO elements (C, N, O, Ne, Mg). For simplicity we group these into two aggregate fluxes N_L (“light”) and N_M (“medium”). The latter are so abundant compared to all possible parent nuclei (except perhaps Fe) that we ignore the contribution of spallation to their abundance (see Fig. 9.2). Using appropriately averaged cross sections, we have

$$\begin{aligned} \frac{\partial \hat{N}_L}{\partial \xi} &= \frac{X}{m_p} \left(\hat{N}_M \sigma_{ML} - \sigma_L \hat{N}_L \right) \\ \frac{\partial \hat{N}_M}{\partial \xi} &= -\frac{X}{m_p} \sigma_M \hat{N}_M, \end{aligned}$$

The solution to this linear system when $N_L(0) = 0$ is

$$\begin{aligned} \hat{N}_M(\xi) &= \hat{N}_M(0) \exp(-\xi \sigma_M X / m_p), \\ \frac{\hat{N}_L(\xi)}{\hat{N}_M(\xi)} &= \frac{\sigma_{ML}}{\sigma_M - \sigma_L} \left(e^{\xi(\sigma_M - \sigma_L)X / m_p} - 1 \right). \end{aligned}$$

The observed relative abundance is $N_L/N_M \approx 0.1$, and the cross sections (appropriately averaged over the elements concerned) are σ_{ML} , σ_M , & σ_L are ≈ 70 , 280, & 200 in units of millibarns ($1 \text{ mb} \equiv 10^{-27} \text{ cm}^2$) respectively. Plugging these numbers (and $X = 0.7$) into the equation above yields $\xi_{\oplus} \approx 3 \text{ g cm}^{-2}$.

A more careful calculation that accounts for the individual species, energy losses, and so forth yields [57]

$$\xi_{\oplus} \approx 5 \text{ g cm}^{-2} \quad (9.6)$$

for the average column density through which the cosmic rays pass, at least at the relatively low energies where their composition is well determined.

9.3.2 Confinement time

The column density (9.6) can be converted to a propagation time given a value for n_H . The latter is believed to be $\approx 1 \text{ cm}^{-3}$ in the solar neighborhood, implying $t = \xi_{\oplus} X / m_p n_H c \approx 2 \times 10^6 \text{ yr}$.

An independent estimate of n_H and hence t can be obtained from the abundance of radioactive spallation products. A particularly important case is ^{10}Be , whose decay time (in its rest frame) is only $\tau_{\text{dec}}(^{10}\text{Be}) = 3.8 \times 10^6 \text{ yr}$. From Tables 5.1 & 9.1 of [33], we may estimate that about 0.16 of the beryllium nuclei produced by spallation of CNO are ^{10}Be . Yet at $E \approx 100 \text{ MeV/nucleon}$, only about 0.05 of the beryllium in cosmic rays observed at Earth is ^{10}Be , about 27% of the relative production rate. This can be accounted for by including the decay term in (9.5), provided that $\langle n_H \rangle \approx 0.12 \text{ cm}^{-3}$; more careful estimates yield $\sim 0.2 \text{ cm}^{-3}$ [57]. Hence the time of flight is larger than estimated above by a factor ~ 5 , or

$$t_{\text{conf}} \approx 10^7 \text{ yr}, \quad (9.7)$$

with an uncertainty of about 50% (this would be $\sim 1.8 \times 10^7 \text{ yr}$ for $\langle n_H \rangle \approx 0.12 \text{ cm}^{-3}$). One assumes that the Earth obtains a representative sample of the cosmic rays, although this might not be true if the nearest CR source happens to be much closer than the mean distance between sources in

the Galaxy. Then it follows that cosmic rays must be lost on the timescale (9.7), presumably by diffusing out of the Galaxy. Hence it is called the **confinement time**.

Since the ^{10}Be argument requires n_{H} to be smaller averaged over the path than it is locally, one infers that the region in which the cosmic rays are trapped is larger than the disk thickness, $2H \sim 500$ pc. Let us write $2H'$ for the thickness of the trapping region. The time to escape from the middle of this region if traveling in a straight line is $\sim H'/c \sim 3000 (H'/\text{kpc}) \text{ yr}$. The time to escape by a random walk of mean free path $\lambda \ll H'$ is longer than this by a factor $\sim H'/\lambda$, *i.e.* $\tau_{\text{esc}} \sim (H')^2/c\lambda$. Setting this equal to t_{conf} , we estimate $\lambda \approx 0.3 (H'/\text{kpc})^2 \text{ pc}$.

This mean free path is probably small compared to the distance to the nearest sources (which are probably supernova remnants). The angular distribution of cosmic rays should therefore be quite isotropic. Indeed, the dipolar anisotropy is $\lesssim 10^{-3}$ at energies $10^{12} - 10^{15} \text{ eV}$.

9.4 Acceleration mechanism

An outstanding question about cosmic rays is how nature manages to endow single nuclei with such large energies. Actually, considerable theoretical progress has been made towards answering this question, at least up to $\sim 10^{15} \text{ eV}$ if not 10^{20} eV .

We have seen that rotating supermassive black holes surrounded by suitable disks might create voltage gaps up to 10^{20} eV . Unfortunately, the black hole at the center of our own Galaxy is both lightweight and (at least at the moment) rather inactive.

Most astrophysicists now believe that cosmic rays below the “knee” at least are accelerated in interstellar shocks. The mechanism is a variant of an idea proposed by [15]. Fermi suggested that in the absence of loss mechanisms, “collisions” between cosmic rays and much larger masses such as interstellar clouds would tend toward equipartition of energy: that is, individual CR particles would *eventually* acquire energies comparable to those of the clouds. (The “collisions” were assumed to be mediated by the interaction between the magnetic field of the cloud and the charge of the CR.) A giant molecular cloud has a typical mass $\sim 3 \times 10^5 M_{\odot} \sim 10^{39} \text{ g}$ and a random velocity $\sim 10 \text{ km s}^{-1}$, hence an energy $\sim 10^{50} \text{ erg} \sim 10^{62} \text{ eV}$!

Of course the Galactic magnetic field is totally incapable of confining particles with such energies, but more importantly, the time required to achieve equipartition is more than astronomical. In a single collision, the energy of the (relativistic) CR will change by a factor

$$\frac{E'}{E} = \gamma^2(1 - \boldsymbol{\beta} \cdot \mathbf{n})(1 + \boldsymbol{\beta} \cdot \mathbf{n}')1 + \boldsymbol{\beta} \cdot (\mathbf{n}' - \mathbf{n}) + [\beta^2 - (\boldsymbol{\beta} \cdot \mathbf{n}')(\boldsymbol{\beta} \cdot \mathbf{n})] + O(\beta^3),$$

where \mathbf{n} is the CR’s directions of motion as measured before scattering in the ‘lab’ frame where the cloud’s velocity is $\boldsymbol{\beta}c$ and its Lorentz factor $\gamma = (1 - \beta^2)^{-1/2}$. The direction \mathbf{n}' is measured after scattering in the *cloud’s* rest frame. Assuming that the dot products have random signs, the energy change vanishes on average to first order. But it is clear that the second-order term is always nonnegative and hence is positive on average, with an average value $\sim \beta^2$. (The exact value depends on the correlation between \mathbf{n} and \mathbf{n}' , if any.) For $\beta \sim 10^{-4.5}$, some 10^9 collisions are required to e-fold the CR energy; if the distance between clouds is measured in light years, then the time required to reach 10^{15} eV starting from a (kinetic) energy $\sim \text{GeV}$ is $\gtrsim 10^{11} \text{ yr}$. This is marginally longer than the age of the universe ($\approx 1.3 \times 10^{10} \text{ yr}$), but more urgently, it is orders of magnitude longer than the inferred confinement time (9.7).

In 1977-1978, several groups independently noticed that a nonzero average of the first-order term can be achieved in a shock, where the flow is systematically converging ($\boldsymbol{\nabla} \cdot \mathbf{v} < 0$): [2], [30], [3], [8]. Very roughly speaking, the effect is analogous to the increase in the internal energy of a gas when it is compressed by a piston.

Consider a non-relativistic shock in the shock rest frame. The pre-shock fluid approaches the front with density velocity $v = -V_{\text{shock}} \ll c$ and density ρ (which we may take equal to the density of rest

mass). The postshock fluid has velocity $v' = v/r$, where $r = \rho'/\rho > 1$ is the shock compression ratio. For a strong shock in an ideal gas with adiabatic exponent γ ,

$$r = \frac{\gamma + 1}{\gamma - 1} = \begin{cases} 4 & \gamma = 5/3 : \text{monatomic nonrelativistic gas} \\ 7 & \gamma = 4/3 : \text{gas of relativistic particles} \end{cases} \quad (9.8)$$

If the thickness of the shock (Δx_{shock}) is very small compared to its radius of curvature we may approximate it as plane-parallel.

Cosmic rays scatter off magnetic irregularities advected with the fluid, so that particles may cross the shock front repeatedly. It is assumed that the scattering preserves the particle's energy viewed in the local fluid rest frame. In the shock rest frame, however, the energy change is

$$\frac{\Delta E}{E} \approx \frac{\mathbf{v} \cdot \Delta \mathbf{n}}{c}$$

to first order, where \mathbf{n} is the direction of motion of the particle. Now the average of $\mathbf{v} \cdot \Delta \mathbf{n}$ is *not* zero for a particle that crosses the shock repeatedly. Consider a particle that crosses the shock upstream—*i.e.* towards the preshock fluid—scatters, and returns to the shock. For simplicity suppose that the velocity of the particle parallel to the shock remains unchanged, so that the angle of motion with respect to the shock normal changes from $\theta \rightarrow \pi - \theta$. In this case $\mathbf{v} \cdot \Delta \mathbf{n} = 2|V_{\text{shock}} \cos \theta / c|$. Next the particle enters the downstream (postshock) flow, scatters and returns again to the shock and to its original direction of motion. For this second event, $\mathbf{v} \cdot \Delta \mathbf{n} = -2r^{-1}|V_{\text{shock}} \cos \theta / c|$, the minus sign occurring because the downstream flow moves away from the shock, so that the particle has to overtake it. Thus the average energy change after one upstream and one downstream shock crossing is

$$\left\langle \frac{\Delta E}{E} \right\rangle \approx \frac{r-1}{r} \frac{2|V_{\text{shock}}|}{c} \langle |\cos \theta| \rangle.$$

For an isotropic velocity distribution of the cosmic rays, $\cos \theta$ is uniformly distributed between ± 1 , but since when averaging over particles we must weight them by the rate at which they cross the shock, and this brings in an additional factor of $|\cos \theta|$:

$$\langle \cos \theta \rangle = \frac{\int_{-1}^1 \cos^2 \theta \, d \cos \theta}{\int_{-1}^1 |\cos \theta| \, d \cos \theta} = \frac{2}{3}.$$

Inserting this above, we have

$$\left\langle \frac{\Delta E}{E} \right\rangle \approx \frac{4(r-1)}{3r} \frac{|V_{\text{shock}}|}{c}, \quad (9.9)$$

Now the typical cosmic ray cannot cross the shock indefinitely often, because the cosmic rays are advected away from the shock by the downstream flow. Let N' be the number density of cosmic rays behind (downstream from) the shock. The rate of upstream crossings per unit area is approximately

$$\frac{N'c}{2} \int_0^1 \cos \theta \, d \cos \theta = \frac{N'c}{4}.$$

since $v' \ll c$ and we assume isotropic velocities. On the other hand, since the cosmic rays are advected downstream, the excess of downstream over upstream crossings (per unit area per unit time) must be $N'v' = N'|V_{\text{shock}}|/r$. We can summarize this situation by saying that each time the particle crosses the shock going downstream, there is a small probability

$$P_{\text{esc}} = 4 \frac{|V_{\text{shock}}|}{rc} \quad (9.10)$$

that it will escape from the shock region and never return.

These results can be combined to determine the energy spectrum of the accelerated cosmic rays. Assume for simplicity that they all start with energy E_0 (before encountering the shock). A cosmic ray that crosses the shock going upstream a total of k times (and therefore crosses downstream $k+1$ times) achieves an energy

$$E_k = E_0 \left(1 + \frac{\Delta E}{E} \right)^k .$$

The fraction of the CR population that crosses k or more times is

$$P_k = (1 - P_{\text{esc}})^k .$$

So CR accelerated to energies $E \gg E_0$ have experienced at least

$$k(E) = \ln \left(\frac{E}{E_0} \right) / \ln \left(1 + \frac{\Delta E}{E} \right) \approx \frac{\ln(E/E_0)}{\Delta E/E}$$

upstream crossings. Hence

$$N(> E) \propto (1 - P_{\text{esc}})^{k(E)} \approx \exp[-k(E)P_{\text{esc}}] \approx \exp \left[-\frac{4|V_{\text{shock}}|/rc}{4(r-1)|V_{\text{shock}}|/3rc} \ln \left(\frac{E}{E_0} \right) \right],$$

where we have use equations (9.9) & (9.10). Notice that V_{shock} cancels out, leaving

$$N(> E) \propto \left(\frac{E}{E_0} \right)^{-3/(r-1)} .$$

Usually one discusses the differential spectrum

$$N(E) \equiv -\frac{dN(> E)}{dE} \propto \left(\frac{E}{E_0} \right)^{-(r+2)/(r-1)} . \quad (9.11)$$

The effective adiabatic index of the interstellar medium is probably intermediate between $\gamma = 5/3$ and $\gamma = 4/3$, since the nonrelativistic component (neutral atoms, ions, and electrons) and the relativistic components (magnetic field and cosmic rays) make comparable contributions to the pressure. (As a rough rule of thumb, the energy densities in all of these components is of order 1 eV cm^{-3} .) Thus we expect $4 \leq r \leq 7$ for strong shocks, leading to $N(E) \propto E^{-p}$ with $3/2 \leq p \leq 2$. Recall that the observed slope $p \approx 2.5 - 3.1$. So the agreement is not perfect, but it is a miracle that this simple argument leads to a power law similar to what is observed, and furthermore that the result does not depend upon the shock velocity, provided at least that the shock is strong.

The picture presented above is by no means complete. One hint of trouble is that the predicted postshock energy density in CR

$$\int_{E_0}^{\infty} E N(E) dE$$

diverges at the upper limit if $p \geq 2$. This indicates that it will be necessary to consider the backreaction of the jump in cosmic-ray pressure on the shock itself in order to obtain an internally consistent solution of the acceleration problem.

Another area to explore is relativistic shocks. The argument presented above, which is essentially that due to [3] and is reproduced in [33], relies upon the smallness of V_{shock}/c at several steps. When $V_{\text{shock}} \sim c$, a particle can gain a large energy in a single shock crossing. Studies of the relativistic shock acceleration problem predict a universal exponent $p \approx 2.2 - 2.3$ (**add references here**).

9.4.1 Energetics

Can supernovae supply enough energy to maintain the cosmic rays? The energy density in the spectrum (9.1) is $\mathcal{U}_{\text{CR}} = 0.3 \text{ eV cm}^{-3}$, or $5 \times 10^{-13} \text{ erg cm}^{-3}$, and most of it at the low end $E \sim \text{GeV}$. Taking the volume of the Galaxy to be $V \sim \pi R^2 H' \sim 300 \text{ kpc}^2 \sim 10^{67} \text{ cm}^3$, the power that must be supplied is

$$P_{\text{CR}} \frac{V \mathcal{U}_{\text{CR}}}{t_{\text{conf}}} \sim 10^{40} \text{ erg s}^{-1}.$$

Each supernova releases $\sim 10^{51} \text{ erg}$, and the rate of supernovae is probably once per century, yielding $P_{\text{SN}} \sim 3 \times 10^{41} \text{ erg s}^{-1}$. The conclusion is that supernovae are indeed sufficient, provided that a few percent of their energy is converted to cosmic rays.

Chapter 10

Compton scattering

Compton scattering is the scattering of light by free electrons or positrons. It affects photons' energies but conserves their number. It is believed to be responsible for the powerlaw X-ray spectra observed from many accreting black holes of stellar and of quasar mass, and neutron stars.

10.1 Compton cross section

The cross section can be calculated classically if the photon energy $h\nu \ll m_e c^2$. Therefore, let an free electron $q = -e$ undergo a forced oscillation due to a plane wave

$$\mathbf{E}_{\text{inc}}(\mathbf{r}, t) = \mathbf{e} E_{\text{inc}} \exp(i\mathbf{k} \cdot \mathbf{r} - i\omega t),$$

where \mathbf{e} is the polarization ($\mathbf{e} \cdot \mathbf{k} = 0$, $\mathbf{e} \cdot \mathbf{e}^* = 1$), and the physical field is the real part of the above. The amplitude of the velocity perturbation is $\sim eE/\omega m_e$, and if this is $\ll c$, then in a frame where $\langle \mathbf{X} \rangle = 0$, we may neglect \mathbf{v} in eqs. (2.8) and use

$$\mathbf{a}(t_{\text{ret}}) \approx -\mathbf{e} \frac{eE_{\text{inc}}}{m} \exp(-i\omega t_{\text{ret}})$$

for the acceleration, so that the reradiated field

$$\mathbf{E}(\mathbf{x}, t) \approx -\frac{e}{cR} \mathbf{n} \times (\mathbf{n} \times \mathbf{a}) \rightarrow \frac{e^2 E_{\text{inc}}}{mcR} \mathbf{n} \times (\mathbf{n} \times \mathbf{e}) e^{-i\omega(t-R/c)}$$

is parallel to the projection of the acceleration onto the plane of the sky—this is a general result when $v \ll c$. The power radiated per solid angle is

$$\frac{dP}{d\Omega} = \frac{cR^2}{8\pi} \mathbf{E} \cdot \mathbf{E}^* = \left(\frac{e^2}{m_e c^2} \right) \frac{cE_{\text{inc}}^2}{8\pi} |\mathbf{n} \times \mathbf{e}|^2.$$

Dividing by the incident energy flux $cE_{\text{inc}}^2/8\pi$ yields the Thomson differential cross section:

$$\left(\frac{d\sigma_T}{d\Omega} \right)_{\text{pol}} = \left(\frac{e^2}{m_e c^2} \right)^2 |\mathbf{n} \times \mathbf{e}|^2. \quad (10.1)$$

The subscript signifies that this is for a definite polarization. Notice that the original wavevector \mathbf{k} doesn't appear in this formula: the re-radiated power is symmetric around an axis parallel to \mathbf{e} and

varies as $\sin^2 \Theta$, where Θ is the angle between \mathbf{n} and \mathbf{e}^1 . Integrating eq. (10.1) over all solid angles gives the total cross section,

$$\sigma_T = \frac{8\pi}{3} \left(\frac{e^2}{m_e c^2} \right)^2 \approx 0.665 \times 10^{-24} \text{ cm}^2. \quad (10.2)$$

The quantity $r_e \equiv e^2/m_e c^2$ is the classical radius of the electron, because before quantum electrodynamics it was conjectured that the mass of the electron might be due entirely to its own electrostatic field.

Often it is useful to have the differential cross section for unpolarized radiation. If \mathbf{e} lies in the plane of \mathbf{n} and \mathbf{k} (but $\perp \mathbf{k}$ of course), then $|\mathbf{n} \times \mathbf{e}|^2 = \cos^2 \psi$, where ψ is the angle between \mathbf{n} and \mathbf{k} , *i.e.*, the angle through which the light is scattered. But if \mathbf{e} is perpendicular to this plane, then $|\mathbf{n} \times \mathbf{e}|^2 = 1$. For completely unpolarized incident light, one averages these two results with equal weight:

$$\left(\frac{d\sigma_T}{d\Omega} \right)_{\text{unpol}} = \left(\frac{e^2}{m_e c^2} \right)^2 \left(\frac{1 + \cos^2 \psi}{2} \right). \quad (10.3)$$

Of course the total cross section is still (10.2). But notice that the re-radiated light at $\psi = \pi/2$ is completely linearly polarized.

At photon energies $\hbar\omega \gtrsim m_e c^2 \approx 511 \text{ keV}$, the classical calculation is not valid. For an initially *stationary* electron, quantum electrodynamics gives the Klein-Nishina formula

$$\left(\frac{d\sigma_{KN}}{d\Omega} \right)_{\text{unpol}} = \frac{3\sigma_T}{16\pi} \left(\frac{\omega'}{\omega} \right)^2 \left(\frac{\omega}{\omega'} + \frac{\omega'}{\omega} - \sin^2 \psi \right), \quad (10.4)$$

where the scattered photon energy is

$$\hbar\omega' = \hbar\omega \left[1 + \frac{\hbar\omega}{m_e c^2} (1 - \cos \psi) \right]^{-1}. \quad (10.5)$$

The electron, of course, recoils with energy $\hbar(\omega - \omega') + m_e c^2$. Notice that whereas the nonrelativistic formula (10.3) is front-back symmetric ($\psi \leftrightarrow \pi - \psi$), the Klein-Nishina formula is strongly peaked in the forward direction if $x \equiv \hbar\omega/m_e c^2 \gg 1$. The exact result for the total cross-section is given in [53]; the high-energy limit is

$$\sigma \approx \frac{3}{8} \left(\frac{\ln 2x + 1/2}{x} \right) \sigma_T \quad (x \gg 1). \quad (10.6)$$

It is instructive to practice dimensional analysis on this formula. In quantum-mechanical calculations, it is useful to think in units where $\hbar = c = 1$ (but $G \neq 1$ because gravity is normally not taken into account). This leaves only one dimension: $[\text{mass}] \leftrightarrow [\text{length}]^{-1}$ because, for example, the reduced Compton wavelength of the electron is $\lambda_e/2\pi \equiv \hbar/m_e c$. Electric charge becomes dimensionless, the square root of the fine-structure constant:

$$\alpha \equiv \frac{e^2}{\hbar c} \approx \frac{1}{137}. \quad (10.7)$$

Now the photon-electron scattering *amplitude* $\propto e^2$ because the force exerted on the electron by the incident photon is $\propto e$, and the re-emission brings in another power of e . The scattering cross-section $\propto (\text{amplitude})^2$. Hence $\sigma \propto \alpha^2 \times (\text{length})^2$. By dimensional analysis, the length should be inversely proportional to some mass or energy, but we have two of these: m_e and ω . (The total cross section should depend on the particle energies before scattering only.) Now the cross section transforms

¹assuming linear polarization; but formula (10.1) itself is valid for general elliptical polarizations.

like a piece of surface perpendicular to the relative motion of the particles before scattering, and therefore σ is invariant with respect to boosts along the direction of relative motion (a general fact). Therefore we can evaluate it in the center-of-mass frame [COM]. If the total COM energy $\gg m_e$, then one expects m_e to be irrelevant; then there is only one energy scale with which to construct the cross section (the photon and electron have opposite momenta in the COM, hence each carries energy $\approx E_{\text{COM}}/2$ if $x_{\text{COM}}/gg1$). Hence

$$\sigma \sim \frac{\alpha^2}{E_{\text{COM}}^2} = \frac{\alpha^2}{m_e(m_e + 2\omega)} .$$

In the final expression, we have evaluated E_{COM}^2 in terms of the incident energies of the photon and electron in the “lab” frame where the electron is at rest; this is most easily done using the invariance of $(\vec{p} + \vec{k})^2$, where \vec{p} and \vec{k} are index-free notations for the 4-momentum of the electron and photon, respectively.² Restoring the appropriate powers of \hbar and c , this predicts that $\sigma \sim r_e^2$ when $x \ll 1$ and $\sigma \sim r_e^2/x$ when $x \gg 1$. This is correct, except that the high-energy formula (10.6) contains a logarithm that “remembers” m_e even at $E_{\text{COM}} \gg m_e$.

10.2 Inverse Compton scattering

This is really the same process as Compton scattering, but viewed in a frame in which the electron is not at rest, so that the photon may *gain* energy by scattering.

Previous results can be applied by transforming into the electron rest frame. The photon is assumed to be soft, meaning that the rest-frame photon energy $h\bar{\nu} \ll m_e c^2$, and recoil of the electron is neglected. Since

$$\bar{\nu} = \nu \gamma (1 - \beta \cos \theta), \quad (10.8)$$

where θ is the angle between the electron 3-velocity $\beta \mathbf{n} \equiv \mathbf{p}/p^0$ and the photon momentum \mathbf{k} in the lab, the corresponding condition on the lab-frame energy is $\gamma h\nu \ll m_e c^2$.

Suppose that the photons are isotropic and monoenergetic in the lab frame:

$$I_\nu(\Omega) = K \delta(\nu - \nu_0), \quad K = \text{constant}.$$

The corresponding specific intensity in the electron rest frame is

$$\bar{I}_{\bar{\nu}}(\bar{\Omega}) = K \delta(\nu - \nu_0) \left(\frac{\bar{\nu}}{\nu}\right)^3 = K \delta(\bar{\nu} - D^{-1}\nu_0) D^{-4}, \quad (10.9)$$

where the Doppler factor is the inverse of the transformation (10.8):

$$D(\bar{\theta}, \beta) \equiv \frac{\nu}{\bar{\nu}} = \gamma(1 + \beta \cos \bar{\theta}) \quad \left[= \frac{1}{\gamma(1 - \beta \cos \theta)} \right],$$

and $\bar{\theta}$ is the angle of propagation in the rest frame. The total energy per unit time striking the electron is

$$\begin{aligned} \left(\frac{d\bar{E}}{dt}\right)_{\text{inc}} &= \sigma_T \int d\bar{\Omega} \int d\bar{\nu} \bar{I}_{\bar{\nu}}(\bar{\Omega}) \\ &= 2\pi\sigma_T K \int_{-1}^1 \frac{d \cos \bar{\theta}}{[\gamma(1 + \beta \cos \bar{\theta})]^4} \\ &= 4\pi\sigma_T K \gamma^2 \left(1 + \frac{\beta^2}{3}\right) = 4\pi\sigma_T K \left(\frac{4\gamma^2 - 1}{3}\right). \end{aligned} \quad (10.10)$$

²Thus $\vec{p} \cdot \vec{k}$ means $\eta_{\mu\nu} p^\mu k^\nu$, and $\vec{p}^2 \equiv \vec{p} \cdot \vec{p} = -m_e^2$.

Since recoil is neglected, the electron simply reflects all of the energy incident upon it. The reflected power carries no net momentum (although the incident power does, see below) because the Thomson differential cross section (10.3) is symmetric between forward and backward scattering, $\psi \rightarrow \pi - \psi$. Because

$$dE = \gamma(d\bar{E} + \boldsymbol{\beta} \cdot d\bar{\mathbf{p}}) \rightarrow \gamma d\bar{E} \quad \text{if } d\bar{\mathbf{p}} = 0, \quad (10.11)$$

and $dt = \gamma d\bar{t}$, it follows that *the emitted power is invariant*:

$$\left(\frac{dE}{dt}\right)_{\text{refl}} = \left(\frac{d\bar{E}}{d\bar{t}}\right)_{\text{refl}} = \left(\frac{d\bar{E}}{d\bar{t}}\right)_{\text{inc}}. \quad (10.12)$$

Therefore, in terms of the photon energy density in the lab $\mathcal{U}_{\text{ph}} = 4\pi K/c$, we have the following expression for the inverse-Compton power per electron:

$$P_{\text{IC}} = \frac{4\gamma^2 - 1}{3} \mathcal{U}_{\text{ph}} \sigma_T c, \quad (10.13)$$

Although derived for monochromatic photons, clearly this applies to any soft and isotropic photon spectrum.

For a nonrelativistic (and nondegenerate) thermal distribution of N_e electrons per unit volume at temperature T_e , $\langle \gamma^2 - 1 \rangle = 3k_B T_e / m_e c^2$, so that

$$N_e \langle P_{\text{IC}} \rangle \approx \left(1 + \frac{4k_B T_e}{m_e c^2}\right) N_e \sigma_T c \mathcal{U}_{\text{ph}} \quad (k_B T_e \ll m_e c^2) \quad (10.14)$$

The “1+” represents the power incident upon the electron, which is independent of the electron velocity β if the photons are isotropic:

$$P_{\text{inc}} = \int d\nu \int d\Omega I_\nu(\Omega) |\mathbf{v}_{\text{ph}} - \boldsymbol{\beta}| = \int d\nu \int d\Omega I_\nu(\Omega) (1 - \beta \cos \theta) = c \sigma_T \mathcal{U}_{\text{ph}}.$$

The ratio $P_{\text{IC}}/P_{\text{inc}}$ is the average increase in photon energy per scattering:

$$\left\langle \frac{\nu'}{\nu} \right\rangle = \frac{4\gamma^2 - 1}{3}. \quad (10.15)$$

The net rate per electron at which energy is input to the photon field is $P_{\text{IC}} - P_{\text{inc}}$, which must be balanced by an energy loss from the electron:

$$\left(\frac{dE}{dt}\right)_{\text{IC}} = -(P_{\text{IC}} - P_{\text{inc}}) = -\frac{4(\gamma^2 - 1)}{3} c \sigma_T \mathcal{U}_{\text{ph}}. \quad (10.16)$$

This is called Compton drag.

10.3 Kompaneets Equation

The methods of the previous section are classical; they would be exact in the limit $\hbar \rightarrow 0$ where the energy and momentum of individual photons would be negligible and electron recoil would completely vanish. But in reality, $\hbar \neq 0$ so that if the electrons were initially completely “cold,” *i.e.* $\langle \gamma \rangle = 1$, or (at least for a nondegenerate gas) $T_e = 0$, recoil effects would tend to heat the electrons until equilibrium with the photon distribution was achieved. In the nonrelativistic regime $\hbar\omega \ll k_B T_e \ll m_e c^2$, this evolution is described by the Kompaneets equation.

Let $n_e(\mathbf{p})$ and $n_{\text{ph}}(\mathbf{k})$ be the number of electrons and photons per mode at momenta \mathbf{p} and $\hbar\mathbf{k}$, respectively. (Both populations are assumed to be completely depolarized, so we do not keep track of spin.) Suppose that in some standard volume V there were a single electron and a single photon at these respective momenta; then define $R(\mathbf{p}, \mathbf{k}; \mathbf{p}', \mathbf{k}')$ to be the probability per unit time that they would scatter to some other momenta $(\mathbf{p}', \mathbf{k}')$. Of course

$$\mathbf{p}' + \mathbf{k}' = \mathbf{p} + \mathbf{k} \quad \text{and} \quad E' + \hbar\omega' = E + \hbar\omega, \quad (10.17)$$

where $E \equiv \sqrt{\mathbf{p}^2 + m_e^2}$ and $\omega \equiv c|\mathbf{k}|$, etc.. Microscopic reversibility dictates that

$$R(\mathbf{p}, \mathbf{k}; \mathbf{p}', \mathbf{k}') = R(\mathbf{p}', \mathbf{k}'; \mathbf{p}, \mathbf{k}). \quad (10.18)$$

One might think that the kinetic equation describing the evolution of n_{ph} should be

$$\frac{\partial}{\partial t} n_{\text{ph}}(\mathbf{k}) = \sum_{\mathbf{p}, \mathbf{k}'} R(\mathbf{p}, \mathbf{k}; \mathbf{p}', \mathbf{k}') [n_e(\mathbf{p}') n_{\text{ph}}(\mathbf{k}') - n_e(\mathbf{p}) n_{\text{ph}}(\mathbf{k})].$$

The first term represents scatterings into the electron mode at \mathbf{k} , and the second term represents scatterings out of that mode. The above equation is indeed correct in the limit that both the electrons and photons are very dilute, *viz.* $n_e, n_{\text{ph}} \ll 1$. But the generally correct equation is

$$\frac{\partial}{\partial t} n_{\text{ph}}(\mathbf{k}) = \sum_{\mathbf{p}, \mathbf{k}'} R(\mathbf{p}, \mathbf{k}; \mathbf{p}', \mathbf{k}') [n'_e n'_{\text{ph}} (1 - n_e)(1 + n_{\text{ph}}) - n_e n_{\text{ph}} (1 - n'_e)(1 + n'_{\text{ph}})], \quad (10.19)$$

in which an obvious shorthand has been used ($n_{\text{ph}} \equiv n_{\text{ph}}(\mathbf{k})$, $n'_{\text{ph}} \equiv n_{\text{ph}}(\mathbf{k}')$). The factors $(1 \pm n)$ reflect Bose-Einstein and Fermi statistics: if the mode at \mathbf{p} is filled, then no scattering into that mode can occur, and the factor $1 - n_e(\mathbf{p})$ enforces this. For the (bosonic) photons, on the other hand, the probability of scattering into the mode at \mathbf{k} increases to the extent that the mean occupation number $n_{\text{ph}}(\mathbf{k})$ is already > 0 (stimulated emission). This argument doesn't explain why the final-state factors are $1 \pm n$ rather than (say) $(1 \pm n)^2$. But consider fermionic and bosonic gases in thermal equilibrium,

$$n_e(\mathbf{p}) = \{\exp[(E + \mu_e)/k_B T] + 1\}^{-1} \quad n_{\text{ph}}(\mathbf{k}) = \{\exp[(\hbar\omega + \mu_{\text{ph}})/k_B T] - 1\}^{-1}.$$

When these forms are inserted, the righthand side of the kinetic equation (10.19) vanishes identically because of energy conservation (10.17). The constants μ_e, μ_{ph} are *chemical potentials* associated with conservation of particle number. For the electrons, $-\mu_e$ is the Fermi energy,³ and the electrons are degenerate if $-\mu_e \gtrsim k_B T$. The chemical potential of a photon blackbody is $\mu_{\text{ph}} = 0$ because photons are not conserved. But pure Compton scattering conserves photons while redistributing their energies and momenta. When Compton scattering dominates, the photons may evolve to $\mu_{\text{ph}} > 0$, meaning that the photon gas is dilute: fewer photons per unit volume than there would be for a black body of the same mean energy per photon.

The derivation of the Kompaneets equation assumes that the electrons are thermal and nondegenerate, so the $(1 - n_e)$ factors are dropped and the electron distribution is Maxwellian,

$$n_e(E) = K e^{-E/k_B T_e}, \quad K = e^{-\mu_e} = \text{const.} \quad (10.20)$$

But the $(1 + n_{\text{ph}})$ factors are retained. The electron and photon distributions are assumed isotropic, so that they can be written as functions of E and ω , as above. Finally, the electrons are nonrelativistic and the photons are soft, so that the fractional changes in photon energy are small,

$$\Delta\omega \equiv \omega' - \omega \ll \omega.$$

³For nonrelativistic electrons, one uses E for the kinetic energy $\mathbf{p}^2/2m$, so the relativistic $\mu_e \rightarrow -(E_F + m_e c^2)$.

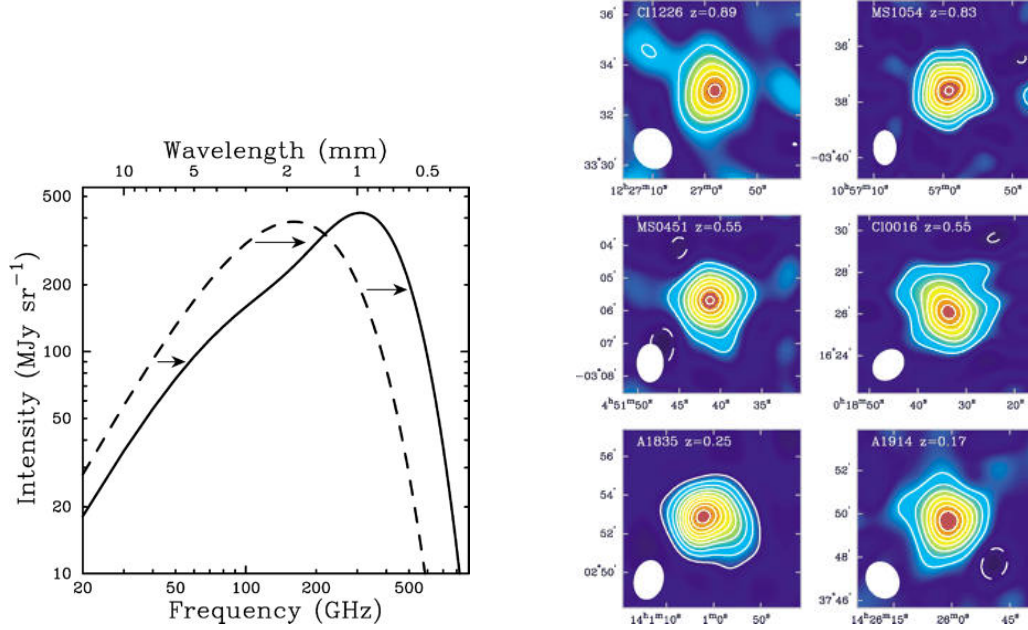


Figure 10.1: *Left panel:* Sunyaev-Zeldovich effect. Hot electrons shift photons from the Rayleigh-Jeans into the Wien part of the spectrum. *Right panel:* Interferometric images of SZ effect in clusters of galaxies. Note that the amplitude of the signal does not depend upon redshift as long as the cluster is resolved [9]

Then the kinetic equation can be reduced to a differential equation by expanding n_e and n_{ph} to second order in energy changes:

$$\begin{aligned} n_e(E') &\approx n_e(E) - \hbar\Delta\omega \frac{\partial n_e}{\partial E} + \frac{1}{2}(\hbar\Delta\omega)^2 \frac{\partial^2 n_e}{\partial E^2} \\ &= \left[1 + \Delta x + \frac{1}{2}(\Delta x)^2 \right] n_e(E), \\ n_{\text{ph}}(x') &\approx n_{\text{ph}}(x) + \Delta x \frac{\partial n_{\text{ph}}}{\partial x} + \frac{1}{2}(\Delta x)^2 \frac{\partial^2 n_{\text{ph}}}{\partial x^2}. \end{aligned}$$

We have introduced a dimensionless photon energy

$$x \equiv \frac{\hbar\omega}{k_B T_e}. \quad (10.21)$$

Putting these expansions into the kinetic equation, we have

$$\frac{\partial n_{\text{ph}}}{\partial t} = \overline{\Delta x} \left[\frac{\partial n_{\text{ph}}}{\partial x} + n_{\text{ph}}(n_{\text{ph}} + 1) \right] + \overline{(\Delta x)^2} \left[\frac{1}{2} \frac{\partial^2 n_{\text{ph}}}{\partial x^2} + \frac{\partial n_{\text{ph}}}{\partial x} (n_{\text{ph}} + 1) \right], \quad (10.22)$$

where the first and second moments of the energy change are

$$\overline{\Delta x} \equiv \sum_{\mathbf{p}, \mathbf{k}'} \Delta x n_e(\mathbf{p}) R(\mathbf{p}, \mathbf{k}; \mathbf{p}', \mathbf{k}') \quad (10.23)$$

$$\overline{(\Delta x)^2} \equiv \sum_{\mathbf{p}, \mathbf{k}'} (\Delta x)^2 n_e(\mathbf{p}) R(\mathbf{p}, \mathbf{k}; \mathbf{p}', \mathbf{k}') \quad (10.24)$$

Labor is saved by realizing that in order to guarantee conservation of total photon number (henceforth we omit the subscript from n_{ph}):

$$N_{\text{ph}} \propto \int x^2 n dx ,$$

it must be possible to cast eq. (10.22) in the form

$$\frac{\partial}{\partial t}(x^2 n) = -\frac{\partial F}{\partial x} , \quad (10.25)$$

By inspection, there must be functions A, B, C such that the number flux F is

$$-F = A(x) \frac{\partial n}{\partial x} + B(x)n + C(x)n^2 . \quad (10.26)$$

Matching coefficients of n, n^2 , and their derivatives, one finds

$$A = B = C = \frac{x^2}{2} \overline{(\Delta x)^2} \quad \text{and} \quad \overline{\Delta x} = \frac{1}{2} e^x \frac{\partial}{\partial x} \left[e^{-x} \overline{(\Delta x)^2} \right] . \quad (10.27)$$

It remains only to compute $\overline{(\Delta x)^2}$. From energy and momentum conservation,

$$\hbar \Delta \omega = E - E' \approx \frac{\mathbf{p}^2 - \mathbf{p}'^2}{2m} \approx \frac{\mathbf{p} \cdot (\mathbf{p} - \mathbf{p}')}{m} = \frac{\hbar \mathbf{p} \cdot (\mathbf{k}' - \mathbf{k})}{m} = \hbar \mathbf{v}_e \cdot \Delta \mathbf{k} ,$$

where $\mathbf{v}_e \equiv \mathbf{p}/m$ is the electron velocity. The square of this expression is already $\propto v_e^2$; since the electrons are non-relativistic, all other factors in the collision can be evaluated as if $\mathbf{v}_e \rightarrow 0$. But if the electrons were at rest, then \mathbf{v}_e and $\Delta \mathbf{k}$ would be uncorrelated, whence

$$\langle (\mathbf{v}_e \cdot \Delta \mathbf{k})^2 \rangle \approx \frac{1}{3} \langle (\mathbf{v}_e)^2 \rangle \langle (\Delta \mathbf{k})^2 \rangle = \frac{k_B T_e}{m} \langle (\Delta \mathbf{k})^2 \rangle ,$$

since $\langle \cos^2 \theta \rangle = 1/3$. Neglecting electron recoil, $|\mathbf{k}'| = |\mathbf{k}|$ when the electron is at rest, so $(\Delta \mathbf{k})^2 = 4\mathbf{k}^2 \sin^2(\psi/2)$ in terms of the scattering angle ψ , and the average of this with respect to the differential cross section (10.3) is $2\mathbf{k}^2 = 2\omega^2/c^2$. The total collision rate per unit volume is of course $N_e \sigma_T c$. Putting these pieces together,

$$\overline{(\Delta x)^2} \approx 2N_e \sigma_T c \frac{k_B T_e}{m_e c^2} x^2 , \quad (10.28)$$

and the Kompaneets equation takes the form

$$\frac{\partial n}{\partial y} = \frac{1}{4x^2} \frac{\partial}{\partial x} \left[x^4 \left(\frac{\partial n}{\partial x} + n + n^2 \right) \right] , \quad (10.29)$$

in terms of a dimensionless time, the Compton y parameter:

$$y \equiv \underbrace{(4k_B T_e / m_e c^2)}_{\langle \Delta \omega / \omega \rangle \text{ per scatt.}} \times \underbrace{N_e \sigma_T ct}_{\# \text{ scatt.}} . \quad (10.30)$$

Notice that for a fixed time t or photon path length ct , $y \propto N_e k_B T_e$, the electron pressure. We will discuss two astrophysical applications of eq. (10.29): the Sunyaev-Zeldovich [SZ] effect, and accretion-disk spectra.

The intergalactic gas in the most massive clusters of galaxies has $k_B T_e \sim 10$ keV ($T \sim 10^8$ K or $k_B T_e / m_e c^2 \sim 0.02$), corresponding to line-of-sight virial velocities $\sim 10^3$ km s $^{-1}$. Optical depths through the centers are $\int N_e \sigma_T dl \lesssim 10^{-2}$, so $y \sim 10^{-4} - 10^{-3}$. The “input” photon spectrum

is the Cosmic Microwave Background [CMB], which is accurately isotropic and has a temperature $T_{\text{ph}} \approx 2.7$ K, so the dimensionless temperature $x \sim 3T_{\text{ph}}/T_e \sim 10^{-7}$. Since x and y are both small, the solution of eq. (10.29) is adequately represented as

$$\begin{aligned} n - n_0 &\approx \frac{y}{4x^2} \frac{\partial}{\partial x} \left(x^4 \frac{\partial n_0}{\partial x} \right), \\ &= y \hat{x} \frac{\partial n_0}{\partial \hat{x}} \left[1 - \frac{\hat{x}(e^{\hat{x}} + 1)}{4(e^{\hat{x}} - 1)} \right] \quad \text{where } \hat{x} \equiv \frac{T_e}{T_{\text{ph}}} x = \frac{\hbar\omega}{k_{\text{B}}T_{\text{ph}}}, \end{aligned} \quad (10.31)$$

and n_0 is the input blackbody:

$$n_0(\omega, T_{\text{ph}}) = [e^{\hat{x}} - 1]^{-1}. \quad (10.32)$$

The reason for writing $n - n_0$ in the final factored form is that if one were to make a small change δT_{ph} in the blackbody temperature, the corresponding change in n would be

$$n_0(\omega, T_{\text{ph}} + \delta T_{\text{ph}}) - n_0(\omega, T_{\text{ph}}) \approx -\frac{\delta T_{\text{ph}}}{T_{\text{ph}}} \times \hat{x} \frac{\partial n_0}{\partial \hat{x}} \quad (10.33)$$

because n_0 depends on T_{ph} and x through the combination $\hat{x} \propto x/T_{\text{ph}}$ only. Therefore the solution (10.31) can be interpreted as a frequency-dependent temperature shift:

$$\frac{\delta T_{\text{ph}}}{T_{\text{ph}}} = y \left[\frac{\hat{x}(e^{\hat{x}} + 1)}{4(e^{\hat{x}} - 1)} - 1 \right]. \quad (10.34)$$

In the Rayleigh-Jeans region $\hat{x} \ll 1$ ($\hbar\omega \ll k_{\text{B}}T_{\text{ph}}$), where most ground-based observations are made, $\delta T_{\text{ph}}/T_{\text{ph}} \approx -y/2$; whereas on the Wien side $\hat{x} \gg 1$, $\delta T_{\text{ph}}/T_{\text{ph}} \approx +\hat{x}y/4$. Thus there is an apparent cooling at low frequencies and an heating at high ones; both effects are caused by a migration of photons to higher frequencies, conserving their number. The temperature shift vanishes at $\hat{x} \approx 3.83$, corresponding to $\lambda \approx 1.4$ mm for $T_{\text{ph}} = 2.7$ K. By measuring y , one determines the line-of-sight integral of the gas pressure; combining this with measurements of the X-ray brightness (due to bremsstrahlung emission from the same gas), one can in principle measure the distance to the cluster and other quantities of interest. After many years of effort and frustration, such measurements have recently become reliable, and the subject holds great promise [cf. 9, for a recent review].

Another important, if less cosmic, application is to the X-ray spectra of accretion disks, especially the inner parts of disks accreting onto black-hole candidates. A typical spectrum for a bright X-ray binary consists of an approximate blackbody at $k_{\text{B}}T_{\text{ph}} \sim 1$ keV, plus a power-law tail extending to much larger energies (in the famous Galactic source Cygnus X-1, the tail may extend to $\hbar\omega \gtrsim 1$ MeV). The ratio of fluxes in the soft (thermal) and hard (power-law) components often varies with time and total flux. It is widely believed that the soft component is emission from the accretion disk, while the hard component results as some of these soft photons are Compton-scattered by much hotter—or possibly relativistic and nonthermal—electrons in a *corona* above the disk. Presumably the corona has something to do with magnetic dissipation.

To see roughly how the hard component might arise, let us modify the righthand side of eq. (10.29) by adding a source function $S(x)$ at small x [*i.e.* $S(x)$ is appreciable only at $x \lesssim x_s \ll 1$], and a sink function $-n/y_c$. The motivation for the latter is that the corona has a finite optical depth

$$\tau_c = y_c \cdot \left(\frac{4k_{\text{B}}T_e}{m_e c^2} \right)^{-1} \sim 1;$$

in our spatially homogenous and isotropic model, we crudely represent this by arranging that the photon has a fixed probability of escaping from the corona per unit “time” y_c . Finally, we seek a

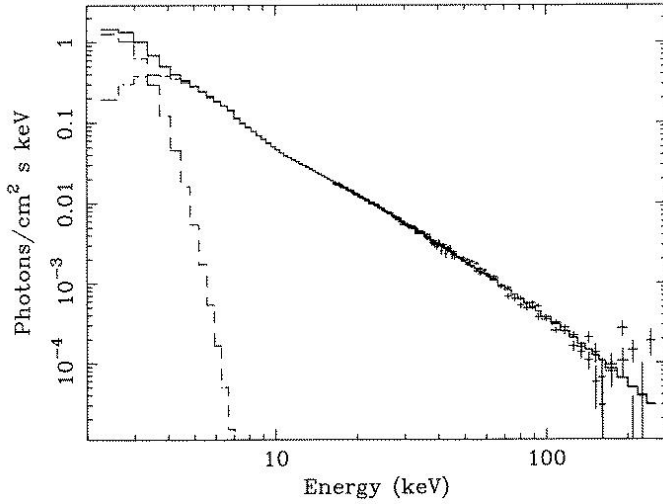


Figure 10.2: Spectrum of Cygnus X-1 measured by RXTE (Rossi X-ray Timing Explorer). Cygnus X-1 is believed to be an accreting black hole with mass $\approx 4 - 5 M_{\odot}$ in a binary system with an O -star companion. X-ray counts shown by points with error bars. Solid histograms show a model fit consisting of a soft thermal component ($k_{\text{B}}T = 0.27 \text{ keV}$), a broken powerlaw (photons per energy per time $\propto E^{-2.95}$ below 10.8 keV and $E^{-1.95}$ above), and an exponential cutoff at 184 keV [13].

steady state, so $\partial n / \partial y = 0$:

$$0 \approx \frac{1}{4x^2} \frac{\partial}{\partial x} \left[x^4 \left(\frac{\partial n}{\partial x} + n + n^2 \right) \right] + S(x) - \frac{n}{y_c}. \quad (10.35)$$

We want to apply this to the high-energy tail, where it is likely that the photons are dilute: $n \ll 1$ whence $n^2 \ll n$, so we drop the nonlinear term. Also, at $x > x_s$ we can ignore $S(x)$ locally (although globally it is crucial to maintain the supply of photons). We now have (with $n' \equiv dn/dx$)

$$\left[x^2 n'' + 4x n' - \frac{4}{y_c} n \right] + [x(xn' + 4n)] \approx 0.$$

The relative scaling of the various terms with x is guesstimated by counting each derivative as a factor of $1/x$ (which is roughly true if the solution resembles a power law, but not if it is exponential). By this accounting, the terms in each set of square brackets scale together, and the second bracket has an extra factor of x with respect to the first. At moderately low frequencies $x_s < x \ll 1$, the first bracket should dominate, and we seek a solution $n \propto x^{-\alpha-2}$; observations are usually quoted in terms of the power-law index of the number of photons per unit energy ($\propto x^2 n$), which is α :

$$\alpha^2 + \alpha - 2 - \frac{4}{y_c} \approx 0 \Rightarrow \alpha \approx -\frac{1}{2} + \frac{3}{2} \sqrt{1 + \left(\frac{4}{3\sqrt{y_c}} \right)^2},$$

since we need the positive root. Hence $\alpha > 1$ so that the total number of photons converges. At large x , ignoring the first bracket in favor of the second leads to $n \propto x^{-4}$: it can be shown that this describes photons injected at *high* energy and *cooling down* toward equilibrium with the electrons (the energy-space flux $F < 0$). If the source is at *low* energies, then the appropriate large- x behavior is found by balancing the two terms with explicit x^2 factors, leading to $n \propto e^{-x}$ as expected for a dilute photon gas in thermal equilibrium.

Thus we are able to model spectra such as that shown in Figure 10.2. One imagines an accretion disk injecting soft photons ($h\nu \sim k_B T_{\text{disk}} \lesssim 1 \text{ keV}$) to a corona containing hot or even relativistic electrons ($\bar{E}_e \gtrsim 100 \text{ keV}$). The soft photons are upscattered to form a powerlaw with photon index $\alpha > 1$ and a cutoff at energies of order \bar{E}_e .

To extend the photon power-law up to $\sim 1 \text{ MeV}$, one therefore needs electron energies of the same order. There is no reason to believe solutions to the differential equation (10.29) when $k_B T_{\text{ph}} \gtrsim m_e c^2$, since all of the approximations by which it was derived break down, and one must go back to the original (integro-differential) kinetic equation. But it can be shown (*e.g.* by Monte-Carlo simulations) that power-law solutions can result, provided there is a population of relativistic electrons.

Bibliography

- [1] M. Abramowitz and I. Stegun, editors. *Handbook of Mathematical Functions*. Dover, 1970.
- [2] W. I. Axford, E. Leer, and G. Skadron. . In *Proc. 15th International Cosmic Ray Conference*, volume 11, page 132, 1977.
- [3] A. R. Bell. . *MNRAS*, 182:147, 1978.
- [4] J. A. Biretta, R. L. Moore, and M. H. Cohen. The evolution of the compact radio source in 3C 345. I - VLBI observations. *ApJ*, 308:93–109, September 1986.
- [5] R. D. Bladford and R. L. Znajek. Electromagnetic extraction of energy from kerr black holes. *MNRAS*, 179:433–456, 1977.
- [6] R. D. Blandford. Astrophysical black holes. In S. W. Hawking and W. Israel, editors, *300 Years of Gravitation*, pages 277–329. Cambridge University Press, 1987.
- [7] R. D. Blandford and C. F. McKee. Fluid dynamics of relativistic blast waves. *Physics of Fluids*, 19:1130–1138, 1976.
- [8] R. D. Blandford and J. P. Ostriker. Particle acceleration by astrophysical shocks. *ApJ*, 221:L29–L32, April 1978.
- [9] J. E. Carlstrom, G. P. Holder, and E. D. Reese. Cosmology with the Sunyaev-Zel’dovich Effect. *ARAA*, 40:643–680, 2002.
- [10] B. Carter. . *Comm. Math. Phys.*, 10:280–310, 1968.
- [11] M. H. Cohen, T. J. Pearson, A. C. S. Readhead, G. A. Seielstad, R. S. Simon, and R. C. Walker. Superluminal variations in 3C 120, 3C 273, and 3C 345. *ApJ*, 231:293–298, July 1979.
- [12] E. Costa et al. GRB 970228. *IAU Circ*, 6572:1–+, March 1997.
- [13] W. Cui, W. A. Heindl, R. E. Rothschild, S. N. Zhang, K. Jahoda, and W. Focke. Rossi X-Ray Timing Explorer Observation of Cygnus X-1 in Its High State. *ApJ*, 474:L57–L60, 1997.
- [14] P. B. Demorest, T. Pennucci, S. M. Ransom, M. S. E. Roberts, and J. W. T. Hessels. A two-solar-mass neutron star measured using Shapiro delay. *Nature*, 467:1081–1083, October 2010.
- [15] E. Fermi. . *Phys. Rev.*, 1949.
- [16] G. J. Fishman. Observed properties of gamma-ray bursts. *A&AS*, 138:395–398, September 1999.
- [17] A. S. Fruchter et al. The Fading Optical Counterpart of GRB 970228, 6 Months and 1 Year Later. *ApJ*, 516:683–692, May 1999.

- [18] T. J. Galama, R. A. M. J. Wijers, M. Bremer, P. J. Groot, R. G. Strom, C. Kouveliotou, and J. van Paradijs. The Radio-to-X-Ray Spectrum of GRB 970508 on 1997 May 21.0 UT. *ApJ*, 500:L97–L100, June 1998.
- [19] D. K. Galloway, M. P. Muno, J. M. Hartman, D. Psaltis, and D. Chakrabarty. Thermonuclear (Type I) X-Ray Bursts Observed by the Rossi X-Ray Timing Explorer. *ApJS*, 179:360–422, December 2008.
- [20] J. Goodman. Are gamma-ray bursts optically thick? *ApJ*, 308:L47–L50, September 1986.
- [21] J. Goodman. Radio scintillation of gamma-ray-burst afterglows. *New Astronomy*, 2:449–460, October 1997.
- [22] NASA: <http://coss.gsfc.nasa.gov/images/epo/gallery/grbs/>.
- [23] D. Guetta, M. Spada, and E. Waxman. Efficiency and Spectrum of Internal Gamma-Ray Burst Shocks. *ApJ*, 557:399–407, August 2001.
- [24] T. Güver, F. Özel, and D. Psaltis. Systematic Uncertainties in the Spectroscopic Measurements of Neutron-star Masses and Radii from Thermonuclear X-Ray Bursts. II. Eddington Limit. *ApJ*, 747:77, March 2012.
- [25] T. Güver, D. Psaltis, and F. Özel. Systematic Uncertainties in the Spectroscopic Measurements of Neutron-star Masses and Radii from Thermonuclear X-Ray Bursts. I. Apparent Radii. *ApJ*, 747:76, March 2012.
- [26] J. W. T. Hessels, S. M. Ransom, I. H. Stairs, P. C. C. Freire, V. M. Kaspi, and F. Camilo. A Radio Pulsar Spinning at 716 Hz. *Science*, 311:1901–1904, March 2006.
- [27] G. Hinshaw et al. Nine-Year Wilkinson Microwave Anisotropy Probe (WMAP) Observations: Cosmological Parameter Results. *ArXiv e-prints*, December 2012.
- [28] K. I. Kellermann and I. I. K. Pauliny-Toth. The Spectra of Opaque Radio Sources. *ApJ*, 155:L71–78, February 1969.
- [29] R. W. Klebesadel, I. B. Strong, and R. A. Olson. Observations of Gamma-Ray Bursts of Cosmic Origin. *ApJ*, 182:L85–L88, June 1973.
- [30] G. F. Krymsky. . *Dokl. Acad. Nauk. USSR*, 234:1306, 1977.
- [31] P. Kumar. Gamma-Ray Burst Energetics. *ApJ*, 523:L113–L116, October 1999.
- [32] J. M. Lattimer and M. Prakash. Neutron star observations: Prognosis for equation of state constraints. *Physics Reports*, 442:109–165, April 2007.
- [33] Malcolm S. Longair. *High Energy Astrophysics*. Cambridge University Press, second edition, 1994.
- [34] NASA/STScI/AURA: <http://hubblesite.org/newscenter/archive/2000/20/>.
- [35] X-ray: NASA/CXC/MIT/H. Marshall *et al.*; Radio: F. Zhao & F. Owen (NRAO); J. Biretta (STScI). Optical: NASA/STScI/UMBC/E. Perlmann and others.
- [36] T. Matheson. The supernovae associated with gamma ray bursts. In P. Humphreys and K. Stanek, editors, *The Fate of the Most Massive Stars*, volume 332 of *ASP Conf. Ser.*, page 416, San Francisco, 2005. ASP.

- [37] M. V. Medvedev and A. Loeb. Generation of Magnetic Fields in the Relativistic Shock of Gamma-Ray Burst Sources. *ApJ*, 526:697–706, December 1999.
- [38] M. R. Metzger, S. G. Djorgovski, S. R. Kulkarni, C. C. Steidel, K. L. Adelberger, D. A. Frail, E. Costa, and F. Frontera. Spectral constraints on the redshift of the optical counterpart to the gamma-ray burst of 8 May 1997. *Nature*, 387:879–+, 1997.
- [39] F. Özel, T. Güver, and D. Psaltis. The Mass and Radius of the Neutron Star in EXO 1745-248. *ApJ*, 693:1775–1779, March 2009.
- [40] W. S. et al. Paciesas. The Fourth BATSE Gamma-Ray Burst Catalog (Revised). *ApJS*, 122:465–495, 1999.
- [41] B. Paczynski. Gamma-ray bursters at cosmological distances. *ApJ*, 308:L43–L46, September 1986.
- [42] B. Paczyński and J. E. Rhoads. Radio Transients from Gamma-Ray Bursters. *ApJ*, 418:L5+, November 1993.
- [43] D. N. Page and K. S. Thorne. Disk Accretion onto a Black Hole. I. Time-averaged structure of the Accretion Disk. *ApJ*, 191:499–506, 1974.
- [44] D. M. Palmer et al. Gamma-ray observations of a giant flare from the magnetar SGR 1820-20. [astro-ph/0502329](#), 2005.
- [45] A. Panaitescu and P. Kumar. Properties of Relativistic Jets in Gamma-Ray Burst Afterglows. *ApJ*, 571:779–789, June 2002.
- [46] P. J. E. Peebles. *Principles of Physical Cosmology*. Princeton University Press, 1993.
- [47] E. Pian et al. Hubble Space Telescope Imaging of the Optical Transient Associated with GRB 970508. *ApJ*, 492:L103–L106, January 1998.
- [48] J. R. Pierce. *Almost all about waves*. MIT Press, 1974.
- [49] T. Piran. Gamma-ray bursts and the fireball model. *Physics Reports*, 314:575–+, 1999.
- [50] R. V. Pound and G. A. Rebka. . *Phys. Rev. Lett.*, 4:337, 1960.
- [51] A. C. S. Readhead. Equipartition brightness temperature and the inverse Compton catastrophe. *ApJ*, 426:51–59, May 1994.
- [52] M. J. Rees and P. Meszaros. Relativistic fireballs - Energy conversion and time-scales. *MNRAS*, 258:41P–43P, September 1992.
- [53] G. B. Rybicki and A. P. Lightman. *Radiative Processes in Astrophysics*. Wiley, 1979.
- [54] B. E. Schaefer, D. Palmer, B. L. Dingus, E. J. Schneid, V. Schoenfelder, J. Ryan, C. Winkler, L. Hanlon, R. M. Kippen, and A. Connors. Gamma-Ray-Burst Spectral Shapes from 2 keV to 500 MeV. *ApJ*, 492:696–702, January 1998.
- [55] W. K. H. Schmidt. Distance limit for a class of model gamma-ray burst sources. *Nature*, 271:525–527, February 1978.
- [56] B. F. Schutz. *A first course in general relativity*. Cambridge University Press, second edition, 2009.
- [57] J. A. Simpson and M. Garcia-Munoz. Cosmic-ray lifetime in the Galaxy: Experimental results and models. *Space Science Reviews*, 46(3-4):205–224, 1988.

- [58] T. Strohmayer and L. Bildsten. New Views of Thermonuclear Bursts. *ArXiv Astrophysics e-prints*, January 2003.
- [59] S. A. Teukolsky. . *Phys. Rev. Lett.*, 29:1114–1118, 1972.
- [60] K. S. Thorne. Disk Accretion onto a Black Hole. II. Evolution of the Hole. *ApJ*, 191:507–519, 1974.
- [61] K. S. Thorne, R. H. Price, and D. A. MacDonald. *Black Holes: The Membrane Paradigm*. Yale University Press, 1986.
- [62] J. van Paradijs. Average properties of X-ray burst sources. *Nature*, 274:650–653, August 1978.
- [63] J. van Paradijs et al. Transient optical emission from the error box of the gamma-ray burst of 28 February 1997. *Nature*, 386:686–689, 1997.
- [64] R. M. Wald. Black hole in a uniform magnetic field. *Phys. Rev. D*, D10:1680–1685, 1974.
- [65] E. Waxman, S. R. Kulkarni, and D. A. Frail. Implications of the Radio Afterglow from the Gamma-Ray Burst of 1997 May 8. *ApJ*, 497:288–293, April 1998.
- [66] S. Weinberg. *Gravitation and Cosmology: Principles and Applications of the General Theory of Relativity*. Wiley, 1972.
- [67] R. A. M. J. Wijers, M. J. Rees, and P. Meszaros. Shocked by GRB 970228: the afterglow of a cosmological fireball. *MNRAS*, 288:L51–L56, July 1997.
- [68] Q. Yu and S. Tremaine. Observational constraints on growth of massive black holes. *MNRAS*, 335:965–976, October 2002.